# Techno-economic evaluation of battery storage systems in industry

Zur Erlangung des akademischen Grades eines

**Doktors der Ingenieurwissenschaften**
**(Dr.-Ing.)**

von der KIT-Fakultät für
Wirtschaftswissenschaften
des Karlsruher Instituts für Technologie (KIT)

genehmigte

**DISSERTATION**

von

**Dipl.-Ing. Fritz Braeuer**

| | |
|---|---|
| Tag der mündlichen Prüfung: | 25. Oktober 2022 |
| Hauptreferent: | Prof. Dr. Wolf Fichtner |
| Korreferent: | Prof. Dr. Orestis Terzidis |

# Abstract

In the context of a changing energy system towards one dominated by renewable energy sources, the demand for flexible energy generation and consumption will increase. Battery storage systems can provide a significant share of this energy flexibility, especially when combined with an industrial manufacturing plant to shift the industrial electricity demand over time. This paper contributes to a better understanding of the business decision when investing in a battery storage system and when marketing energy flexibility. For this purpose, the work considers the techno-economic and regulatory framework for flexibility measures and examines the optimal investment and dispatch planning for a battery storage system in an industrial company.

The studies in this thesis focus on three central aspects. As a first aspect, the various revenue streams for the stored electricity are analysed and how these influence the profitability of a battery storage system. In particular, the provision of frequency containment reserve power, peak load shifting or peak shaving, arbitrage trading on the energy markets and the increase in self-consumption through photovoltaic self-generation are addressed. For this purpose, an optimisation model is formulated as a discrete, linear programme that maps the economic framework of the flexibility markets and integrates the technological constraints of the battery storage system. As a second aspect, uncertainties about market prices, load and generation behaviour are integrated into the optimisation model and the influence on the investment decision is investigated. This is done on the one hand by a two-stage robust optimisation model, which represents the uncertainty about the market success on the intraday market. On the other hand, the significance of the sequence of uncertain market decisions is illuminated through a multi-stage stochastic optimisation model. As a third aspect, the trade-off between the economic and ecological use of a battery storage system is analysed. For this purpose, an ecological, $CO_2$-minimal dispatch is calculated by deriving national $CO_2$-emission factors and compared with an economically optimal dispatch.

The case studies are analysed based on real industrial load data from small, medium and large enterprises. The thesis discusses the technical and economic framework conditions, with the main focus on Germany. However, a comparison between the countries Germany, Denmark, and Croatia is also presented.

The results show that peak shaving and the provision of frequency containment reserve are complementary and make the investment in a battery storage system economically viable. Self-generation through a photovoltaic system can reduce the risk arising from uncertain energy

market prices. However, the sequence of uncertain decisions has a significant impact on the design of the battery storage system. Economically feasible operation through arbitrage trading, on the other hand, is not possible due to the small price differences in the markets and limitations due to battery ageing and efficiency. These battery characteristics also influence the use of a battery storage system for $CO_2$-reduction. Due to the limited number of cycles and relatively high charging losses, battery technology is currently unsuitable for $CO_2$-minimal storage use. Nevertheless, the economic and ecological potential of battery storage systems strongly depends on individual factors such as local grid charges, the selected battery technology and the individual industrial load profile. Advances in battery technology, such as increased lifetime, and possible new flexibility markets, such as dynamic grid charges, offer new application and marketing opportunities that could increase the economic viability of a battery storage system.

# Acknowledgments

This dissertation was written for the most part during my time as a research assistant at the Chair of Energy Economics at the Institute for Industrial Production (IIP) at Karlsruhe Institute of Technology (KIT). The thesis was completed while I was working at the federal Ministry of Economic Affairs and Climate Action (BMWK). During these six and a half years from 2016 to 2022, I had the privilege to work in an enriching and stimulating environment. I had the opportunity to make a scientific contribution to various research projects funded by the BMWK and the car manufacturer BMW. Through my activities, I have had the chance to meet and learn from many different people.

First and foremost, I would like to thank my doctoral supervisor Prof. Dr. Wolf Fichtner for his many years of support and constructive discussions. Through him, I have learned the fundamentals that help me professionally every day. I would also like to thank Prof. Dr. Orestis Terzidis for his role as co-reviewer, as well as Prof. Dr. Stefan Nickel and Prof. Dr. Andreas Oberweis serving as committee members.

Special thanks go to Prof. Dr. Russell McKenna, who has played a major role in my scientific success as a group leader for many years. Russell has always brought in new impulses and pointed out new research possibilities. I credit Russell's ability to discuss, argue and disagree while always being supportive. Special thanks go to all colleagues at the IIP and in particular to Florian Zimmermann, Dr. Joris Dehler-Holland, Elias Naber, Maximilian Kleinebrahm, Dr. Patrick Jochem, Dr. Kai Mainzer, Manuel Ruppert, Victor Slednev and Johannes Schäuble. Special thanks also go out to my co-authors Prof. Dr. Fabian Scheller, Dr. Julian Rominger, Nikolina Čović and Prof. Dr. Hrvoje Pandžič. Finally, I would also like to thank the Gesellschaft für Energiewissenschaft und Energiepolitik (GEE) and my fellow board members Prof. Dr. Aaron Praktiknjo, Prof. Dr. Michael Bucksteeg, Dr. Philipp Riegerbauer and Dr. Maximilian Happach.

The biggest thanks, however, go to my wife Jule, who supported me throughout the whole process in all its draining length and made it all seem like a matter of course. I would also like to thank my family and especially my parents, who made this possible for me in the first place. Thank you!

Berlin, January 2023

Fritz Braeuer

# Table of content

# Nomenclature

### Abbreviations

| | |
|---|---|
| aFRR | Automated frequency restoration reserve |
| AEF | Average emission factor |
| BEM | Balancing energy market |
| BMS | Battery management system |
| BSS | Battery storage system |
| BNetzA | Federal regulation authority |
| $CO_2$ | Carbon dioxide |
| C-rate | Charging rate |
| KSG | Climate Protection Act |
| CHP | Combined heat and power |
| DoD | Depth of discharge |
| DSO | Distribution system operator |
| DRO | Distributionally robust optimisation |
| EV | Electric vehicle |
| StromNEV | Electricity grid charges ordinance |
| EF | Emission factor |
| EoL | End-of-Life |
| EU | European Union |
| BMWi | Federal Ministry for Economic Affairs and Energy |
| FCR | Frequency containment reserve |
| HV | High voltage |
| HSRO | Hybrid stochastic robust optimisation |

| | |
|---|---|
| SOL | Immediately interruptible loads |
| JCEU | Justice Court of the European Union |
| LP | Linear Problem/Programme |
| LFP | Lithium iron phosphate |
| LTO | Lithium titanate |
| Li-ion | Lithium-ion |
| LV | Low voltage |
| mFRR | Manual frequency restoration reserve |
| MPM | Marginal power mix |
| MPP | Marginal power plant |
| MSR | Marginal system response |
| MV | Medium voltage |
| MILP | Mixed-integer linear problem/programme |
| MINPL | Mixed-integer non-linear problem/programme |
| NMC | Nickel-Manganese-Cobalt |
| NLP | Non-linear problem/programme |
| AbLaV | Ordinance for interruptible loads |
| OTC | Over-the-counter |
| PV | Photovoltaics |
| SNL | Quickly interruptible loads |
| RES | Renewable energy sources |
| EEG | Renewable Energy Sources Act |
| SEI | Solid Electrolyte Interface |
| SOC | State of Charge |
| TSO | Transmission system operator |

**Model names**

| | |
|---|---|
| BSS-Opt model | Linear optimisation model |

| | |
|---|---|
| BSS-robust-model | Two-stage robust optimisation model |
| BSS-mult-stg-model | Multi-stage stochastic optimisation model |
| BSS-two-stg-model | Two-stage stochastic optimisation model |
| BSS-$CO_2$-model | $CO_2$-minimal dispatch model |

### Symbols

| | |
|---|---|
| $\gamma$ | Decision stage |
| $\gamma arb$ | Arbitrage decision level |
| $\gamma fcr$ | FCR decision level |
| $\Gamma$ | Uncertainty budget |
| $\Delta c^{ID}$ | Price deviation on the intraday market |
| $\pi$ | Probability factor |
| $\rho$ | Weighting factor |
| $Ann^{BSS}$ | Annuity payment for BSS |
| $Ann^{BSSaged}$ | Annuity payment for BSS ageing |
| $Ann^{PV}$ | Annuity payment for PV system |
| $bin$ | Binary decision variable |
| $c^{DA}$ | Day-ahead market price |
| $c^{FCR}$ | FCR price |
| $c^{fees}$ | Taxes, levies and fees |
| $c^{ID}$ | Intraday market price |
| $c^{peak}$ | Annual capacity price |
| $cap^{BSS}$ | Capacity of the BSS |
| $cap^{FCR}$ | Capacity blocked for FCR activities |
| $cap^{PV}$ | PV system capacity |
| $cost$ | Total cost |
| $d$ | Production load |
| $EF$ | Dynamic emission factor |

| | |
|---|---|
| $FCR$ | Frequency containment reserve |
| $m^{CO2}$ | Amount of $CO_2$-emissions |
| $P^{BSS,prod}$ | Power flow from BSS to production |
| $P^{FCR}$ | FCR power provided |
| $P^{grid,BSS}$ | Power flow from the power grid to the BSS |
| $P^{grid,prod}$ | Power flow from the power grid to production |
| $P^{grid}$ | Power flow from and to the power grid |
| $P^{peak}$ | Annual peak load |
| $Pcap^{BSS}$ | Maximum power capability of the BSS |
| $r^{FCR,puff}$ | FCR buffer factor |
| $u$ | Unserved load |
| $u^{VoLL}$ | Penalty term for unserved load |
| $x^{BSS,prod}$ | Power flow from BSS to production |
| $x^{grid,BSS}$ | Electricity flow from the power grid to the BSS |
| $x^{grid,in}$ | Electricity flow from the power grid |
| $x^{grid,prod}$ | Electricity flow from the power grid to production |
| $x^{grid}$ | Electricity flow from and to the power grid |

### Indices

| | |
|---|---|
| $h$ | Hour |
| $n$ | Nodes of the scenario tree |
| $q$ | Quarter-hour |
| $s$ | Two-stage scenario |
| $sc$ | Multi-stage scenario |
| $w$ | Week |

### Sets

| | |
|---|---|
| $H$ | Set of hours considered |

| | |
|---|---|
| $Q$ | Set of quarter hours considered |
| $S_{\gamma arb}$ | Set of nodes on the arbitrage decision level |
| $S_{\gamma fcr}$ | Set of nodes on the FCR decision level |
| $S$ | Set of the two-level scenarios considered |
| $N$ | Set of nodes of the scenario tree |
| $W$ | Set of weeks considered |

# List of Figures

# List of Tables

# Part I

# Framework

# 1 Introduction

## 1.1 Motivation and research question

The Paris Agreement of 2015, which aims to limit global warming to 1.5 degrees, has set ambitious emissions targets. At the national level, these targets are driving the transformation of the conventional energy system to one dominated by renewable energy sources (RES). Here, largely weather-dependent RES plants are replacing dispatchable energy supply from conventional power plants. The removal of these dispatchable, conventional generation units means that the role of flexibility measures in the power system becomes more significant (Lund et al. 2015). Flexibility measures can shift and match electrical load and generation in a power system over time. This is achieved by either temporarily storing electricity in various forms (e.g. a battery storage system) or by reducing or avoiding electricity generation or consumption. In this way, congestions in the power grid can be avoided (Ruppert et al. 2020), the share of RES in the system can be increased (Gils 2014), and $CO_2$-emissions can be reduced (Jochem et al. 2015). Various approaches in Germany and the European Union (EU) aim to promote the provision of flexibility. Among other things, flexibility can be offered as balancing reserve power or for arbitrage trading[1] on energy markets. The extent to which incentives are sufficient to provide the appropriate level of flexibility for the power system depends on technical and economic factors.

This thesis analyses the use of a battery storage system (BSS) as a key flexibility measure in the transformation process of the energy system. A BSS stores electricity in chemical form and can provide flexibility on both the load and generation sides. Especially in the case of BSS based on lithium-ion technology (Li-ion technology), their flexibility potential is determined by their technological attribute of being able to provide relatively high amounts of electrical power and energy in a relatively short time compared to other battery technologies (Stadler et al. 2014, p. 605). This attribute makes the BSS suitable for various flexibility marketing options at the same time. This flexibility potential can be additionally increased if the BSS is combined with an electrical consumer such as a household or an industrial plant. Through

[1] In this paper, the term arbitrage trading describes the exploitation of temporal price differences and price differences between different energy markets. The term is guided by the definition and application in Walawalkar et al. (2007, p. 2599), Sioshansi et al. (2009, p. 270), Bradbury et al. (2014, p. 513), Sakti et al. (2017, p. 284), and Campana et al. (2021, p. 2). Brealey et al. (2011, p. 327) points out, however, that in the textbook definition arbitrage trading takes place without risk, but in practice they usually involve risk. This is also true for the time arbitrage of this paper, which is also described by Next Kraftwerke GmbH (2022) as “quasi-arbitrage trades”

this combination, additional flexibility can be offered by shifting the load (peak shaving) or optimising the consumption of self-generated electricity.

Especially in industry, there is a "significant potential" (Stede et al. 2020, p. 2) to introduce flexibility into the energy system through load shifting. Paulus and Borggrefe (2011, p. 440) estimate that flexibility measures of industrial processes in Germany could "provide approximately 50% of capacity reserves for the positive tertiary balancing reserve market in 2020" and Stede et al. (2020, p. 111893) calculate an industrial load reduction potential between 3.8% and 5.5% of the peak load in Germany. The fact, that most industrial companies have an active energy management system favours the implementation of flexibility measures. However, process flexibility goes along with high activation cost (Müller and Möst 2018, p. 191) and flexibility measures must not result in loss of production (Gruber 2017, p. 133). Installing a BSS at an industrial company allows the company to offer energy flexibility to the system without affecting the production process (Materi et al. 2021, p. 677).

From a business perspective, a BSS can contribute to reducing the energy costs and simultaneously lowering $CO_2$-emissions of an industrial operation (Figgener et al. 2020). However, three attributes complicate the economical evaluation of a BSS operation[2], despite falling BSS prices[3]: firstly, the various marketing opportunities for the energy stored in the BSS; secondly, the heterogeneous load behaviour of many industrial operations; and thirdly, the technical characteristics of a BSS. In addition, for an economic investment in a BSS, it is important to consider the uncertainties about the future behaviour of market prices and electrical load.

In this context, this thesis investigates the techno-economically optimal investment and dispatch of battery storage systems (BSS) in industrial plants, addressing the following research questions:

1. What influence does the consideration of different revenue streams, offering frequency containment reserve, peak shaving, arbitrage trading and optimised self-consumption, have on the economic performance of a BSS in an industrial plant?
2. What influence do uncertainties regarding market prices, electrical load and self-generation have on the economic performance of a BSS in an industrial plant?
3. What is the influence of optimised dispatch of a BSS in an industrial plant on the plant's $CO_2$-emissions?

To answer these questions, a discrete linear optimization model is developed to minimize the overall energy costs of an industrial manufacturing site with the option to invest in a BSS. The capacity and dispatch of the BSS is a model endogenous decision variable. For the model calculations, mainly German market prices for the day-ahead, intraday and frequency containment

[2] Sandia National Laboratories (2022) shows a relative stagnation of the worldwide installed capacity of Li-ion BSS compared to other electrochemical storage technologies in terms of large-scale battery storage systems.

[3] For example, according to Eble (2021), prices for large BSS fell by a third between 2015 and 2021.

reserve markets as well as German grid charges are considered. As exogenous load parameters, the studies are applied to 50 real industrial load profiles. The load profiles are the recorded power demand of manufacturing plants of small- and medium-sized enterprises in 15-minute time steps, continuous for one year. To consider uncertainties, the discrete model is extended to a two-stage robust optimisation model, a two-stage stochastic and a multi-stage stochastic optimisation model. The value of the uncertainty consideration is shown by comparing the results of the respective optimisation models.

## 1.2 Structure of the thesis

This thesis is written as a cumulative dissertation and includes the publications listed below. The thesis is structured in such a way that Part I sets the thematic framework and explains the basics to discuss the publications. In Part I, Chapter 2 highlights the technological and economic framework for the use of a BSS in industry. Chapter 3 gives an overview of the methodologies used in the publications. Chapter 4 summarises the results of the publications. Chapter 5 provides a critical review of the results, and chapter 6 concludes Part I with an overall summary of the thesis. Finally, Part II recites the publications that are considered in this thesis, which are the following:

**Publication A** (Braeuer et al. 2019b)
F. Braeuer, J. Rominger, R. McKenna, W. Fichtner. Battery storage systems: An economic model-based analysis of parallel revenue streams and general implications for industry. *Applied Energy*, 239:1424–1440, 2019. doi:10.1016/j.apenergy.2019.01.050 .

**Publication B** (Covic et al. 2021)
N. Čović, F. Braeuer, R. McKenna, H. Pandžič. Optimal PV and battery investment of market-participating industry facilities. *IEEE Transactions on Power Systems*, 36: 3441–3452, 2021. doi:10.1109/TPWRS.2020.3047260 .

**Publication C**
F. Braeuer, M. Ruppert, W. Fichtner. Stochastic optimization of battery storage investment in industry – Comparing a two-stage and multi-stage approach. Submitted to *Annals of Operations Research* on 05/05/2022.

**Publication D** (Braeuer et al. 2020)
F. Braeuer, R. Finck, R. McKenna. Comparing empirical and model-based approaches for calculating dynamic grid emission factors: An application to $CO_2$-minimizing storage dispatch in Germany. *Journal of Cleaner Production*, 266:121588, 2020. doi:10.1016/j.jclepro.2020.12 .

Figure 1.1 shows the relationship between the publications considered and the research questions. In addition, the figure depicts the relationship between the models used in the publications.

***Publication A*** addresses the first research question. The consideration of the different revenue streams requires a systematic techno-economic approach. For this purpose, a deterministic, linear optimisation model is developed for the design of a BSS in an industrial manufacturing plant. The BSS has the option of offering frequency containment reserve (FCR), arbitrage trading on the day-ahead or intraday market, or reducing the charges for the annual peak load by peak shaving. The optimisation model developed in Publication A, which optimises a BSS in industry (BSS-Opt model), is the basis for all further publications used in this thesis.

***Publication B*** extends the BSS-Opt model and includes a further technology and marketing option with self-generation from a photovoltaic system (PV system). In addition, Publication B illuminates the second research question and maps uncertainties in the optimal decision by adding a stochastic and a robust component to the BSS-Opt model. For this purpose, a two-stage stochastic optimisation approach is developed to design a BSS together with a photovoltaic (PV) system in an industrial plant. A robust optimisation formulation is integrated into this approach. This evaluates the stochastic market and load behaviour as well as the uncertainty about the market success on the intraday market.

***Publication C*** builds on this and develops the BSS-Opt model into a multi-stage stochastic linear problem. Publication C compares the multi-stage with a two-stage approach in the analysis. Through the comparison, the influence of a sequence of uncertain prices and decisions on the design and economic efficiency of a BSS can be examined in more detail. This allows the inaccuracies in the comparison of the approaches to be highlighted, as well as the importance of the sequence of uncertain market decisions.

***Publication D*** answers the third research question and explores the possible trade-off between an ecological and economic charging strategy. For this purpose, Publication D compares different $CO_2$-emission factors of German electricity generation. Based on the BSS-Opt model, the paper investigates the differences between profit-maximising and $CO_2$-emission-minimising battery operation.

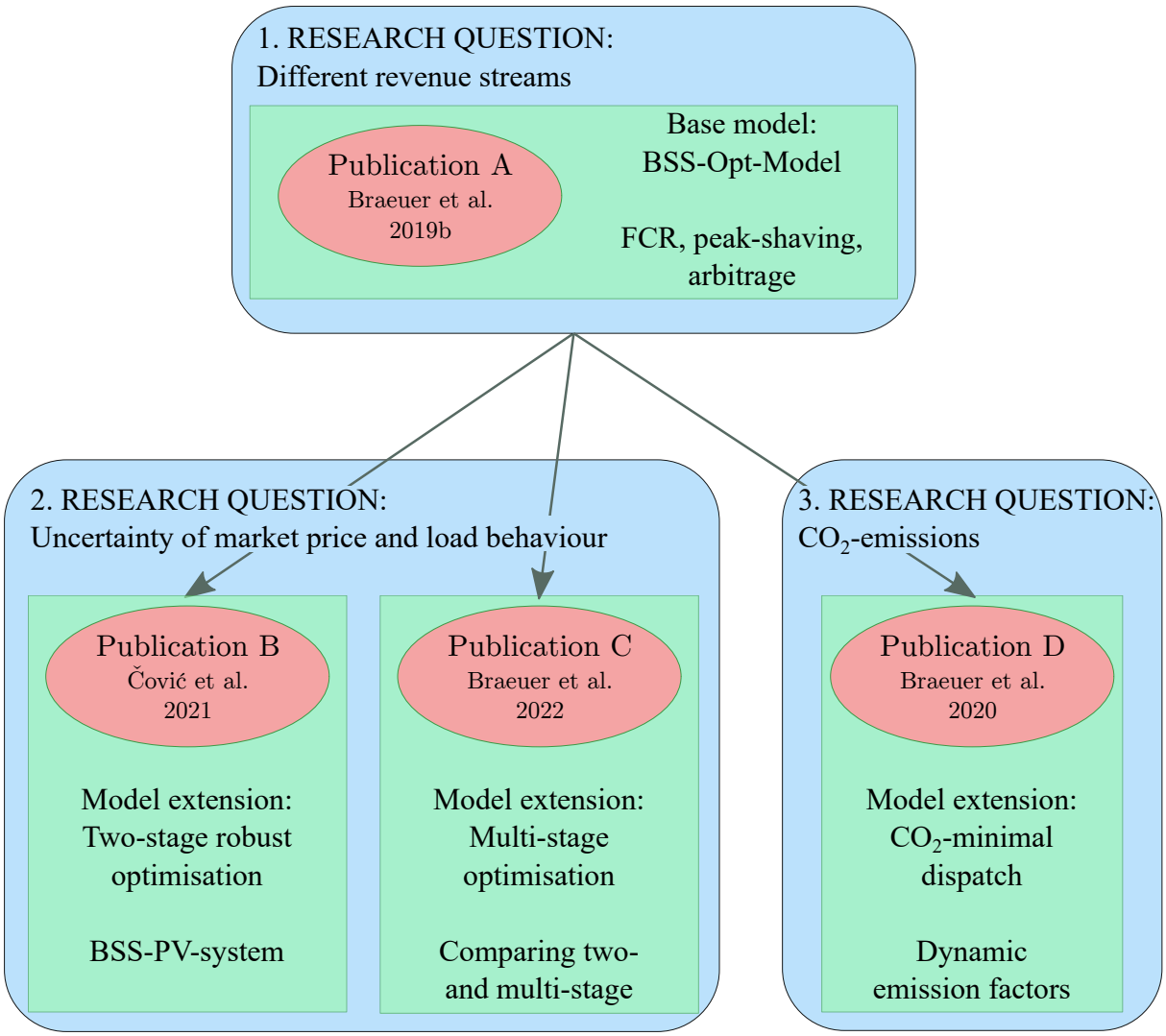


**Figure 1.1:** Graphic representation of the relationship between the considered publications, the research questions and the model extensions

.

# 2 Background

This chapter explains the basics for understanding investment and dispatch planning[1] for a BSS in an industrial company. The first Section 2.1 shows the thematic framework, in which this thesis is located. The subsequent Section 2.2 summarises the technical characteristics of a BSS, which enable the BSS to offer flexibility for the energy system. Section 2.3 explains how the transformation of the German energy system will increase the need for flexibility, and which flexibility markets and products already exist to address this need. Section 2.4 concludes the chapter by highlighting the regulatory framework and market structures in Germany to provide flexibility from the perspective of an industrial customer.

## 2.1 Thematic framework

This section highlights the thematic framework of investment and dispatch planning of energy flexibility measures. The research focus in this framework includes both a technical and an economic component. In addition, since investment periods in most cases last several years, this framework includes a long-term perspective. In contrast, research that focuses primarily within a short-term time frame on storage or battery management, system controls, energy management, or bidding strategies is not included. The following explanation of the framework does not claim to be exhaustive.

To give the reader a notion of the manifold possibilities to view this topic, this section introduces three relevant dimensions to describe the thematic framework. The first dimension to consider, Section 2.1.1, is the different flexibility measures that could be used to store energy or allow for flexible energy generation or consumption. The second dimension, Section 2.1.2, is the location where the flexibility measures are installed. The third dimension, Section 2.1.3, describes possible applications, use cases and revenue streams for flexibility measures.

[1] Other terms used in the scientific literature are capacity and dispatch planning, as well as design and dispatch planning.

### 2.1.1 Flexibility measures

The first dimension of the thematic framework describes the flexibility measures. In the context of this thesis, flexibility measures include technological installation as well as structural or organisational changes from a micro-economic perspective. They allow for a temporal or spatial shift of electricity consumption. The selected flexibility measure sets the technological constraints for operation and the price of the investment, which both need to be considered to assess the economic potential. This thesis distinguishes five different types of flexibility measures explained in the following:

- Lithium-ion BSS,
- other BSS,
- other storage technologies,
- sector coupling technologies, and
- organisational flexibility.

Lithium-ion (Li-ion) BSS are the main focus of this thesis and are discussed in detail in Section 2.2. However, the market for Li-ion BSS presents multiple types of battery cells, which mostly vary in their chemical composition. Nevertheless, these types differ in their technological attributes such as calendar or cycle life[2], charging curve, thermal operation conditions and hazardous assessment of operation. For stationary applications, the size or the power density of the different battery cells plays a minor role. As the different Li-ion BSS present varying states of maturity, the markets offer a large range of prices.

The category of other BSS includes systems, such as the sodium sulphur (NaS) battery or the redox flow battery, as described in IRENA (2017, p.36). The main characteristics where these systems differ are their reaction time, power density and energy density. NaS BSS and redox flow BSS are suitable for long-term storage applications of more than one day (Al-Humaid et al. 2021, p. 162963) as they present longer reaction times than Li-ion batteries. Both systems are installed in relatively large sizes compared to Li-ion batteries. In particular, the NaS battery offers very low discharge rates but coincides with high operational costs as sodium and sulphur are stored in liquid form at high temperatures. For redox flow systems, the cycle life is no concern (Tohidi and Gibescu 2019, p. 556) and the energy capacity can be expanded by increasing the tank size storing the electrolyte. This is an economic advantage (IRENA 2017, p. 87). The disadvantages are the relatively low efficiency and high system cost compared to the Li-ion BSS.

[2] For an explanation of battery parameter, please refer to Section 2.2.2. The parameter definitions for BSS can be adapted to explain other flexibility measures as well. Briefly, calendar life describes the number of years until the end-of-life condition of the flexibility measure is reached. Cycle life describes the number of full charging cycles until the end-of-life condition is reached.

The category of other storage technologies utilises an electro-mechanical storage principle, such as flywheels, pumped water storage or compressed air storage. The flywheel storage system has a very short reaction time and high power density. Compared to a Li-ion BSS, it has a long lifetime, almost no cycle life limitations or degradation effects (Choudhury 2021). However, IRENA (2017, p.61) name its low energy density and high self-discharge rate as a disadvantage. Pumped hydro storage or the compressed air storage system, the latter is "less proven at a commercial scale" (Jones et al. 2021, p. 1), are considered large-scale storage systems. They function as power storage as well as energy storage with a long life and "long storage periods" (IRENA 2017, p. 51). Nevertheless, pumped hydro storage requires a high initial investment and long construction time. Both systems depend on geographic conditions. These conditions are restrictive, as pumped hydro systems need space for a reservoir and a height gradient, and compressed air systems require a cavern or a large body of water[3].

The category of sector coupling technologies or power-to-x technologies summarises another set of flexibility measures, where electricity is converted into a second energy carrier such as heat, cold, or hydrogen or used for other means such as mobility in electric vehicles. In most cases, this limits some revenue streams, as electricity is not fed back into the grid. At the same time, sector coupling offers additional revenue streams, as hydrogen can be used as process gas in industry, heat can be used for process heating in industry or space heating in residential and commercial buildings.

Finally, the category of organisational flexibility or "functional energy storage" (Gruber 2017, p. 1) describes a flexible operational mode of electricity consumers. In industry, this could be executed through variation of the process schedule, flexible stock planning or a behavioural change of the machine operators (Behrens et al. 2022, p. 633). In the commercial and residential sector, the process flexibility is limited compared to the industry sector but could be achieved through temperature variation in heating and cooling systems or a temporally delayed operation of devices. Nevertheless, these measures differ in terms of activation time, activation cost and the individual must-run conditions of the processes. For most of the organisational flexibility measures, cycle life is an issue, as interrupted processes or a reduced operation influence the durability of the process materials.

### 2.1.2 Flexibility location

The second dimension describes the location of the flexibility measure, as the optimal investment and dispatch decision depends on the chosen location. Therefore, the flexibility measure can either be installed:

[3] Underwater compressed air storage systems store compressed air in capsules underwater at the ground of a lake or an ocean. The air pressure is the same as the underwater pressure storing air at an isobaric state. Nevertheless, this technology should be considered relatively immature (Budt et al. 2016, 265).

- at an industrial manufacturing plant,
- in a commercial building,
- in a residential home or area,
- at a power plant, or
- directly at grid level.

This thesis studies the industrial sector as the flexibility location. However, industrial manufacturing plants are heterogeneous in terms of size, peak electricity demand, load behaviour and predictability of load changes. Even within the same industrial branch, the load behaviour of different companies can differ significantly (Nystrup et al. 2021, p. 2). The individual energy demand depends, for example, on the organisational structure, the production design, order situation and capacity utilisation of the business. Comparing single companies, the economic potential may also depend on individual energy contracts, tariffs, grid access, or choice of energy carrier.

With a lower energy demand, the commercial sector offers various use cases for flexibility measures (Campana et al. 2021). Commercial buildings such as supermarkets usually have a high demand for cooling energy in their food storage, while hotels require space heating and cooling as well as process heat for hotel laundry. Moreover, delivery services may employ a fleet of electric vehicles. Additionally, many commercial buildings offer idle space for the installation of PV on rooftops. However, in many commercial businesses, energy cost plays a significant role and energy cost reduction affects the overall business performance. This is to the economic advantage of flexibility measures.

The residential sector shares some characteristics with the commercial sector. A sector coupling potential exists as well because residents require electricity, heating, cooling and mobility. Furthermore, a self-generation potential exists through PV or solar panels on rooftops. Nevertheless, available electricity tariffs or grid charges may differ compared to the industry sector and commercial sector. Additionally, the ownership structure, especially in multifamily residential buildings, may diminish the flexibility potential (Braeuer et al. 2019a).

The sight of a power plant as a location for flexibility measures represents a different case to the former three locations, as only electricity generation and no consumption plays a role. In this regard, the flexibility measure can either be part of a virtual power plant[4] or be integrated into the operation of a conventional power plant. Integrating a storage system into a virtual power plant allows the operator to not just sell electricity on the electricity markets, but also provide ancillary services. Integrated into a conventional power plant, the storage system allows for a

[4] Virtual power plants describe the centralised, aggregated management of decentralised generators and consumers (Naval and Yusta 2021)

more steady operational mode, most relevant for fluctuating peak load power plant operations such as open cycle gas turbines. The steady operation mode increases the duration of the turbine and decreases the $CO_2$-emissions while expanding electricity marketing options.

Finally, among the considered flexibility measures, installation at grid level mainly aims at storage systems and sector coupling technologies. The systems may be operated by the grid operator, a power plant operator or an independent third party. Such systems may defer or even avoid grid expansion at the distribution or transmission level. In this case, the storage system locally offers generation or consumption capacities in times of high grid utilisation, thus, relieving possible grid congestions. Additionally, such systems improve resource adequacy through long-term energy storage for more than a day, week, or month. The systems are also well suited for the provision of ancillary services.

### 2.1.3 Flexibility application

The final dimension describes possible applications, revenue streams and use cases for flexibility measures and storage operations. Its applicability and economic performance depend on the chosen flexibility measure as well as the location of said measure. The nine categories of this dimension cannot be clearly separated from each other, as there are various intersections between individual categories. For this thesis, the flexibility applications are categorised as follows:

- Balancing ancillary services,
- energy spot market trading,
- grid charge reduction,
- optimised self-consumption,
- non-frequency ancillary services,
- power quality and reliability,
- resource adequacy,
- optimised plant operation, and
- optimised grid operation.

The first four categories are extensively studied in this thesis and, therefore, addressed in detail in Section 2.4. First, balancing ancillary services categorise activities on the balancing reserve markets such as frequency containment reserve (FCR), automated frequency restoration reserve (aFRR), or manual frequency restoration reserve (mFRR). Multiple flexibility measures can provide balancing ancillary services at all considered locations. The category of energy markets describes first of all activities on all the electricity markets, a revenue stream applicable to all

flexibility measures and locations, but furthermore addresses markets for other energy carriers relevant for sector coupling technologies (Zare Oskouei et al. 2021). The category of grid charge reduction aims at all activities that reduce grid charges, such as peak shaving or peak shifting. It applies only to the industrial, residential or commercial location. Such is the category of optimised self-consumption. Here, the flexibility measure optimises or increases the consumption of self-generated electricity through PV or combined heat and power (CHP) plants.

Compared to the first categories, the following categories are less standardised and the business models behind these applications are more heterogeneous and less mature. The markets for these applications are less transparent, and the economic evaluation of the delivered services is challenging, i.e. some applications are not directly linked to earnings or revenue streams.

Non-frequency ancillary services are described in Subsection 2.4.4. Among these services, at least for the reactive power provision and black start capability, a transparent and non-discriminatory market is to be created. BSS or flywheels are particularly suitable for these cases regardless of location, especially, due to their self-sufficient operation. Furthermore, such non-frequency ancillary services play an important role in isolated, decentralised power grids as they lack the physical attributes of large conventional energy systems.

The category of power quality and reliability is a special use case for the industrial sector, but may also inflict on the residential and commercial areas. This use case is also addressed by uninterruptible power supply (UPS) systems, which are usually combined with a storage unit (Zhao et al. 2021). Mainly, it addresses the issue of manufacturing processes, facilities, or devices that react highly sensitive to frequency or voltage deviations (Tang et al. 2022, p. 208). In these cases, a BSS is well suited to guarantee a stable power supply with few frequency and voltage deviations. Power reliability includes risk mitigation measures against power outages, mostly through backup generators, BSS, or hydrogen CHP.

Resource adequacy as a category mainly describes the perspective of a regional or national energy system planner to guarantee sufficient energy supply during all times of a year[5]. Fitzgerald et al. (2015, p. 16) describe resource adequacy as the means “to incrementally defer or reduce the need for new generation capacity and minimise the risk of overinvestment in that area”. By installing flexibility measures in different locations, investments in generation capacities such as open cycle gas turbines to match inelastic peak electricity demand might be avoided. Thereby, the cost of the energy system could be reduced. Nevertheless, in absence of capacity mechanisms for other technologies but conventional power plants (Bublitz et al. 2019), resource adequacy should be viewed as a secondary benefit of electric market activities of flexibility measures, since it is not directly remunerated.

[5] Article 23, Paragraph 1, regulation 2019/943 of the European Parliament and of the council of 5 June 2019 on the internal market for electricity defines the adequacy assessment to assess “the overall adequacy of the electricity system to supply current and projected demands for electricity”.

Integration of flexibility measures, mostly storage systems, into a power plant fosters operation flexibility, which improves economic, emission and technological aspects of the plant operation, as indicated by Bulut and Özcan (2021). The authors show that combing a natural gas power plant with a BSS prolongs the health of the equipment, generates higher revenues and lowers $CO_2$ emissions. In a thermal-driven CHP, a BSS allows for a more flexible electricity marketing strategy (Rouzbahani et al. 2021). Nevertheless, a larger number of system components requires higher coordination efforts among these components. In this regard, Rouzbahani et al. (2021) review virtual power plant concepts, where storage systems are an integral part, and discuss different scheduling methods.

Finally, the category of optimised grid operation defines measures that relieve strain on the grid and defer grid investments. As studied by Richter and Porst (2022), in Germany grid operators usually own such flexibility measures[6]. Because of the European unbundling of the electricity market, a grid operator-owned storage system would not be allowed to offer its service on any other market. The profitability of such a system can only be estimated considering the grid operation as a whole, as the storage operation defers otherwise needed grid investments (He et al. 2021). Other marketing concepts are possible, where grid operators offer monetary incentives for owners of flexibility measures to support an optimised grid operation. However, a "well-functioning remuneration system is crucial for successful implementation" (Brinkel et al. 2022, p. 8).

### 2.1.4 Further considerations

The previous subsections show how the selected flexibility measure and its technological constraints define for what application such measures might be feasible. An economically successful operation depends on the location, which influences the flexibility potential, and what revenue streams are associated with the respective application. Nevertheless, this highlights only a section of the overall thematic framework. The following elaborates on further considerations in this field.

Potential revenues additionally depend on geographical attributes. Different regions or countries may apply other legal regulations and incentive schemes, or present other market conditions, concerning competitors, prices, or entry barriers. The climatic conditions may also differ, which results in varying self-generation potential through PV and may also affect the sector coupling potential as heating demand changes. Geographical features define the sector coupling potential, as pumped hydro and compressed air storage systems require certain geo-conditions and

[6] In line with directive 2019/944 of the European Parliament and of the Council of 5 June 2019 on common rules for the internal market for electricity, the German parliament changed legislation to allow grid operators to own and operate storage systems for congestion relief, so called "Netzbooster" (Bathke 2021). The transmission grid operator plans to run such a sight in the South of Germany by the year 2026 (TransnetBW 2021).

conversion to hydrogen or e-mobility depends on the connectivity to other energy and transport infrastructure. Sector coupling and organisational flexibility consideration also include local societal characteristics as a variation of heating, driving, or working patterns that coincide with behavioural changes and require a high level of social acceptance.

From a business perspective, multiple approaches exist to evaluate the economic efficiency of an investment. Most commonly used among company decision makers are the usage of the net present value (NPV) and the internal rate of return (IRR) (Brealey et al. 2011, p. 104). Both approaches consider the time value of money, the projected future cash flow and the opportunity cost of capital. The NPV subtracts the discounted cash flow over the investment period from the initial investment. The IRR describes the discount rate when the NPV would be equals zero. Both approaches yield similar results, but the IRR method "can also be a misleading measure" (Brealey et al. 2011, p. 108). The calculation of the equivalent annual cash flow is a variation of the NPV method, most appropriate if the annual cash flow is constant. A way to consider the financing situation of companies in the decision process is by using the weighted average cost of capital (WACC) instead of the estimated opportunity cost of capital. Additionally, some decision makers calculate the payback period without discounting future cash flows, ignoring the time value of money or the discounted payback period with the discounted cash flow. The payback period defines the time until the cumulated cash flows surpass the initial investment. However, both payback period approaches ignore cash flows occurring after the payback period and should not be used isolated without other investment measures.

Finally, for the identification of the optimum BSS investment and dispatch, various methods can be applied. These methods also consider uncertain market and load behaviour in multiple ways. Section 3 summarizes the different methodological approaches.

### 2.1.5 Categorisation of this thesis

With its quick reaction time and relatively long storage periods, the Li-ion BSS is well suited to serve multiple short- and medium-term applications simultaneously. Installed at an industrial site, the BSS is asserted with a high flexibility potential. It is the focus of this thesis to better understand the techno-economic evaluation of such flexibility measures and to answer the in Section 1 raised research questions. Therefore, within the thematic framework, this thesis focus lies on Li-ion BSS as a flexibility measure located at an industrial manufacturing plant. The BSS's applications are balancing ancillary services, energy markets, grid charges and optimised self-consumption.

The Li-ion technology has reached a high level of maturity, and multiple large-scale stationary BSS already exist globally. Therefore, broad knowledge of its technical attributes and its system prices exists. The market for Li-ion BSS indicates fewer price variations than markets of immature

storage technologies. Additionally, the BSS technology is independent of geographic conditions and can be installed in a variety of sights in the same manner.

By itself, a BSS system, connected at grid level, can serve the balancing reserve market as well as trading electricity on the energy markets. The combination with an industrial manufacturing plant allows the inclusion of two additional applications, reduction of grid charges and the optimised self-consumption of self-generated electricity. For this thesis, the options for the BSS operator are to offer FCR, do arbitrage trading on the day-ahead and intraday electricity market, reduce the peak load to avoid grid charges, and optimise the consumption of self-generated PV electricity.

This thesis' focus is on the German national level. It partly neglects specific legal, regulatory, and economic conditions, such as market entry conditions, metering operation conditions, specific fees and taxes, as well as ownership and financing conditions. The objective of the thesis' optimisation model is to minimise the equivalent annual cash flow. The optimisation approach simplifies energy management system constraints as well as the control system constraints of a real-life BSS operation.

## 2.2 Battery storage systems

This section highlights the technological characteristics and specific attributes of BSS, with the main focus on Li-ion BSS. First, the basic principle of a Li-ion battery cell is explained. Second, for this thesis, the most relevant battery parameters are introduced. The final subsection lists the main Li-ion battery types and gives an overview of the Li-ion battery market.

According to the Sandia National Laboratories (2022) database, Li-ion storage systems currently account for around 26% of the world's installed large-scale electrochemical storage capacity. Li-ion technology is characterised by "large specific energy, large specific power, high charging and discharging efficiency and low self-discharge" (Korthauer 2013, p. 15). A comprehensive insight into Li-ion technology is provided for example by Jossen and Weydanz (2006), Korthauer (2013), Julien et al. (2016), Kaschub (2017) and Maiyalagan and Elumalai (2021). For information on other battery technologies, please refer to Jossen and Weydanz (2006), Wietschel et al. (2015) and Kularatna and Gunawardane (2021), among others.

### 2.2.1 Basic principle

BSSs are composed of individual battery cells. In battery cells, chemical energy is converted into electricity through an electrochemical process. Secondary batteries, also called rechargeable batteries or accumulators, have the important property that they can reverse this electrochemical process and thus absorb and release electricity through charging and discharging. One of these

secondary batteries is the Li-ion battery, whose significance, driven by its use in electric vehicles, has also increased in the energy industry.

The functional principle of the Li-ion battery cell as for all electrochemical processes is based on the reduction and oxidisation of two electrodes, also named redox reaction. During oxidisation, one electrode emits an electron, which in the reduction process is attached to the other electrode. In the Li-ion battery, the electrodes are comprised of Lithium compounds. Since Lithium has an "extremely low electrode potential ($-3.04\ V$ vs. standard hydrogen electrode)" (Xie and Lu 2020, p. 1), Li-ion battery cells can reach a rated voltage of up to $4\ V$, dependent on the other compound elements. Compared to Lead-acid battery cells with a rated voltage of around $2\ V$, the Li-ion battery cells exhibit relatively high energy densities.

According to Choi et al. (2021, p. 7), Kurzweil (2020, pp. 143-145) and Kaschub (2017, pp. 48-49), in the Li-ion battery cell, lithium atoms are embedded in the active materials of the two electrodes. The two electrodes are separated by a porous separator, which is surrounded by a liquid electrolyte[7]. During the charging and discharging process, one lithium atom at a time is ionised through oxidisation by releasing an electron. These Li-ions are carried from one electrode to the other by the ion-conducting electrolyte, while the released electron travels across the conductors applied to the electrodes. Arriving at the other electrode, the Li-ions are reduced, taking up the electron again, and are neutralised. When discharging, the Li-ions are released from the negative electrode, also called the anode, and flow to the positive electrode, the cathode. When charging, the process is reversed.

To make use of the energy and power of the individual battery cells, they are connected in series or parallel and assembled in a BSP. The correct composition of these battery cells in a BSS should ensure "efficient, reliable and safe operation of the energy storage system over a very long period of time" (Korthauer 2013, p. 95). Here, it is necessary to regulate the mechanical, electronic and thermal characteristics of battery operation, as well as to establish communication between cells within a BSS and to the outside. For stationary use, the battery cells are usually combined into *modules* [8], which in turn are assembled as *racks*. These are assembled in containers or even buildings, depending on the desired performance and capacity. For safe, efficient and gentle operation, a coordinated thermal and electrical control is required at the level of the individual cells, the module, the rack and the overall system, as also described in Hesse et al. (2017) and Lawder et al. (2014). Here, the battery management system (BMS) constantly monitors the voltage, current, and temperature at the cell level and ensures charge equalisation between the individual cells. The thermal management system at all levels stabilises the temperature of the battery cells to ensure safe and long-lasting operation. Moreover, the thermal and electronic

[7] In the case of the solid-state battery, the electrolyte does not occur in a liquid state, but in a solid state, so that the use of a separator is not necessary.

[8] "In the case of large stationary lithium storage systems, current concepts pursue a modular design of individual cells connected in parallel and series to be able to meet the necessary energy and performance requirements" (Korthauer 2013, p. 424).

control is controlled by the higher-level energy management system, which also includes the power electronics for connecting the BSS to the power grid. For the case studies of this thesis, the BMS is not further investigated, but an efficient BMS is assumed.

### 2.2.2 Battery parameters and battery ageing

To make the decisive battery properties comprehensible, it is necessary to define the most important battery parameters. Here, we refer to the definitions according to Fischhaber et al. (2016, p. 29) or Petrovic (2021, pp. 21-22) and assume the energy units for energy in $kWh$ and power in $kW$. The *capacity* of a BSS is given in $kWh$. Some manufacturers and scientific publications distinguish between *nominal capacity* and *usable capacity*. The useful capacity is smaller than or equal to the nominal capacity. The difference between these two values describes the part of the nominal capacity that is not used for safety and ageing reasons. In this work, it is assumed that the useful capacity is equal to the nominal capacity. The *state of charge* or *SOC* of a BSS describes the relationship between the charged amount of energy and the useful capacity. The SOC usually quantifies the charge ratio as a percentage, but can also be specified as an absolute state of charge in $kWh$, if applicable. The *Depth of Discharge* or *DoD* indicates what proportion of the available energy in the BSS is discharged during a discharge process and ranks between 0%, no discharge, and 100%, complete discharge.

The *charging rate* or *C-rate* indicates how fast a BSS is completely discharged. Roughly, the parameter can be calculated as the ratio between discharge power and useful capacity, but it is dimensionless. With a C-rate of 1, the BSS is completely discharged within one hour, with a C-rate of 2, only 30 minutes are needed and with a C-rate of 0.5, again 2 hours. The *life* of a battery cell is distinguished between a *cycle* life and a *calendar* life. The cycle life is described in this context as the achievable number of *equivalent full cycles* until the end of life of the battery cell. An equivalent full cycle is "generally understood to be a charge throughput twice the nominal capacity" (Fischhaber et al. 2016, p. 32). The calendar life describes the duration in months or years until the end of life is reached. The end of life in turn is described by the *End-of-Life-criterion* (EoL). The EoL indicates in percent what proportion of the nominal capacity is still available as useful capacity at the end of the service life. If the EoL criterion is reached, it can be assumed that the BSS deviates from the original operating behaviour and that the intended application can no longer be adequately served (Kaschub 2017, p. 51). Often, a residual capacity of 80% is assumed[9], but lower values may be possible, especially in the stationary sector (Kaschub 2017, p. 52). Overall, the real EoL depends strongly on the "subjective" mode of operation (Fischhaber et al. 2016, p. 35).

[9] "In the "Electric Vehicle Battery Test Procedures Manual" of the USABC, an EoL = 80%, which is to be understood merely as a rough guideline value, was first stated in 1996. This value is still adopted or only slightly varied in almost all publications today" (Fischhaber et al. 2016, p. 35). Moreover, Petrovic (2021, p. 22) and Choi et al. (2021, p. 13) name 80% as the EoL criterium for many batteries.

### 2.2.3 Charging and discharging behaviour

The charging and discharging process of common secondary battery cell types depends on various parameters, such as current or C-rate, voltage, or temperature. For a better understanding of the operational behaviour of battery cells, Figure 2.1 illustrates the discharging current and voltage curve of a hypothetical battery cell. According to Petrovic (2021, pp. 30-31), Figure 2.1 depicts three operational modes, the constant power, constant current and constant resistance mode. The solid line in Graph (a) shows a constant current for the full discharge of the battery. Corresponding in (b), the solid line indicates the voltage behaviour during discharge in constant current mode. The voltage curve can be divided into three phases, a steep decline at the beginning of the discharging process, a linear decline during the majority of the process and another steep decline at the end. Overall, the voltage decreases because the amount of active material in the anode is reduced through oxidisation. This leads to a lower potential difference between the two electrodes, as charges move from anode to cathode. Finally, lower electrode potential results in lower voltage. The steep decline at the beginning is attributed to the activation overpotential that starts the reaction process and that is needed to overcome kinetic limitations (Kasnatscheew et al. 2016). The steep decline at the end indicates, that no further active material exists for the reaction.

For the other two operational modes, the curves can be deducted from the electro-technical relationship of voltage, current, resistance, and power. For constant power, the product of voltage and current, a decreasing voltage requires an increase in current for the product to be constant. For the constant resistance, the quotient of voltage and current requires a decreasing current to compensate for lower voltage levels.

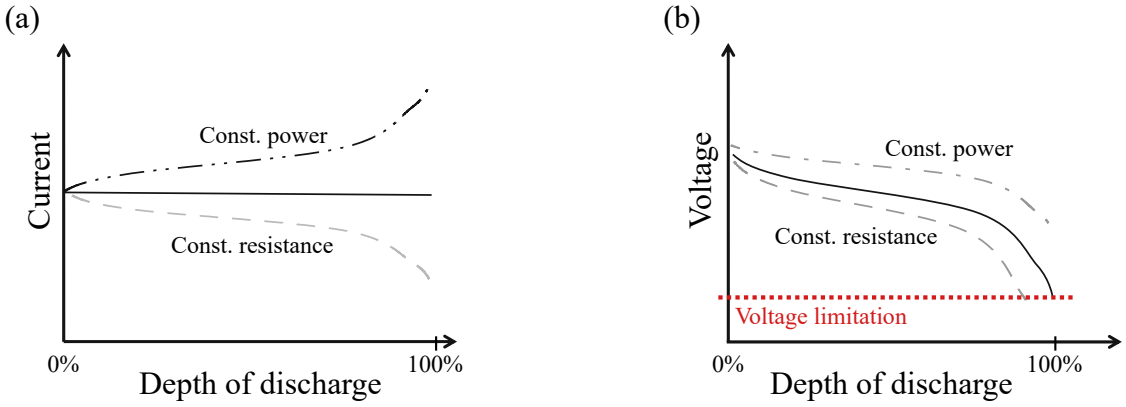


**Figure 2.1:** (a) Discharging current curve of a battery cell with different charging modes, (b) corresponding discharging voltage curve according to (Petrovic 2021, pp. 30-31). The curves do not represent real data, they illustrate the concept.

A crucial battery cell attribute is the voltage limitation. Battery cells should not be discharged under the voltage limit. Similarly, for the charging process, the upper voltage limit should not be exceeded. Although Wang et al. (2021) show advantages in performance for overcharging

a battery cell for $SOC < 108\%$, exceeding the limit and repeatedly overcharging leads to significant capacity losses of the cell. Additionally, exceeding the limit may "result in physical damage to the battery and immediate as well as long-term negative effects [...] even thermal runaway and explosion" (Petrovic 2021, p. 23). One of the tasks of the BMS is to stay within these voltage limitations (Lawder et al. 2014, p. 1016).

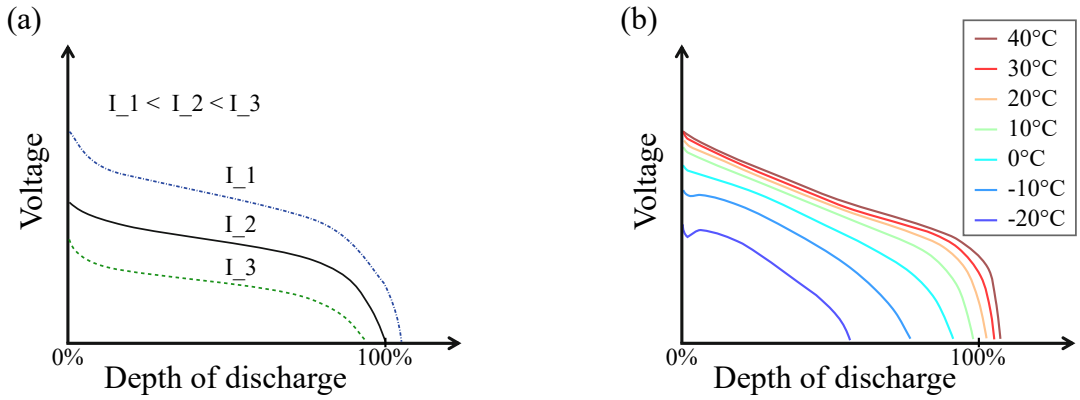


**Figure 2.2:** (a) Discharging voltage curve of a battery cell with different constant current according to Petrovic (2021, pp. 30-31). The curves do not represent real data, they illustrate the concept. (b) Discharging voltage curve for constant current at different temperature levels according to Buchmann (2021).

Figure 2.2 Graph (a) elaborates on the current-voltage relationship further. The illustration according to Petrovic (2021, pp. 33) indicates that higher currents or C-rates coincide with lower voltage levels. Vice versa, lower currents or C-rates coincide with higher voltage levels. Higher currents translate to a faster transport of electrons from anode to cathode. Thus, also the potential and subsequently the voltage decreases faster. Therefore, the manufacturer usually declares a nominal current as well as a nominal voltage for the battery to operate. If the charging process deviates from the nominal current, so does the voltage curve. Considering the hypothetical case in Figure 2.2, it is obvious that higher C-rates also diminish the usable battery capacity. So, a deviation from the nominal current also varies the nominal capacity. Petrovic (2021, p. 35) state that "an increase in C-rate from 1 to 8 C can typically lower the usable capacity by 20%-30%". Consequently, the nominal current and nominal capacity should be considered according to the selected battery use case, or the battery behaviour for higher C-rate needs to be properly included as suggested by (Li et al. 2019).

Finally, the temperature at which the battery is operated or stored has a strong influence on cell behaviour according to Ma et al. (2018, p. 654). Figure 2.2 (b) shows the voltage curve at constant current mode for different temperature levels. It indicates, that the voltage level decreases for lower temperatures. Accordingly, the usable capacity is also reduced at low temperature levels. This is a phenomenon known from electric vehicles (EVs) during winter. This is because the temperature influences the chemical reactivity. Chemical systems are less reactive at low temperature and more reactive at high temperature (Petrovic 2021, p. 34). Thus, the redox reaction can ionise fewer Li-atoms than at nominal temperature. At higher than nominal temperature, higher reactivity

results in higher usable capacity. Therefore, higher temperatures may appear advantageous for battery operations. However, increased reactivity influences not only the main redox reaction but also side reactions that have negative effects on battery characteristics. Effects on ageing and degradation are discussed in the following section.

### 2.2.4 Battery ageing and degradation

The mode of operation has a significant influence on the ageing of the battery cells. In particular, the DoD, SOC, C-rate and the temperature, at which the battery cell is operated, can influence the capacity reduction and impedance increase of the cell (Paarmann 2021, p. 17). In general, both "cycling and storage of the cells lead to a loss of active lithium and, therefore, to a loss of cell capacity" (Lang 2018, p. XV). The ageing or degradation due to cycling and storage of the battery cell is also referred to as cycle or calendar ageing. In addition to the loss of active lithium, there is also a loss of active material in the electrodes and an increase in the internal resistance of the cells (Barré et al. 2013, p. 682). Korthauer (2013, p. 17) cites three ageing effects for this, the increase in the "solid electrolyte interface" (SEI), cracking in the active material due to mechanical stress and the volume change due to the intercalation of Li-atoms in the active material. The SEI affect the anode and is a "durable layer [...] built up on the active material of the negative electrode during production" (Korthauer 2013, p. 17). The SEI is immanent for battery operation, as it protects the anode from direct contact with the electrolyte, which would result in the decomposition of material. Nevertheless, an increased SEI binds Li-atoms, which decreases the capacity. Furthermore, it reduces ionic conductivity, which increases the impedance. Cracking of the electrodes leads to a reduced surface area through oxidisation. Volumetric changes result in loss of contact within the electrode, which decreases the capacity through loss of active material and increases impedance through reduced conductivity (Weiss 2019, pp. 19-21).

As mentioned above in Section 2.2.3, the temperature during rest and operation of the cell increases the chemical reactivity of cell material. It also fosters side reactions, such as growth of SEI layer, oxidisation or electrolyte decomposition. Liu et al. (2021) give an overview of the temperature effects on battery degradation. Additionally, the operational attributes influence each other, as high C-rates increase the internal cell temperature. Therefore, Xu et al. (2021) attribute the cell degradation to the effect of a C-rate induced temperature rise and to an isolated effect of high temperatures and high C-rates. Therefore, high C-rates could result in cracking of the cathode diminishing the battery capacity. Furthermore, higher temperatures reduce the thermal resistance within the cell, which allows for higher DoDs. At the same time, high DoDs negatively affect battery capacity (Ecker et al. 2014). Finally, circular dependencies exist as higher ohmic resistance, because of capacity losses, results in higher cell temperature during operation, which in turn fosters higher capacity losses (Xu et al. 2021). Moreover, Choi et al. (2021, pp. 11-12) name additional reversible and irreversible heat generating processes during

battery operation. Therefore, efficient thermal management to control the ambient temperature and the cell temperature is a decisive factor for battery degradation. However, a quantification of the ageing effects is difficult as it depends on the battery cell materials, its chemical composition, the production process, and the operational mode (Barré et al. 2013).

### 2.2.5 Li-ion battery types and market overview

The battery properties are particularly dependent on the chemical composition of the cathode and anode. Therefore, this chemical composition is often used in the naming of different battery types. The battery types currently used in electric mobility usually have a nickel-manganese-cobalt (NMC) compound as the cathode material, with graphite as the anode material[10]. These battery types are characterised by a "good compromise between energy density, cost and safety" (Doppelbauer 2020, p. 155). However, the availability of the raw materials manganese and cobalt is relatively scarce, resulting in relatively high prices on the world market. Therefore, lithium iron phosphate (LFP) is a possible alternative cathode material for stationary use. Even though the energy density is lower, LFP cathodes have a price advantage over NMC cathodes and are at the same time very safe regarding the fire hazard (Korthauer 2013, p. 41). When selecting the anode material, it is possible to deviate from graphite and replace it with lithium titanate (LTO). [11]. LTO battery cells are safer and more durable in use.

Looking at the market for stationary BSS, NMC, LFP and LTO are the most common battery types. Figure 2.3 shows the shares of the individual battery types in relation to the total installed capacity of BSS active worldwide. The figures come from the Sandia National Laboratories (2022) database and show that the majority of the world's BSS use lithium iron phosphate as the cathode material, followed by nickel manganese cobalt. 17.6% still go back to lithium titanate as anode material, although here the cathode material is not known. These three types also determine the German market according to the figures of C.A.R.M.E.N. e.V., who has compiled an overview of suppliers of stationary BSSs in writing (C.A.R.M.E.N. e.V. 2021b) and online (C.A.R.M.E.N. e.V. 2021a). The online version lists 32 manufacturers and 449 BSS products online. 77% of the systems can be assigned to the three types NMC, LFP and LTO. The system sizes listed in the database range from $1.41\,kWh$ to $4,220\,kWh$. Table 2.1 summarises the most important findings. Most suppliers offer LFP systems, followed by NMC suppliers. LTO cell types are only listed by one supplier in the database. The stated characteristics for the cycle life of the BSS vary greatly for the NMC and LFP battery types, from a minimum of 1,500 equivalent full cycles to 10,000 full cycles. The service life of the LTO systems is particularly striking, with 20,000 equivalent full cycles. The database also shows an average price for large-scale storage of $854\,€/kWh$ for the year 2021 (Eble 2021).

[10] NMC "is currently the standard material for the batteries in many electric cars" (Doppelbauer 2020, p. 155)

[11] "The $Li_4Ti_5O_{12}$ (LTO) spinel is considered as the most appropriate titanium-based oxide for use as anode in Li-ion batteries, and is actually considered as a viable anode for Li-ion batteries" (Julien et al. 2016, p. 354)

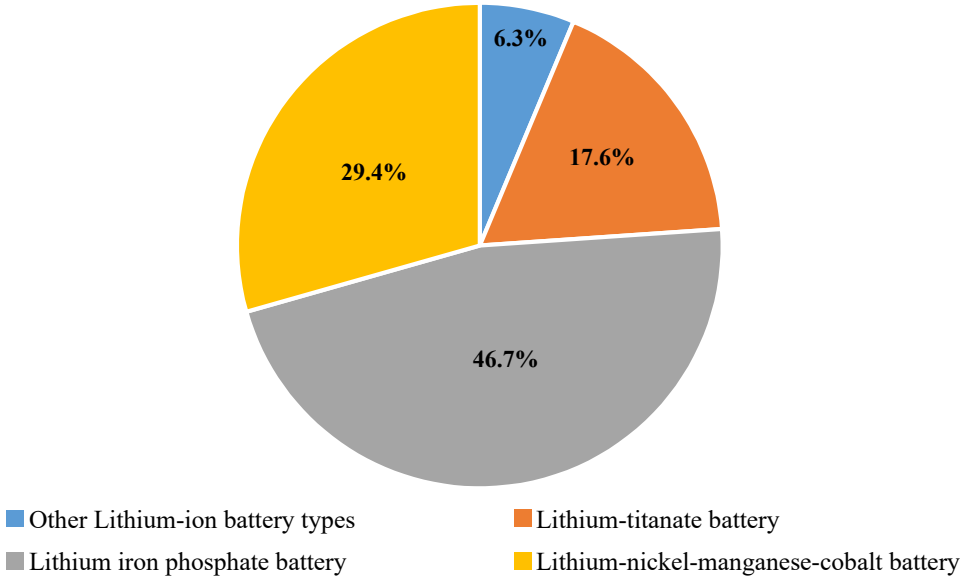


**Figure 2.3:** Pie chart of globally active BSS in terms of installed capacity according to Sandia National Laboratories (2022) with a total capacity of around 503 $MW$ in 2020.

| Battery type | Number of suppliers | Cycle Life |
|---|---|---|
| NMC | 7 | 1,500-10,000 |
| LFP | 14 | 3,650-10,000 |
| LTO | 1 | 20,000 |

**Table 2.1:** List of Li-ion BSS suppliers in Germany and the provided battery types according to C.A.R.M.E.N. e.V. (2021a).

## 2.3 Flexibility in the energy system

The national and global $CO_2$-emission targets require a change in the generation portfolio in the energy system, through which a growing share of RES replaces conventional fossil energy sources. However, conventionally operated power plants such as gas or coal-fired power plants are regarded as dispatchable generation capacities in the sense that they, to a certain extent, can adapt their generation to the load. They, therefore, provide the flexibility to keep generation and load in balance. A loss of these generation capacities also results in a loss of flexibility, which can only be replaced to a limited extent by RES plants. This section describes how the future demand for flexibility will increase and which measures have already been installed to stimulate the supply of flexibility.

### 2.3.1 Flexibility demand

As mentioned above, some conventional fossil-fuelled power plants are dispatchable in the sense that electricity generation is determined by the fuel supply and the fuel is a largely controllable

production factor. Conventional power plants can therefore adapt their electricity generation to a certain extent to load changes in the power grid by varying the fuel supply. In contrast, wind and solar energy sources are volatile and intermittent and, above all, not dispatchable[12]. Consequently, wind and solar power plants are rather limited in their adaptability to changing load conditions. Modern wind and solar power plants can throttle their generator output to counteract load reduction in the grid, but an increase in power supply depends on the availability of renewable energies. This is most evident at night when no sunlight is available. Therefore, a higher share of renewables in the system is associated with a higher degree of volatility and intermittency on the supply side.

Among the conventional power plants, some plants are better suited to adapt their generation than others, depending on their techno-economic constraints. Base load power plants such as nuclear, lignite, or run-river power plants are usually "not designed to respond to major shifts in output" (Shivakumar et al. 2017, p. 152). This is due to relatively low fuel costs and long start-up times. Intermediate load power plants such as hard coal and combined cycle gas power plants are designed to operate at partial-load with fewer full-load hours (Strauß 2009, p. 32). Therefore, these plants are equipped to address load variations during the day. The fastest reacting conventional power plants are the peak-load power plants, such as open-cycle gas turbines or pumped hydro storage plants. Open-cycle power plants coincide with low investment and relatively high fuel costs. These plants are designed to operate only a few hours a day and to adapt their generation to sudden load changes within minutes (Shivakumar et al. 2017, p. 153).

A reduction in dispatchable generation capacity in the systems also affects the ability to balance short-term fluctuations in load and generation in the power grid, observable as frequency deviations. The mechanical shaft in rotating synchronous machines such as a power generator in a conventional power plant provides the inertia needed to spontaneously balance supply and demand in the power grid. Therefore, many conventional power plants are particularly good at responding to momentary imbalances. Even though it is technologically possible to enable instantaneous response time of RES power plants (Agricola et al. 2014, p.54), these systems are not yet commercially available (Kraiczy 2021, p. 11). "Generally, the more rotating synchronous machines, the higher the inertia and the slower the rate of change of the frequency deviation" (Ela et al. 2011, p. 24).

In addition to the temporal uncertainty and variability of generation from RES plants, there is also a site-specific component according to Kondziella and Bruckner (2016, p. 11). Conventional power plants are built where a high load must be satisfied. RES plants, on the other hand, are built in locations where the RES potential is high, i.e. in places with high solar irradiation and a high number of strong wind hours. This allows these plants to operate with high economic efficiency. As a result, the need for flexibility has to be assessed site-specifically and also

[12] Some RES, on the other hand, can be considered dispatchable, e.g. hydropower, pumped storage, biomass, and geothermal energy

depending on the utilisation of the power grid. In addition, Brunner et al. (2020) point out that the flexibility demand of a power system varies under different system configurations. For example, the flexibility demand depends on the share of RES, the grid expansion, the import and export capacities as well as the operating mode of the RES plants.

Various scientific studies have assessed the flexibility needs of an energy system (Kondziella and Bruckner 2016). Studies assume that the increasing share of renewable energies in the energy system will require a higher degree of flexibility than the traditional energy system (Ma et al. 2013, Sterner and Stadler 2014, Beucker et al. 2020).

Several definitions and characterisations of flexibility exist (Fraunhofer IFF 2020, Michaelis et al. 2017, Alizadeh et al. 2016). This thesis refers to Beucker et al. (2021, p. 11), who define flexibility in terms of the following attributes:

1. Direction of power demand, positive or negative
2. Duration of power demand
3. Activation time of the power demand.

The direction refers to whether there is a positive or negative residual load. In this thesis, the residual load can be described as the difference between the load and the non-dispatchable RES generation. As no uniform definition exist, residual load may also include must-run thermal generators and other generators "assumed to be inflexible" (Schill 2014, p. 67). Positive residual load applies to the case, where conventional generation is smaller than the residual load. Vice versa, for negative residual load, the residual load is smaller than the conventional generation. Positive residual load is balanced by downward flexibility and is achieved in the conventional energy system by increasing the generation of power plants. Negative residual load is compensated by upward flexibility, which can be achieved by throttling and curtailment of generators. In addition, there is shifting flexibility, where power is shifted spatially or temporally. A spatial shift occurs through the utilisation of power grid capacities, and a temporal shift occurs primarily through the intermediate storage of energy (Michaelis et al. 2017, p. 1). The duration of the power demand results in requirements for the flexibility measure, as the duration provides information on the amount of energy required, and energy is defined as the integral of power over time. For example, a storage system's ability to provide energy is restricted by its storage capacity. Thus, in the case of negative flexibility, as soon as a storage facility is fully charged, another storage system must be activated (Michaelis et al. 2017, p. 3).

The activation time is decisive for the reaction time of the flexibility measure, and the activation time depends on the source of the system imbalance. As Hirth and Ziegenhagen (2015, p. 1039) state, negative or positive residual load arises from stochastic forecast errors or deterministic "schedule leaps". Schedule leaps are linked to the step-wise electricity market schedules, where market products are offered in quarter-hourly or hourly time frames. For example, a PV power plant operator offers a 15-minute energy packet signalling a constant power generation for these

15 minutes. However, this constant 15-minute schedule value will differ from the real-time continuous physical generation values. “Deterministic sources of system imbalances can be forecast quite easily” (Hirth and Ziegenhagen 2015, p. 1040). The stochastic errors occur from load and forecast errors of load and generation, as well as unplanned outages of generators or transmission lines. Therefore, the less time is between the detection of the forecast error and the imbalance realisation, the shorter the activation time. Depending on individual ramp rates and start-up time, conventional power plants can adjust their schedules accordingly. The shorter the activation time, the fewer power plants can adjust their schedules due to individual reaction time. Most conventional power plants are able through a “combination of electrical, mechanical, and hydraulic means to adjust the input to the turbine (e.g., opening steam valves in a steam turbine generator)” (Ela et al. 2011, p. 25). Nevertheless, it becomes clear that, based on the attributes described, different types of power plants can address the demand for flexibility. Among conventional power plants, gas-fired power plants have the highest operational flexibility (Agora Energiewende 2017, 47). The phase-out of conventional power plants, therefore, leads to increasing demand for temporal and spatial flexibility through other technologies (Heffron et al. 2020, p. 5).

### 2.3.2 Flexibility markets

The previous section described the transition of the energy system and the resulting need for other flexibility measures. To stimulate the provision of flexibility, different markets and products have been introduced. These can be distinguished according to the division of the German energy market design into the energy market and the grid sector (Fraunhofer IFF 2020, p. 46). Thus, electricity producers, traders, and distributors can offer their flexibilities on the energy markets. In the grid sector, it is possible to offer flexibilities as ancillary services or in the context of avoiding grid congestions (Beucker et al. 2021, p. 11).

These markets address both the generation and the supply side of the energy system and use different signals to activate flexibility options. The following section briefly explains the different markets and products. In Section 2.4 the market framework is explained in more detail.

The electricity market balances the medium to long-term generation and load of the power system. The need for flexibility results from short-term divergences, between 15 minutes and a few days, between electricity supply and demand. This need for flexibility is considered by the energy exchanges, namely the day-ahead market, the intraday day-ahead market and the continuous intraday market. On these markets, the fluctuation of market prices signals the need for flexibility. In Europe, on the day-ahead market, electricity quantities are traded for every hour of the next day. On the intraday day-ahead markets, electricity is traded for every 15 minutes of the next day, and it allows for systemic deviations between the hourly and quarter-hourly schedules to be balanced. In the continuous intraday market, 15-minute power quantities are

traded up to five minutes before physical delivery[13]. The continuous market offers the possibility to balance divergences between market activities and updated forecasts for load and generation. The short-term characteristic of the continuous market technically limits flexibility measures and increases the market price spread compared to the day-ahead market.

The ancillary services consider the instantaneous to short-term flexibility, from seconds up to one hour, required for stable operation of the power grid and grid restoration. Ancillary services include frequency and voltage stability measures, namely balancing reserve power, interruptible loads or reactive power compensation. Restoration measures include, above all, black start capabilities and isolated operation capabilities. The activation of ancillary services is usually not signalled by market prices, but either directly by the grid operator or automatically by frequency measurements. The provision of such services is either offered and remunerated on special marketplaces such as the control reserve market or through bilateral agreements between the grid operator and the service provider. All ancillary services differ in terms of their activation time, duration, and energy or power demand. They, therefore, address different flexibility measures or technologies. The system services are described in more detail in Section 2.4.4.

Finally, the measures to avoid grid congestion target local flexibility needs in the power grid. In Germany, these activities mainly target the supply side and include redispatch and curtailment measures. On the demand side and especially on the lower grid levels, interruptible loads can be used to avoid grid congestion. Activation is signalled directly by the grid operator. In Germany, there are also various regulations that create incentives for electricity consumers to reduce, adjust or shift their peak load through demand flexibility (Lange 2021). This demand flexibility is also referred to as peak shaving. While these schemes were introduced with the intention of reducing the load on the grid, Fritz et al. (2021) argue that these schemes are outdated and may achieve the opposite effect as they do not reflect the flexibility needs of today's volatile energy system. This is explained in more detail in Section 2.4.3.2.

In the following Section 2.4, the market and regulatory frame are described in more detail. This thesis particularly addresses the perspective of an industrial company, as the industrial flexibility potential enables a good adaptation to an increasing intermittent RES supply (Heffron et al. 2020, p. 2).

## 2.4 Market structure for flexibility measures

This section takes a closer look at the regulatory framework and the market structure of flexibility products. In particular, the perspectives of an industrial company in Germany are considered. This includes the electricity price composition for industrial customers with a special focus on

[13] For a detailed presentation of the sequential timing of market products, please refer to Kraft (2022, p. 14).

electricity marketing and grid charges, as well as the provision of ancillary services through participation in balancing reserve markets.

### 2.4.1 Electricity prices for industrial customers

Industrial customers differ greatly from household customers due to their demand profile for electricity. Especially because of the larger quantities of electricity, industrial customers usually have to pay lower electricity prices than household customers. The German Association of Energy and Water Industries e.V. (BDEW 2022) publishes the electricity prices of different sectors in Germany and their components every year. Figure 2.4 shows the development of the annual average electricity prices for industrial customers in Germany. The different components of the electricity price are highlighted in colour. This shows that the largest share of the electricity price is attributable to procurement, grid charges and operation. The composition of this price component can be seen as heterogeneous, as it depends strongly on the quantity purchased, the geographical location, as well as the willingness to take risks and the procurement strategy. To shed more light on this, the following section takes a closer look at electricity procurement. The attached Section 2.4.3 provides explanations on the grid charges.

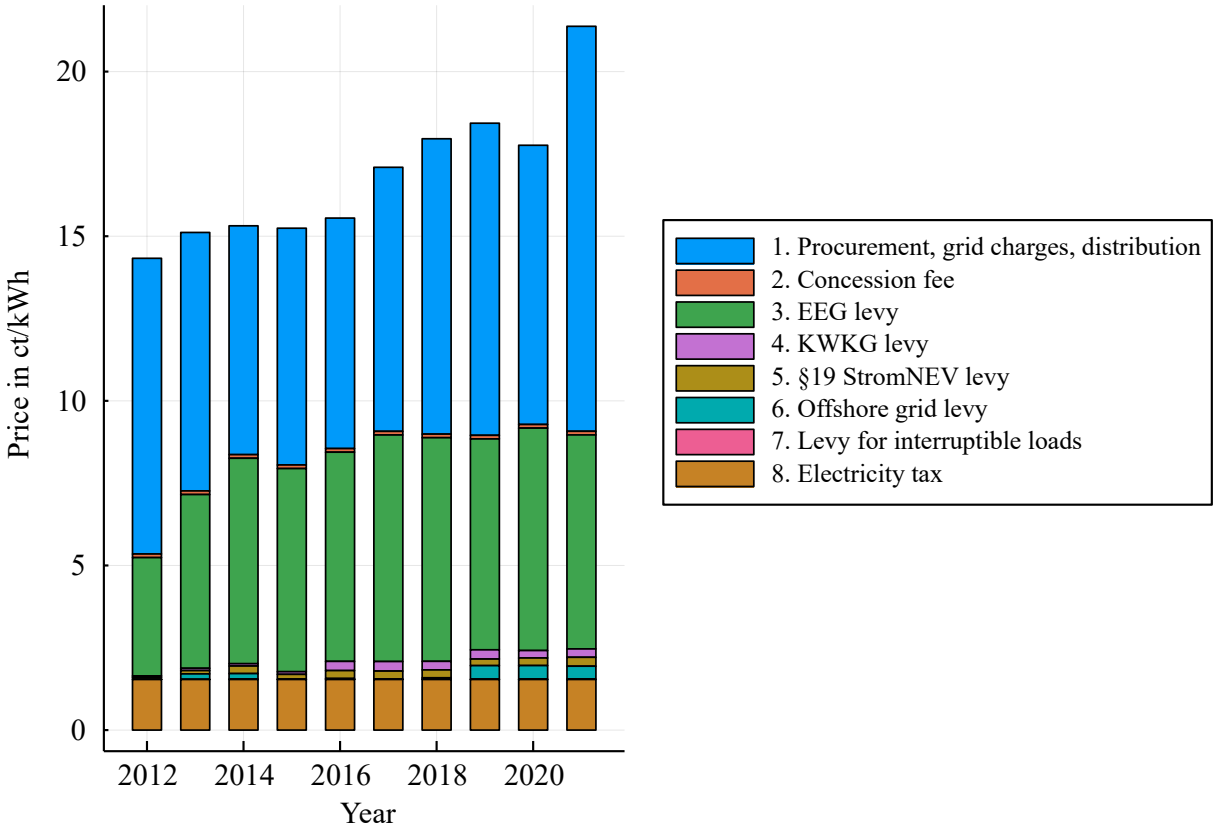


**Figure 2.4:** Industrial electricity prices in Germany for the medium voltage level and a consumption between $160,000\,kWh$ and $20,000\,MWh$, as of 01.2022 according to BDEW (2022).

### 2.4.2 Electricity procurement for industrial customers

Zimmermann and Breuer (2019) present a detailed overview of the electricity procurement options of an industrial company in Germany. According to this, an industrial company can either obtain electricity directly from an energy utility company, purchase electricity quantities in an over-the-counter transaction (OTC transaction) or trade on the power exchange. In the latter two cases, it is possible either to conclude longer-term forward transactions or to become active on the spot market for short-term purchases. Direct supply by a utility company enables a risk-free electricity supply for the industrial company, as a fixed electricity tariff is usually agreed upon. The risk of fluctuating prices lies with the utility. OTC transactions can be concluded either via a broker or bilaterally. However, in both cases, there is a contractual risk of non-performance. OTC transactions can generally be described as rather non-transparent and inconsistent. The majority of German electricity volumes are traded in an OTC transaction (European Commission 2021, p. 20) and mostly concern long-term supply contracts. However, long-term forward transactions can also be settled on the power exchange. Here, uniform, transparent and mostly anonymous electricity quantities are traded.

According to Fraunhofer IFF (2020, p. 53), it is most advantageous for industrial companies to combine the possibilities of forward transactions with those of the spot market when procuring electricity. In this way, the quantities of electricity that can be predicted in the long term are purchased via the futures market and uncertainties in the load forecast can be compensated flexibly and at short notice via the spot market (Zimmermann and Breuer 2019, p. 18).

Therefore, the spot market on the power exchange is a natural area of application for flexibility measures. Here, uniform, transparent and, in particular, short-term electricity products are traded. These are short-term in the sense that there can be a maximum of 36 hours and a minimum of five minutes between the conclusion of the trading transaction and the physical delivery of the electricity. Furthermore, the electricity quantities can be traded as a block, for every hour or every 15 minutes of a day. In relation to the German market area, EPEX SPOT in Paris is the spot market exchange with the largest traded energy volume. Here, a distinction is made between different markets according to the time interval between the conclusion of the trade and the realised electricity delivery, the electricity as quarter-hourly or hourly quantities and the type of pricing. In the latter case, either a market clearing price or a bid price can be determined. In the case of market clearing price, the bids are sorted in ascending order by price at the end of the auction and the last bid accepted is identified. The price of this bid then applies to all accepted bids on the respective product. Thus, the market-clearing price follows the merit-order, where the generation types are ranked by their marginal cost. In contrast, the bid price according to the so-called pay-as-bid procedure refers to the fact that a sell offer is matched with a buy offer at the same bid price. The transaction is then carried out at this price. This results in several pairs of transactions with different bid prices for the same product.

The following is a summary of the spot markets for the German market area and their characteristics (EPEX SPOT 2021):

- Day-ahead market: auction for each hour of the following day; auction closes at 12 noon; market clearing price.
- Intraday auction market: auction for each quarter-hour of the following day; auction closes at 3 p.m.; market clearing price.
- Continuous intraday market: continuous trading of electricity up to five minutes before delivery; hourly or quarter-hourly products; from 3 p.m. or 4 p.m. of the previous day; bid price.

In Europe, Germany is the largest and most liquid market area for electricity trading. Even though the largest amount of electricity is traded via OTC transactions, about two-thirds, the remaining share is traded in exchange transactions. This share increased by 3% in Germany from 2020 to 2021 (European Commission 2021, p. 19). As can be seen in Figure 2.5, at EPEX-SPOT the traded volume of electricity on the intraday market has continuously increased in recent years and doubled between 2014 and 2019. The volume on the day-ahead market, on the other hand, has fallen by 14% in the period (Bundesnetzagentur and Bundeskartellamt 2020, p. 236).

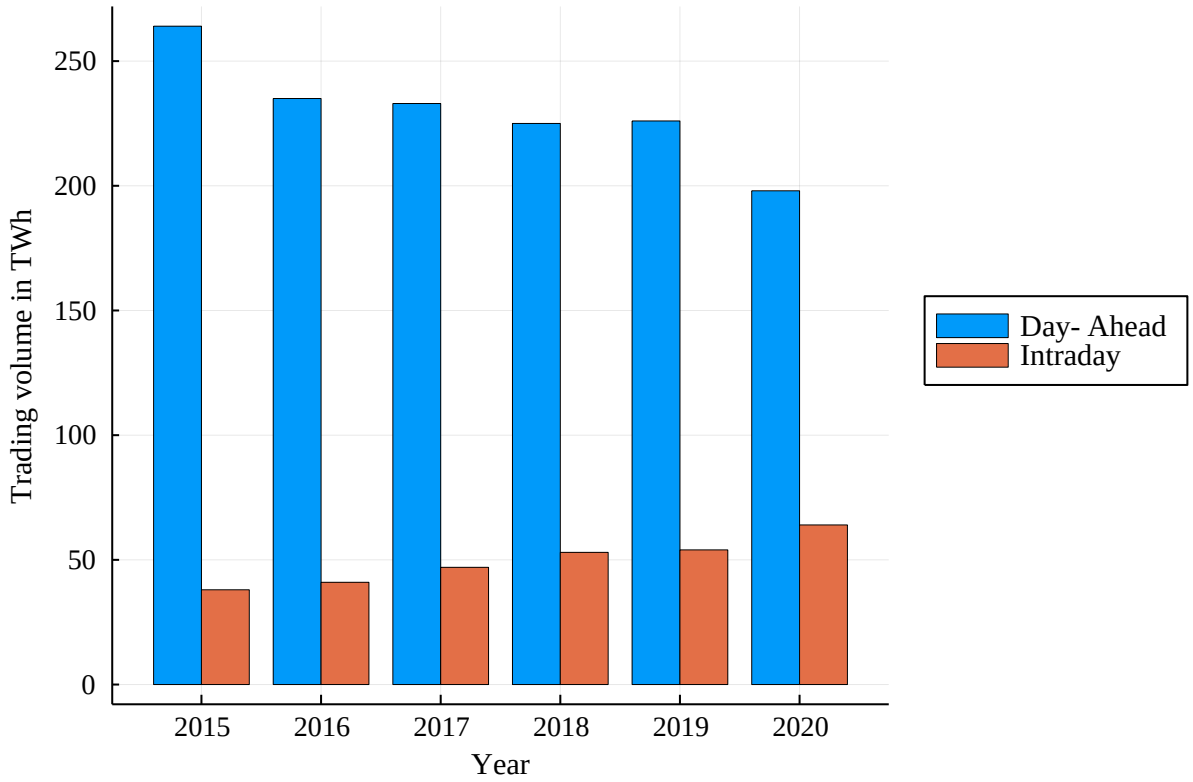


**Figure 2.5:** EPEX SPOT trading volume for the German market area, based on Bundesnetzagentur and Bundeskartellamt (2022, p. 249).

Participation in the power exchange can be either direct or indirect. To trade directly on the exchange, an exchange admission is required. The admission is linked to requirements such as a balancing group responsibility. Indirect participation in the exchange, on the other hand, can take place via an intermediary, such as a direct marketer or an aggregator. The intermediary charges a fee for this service. For an industrial company, it depends on its energy needs whether direct or indirect participation in the exchange is worthwhile. Here it is important to compare the costs for a stock exchange admission as well as the trading fees of a direct marketer.

### 2.4.3 Grid charges for industrial customers

Industrial customers that have power metering pay grid charges that are divided into both a capacity price[14] and an energy price[15]. This is one of the ways in which the grid charges for industrial customers differ from those for residential customers, which usually only refer to an energy price in $€/kWh$. The current grid charge regulation for industrial customers was introduced to ensure a balanced and fair participation of all end consumers in the grid costs (keyword "the-user-pays"). The determination of the amount of the grid charge is regulated in the Electricity Grid Charges Ordinance (StromNEV), in particular in §§ 16 and 17 as well as in Annex 4. For a clear explanation of the current grid charge regulations, please refer to Fritz et al. (2021) and (Jeddi and Sitzmann 2019).

The grid charges for industrial customers in Germany have the following main features:

- differentiation into capacity and energy prices,
- "inflection point" at 2,500 annual full load hours[16],
- distinction between grid operators, and
- distinction between voltage levels.

These features are explained in more detail below. Section 2.4.3.1 thereby shows the legal framework for determining the level of grid charges and addresses the specifics of the "inflection point" as well as the price differences between voltage levels, grid areas and over the years. Furthermore, in Section 2.4.3.2 the possibilities of grid charge reduction are discussed and, finally, in Section 2.4.3.3 the problem of the lack of conformity of the German grid charge regulation with the European legal framework is addressed.

[14] The capacity price refers to the maximum electrical power, measured in $kW$, with which electricity is drawn from the power grid in a certain period, usually a year.

[15] The energy price refers to the total amount of electricity, measured in $kWh$, which is drawn from the power grid in a certain period of time, usually one year.

[16] The annual full load hours, annual full load hours or also annual usage period is the quotient between annual energy demand and annual peak load. The value describes how many hours a company would theoretically draw electricity if it constantly drew electricity at the level of the annual peak load.

#### 2.4.3.1 Determination of grid charges

For their industrial customers, the grid operators specify their grid charges for each voltage level[17] with a specific capacity price and a specific energy price. As Annex 4 StromNEV shows, the prices differ for consumption with less than 2,500 annual full load hours and consumption with at least 2,500 full load usage hours. For an exemplary clarification of this process, table 2.2 presents the grid charges of the Pforzheim municipal utility for three exemplary voltage levels in 2016.

| | Annual full load hours $< 2.500h/a$ | | Annual full load hours $>= 2.500h/a$ | |
|---|---|---|---|---|
| | Capacity price in $€/kW$ | Energy price in $ct/kWh$ | Capacity price in $€/kW$ | Energy price in $ct/kWh$ |
| High voltage (HV) | 6.77 | 2.46 | 67.28 | 0.04 |
| Medium voltage (MV) | 8.39 | 2.79 | 64.68 | 0.54 |
| Low voltage (NV) | 9.74 | 4.18 | 71.58 | 1.71 |

**Table 2.2:** Grid charges of Stadtwerke Pforzheim GmbH & Co. KG for three exemplary voltage levels in 2016.

The prices are determined using a commonality function and commonality degree in Annex 4 StromNEV and consider the consumption behaviour and peak load in a grid area. The table shows that the ratio of the price components changes drastically at a threshold value of 2,500 annual full load hours (indicated with the unit *h*). This threshold value is so specified in Annex 4 StromNEV and is also referred to in the standard as "inflection point".

For the range of less than 2,500 annual full load hours, the level of the grid charge is primarily determined by the energy price. This turns around for the range of at least 2,500 annual full load hours. In this range, the influence of the capacity price on the grid charges is greatest. In addition, table 2.2 indicates that prices decrease with each higher voltage level.

As Fritz et al. (2021) note, the "inflection point" not only changes the price ratio but also sets other incentives to adjust the load profile of consumption to the grid charge level. To elaborate on this point, figure 2.6 serves as an explanation. This figure shows the specific grid charge in $ct/kWh$ as a function of the annual full load hours for the medium voltage level of Stadtwerke Pforzheim from 2016[18]. The share of the capacity or energy price in the grid charge is highlighted in colour.

[17] Voltage levels describe the seven grid levels into which the German power grid is divided, with the voltage levels low voltage, medium voltage, high voltage and extra high voltage, as well as the respective transformer levels between these voltage levels

[18] The possibilities of reduced grid charges according to § 19 (2) StromNEV are not considered here. As explained in Section 2.4.3.2, this includes atypical grid usage according to § 19 (2)(1) StromNEV and uniform electricity consumption according to § 19 (2)(2) StromNEV

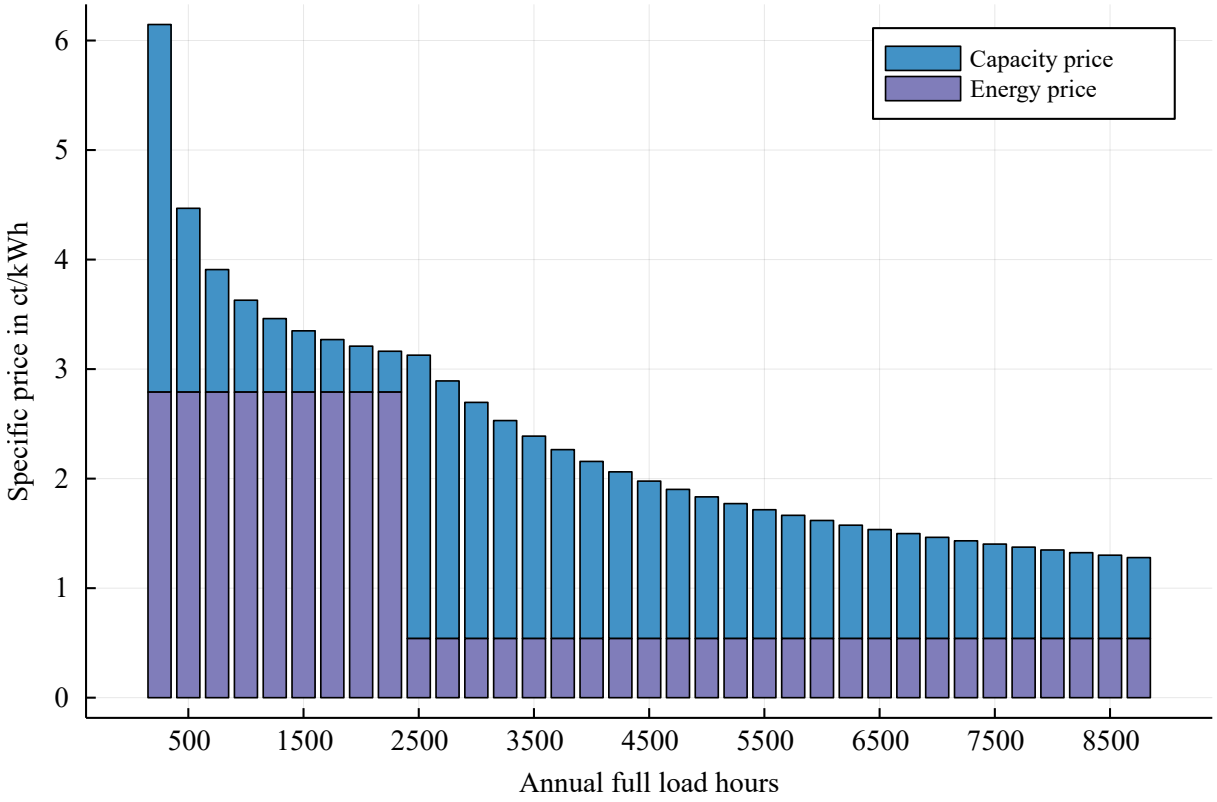


**Figure 2.6:** Grid charges in reference to the annual full load hours using the example of Stadtwerke Pforzheim, medium voltage level in 2016.

At the "inflection point" of 2,500 annual full load hours, the ratio of the price components changes visibly and the trend of the grid charge also changes.

In general, Figure 2.6 makes it clear that the grid charge regulation stimulates high annual full load hours. This leads to consumers being encouraged to reduce the annual peak load. However, the incentives to reduce electricity consumption through the level of the energy price component of the grid charges are much lower for consumers with more than 2,500 annual full load hours than for consumers with less than 2,500 annual full load hours.

From the consumer's perspective, the grid charge regulation, therefore, has the effect that encourages the use of flexibility measures for peak load reduction or peak shaving for consumption with at least 2,500 annual full load hours and encourages energy-saving measures for the range smaller than 2,500 annual full load hours. However, Fritz et al. (2021) point out that this individual flexibility incentive runs counter to the systemic need for flexibility and is even retroactive. Thus, peak shaving is carried out independently of the actual dynamic grid load and the strain on the grid (Perez-Arriaga et al. 2017, p. 76). Even if a continuous demand, analogous to a high number of annual full load hours, results in a demand that can be planned in the long term, the grid charges in their structure do not include an incentive to provide flexibility for short-term grid bottlenecks.

In addition, the high energy prices, especially in the range of less than 2,500 annual full load hours, can reduce the flexibility incentive. This can be explained using the example of a production-related flexibility measure, which involves shifting production steps over time[19]. In the case that price differences on the electricity market serve as a signal for a need for flexibility, low electricity prices may even indicate a surplus of electricity. In this case, production-related flexibility measures in a plant with a high energy price component are economically disadvantaged compared to a plant with a lower energy price component, as the production costs would be higher in the former. According to Fritz et al. (2021, p. 17), this leads to an "economically suboptimal" use of flexibility capacities. Richstein and Hosseinioun (2020, p. 9) also describe that this results in "significant economic distortions". In this context, Jeddi and Sitzmann (2019) discuss possible alternative grid charging systems with a view to Europe, which are more responsive to the changing challenges for the energy system.

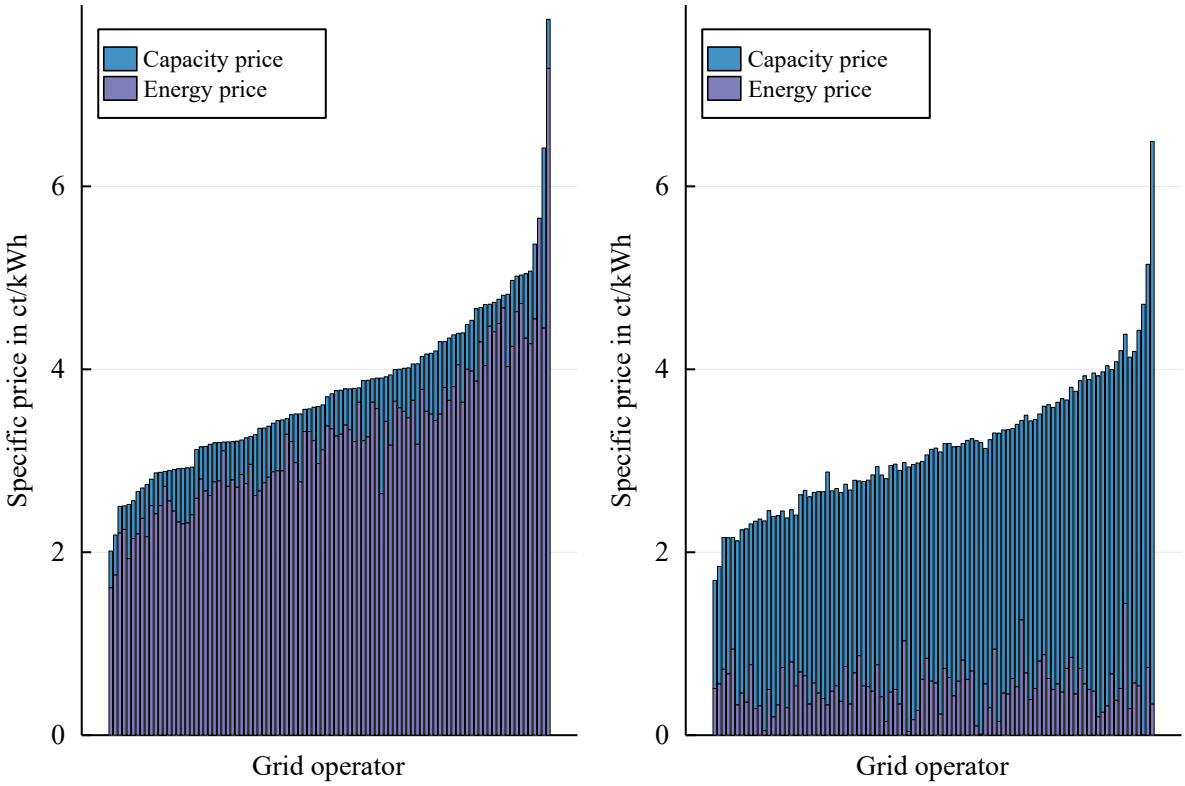


**Figure 2.7:** Grid charges for 100 grid operators in Baden-Württemberg for the medium voltage level in 2016; left graph refers to 2,000 annual full load hours; right graph refers to 3,000 annual full load hours.

As mentioned above, it is also important to consider the dependency on location and voltage level, which are explained graphically in Figure 2.7 and Figure 2.8 respectively. Figure 2.7 shows the grid fees together with the two price components for 100 grid operators in Baden-Württemberg sorted by size. Shown are the grid charges for the medium voltage level. The left graph shows

[19] The possibility of shifting consumption is described, for example, in Friedrichsen (2015).

the specific grid charges for 2,000 annual full load hours and the right graph those for 3,000 annual full load hours. The coloured distribution shows the drastic change in the relationship of the price components to each other, which, as described above, begins at the "inflection point". In the comparison of the grid areas, the difference between the lowest and highest grid charge is the factor of almost four for 2,000 annual full load hours and just under three for 3,000 annual full load hours, respectively. The level of the grid fee depends on the layout of a grid area as well as "the typical settlement structure of the area, the consumer structure, the degree of utilisation and the age structure of the equipment" (Fritz et al. 2021, p. 18) in this network area. In this context, high grid charges can arise especially from the integration of RES plants and less from local consumers. In addition, grid charges are usually higher in rural areas than in cities, just as they are usually higher in the north of Germany than in the south.

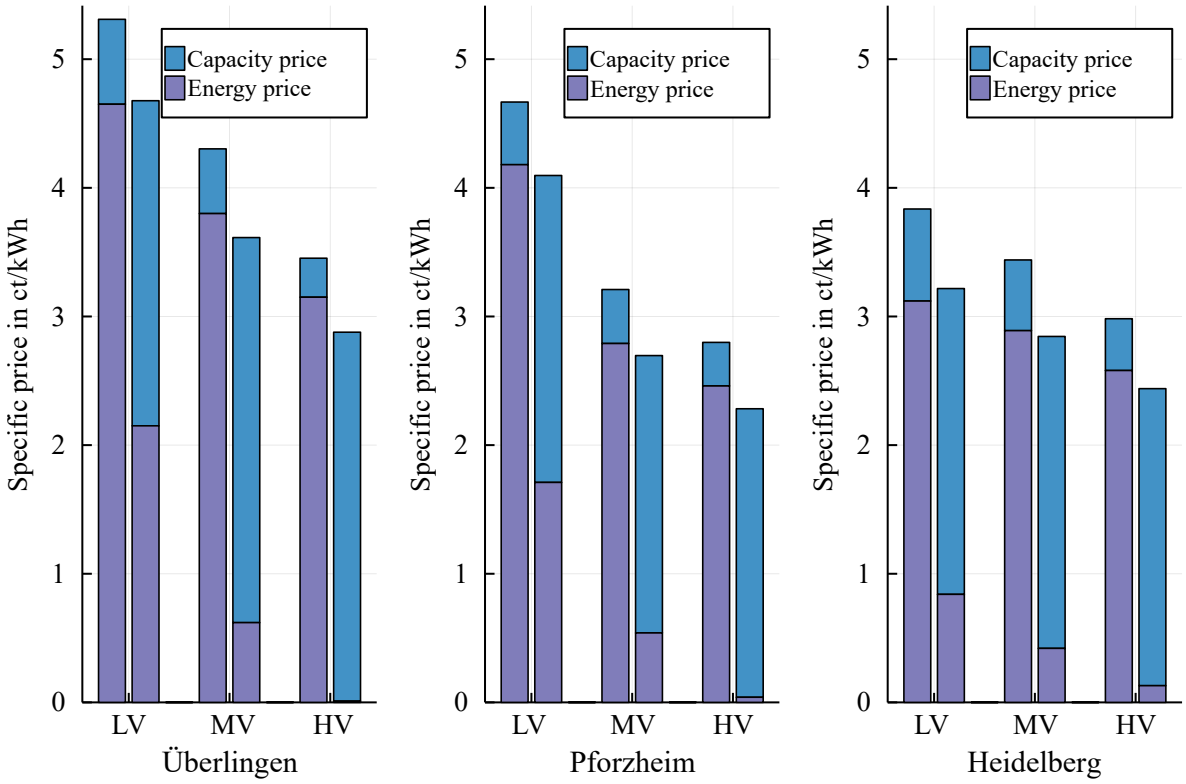


**Figure 2.8:** Comparison of grid charges for different voltage levels; left bar of the bar pairs refers to 2,000 annual full load hours in each case; right bar refers to 3,000 annual full load hours.

Figure 2.8 compares the grid fees for different voltage levels for three exemplary network operators from Baden-Württemberg, the municipal utilities of Überlingen, Pforzheim and Heidelberg. The specific grid charges for the low-voltage (LV), medium-voltage (MV) and high-voltage (HV) levels are shown. The grid charges are each shown as a pair; the left bar of such a pair represents the grid charge for 2,000 annual full load hours and the right bar for 3,000 annual full load hours. The price components are highlighted in colour and again indicate a strong change in the grid charge composition at the "inflection point". Furthermore, it can be seen that the grid

charges decrease with each higher voltage level. However, the differences between the voltage levels vary regionally. For example, the grid charges decrease from low voltage to high voltage by a maximum of 44% (Pforzheim, 3,000 annual full load hours) and a minimum of 22% (Heidelberg, 2,000 annual full load hours). However, it can be observed that especially for 3,000 annual full load hours, the capacity price only changes insignificantly depending on the voltage level compared to the energy price.

The development of the nationwide grid fees shows a constantly increasing trend over the last ten years (Bundesnetzagentur and Bundeskartellamt 2020, p. 162). For example, commercial grid charges increased by approximately 12% from 2015 to 2020; for industrial customers, grid charges increased by approximately 27% in the same period. However, the figures only reflect an average value for Germany. The development of grid charges at the distribution grid level can indeed show significant regional differences (Bundesnetzagentur 2021-01-14). As an example, figure 2.9 shows the development of grid charges for three voltage levels of Stadtwerke Pforzheim between 2015 and 2021. The increase in grid charges fluctuates between around 61% and 72% over the seven years. The development is thus in stark contrast to the national average.

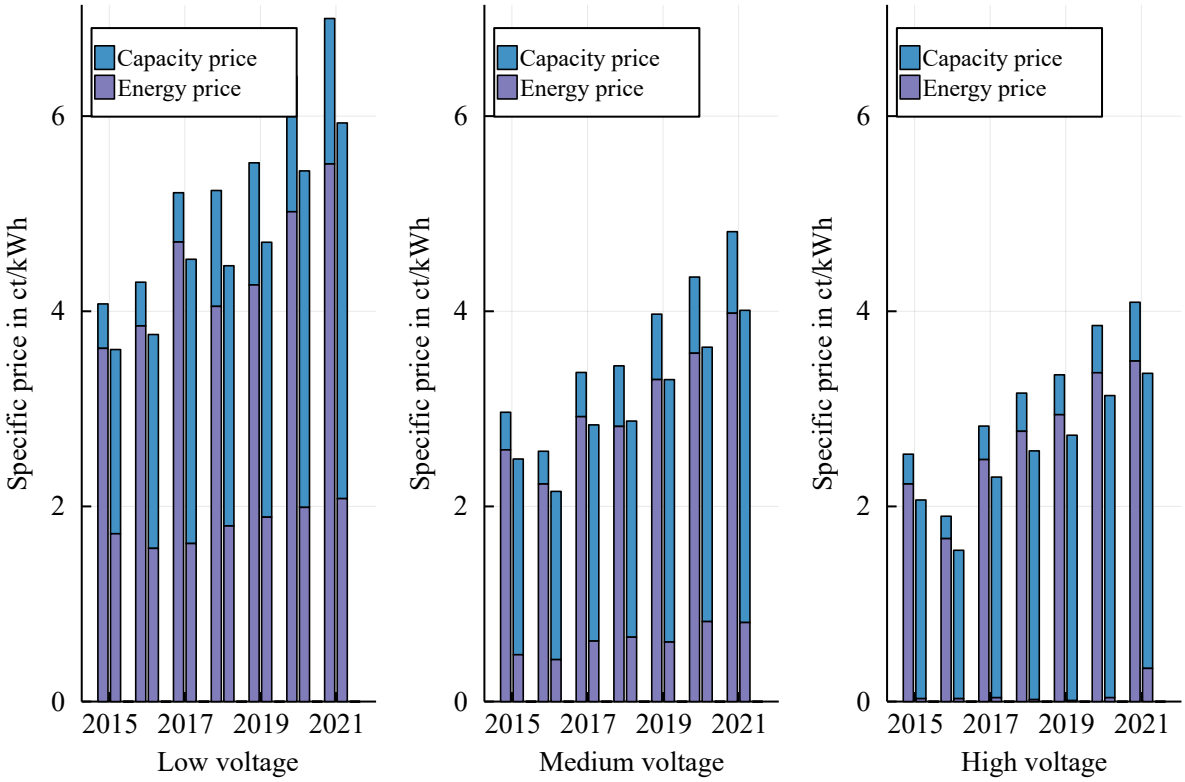


**Figure 2.9:** Development of grid charges for Stadtwerke Pforzheim; left bar of the pair of bars refers to 2,000 annual full load hours; right bar refers to 3,000 annual full load hours.

#### 2.4.3.2 Reduction of grid charges

To reduce grid charges, industrial companies have the option of reducing their peak load, thus reducing the capacity price component of grid charges. This is described by the term peak shaving. In Germany, peak shaving is currently incentivised via the annual capacity price. In addition, the German legal framework currently stipulates that consumers whose individual load peaks deviate from the load peaks of a grid area are to be offered an individual grid charge in accordance with § 19 (2) StromNEV. This includes atypical grid usage according to § 19 (2)(1) StromNEV and uniform electricity consumption according to § 19 (2)(2) StromNEV. The respective individual grid charge must be approved by the competent regulatory authority.

**Peak shaving** describes the shifting of the peak load of an industrial company. The definition period for peak load can refer to a year, a month, as in the Croatian case in Publication B, or variable high-load time windows, as in the case of atypical grid usage. A general overview of the concept of peak shaving is given in Uddin et al. (2018). In this context, peak shaving is applied in different areas through different load shifting technologies. For example, Campana et al. (2021) investigate the use of Li-ion storage in a commercial building for peak shaving and Cossutta et al. (2022) investigate the use of neighbourhood storage with PV self-generation. Lee et al. (2021) look at the possibilities of second-life battery storage, Chen et al. (2021) consider sector coupling at the building level and Golmohamadi (2022) analyses load shifting possibilities on the process-side in heavy industry. Thus, peak shaving can hold economic benefits for the end-user, but peak shaving also represents an opportunity to avoid costs at the grid level. He et al. (2022) show, for example, the economic benefits in the operation of a distribution network. However, this paragraph is only intended as a brief mention of the concept of peak shaving. Please refer to Publication A for a more detailed explanation.

**Atypical grid usage** describes the possibility that a consumer only pays grid charges for the energy and power drawn within a high-load time window. This encourages the consumer to draw most of his load outside these high-load time windows, which makes the use of flexibility measures economically interesting (Weinand et al. 2021). A consumer can only apply for such an individual grid charge of atypical grid usage for a subsequent year. Whether an actual claim exists can in turn only be determined ex-post following the subsequent year. The high-load time windows are decisive for this.

These high-load time windows are determined by the distribution system operator by 31 October of each year for the following year. They are adapted to the grid load in the grid area and determined for each of five seasons (winter, spring, summer, autumn, and winter). A high-load time window describes a continuous period of a day to the nearest quarter of an hour, for example, between 2:15 pm and 4:00 pm of a day. Several time windows per day can be named, which in

turn can differ according to season. It is also possible to specify no high-load time windows for certain times of the year.

The individual grid charge then refers to the annual peak load within the high-load time window, which is multiplied by the corresponding capacity price of the grid operator. The energy component of the grid charges is not affected. However, the grid charge may not be less than 20% of the original grid charge without individual reduction. As a further economic incentive, consumers with less than 2,500 annual full load hours can also choose prices for at least 2,500 annual full load hours.

For atypical grid usage, the criteria of relevance threshold and relevance gap must also be met. The relevance threshold describes the percentage deviation between the peak load within the high-load time window and the load outside the time window. Depending on the voltage level, an amount of at least 5% (extra-high voltage level) and 30% (low voltage level) must be reached. The relevance gap describes the difference between the peak load within a high-load time window and that outside, which must be at least $100\ kW$. The introduction of the two relevance criteria is to promote active load shifting and to exclude possible "random finds".

However, the design of the individual grid charges pursuant to § 19 (2)(1) StromNEV shows large regional differences, as is already the case with the level of the regular grid charges. In addition, there is a strong annual variation. This variation relates less to the level of the capacity and energy prices than to the determination of the high-load time windows. These high-load time windows can vary considerably from year to year. This makes long-term planning more difficult.

Friedrichsen et al. (2016) and Weinand et al. (2021) have shown that the concept of atypical grid usage can support investment in flexibility measures. However, atypical grid usage can also promote energy inefficiencies if, for example, to comply with the relevance criteria, the load peaks outside the high-load time windows are increased without any production-related necessity. In addition, it remains questionable whether the rigid structure of annual high-load time windows is sufficient to cope with the dynamic grid load caused by an increasingly decentralised and intermittent energy system (Fraunhofer IFF 2020, p. 66). However, the basic principle of atypical grid usage can be understood as a first stage of time-variable grid charges, as called for by Fritz et al. (2021, p. 22). All the more, further designs of the regulatory principle (Seidl et al. 2018) as well as a more dynamic formation of high-load time windows (Connect Energy Economics GmbH et al. 2015) have already been discussed.

**Uniform electricity consumption** according to § 19 (2)(2) StromNEV as another type of individual grid charges enables energy-intensive industry, in particular, to reduce their grid charges, see Fraunhofer IFF (2020) for a more detailed explanation. It is aimed at companies that have an electricity consumption from the grid of more than $10\,GWh$ per year at one location with more than 7,000 annual full load hours. At present, these are mostly companies from the

aluminium, paper and chemical industries. Depending on the annual full load hours, a minimum share of the otherwise applicable grid fees must be paid. For at least

- 7,000 annual full load hours at least 20%,
- 7,500 annual full load hours at least 15%, and
- 8,000 annual full load hours at least 10%

shall be paid.

The assessment of the level of grid charges also considers the "physical path". This assumes a theoretical direct line to the nearest real generator capable of meeting the consumer's electricity demand. Such generation plants are usually conventional power plants. Particularly, due to the coal phase-out and the reduction of conventional power plant capacities, the physical paths and the associated individual grid charges may increase.

The regulation on uniform electricity consumption may well stimulate individual flexibility measures to achieve the minimum number of annual full load hours (Fraunhofer IFF 2020). However, this also encourages inefficiencies, as in the case of atypical grid usage, in that an increase in full load hours that is not necessary from a production perspective to reach the threshold could be economically advantageous. Uniform electricity consumption also precludes the provision of ancillary services, as these are either not allowed in combination or can negatively influence the level of grid charges. A detailed explanation of the obstacles of this regulation for the provision of system-beneficial flexibility is given by Seidl et al. (2018) and Fritz et al. (2021).

#### 2.4.3.3 Compliance with the European legal framework

However, the legality of the German grid charge regulation and in particular the regulation on the grid charge reduction for uniform electricity consumption is increasingly being questioned. In this context, the European court has assessed the grid charge exemption from 2012 and 2013 pursuant to § 19 (2)(2) StromNEV as unlawful aid within the meaning of European law. This ruling is currently still being appealed (Die BBH-Gruppe 2021). Nevertheless, this creates legal uncertainty that could result in repayments in the millions. These explicit uncertainties affect energy-intensive businesses in particular.

The ruling of the Court of Justice of the European Union (CJEU) (Der Gerichtshof der europäischen Union 2021) also contains much broader uncertainties for the entire electricity sector and calls into question the fundamental grid charge regulation. In this case, the CJEU upheld the European Commission's action against the Federal Republic of Germany. According to the court, Germany has not properly implemented the requirements of the EU Electricity and Gas Directives and has not properly considered the independence of the federal regulation authority (BNetzA) in setting grid charges (dpa 2021). What concrete effects this will have on the energy

sector cannot be estimated at this point. However, it cannot be assumed that the ruling will result in radical changes in German energy law in the short to medium term, which is also confirmed by the BNetzA in a press release (Bundesnetzagentur 2021-09-02). Anything else would be incompatible with the objective of "predictable and reliable framework conditions" (Bundesnetzagentur 2021-09-02, p. 2) and would also negatively affect the necessary investment security and thus system stability.

### 2.4.4 Ancillary services

Another possibility for marketing flexibility measures is to offer ancillary services. Ancillary services enable secure and stable grid operation, which is the core task of the grid operators according to § 11 EnWG. The ancillary services, which are the main responsibility of the transmission system operators (TSOs) according to § 13 EnWG, can be divided into the areas of frequency and voltage control, operational management and supply reconstruction (BDEW Bundesverband der Energie- und Wasserwirtschaft e.V. 2018, p. 6). Specifically, ancillary services for frequency control, balancing power, interruptible loads and balancing group settlement are explained in more detail below. Other services such as the provision of reactive power for voltage control, congestion management for optimised operation management or black start capabilities for supply reconstruction are only mentioned in passing. The latter services are less standardised and less transparent and are not the focus of this thesis.

#### 2.4.4.1 Balancing reserve

The European power grid oscillates across countries at a frequency of 50 Hz. In order for this frequency to remain constant at 50 Hz at all times, it is necessary that the generation and the load in the power grid are always balanced. If the ratio between generation and load deviates from this state of equilibrium, the frequency changes. If, from one moment to the next, the generation increases while the load remains constant, the power grid "overtorques" and the frequency increases; if the generation decreases while the load remains constant, the power grid "overloads" and the frequency decreases. The same applies in the opposite direction for an increasing or decreasing load with constant generation.

At least in the quarter-hourly or hourly range, a balance between generation and load is generally given via the electricity market. However, there can always be a mismatch between electricity supply and demand in the period up to a quarter-hour. For example, this is due to inaccurate forecast data, sudden weather changes or unforeseen power plant outages (Next Kraftwerke GmbH 2021b). This imbalance leads to frequency fluctuations that are easily measurable. In this context, figure 2.10 shows an example of the frequency curve as measured in the German power grid in May 2016.

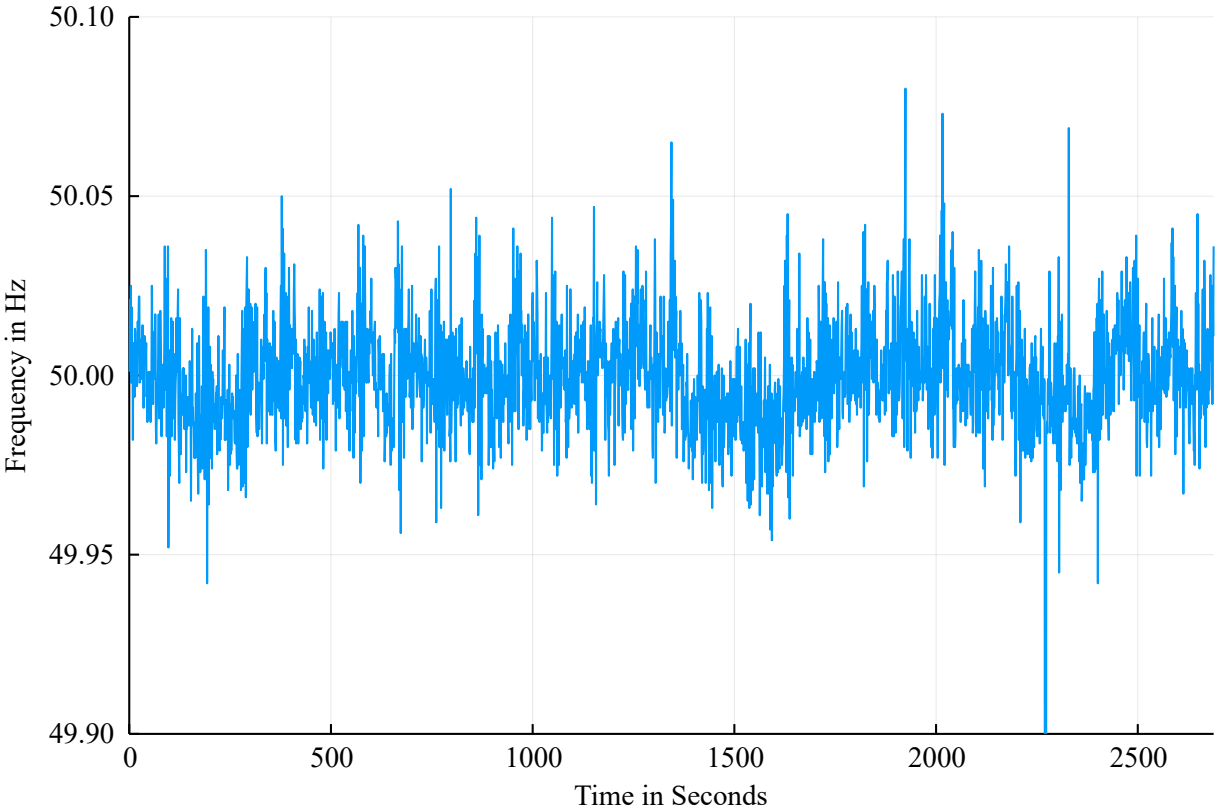


**Figure 2.10:** Frequency curve in second-by-second values in May 2016 in the European power grid, available on the homepage of 50Hertz Transmission GmbH (2022).

Figure 2.10 clearly shows that the measured frequency values fluctuate around the normal frequency of 50 Hz during the month. To balance these fluctuations, balancing reserves, in the form of energy or power, is needed. In this thesis, the power component is referred to as balancing reserve and the energy component as balancing energy. A distinction is made between positive and negative balancing reserve. Positive balancing reserve is required when the system is in a range smaller than 50 Hz and either additional power must be supplied to the system or load must be reduced. In the opposite case of negative balancing reserve, the frequency exceeds 50 Hz and power supplied to the system must be reduced or load increased.

The current system knows four[20] types of balancing reserve or energy, which can be distinguished primarily based on reaction time. First, the instantaneous reserve reacts to a frequency deviation. As the name suggests, the instantaneous reserve reacts at the exact moment of the frequency deviation. In the conventional power system, the instantaneous reserve is provided by the inertia of the rotating mass in conventional power plants, the rotating drive shaft. However, it can theoretically also be provided by electronic circuits in inverters or by the rotors in wind turbines.

[20] There is debate whether the instantaneous reserve should be counted as balancing reserve (Next Kraftwerke GmbH 2021a). In this thesis, it is included because in a future power system it may no longer be an intrinsic physical property of the power system due to the elimination of conventional rotating mass, but may have to be activated separately.

Since physical inertia is currently used, the instantaneous reserve does not have to be activated by a separate signal. However, it is not remunerated separately.

Following the instantaneous reserve, the primary, secondary and minute reserve power are activated, which are also named Frequency Containment Reserve (FCR), automatic Frequency Restoration Reserve (aFRR) and manual Frequency Restoration Reserve (mFRR) respectively. These three types are offered by energy plant operators and purchased by the transmission system operators (TSOs). Trading takes place on a separate control reserve market. Table 2.3 summarises the most important characteristics of the three types of control reserve.

In the first 30 seconds of the frequency deviation, the FCR is activated. FCR is automatically activated via the frequency measurement at the provider's location and activation occurs in both positive and negative directions. FCR is activated at a deviation from the normal frequency of 50 Hz plus/minus 0.01 Hz. Providers must have the assured FCR fully activated within 30 seconds and be able to maintain it for 15 minutes. FCR is offered for six time slices per day of four hours each and must be available at any time during a time slice. Until July 2019, FCR had to be provided in weekly time slices and until July 2020 in daily time slices. Market procurement takes place the day before each day, and the price is determined as a market clearing price per time slice. A balancing reserve quantity with an associated capacity price is offered.

| | FCR | aFRR | mFRR |
|---|---|---|---|
| Activation time | 30 seconds | 5 minutes | 15 minutes |
| Activation | Frequency controlled:<br>Independent measurement/intervention on site by FCR provider | By control zone-responsible TSO<br>- automatically replaces FCR. | By control area-responsible TSO<br>-manual request by TSO |
| Minimum bid size | $\pm 1MW$<br>(pos. and neg.) | $1MW$*<br>(pos. or neg.) | $1MW$*<br>(pos. or neg.) |
| Tender period | Daily<br>(for the next day) | Power: Daily<br>(for the next day)<br>Work: Up to 1 hour before activation | Power: Daily<br>(for the next day)<br>Work: Up to 1 hour before activation |
| Daily time division | 6 time slices with a duration of 4 hours each. | 6 time slices with a duration of 4 hours each. | 6 time slices with a duration of 4 hours each |
| Remuneration | Capacity price<br>(market-clearing) | Capacity price and energy price<br>(pay-as-bid) | Capacity price and energy price<br>(pay-as-bid) |

*For suppliers submitting only one bid per time slice and product.

**Table 2.3:** Balancing reserve market criteria according to Beucker et al. (2021, p. 14).

The FCR is replaced by the aFRR. This must be available after 30 seconds at the latest, be fully operational after five minutes at the latest and be maintained for 15 minutes. Similar to FCR, the auction takes place the day before for six time slices of 4 hours each per day. However, aFRR is offered either as positive or negative control reserve. aFRR is activated automatically by the responsible TSO. aFRR is followed by the mFRR, which is activated after 15 minutes. mFRR is activated either automatically or manually by the TSO. If the frequency deviation lasts

longer than one hour, the balancing group manager in whose balancing group the cause of the imbalance occurred takes over by adjusting the power plant schedules or by trading electricity on the electricity markets.

In the case of aFRR and mFRR, a balancing reserve quantity was offered until November 2020 together with a capacity price and an energy price. Since then, a balancing energy market (BEM) (SMARD 2020) has been introduced. Now, the balancing reserve auction continues to take place the day before. Here, a balancing reserve quantity is bid together with a capacity price. The accepted bid is remunerated according to the pay-as-bid procedure for the provision of balancing reserves. The actual activation of the balancing reserve or balancing energy is only organised via the BEM. Here, suppliers without an accepted balancing reserve bid may also submit bids in the form of balancing energy quantity and price. The bids are drawn up according to the merit order and awarded according to demand. Bids may also be submitted at short notice up to one hour before activation.

Suppliers of balancing reserves must be prequalified by the TSO. This includes, among other things, the fulfilment of the technical requirements for communication and control as well as a test run. The associated investments and expenses represent a non-negligible barrier to entry, which is, however, lower for the provision of aFRR and mFRR than for the provision of FCR power (Fraunhofer IFF 2020, p. 55). Another barrier is the minimum supply size. For plants that do not reach the threshold of $1\ MW$, it is necessary to pool the balancing reserve supply via an aggregator, which usually involves additional costs.

Since the end of 2006 and 2007 respectively, the mFRR, the aFRR and FCR have been jointly tendered by the four TSOs in Germany. The tendering is carried out via the internet platform *regelleistung.net*. In addition, the four TSOs have gathered in a grid control group to avoid, among other things, "balancing against each other" (EnBW Energie Baden-Württemberg AG 2010). Through the grid control group, the providers of aFRR and mFRR offer their ancillary services in the entire German grid area. The concept of the national grid control group is also to be extended to an international grid control group (Regelleistung.net 2021a). Since 2019, there is a cooperation between Austria and Germany for aFRR. FCR auctioned via *regelleistung.net* already includes several market participants outside Germany as well [21].

Figure 2.11 shows the tender volume for the different balancing reserve products as annual averages. It can be seen that the tendered balancing reserve quantity varies greatly between 2009 and 2020. This variation is due to a continuous change in the market structures, such as the reduction of the time slices, reduction of the minimum bid size, change in pricing, introduction of a balancing energy market or the expansion of the market area. This had an influence on both the tender quantity and the market participants and prices. The annual average values shown are

[21] Currently, FCR demand from the Netherlands (since 2014), Austria and Switzerland (since 2015), Belgium (since 2016), France (since 2017) and Denmark and Slovenia (since 2021) is also partly covered via *regelleistung.net*

taken from Bundesnetzagentur and Bundeskartellamt (2020) and show the tendered demand of the four German TSOs. Looking at the FCR demand for Germany only, it is striking that the demand has not changed. However, due to the integration of international grid operators, the FCR quantity offered via *regelleistung.net* has more than doubled since 2009, see red bars for "FCR, regelleistung.net". These formerly mentioned changes in market structure are one of the reasons why FCR prices are subject to high fluctuations (Kern 2021). Concerning the unchanged FCR demand, Hirth and Ziegenhagen (2015, p. 1041) name possible explanations, such as improvement in load and weather forecasting, reduced plant outages, and improved liquidity on the continuous intraday market.

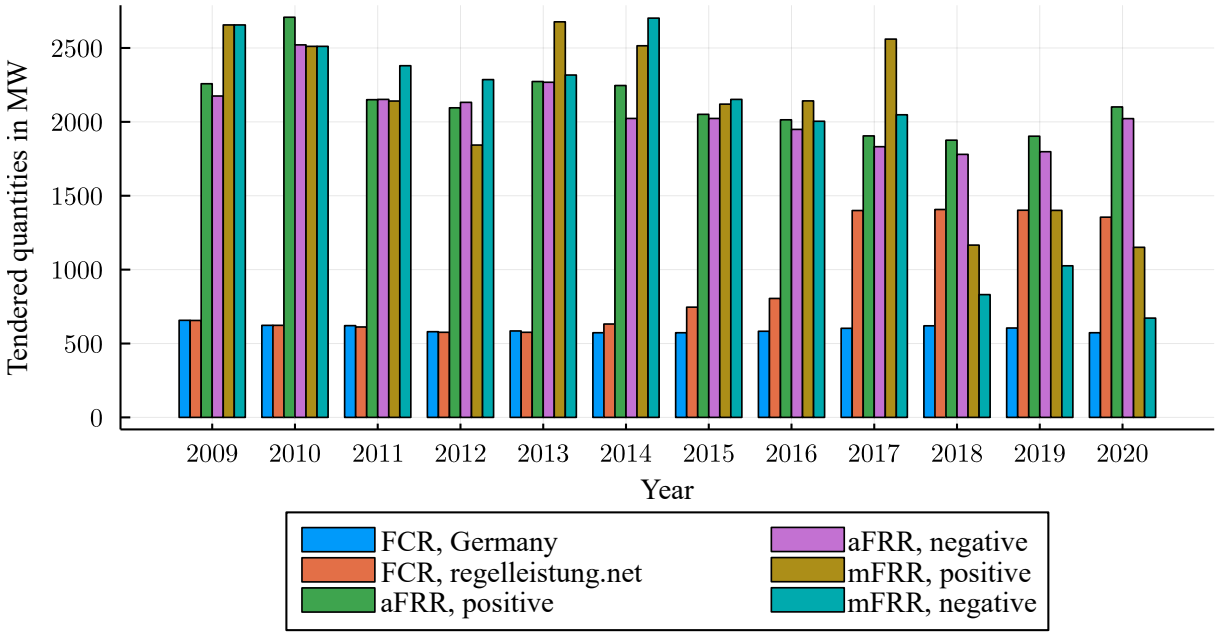


**Figure 2.11:** Tendered balancing reserve demand from the perspective of a German provider (Bundesnetzagentur and Bundeskartellamt 2020, Regelleistung.net 2021b).

#### 2.4.4.2 Interruptible loads

Another ancillary service to be mentioned is the interruptible loads according to the ordinance on interruptible load loads (AbLaV). These are used for system balancing, mostly in connection with mFRR, as well as for redispatch (Bundesnetzagentur and Bundeskartellamt 2022, p. 224). The interruptible loads are divided into immediately interruptible loads (SOL) and quickly interruptible loads (SNL). Both are traded weekly by the TSOs via the internet platform *regelleistung.net*. The capacity held in reserve is remunerated via a capacity price and the activated energy via an energy price. The activation period for which SOL or SNL are provided varies quarter-hourly between a quarter of an hour and eight hours. The minimum bid size is $5\,MW$ but can also be provided by forming a consortium. Here, all consortium members must be located at the same extra-high voltage node. In addition, the SOL and SNL providers must be connected at least at

the extra-high voltage level. The AbLaV, which regulates the procurement of interruptible loads, came into force in 2013, was amended in 2016 and was valid in this form until 01.07.2022.

The interruptible loads are intended to provide an "incentive for the voluntary disconnection of industrial processes" (Next Kraftwerke GmbH 2021c). However, the market situation, especially in the SOL market, can be described as oligopolistic (Fraunhofer IFF 2020, p. 60). According to Regelleistung.net (2020), there are four framework contracts between suppliers and TSOs for SOL, and at least 15 contracts for SNL. According to Bundesnetzagentur and Bundeskartellamt (2022, p. 223), there are a total of nine pre-qualified SOL facilities with a total interruptible capacity of $802\,MW$ and 41 SNL facilities with $1559\,MW$ respectively. However, the weekly demand is fixed in § 8 (1) AbLaV at $750\,MW$ each for SOL and SNL.

In 2020, interruptible loads were used on "nine days to maintain the system balance, i.e. comparable to balancing reserves" (Bundesnetzagentur and Bundeskartellamt 2022, S. 224). By reporting unavailability in due time, the offered services can be marketed on the day-ahead or balancing reserve markets. This makes interruptible loads attractive as a business model for those providers who are already active on other markets. Here, however, the revenues are offset by investments in control and communication technology, as well as high wear and tear costs due to the rapid start-up and shutdown of industrial processes (Fraunhofer IFF 2020, p. 60-61).

The counterpart to interruptible loads at transmission grid level are the "controllable consumption facilities", formerly "interruptible consumption units", at distribution grid level. These are regulated in § 14a EnWG. This regulation addresses, for example, night storage heaters, heat pumps, cooling systems and explicitly electric mobility (Fraunhofer IFF 2020, p. 62). According to this, suppliers in the low-voltage sector can negotiate a reduced grid charge with their DSO, provided they enable the grid-beneficial control of a part of their facilities. Bundesnetzagentur and Bundeskartellamt (2022, p. 199) counts about 1.8 million controllable consumption facilities at more than 80% of the DSOs; significantly more than half are offered in North Rhine-Westphalia, Baden-Württemberg and Bavaria. According to Bundesnetzagentur and Bundeskartellamt (2022, p. 200), an "average reduction of the grid charge of approximately 57%, which corresponds to an average absolute reduction of 3.76 ct/kWh", with a maximum value of 84% and a minimum value of 5%.

Around 94% of the controllable facilities are either night storage (64%) or heat pumps (33%) (Bundesnetzagentur and Bundeskartellamt 2022, p. 200)[22]. Only 1% is attributable to electric mobility. "In future, all installations [...] must be mandatorily equipped with an intelligent metering system." (Bundesnetzagentur and Bundeskartellamt 2022, S. 201). However, to date, "intelligent control" is only possible for a small proportion of facilities, as many are still controlled by timers. This represents an obstacle to grid-beneficial control (Fraunhofer IFF 2020, p. 63). § 14a (1)(3) EnWG empowers the Federal Government to specify the requirements by ordinance.

[22] As of July 2021.

However, up to now, there is neither a preliminary regulation on this nor an amendment to § 14a. Possible redesigns have already been discussed, among others, in an expert opinion commissioned by the Federal Ministry for Economic Affairs and Energy (BMWi) (Zander et al. 2018) or by Dreisbusch et al. (2020).

#### 2.4.4.3 Other ancillary services

In addition to frequency regulation, the other ancillary services, voltage control, operational management and supply restoration, are summarised in the non-frequency ancillary services. For these non-frequency ancillary services, the European Electricity Market Directive (2019/944/EU, Article 40(5)) requires member states to procure them on a market basis or at least to evaluate the efficiency of such a market. Germany implemented this directive on 27 November 2020 with the "Act amending the EnWG on market-based procurement of ancillary services" and in this context newly introduced § 12h EnWG. § 12h names the following ancillary services:

1. "services for voltage regulation", primarily the provision of reactive power,
2. "inertia of local grid stability", primarily instantaneous reserve,
3. "short-circuit current", primarily the initial short-circuit current through synchronous machines,
4. "dynamic reactive current support", primarily the voltage maintenance in case of fault,
5. "black start capability", the ability of a plant to resume operation without external support, and
6. "island operation capability", the ability to regulate voltage and frequency in an isolated network operation.

According to § 12h EnWG, it is the task of the BNetzA to evaluate the possibilities of "transparent, non-discriminatory and market-based" procurement. If this type of procurement is deemed to be economically inefficient, the BNetzA must define an exception for the corresponding service and specify an alternative procurement. If market-based procurement is assessed as efficient, the BNetzA must specify the rules of such a market (Halbig 2021, p. 10). The efficiency question was examined in an expert report by Schlecht et al. (2020). The Ruling Chamber 6 of the BNetzA followed this assessment and ruled out economic efficiency for all non-frequency ancillary services except for the "voltage regulation service" and the "black start capability", see Beschlusskammer 6 (2020).

The implementation possibilities of a market for the procurement of reactive power (voltage regulation) and for the contracting of black-start capable plants have already been discussed in detail in the expert reports by Blumberg et al. (2021) and Wagner et al. (2020). Currently, however, no market specifications are in force. However, on 20.12.2021 BNetzA opened two

specification procedures for “black start capability”. In one, the distribution system operators are to be exempted from market procurement (Beschlusskammer 6 2021a), in the other, the market structures are to be specified for procurement by the TSOs (Beschlusskammer 6 2021b).

# 3 Methodology

To support the investment and dispatch decision for a BSS, energy modelling techniques can be used (Gargiulo and Gallachóir 2013). In this field, Ringkjøb et al. (2018, p. 444) distinguish between three methodological approaches: simulation models, optimisation models and equilibrium models. To narrow down the broad field of energy modelling and to focus on the core of this thesis, the following section explicitly addresses the methodology of optimisation models.

The optimisation model or problem can be differentiated according to certain criteria. First and foremost, the

- the differentiation according to problem classes and
- the differentiation according to the way uncertainties are considered.

These criteria are explained in more detail in the following two sections, Section 3.1 and Section 3.2. The explanations serve to facilitate the understanding of the basic structure of the optimisation models used in this thesis. These optimisation models are described in Section 3.3 briefly to clarify how the models are built on top of each other. A detailed description can be found in the publications in Part II.

## 3.1 Problem classes

The optimisation problem classes can be divided into linear and non-linear classes. These subclasses can be further distinguished between problems with only continuous variables, linear problems (LP) and nonlinear problems (NLP), or with additional integer variables, mixed-integer linear problems (MILP) and mixed-integer nonlinear problems (MINLP). With reference to mathematical programming, the problems are also called programmes. Before the program classes are explained, the optimisation model and its standard form is briefly recapitulated.

In a decision-making process, an optimisation model calculates the optimal path to achieve a goal (Dantzig 2002, p. 42). In an economic sense, this often means finding the minimum-cost use of resources. The general formulation of an optimisation problem is as follows:

$$\min_{x \in \mathbb{R}^n} \quad z = f(\boldsymbol{x}) \tag{3.1}$$

$$s.t. \quad g_i(\boldsymbol{x}) = 0, \forall i \in \{1, 2, ..., p\} \tag{3.2}$$

$$h_j(\boldsymbol{x}) \leq 0, \forall j \in \{1, 2, ..., q\} \tag{3.3}$$

Accordingly, Equation 3.1 represents the objective function or cost function of the vector $\boldsymbol{x}$. $\boldsymbol{x}$ is an n-dimensional vector that contains all decision variables. The optimal size of the decision variables in $\boldsymbol{x}$ is determined via the objective function. In addition, the optimal solution must satisfy the constraints given as the equality constraint (Equation 3.2) and the inequality constraint (Equation 3.3) (Graichen 2016, p. 2). The solution of the optimisation problem thus describes a decision vector $\boldsymbol{x}$ which yields a minimum value for the objective function $z$ without violating any of the constraints.

**Linear problems** have the property that all equations in the objective function and constraints are linear and the decision variables are continuous. "Linear programming is the best developed part" (Zimmermann 2008, p. 68) of optimisation and can "still be solved relatively easily" (Kallrath 2013, p. 16). However, the development of an LP is usually accompanied by the need to abstract reality, which leads to inaccuracies in the model results. Thus, often actually non-linear correlations are only represented in a linearised way or continuous quantities are assumed, although, in reality, only whole numbered quantities are possible. The "best known method" (Kallrath 2013, p. 72) for solving LP is the *simplex* method. As other solution approaches, the solution of the dual problem, the interior point method or the ellipsoid method can also be mentioned (Rominger 2020, p. 36). All LP are convex and thus an exact solution with a local optimum as a simultaneous global optimum is possible (Schwarz et al. 2018, p. 46).

**Mixed integer linear problems** (MILP) consider the decision variables to be partially discrete. This means that they are either binary or integer. Solving such problems can be much more computationally complex than solving LP, which is also indicated by the exponential increase in the computational runtime to solve the MILP depending on the number of discrete variables (Kallrath 2013, p. 16). However, real processes can be represented more accurately in this way, such as the must-run condition of power plants or the minimum output of combined heat and power (CHP) plants (Braeuer et al. 2022). Furthermore, a piecewise linearisation of non-linear processes is possible through the formulation, such as decreasing marginal costs for large investments (Merkel 2016). In the same way, whole numbered supply or demand quantities can also be represented, as in the electricity markets.

Heuristics can be used to solve MILP, but also exact methods such as the *Branch&Bound*- or *Branch&Cut*-method. In the last two cases, the MILP is relaxed and represented as several

sub-problems in the form of an LP. By solving the sub-problems, the solution space in which the global optimum is located can be narrowed down step-by-step. The optimal solutions of the relaxed sub-problems represent the boundary values of the MILP solution space. This makes it possible to approach the global optimum. Finding a sufficiently exact solution is not possible for many MILP even with current computational technology (Schwarz et al. 2018, p. 47).

**Nonlinear problems** have a non-linear equation in either the objective function, one of the constraints, or both. The problems can contain either only continuous decision variables (NLP) or also integer ones (MINLP). In contrast to linear problems, the solution space is not necessarily convex, which means that several local and global optima can occur (Zimmermann 2008, p. 188). This creates the dilemma of some solution approaches that the optimality of a point cannot be guaranteed. This can cause a solution algorithm to get "stuck" at a local minimum (Rominger 2020, p. 37). Stein (2021) presents possible solution methods for an NLP, such as the convex relaxation approach that extends the feasibility space.

NLP or MINLP offer the possibility to represent reality with relatively high accuracy compared to linear models. However, this is accompanied by a relatively high degree of computational complexity and runtime for the solution of such a problem.

## 3.2 Consideration of uncertainties

Optimisation models can also be distinguished according to the way they account for uncertainties. Following Schwarz (2019, p. 49), Svetlova and van Elst (2013, p. 1), Stirling (2003, p. 124) and Oehmen et al. (2020, p.331), this thesis divides uncertainty into three subgroups: risk, uncertainty as ambiguity and uncertainty as ignorance. Risk is to be understood without value judgement as the possibility of a future realisation of a known event or state, where also the probability of this realisation is known. In the case of ambiguity, the event or state is known, but the probability of realisation is not. Finally, ignorance describes the state in which neither the event nor state nor the probability of realisation is known.

One way to distinguish models regarding uncertainty is to use the following four subgroups:

- deterministic optimisation,
- sensitivity and scenario analysis,
- robust optimisation and regret minimisation, and
- stochastic programming.

**Deterministic optimisation** explicitly does not consider uncertainties. It is assumed that all future states are known and will occur in this way. Compared to stochastic programming, the computational complexity is relatively low. This offers the possibility to better address system details than with stochastic models (Rebennack 2010, p. 45). Among other things, this allows insights into techno-economic relationships that are not intuitively apparent. In addition, the results of deterministic investigations are well suited as a benchmark for other possible investigations of uncertainties.

**Sensitivity and scenario analysis** represents a "very common and classical form" (Schwarz et al. 2018, p. 52) to investigate the influence of uncertainties on deterministic model results. A good overview of sensitivity and scenario analyses is provided by Borgonovo and Plischke (2016), Saltelli et al. (2000), Ward and Wendell (1990), Mietzner (2010). In sensitivity analysis, either the objective function or the input parameters are varied. This makes it possible to gain insight into how the model behaves when the assumed structure changes or input parameters deviate from the assumed values. In this sense, sensitivity analysis can be distinguished between a local (for example *one factor at a time*) and a global (for example *monte carlo*) analysis (Borgonovo and Plischke 2016, p. 869).

Scenario analysis is less concerned with model behaviour; rather, it serves to determine an action plan for future events by analysing "the results of the more extreme outcomes (with high probability and/or more severe impacts)" (Balaman 2018, p. 139). Possible developments and future states of individual model parameters are combined into scenarios. This creates a scenario funnel that expands further with each time step into the future. Thereby, it ensures that the difference among the scenarios increases the further one looks into the future. This wide-ranging scenario space ultimately offers the possibility of identifying a best-case or desired scenario, as well as a trend scenario and a worst-case scenario.

**Stochastic programming** or stochastic optimisation is considered a very popular method, especially for decision support in investment and operational planning (Lara et al. 2019, p. 2). A detailed basic treatment can be found in Kall and Wallace (1997) and Birge and Louveaux (2011). It deals with the risk part of the uncertainty definition, where the outcome of a future event and its associated probability distribution is known. In stochastic programming, the problem is divided into decision stages, which are lined up in chronological order. The first stage is called the *here-and-now* stage. In this initial stage, the decision is made deterministically without knowing the realisation of uncertain states in the future. In the investment and dispatch planning stage of an asset, the investment is decided without knowing exactly how it will be dispatched in the future. The second and all subsequent stages are called *Wait-and-See* stages which means that a decision at this stage has to be made only when it is known how the future will develop, i.e. the realisation of an uncertain future state is known. It is immanent at each stage that, at the time of

the decision, all previous decisions and realisations are known, but all decisions and realisations of the following stages are uncertain. If the stochastic programme consists of only two stages, it is called a two-stage stochastic programme; if there are more than two stages, it is called a multi-stage stochastic programme.

Stochastic programming has the advantage of determining less conservative decisions than robust programming (Lara et al. 2019, p. 2), explained in the final segment of this section. The decision considers a finite number of possible states, of which the probability distribution is known. However, this distribution is also a disadvantage of stochastic programming, since the result of the optimisation can strongly depend on the assumed probability distribution (Lara et al. 2019, p. 2).

In solving stochastic programmes, Rebennack (2010, p. 44) distinguishes between a scenario-based approach and a sample-based approach. The scenario-based approach is sometimes also understood as the LP approach. Here, possible scenarios with an associated probability of realisation are derived from the random space under consideration. Using these scenarios, a scenario tree can be built and the deterministic equivalent to the stochastic programme can be derived. This can be solved with known deterministic optimisation methods. Especially, two-stage optimisation models can be solved with a large number of scenarios. In the multi-stage case, however, the number of scenarios is relatively limited because the computational complexity of the model increases exponentially with each stage.

The sample-based solutions usually refer to dynamic programming approaches. Here, the stochastic programme is subdivided into recursive, single-stage programmes using decomposition methods (Rebennack 2010, p. 49). In this way, especially the exponentially growing complexity of multi-stage stochastic optimisation models can be mastered. The decomposition approaches have been researched in detail and can in turn be divided into scenario-based and stage-based approaches, which usually use the Lagrange method and the Benders method respectively (Lara et al. 2019, p. 3).

**The robust optimisation** considers the worst-case scenario, in the sense that the optimisation model is only calculated for the worst possible case (Birge and Louveaux 2011, p. 86). This "guarantees feasibility" (Lara et al. 2019, p. 2) of the decision and, at the same time, other future scenarios do not have to be considered. This is achieved through a relatively low computational effort compared to stochastic programming. Due to the focus on the worst-case, the decision must be regarded as "more conservative" (Lara et al. 2019, p. 2) or even "extremely pessimistic" (Schwarz et al. 2018, p. 59). However, an advantage of robust optimisation, apart from the relatively low computational complexity, is that no knowledge about the probability of realisation of the scenarios is required, which makes robust optimisation particularly suitable for mapping uncertainties as ambiguities. A further discussion of robust optimisation is provided by Ben-Tal (2009).

Regret minimisation can be seen as an extension of robust optimisation, as applied by Schwarz et al. (2018). Regret is the deviation from the best possible decision (Birge and Louveaux 2011, p. 90). Here, the worst- and best-case scenarios are combined. The optimal solution indicates at which point in the worst-case the regret is minimal. From the conceptual structure of robust optimisation and regret minimisation, it is evident that the result depends on the selected scenarios and that such models can react sensitively to extreme scenarios.

Another variation of robust optimisation is stochastic p-robust optimisation, as described in Snyder and Daskin (2006). It combines stochastic programming, where the optimum does not hold in every scenario, with robust optimisation, where the optimum is determined only for a worst-case scenario with very low probability of realisation. The result achieves "the highest level of profit and the lowest level of regret. (Najafi-Ghalelou et al. 2022, p. 7). The level of regret is determined by the robustness level $p$. This approach combines the advantages of stochastic programming and robust optimisation. Cai et al. (2022, p. 456) show, in the case of a virtual power plant, that a "robust operation of the system under the worst-case scenario" can be achieved, with only a small increase in operational costs compared to a stochastic programming approach. Similar observations are made by Sriyakul and Jermsittiparsert (2020) for the charging schedule of an electric vehicle fleet. For the scheduling of a microgrid, Mazidi et al. (2019, p. 253) show that the approach is "adjustably robust and computationally tractable and also financially effective at the same time".

Li et al. (2022) lists two other variations of robust optimisation, distributionally robust optimisation (DRO) and hybrid stochastic robust optimisation (HSRO). DRO addresses the drawback of stochastic programming that the probability distribution of the random variables under consideration must be known, and that stochastic programming is not applicable if "ambiguity in the choice of a distribution for the random parameters" (Delage and Ye 2010, p. 595) exists. Accordingly, "DRO minimises the worst-case expected cost over an ambiguity set" (Li et al. 2022, p. 670). The ambiguity set describes the set of possible distributions of the random variables. The creation of different ambiguity sets for the operation of energy hubs is presented at Zhao et al. (2020), Ding and McCulloch (2021), Xu et al. (2020) and Parvar and Nazaripouya (2022). DRO offers computational advantages over stochastic programming and "clear statistical interpretations, and the conservatism of solutions can be significantly ameliorated" (Shang and You 2018, p. 920).

HSRO combines stochastic programming with robust optimization in such a way that they "deal with different uncertainty sources" (Li et al. 2022, p. 671). Thus, Zare Oskouei et al. (2021) optimise the dispatch plan of a multi-energy-retailer, where the uncertain energy demand is mapped via scenarios in a stochastic programme. The uncertainty in market prices is integrated into the stochastic programme as a sub-problem via a robust optimisation approach. For a multi-energy system, Nasiri et al. (2021) combines the stochastic dispatch problem with a robust wind generation problem. In Liu et al. (2016), a stochastic program defines the day-ahead micro-grid

schedule, while a robust formulation balances real-time energy demand. As a result, the proposed hybrid model is "robust against uncertain real-time market prices" (Liu et al. 2016, 235). With the HSRO, the decision is less conservative than in a pure robust optimisation and random variables without knowledge of their distribution can be integrated. Additionally, random variables where the worst-case should be considered can be integrated into a stochastic program. Finally, through a robust control parameter or uncertainty budget $\Gamma$ the risk acceptance level of the decision makers can be considered.

## 3.3 The BSS-opt-model

The previous section showed the manifold ways to deal with uncertainty in optimisation models. In this thesis, an optimisation model is developed for the investment and dispatch planning of a BSS in an industrial manufacturing plant. The base model referred to as the BSS-opt-model is described as a deterministic LP. It allows the initial investigation of technical and economic dependencies. Furthermore, the BSS-opt-model is adapted and extended with reference to the respective research question and consideration of various uncertainties. The BSS-opt-model and its extensions are described in detail in the publications associated with this thesis, in Part II. In this section, the methodological approach will only be summarised to generate a coherent understanding.

### 3.3.1 Base model

The base model is described in detail in Publication A and provides the methodological basis for the further publications B, C and D.

Figure 3.1 represents the base model graphically and illustrates the most important power and energy flows as well as the underlying economic application possibilities of a BSS in an industrial enterprise. The underlying concept of the model is that an industrial company has to meet its energy demand, which comes mostly from production. This demand is given as an exogenous load profile and cannot be changed by the model. The demand is met by purchasing electricity from the power grid. Now there is the possibility for the industrial company to install a BSS and use it in different business models, especially the provision of frequency containment reserve, peak shaving and arbitrage on the day-ahead and intraday market.

Figure 3.1 shows the electricity flow with blue arrows and an $x$, whereas the power flows are shown with red arrows and a $P$. Thus, the production load on the left-hand side can be covered either by direct purchase from the power grid or via intermediate storage in the BSS. For the use of the BSS, it must be decided how much reserve power is to be offered on the FCR market. A corresponding amount of BSS capacity must be blocked for these FCR activities ($cap^{FCR}$). The

remaining idle capacity of the BSS can now be used for peak shaving or arbitrage trading on the energy markets. For a more detailed explanation of the business models, see Section 2.4.

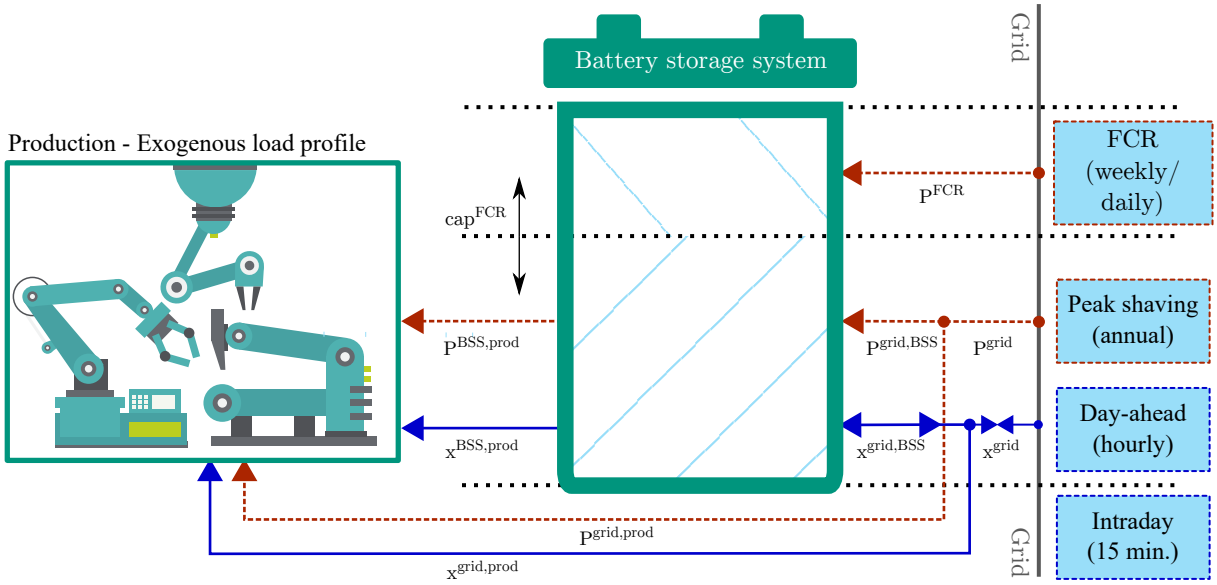


**Figure 3.1:** Graphical representation of the BSS-opt-model according to Braeuer et al. (2019b, p. 1428).

The optimisation model identifies the optimal size or capacity of the BSS in which the industrial company should invest, as well as the optimal dispatch of the BSS, at what time it is charged and discharged and how much capacity is kept available for the reserve power market. Here, the optimum is defined by the economic objective function that minimises the total costs, see equation 3.4. For the total cost calculation, the annuity payment for the investment in the BSS ($Ann^{BSS}$) is considered, as well as the costs for buying and selling electricity on the energy markets, Intraday ($x^{ID} \cdot c^{ID}$) and Day-Ahead ($x^{DA} \cdot c^{DA}$), the revenue from offering FCR ($P^{FCR} \cdot c^{FCR}$) and the annual cost of grid charges ($P^{peak} \cdot c^{peak}$). The additional expenses incurred due to the ageing of the BSS are also considered ($Ann^{BSSaged}$).

$$\begin{aligned} \min cost = & Ann^{BSS} + Ann^{BSSaged} + \\ & \sum_{w=1}^{52} \left( \sum_{h=1}^{168} \left( \sum_{q=1}^{4} (x^{ID}_{q,h,w} \cdot c^{ID}_{q,h,w}) + x^{DA}_{h,w} \cdot c^{DA}_{h,w} \right) - \right. \\ & \left. P^{FCR}_{w} \cdot c^{FCR}_{w} \right) + \\ & + P^{peak} \cdot c^{peak} \end{aligned} \tag{3.4}$$

The base model is calculated in 15-minute steps for a whole year. To get a better impression of the model, four more essential constraints are listed below. Thus, in the model, in every time step (every quarter-hour $q$ out of every hour $h$ in every week $w$), the energy demand from

the production of the industrial enterprise ($d_{q,h,w}$) must be satisfied, see equation 3.5. This is done either by discharging the BSS ($x_{q,h,w}^{BSS,prod}$) or by drawing electricity from the power grid ($x_{q,h,w}^{grid,prod}$). Equation 3.6 indicates that when the BSS is discharged, the electricity either flows into the production ($x_{q,h,w}^{BSS,prod}$) or is fed into the grid ($x_{q,h,w}^{BSS,grid}$). This amount of electricity must not be greater than the installed BSS capacity ($cap^{BSS}$) minus the weekly capacity blocked for FCR provision ($cap_w^{FCR}$). As described in equation 3.7, this FCR capacity is calculated via the weekly reserve power offered on the FCR market ($P_w^{FCR}$) multiplied by a buffer factor ($r^{FCR,puff}$). Finally, equation 3.8 describes peak shaving, in which the model is required to keep the annual peak load ($P^{peak}$) as low as possible. Accordingly, the electricity drawn from the grid ($x_{q,h,w}^{grid}$) must not be greater at any time step than the peak load[1].

$$d_{q,h,w} = x_{q,h,w}^{BSS,prod} + x_{q,h,w}^{grid,prod} \qquad \forall q,h,w \tag{3.5}$$

$$x_{q,h,w}^{BSS,grid} + x_{q,h,w}^{BSS,prod} \leq cap^{BSS} - cap_w^{FCR} \qquad \forall q,h,w \tag{3.6}$$

$$cap_w^{FCR} = r^{FCR,puff} \cdot P_w^{FCR} \qquad \forall w \tag{3.7}$$

$$P^{peak} \geq x_{q,h,w}^{grid} \cdot \frac{4}{1000} \qquad \forall q,h,w \tag{3.8}$$

The decision variables of the base model are the installed BSS capacity, and the energy quantities for charging and discharging the BSS, such as the energy purchase and the feed-in from and into the general power grid. Additional decision variables are the amount of energy traded on the energy markets as well as offered FCR quantities and the BSS capacity blocked by FCR trading.

The basic assumptions of the base model are the following:

- In the energy and reserve power markets, the respective buy and sell bids of the industrial enterprise under consideration are always awarded. The enterprise only acts as a price-taker on the respective markets.
- The calculated year is considered representative for the entire investment period.
- Perfect foresight prevails. This means that demand and prices are known for each time step at the time of the investment.

[1] The factor $\frac{4}{1000}$ is used to convert the unit energy into the unit power

### 3.3.2 Stochastic programming and robust optimisation

One of the assumptions of the base model is perfect foresight, which, as described in Section 3.2, comes with large uncertainties related to the informativeness of the result. To address these uncertainties, Publication B and Publication C present an extension of the base model that considers uncertain future load behaviour as well as uncertain future price patterns using stochastic programming and robust optimisation.

In reality, the economic decisions for the different revenue streams are strongly dependent on each other but are made at different points in time. Taking this temporal sequence into account is a challenge, as this is accompanied by a considerable increase in model complexity. Therefore, when extending the model, it must be considered which uncertainties are included and in what way. Publication B and Publication C present different approaches in this context, which focus on different revenue streams. Thus, the model in Publication B integrates as a two-stage robust optimisation the uncertain intraday activities as well as possible load deviations. These represent the short-term decisions and offer the possibility to react to previously made decisions. The model from Publication C, as a multi-stage model, focuses on the temporal sequence of different decisions. The following subsection, first, presents the two-stage robust optimisation model and, second, the two-stage and multi-stage stochastic optimisation approach.

#### 3.3.2.1 Two-stage robust optimisation

Publication B considers the uncertainty of market prices and load demand. In addition, the base model is extended to include the possibility of installing a PV module and benefiting from self-consumption of the generated PV electricity. At the same time, the uncertainty of solar radiation is considered. Finally, additional demand flexibility is integrated into the extended model as part of the load demand can also be unnerved.

The model, referred to as *BSS-robust-model* for this thesis, is formulated as a two-stage stochastic problem in the form of an MILP. Equation 3.9 shows the objective function for this. In the first stage, the investment and market decisions are made on the day-ahead and FCR markets. The stochastic uncertainty of the day-ahead and FCR prices enters the model via the weighted average price so that the decision on these two markets is made with perfect foresight. In the second stage, with knowledge of the realisation of the first stage, the decision is made on the BSS dispatch and the quantities of electricity purchased on the intraday market. The intraday behaviour is formulated as a robust optimisation problem to account for the pay-as-bid market structure and the continuous bidding process.

In equation 3.9, the first four rows indicate the first stage. The fifth and last row define the second stage and consider possible price realisations via the average intraday price ($c^{ID}_{q,h,w,s}$) from the scenarios $S$. Matching this, an optimal decision is made for the amount of electricity purchased

on the intraday market ($x^{ID}_{q,h,w,s}$) and for the unserved load demand ($u_{q,h,w,s}$), which is priced with a penalty term ($c^{VoLL}$).

$$
\begin{aligned}
\min_{\Psi} cost =& Ann^{BSS} + Ann^{PV} + \\
& P^{peak} \cdot c^{peak} + \\
& \sum_{w=1}^{W} \rho_w \cdot \left( \sum_{h=1}^{H} \left( x^{DA}_{h,w} \cdot (c^{fees} + \sum_{s=1}^{S} \pi_{w,s} \cdot c^{DA}_{h,w,s}) \right) - \right. \\
& P^{FCR}_{w} \cdot \sum_{s=1}^{S} \pi_{w,s} \cdot c^{FCR}_{w,s} + \\
& \left. \sum_{s=1}^{S} \pi_{w,s} \cdot \sum_{h=1}^{H} \sum_{q=1}^{Q} \left( x^{ID}_{q,h,w,s} \cdot (c^{fees} + c^{ID}_{q,h,w,s}) + u_{q,h,w,s} \cdot c^{VoLL} \right) \right) + \\
& \max_{bin_{q,w,h,s}} \sum_{w=1}^{W} \rho_w \cdot \left( \sum_{h=1}^{H} \sum_{q=1}^{Q} \sum_{s=1}^{S} \pi_{w,s} \cdot x^{ID}_{q,h,w,s} \cdot \Delta c^{ID}_{q,h,w,s} \cdot bin_{q,h,w,s} \right), \\
\Psi =& \{ x^{DA}_{h,w}, x^{ID}_{q,h,w,s}, P^{FCR}_{w}, u_{q,h,w,s}, P^{peak}, cap^{BSS}, Pcap^{BSS}, cap^{PV} \}
\end{aligned}
\tag{3.9}
$$

$$
\sum_{h=1}^{H} \sum_{q=1}^{Q} bin_{q,h,w,s} \leq \Gamma, \qquad \forall w, s \tag{3.10}
$$

$$
0 \leq bin_{q,h,w,s} \leq 1, \qquad \forall q, h, w, s \tag{3.11}
$$

The last line represents the robust decision-making and maximises as a sub-problem the damage that can occur in intraday trading. The damage is caused by adding the maximum price deviation on the intraday market ($\Delta c^{ID}_{q,h,w,s}$) for the corresponding time step. Whether the maximum intraday price is thereby paid in a time step depends on the relaxed binary decision variable $bin_{q,h,w,s}$. This binary variable depends on the uncertainty budget $\Gamma$ in equation 3.10. $\Gamma$ represents in how many time steps the maximum price should be considered. With a value of $0$, only the average price is assumed and no further uncertainty due to price deviations is considered. At most, $\Gamma$ can assume the value of the product of $H$ and $Q$, so that the maximum price is assumed in every time step. To solve the optimisation problem with two opposite objectives (minimisation and maximisation), the sub-problem of maximising the damage in Publication B is reformulated as a dual problem[2].

[2] For further explanation of the dual problem, see, among others, Kallrath (2013, p. 324 ff.).

#### 3.3.2.2 Two-stage and multi-stage stochastic optimisation

The model extension in Publication C considers the sequence of different uncertain market decisions. For this purpose, the base model is developed into a two-stage stochastic optimisation problem (*BSS-two-stg-model*) as well as a multi-stage stochastic optimisation problem. Both models are formulated as deterministic equivalents in the form of an LP.

Equation 3.12 represents the objective function of the BSS-two-stg-model. Analogous to the BSS-robust model, the investment decision is made at the first stage and the annual peak load is determined for peak shaving. In contrast to the BSS-robust-model, however, the costs due to battery ageing are considered ($Ann^{BSSaged}$). These depend on the dispatch decision of the BSS at the second stage and are included as a weighted average value over all time steps for each possible realisation of the second stage. An additional distinction is that all market decisions are made at the second stage after the investment decision, see lines 3 and 4 in equation 3.12. The market and BSS dispatch decisions take place simultaneously. Thus, there is knowledge of which price or demand scenario has been realised and which decision has been made on the FCR market, the day-ahead market as well as the intraday market. The consecutive order of these decisions, in reality, is therefore neglected.

To better represent this consecutive order, in Publication C the base model is also formulated as a multi-stage optimisation problem (*BSS-mult-stg-model*). The multi-stage stochastic problem is solved via a scenario tree. The objective function of the deterministic equivalent derived from this is captured in equation 3.13. In the model, as in the two-stage case, the investment decision, as well as the decision on the peak load, is made at the first stage. The first stage is followed by an FCR stage from the set $\gamma fcr$, where the FCR decision for the first time frame is made, see line 4 in equation 3.13. The FCR stage is followed by an arbitrage stage from the set $\gamma arb$. Here, in relation to the first time frame, both the decisions on the day-ahead and intraday market are made as well as the dispatch decision of the BSS, see line 3 in equation 3.13. This stage is followed by the second time frame starting with an FCR stage, followed by an arbitrage stage. This order continues depending on how many time frames are considered. The BSS ageing costs are considered as a weighted average cost over all considered multi-stage scenarios, see line 2 in equation 3.13.

$$
\begin{aligned}
\min cost = & Ann^{BSS} + P^{peak} \cdot c^{peak} + \\
& Ann^{BSaged} + \\
& \sum_{w} \left( \rho_w \sum_{s} \pi_{w,s} \cdot \left( \sum_{h} \left( \sum_{q} \left( x^{ID}_{q,h,w,s} \cdot c^{ID}_{q,h,w,s} \right) + x^{DA}_{h,w,s} \cdot c^{DA}_{h,w,s} \right) - \right. \right. \\
& \left. \left. P^{FCR}_{w,s} \cdot c^{FCR}_{w,s} \right) \right), \\
& with \sum_{s} \pi_{w,s} = 1 \; \forall w
\end{aligned}
\tag{3.12}
$$

$$
\begin{aligned}
\min cost = & Ann^{BSS} + P^{peak} \cdot c^{peak} + \\
& \sum_{sc} \left( \pi_{sc} \cdot Ann^{BSaged}_{sc} \right) + \\
& \sum_{n \in S_{\gamma arb}} \left( \pi_n \cdot \rho_n \cdot \sum_{h} \left( \sum_{q} \left( x^{ID}_{q,h,n} \cdot c^{ID}_{q,h,n} \right) + x^{DA}_{h,n} \cdot c^{DA}_{h,n} \right) \right) + \\
& \sum_{n \in S_{\gamma fcr}} \left( \pi_n \cdot \rho_n \cdot (-P^{FCR}_{n}) \cdot c^{FCR}_{n} \right), \\
& with \sum_{n \in S_\gamma} \pi_n = 1 \; \forall \gamma \; and \sum_{sc} \pi_{sc} = 1
\end{aligned}
\tag{3.13}
$$

### 3.3.3 $CO_2$-minimal dispatch

The base model is used in Publication D and extended to investigate an ecologically optimal use of the BSS (BSS-$CO_2$-model). The ecological optimum was formulated as the objective to minimise the $CO_2$-emissions associated with the electricity purchased from the grid. The methodology is described in detail in Publication D; here the approach will be explained using the modified objective function, see equation 3.14.

$$
\min m^{CO2} = \sum_{w=1}^{52} \left( \sum_{h=1}^{168} \left( \sum_{q=1}^{4} (x^{grid,in}_{q,h,w} \cdot EF_{q,h,w}) \right) \right) \tag{3.14}
$$

Equation 3.14 minimises the $CO_2$emissions ($m^{CO2}$) at each time step of the year. The $CO_2$emissions are defined in each time step as the product of the electricity purchase from the power grid ($x^{grid,in}_{q,h,w}$) and the corresponding emission factor ($EF_{q,h,w}$). For a detailed analysis, Publication D presents four emission factors based on different methodological approaches, denoted as:

1. average emission factor (AEF),
2. marginal system response (MSR),
3. marginal power mix according to Hawkes (2010) (MPM) and
4. marginal power plant (MPP).

The first three emission factors are based on empirical data generated by a novel combination of two databases. These two public databases, which document power plant dispatch and power plant emissions, are combined for the first time in Publication D and the allocation key is published in the additional information. The final emission factor is the result of a European energy system model.

# 4 Summary of results

This chapter summarises the results of the publications of this thesis. The summary builds on the methodological approaches introduced in Section 3.3 and serves to answer the research questions of this thesis.

## 4.1 Publication A – Battery storage systems: An economic model-based analysis of parallel revenue streams and general implications for industry

As shown in Section 2.3, energy demand and supply flexibilities are an important component of upcoming energy systems that rely to a large extent on generation from intermittent RES plants. Publication A argues that due to high energy demand, industrial plants can take on a special role. Various markets and incentives already exist that economically stimulate demand-side flexibility. However, various flexibility measures can have a direct influence on production processes. At this point, however, the economic risk of failure in production is disproportionate to the current returns from providing energy flexibility.

To counteract this economic imbalance, Publication A proposes the notion of "pseudo-flexibility". By integrating an energy storage system, explicitly a BSS, it is possible to temporarily shift the energy purchase from the power grid without influencing the load of the production process. It is precisely this possibility of demand flexibility without changing the production load that is referred to as "pseudo-flexibility". For further investigations, the base model of a BSS in industry, *BSS-Opt-Model*, described in Section 3.3.1, is developed in Publication A. The model is used to techno-economically optimise the investment and dispatch of a BSS. Three revenue streams, which are introduced in Section 2.4, are considered: Offering frequency containment reserve, arbitrage trading on the day-ahead and intraday market and peak shaving.

The model is applied to 50 German small and medium-sized enterprises, each of which is included in the calculation with their annual load profiles in 15-minute increments. The results are used to examine the profitability of the individual revenue streams and to what extent the simultaneous pursuit of several revenue streams increases the profitability of the BSS. Furthermore, the influence of newly introduced load indicators on profitability is examined via stepwise regression.

The most important result is that the highest profitability is achieved when a BSS is installed and all three revenue streams are pursued simultaneously. Only a single revenue stream, on the other hand, does not achieve a positive net present value for the investment in a BSS. Rather, the combination of FCR marketing and peak shaving achieves a complementary effect and drives profitability upwards. Accordingly, a profitable operation in terms of revenue is on average 75% attributable to the marketing of FCR and 24% to peak shaving.

Due to the contribution of peak shaving, profitability is strongly dependent on the individual load profiles of the companies[1]. Thus, among the 50 companies, there is a trend that the optimal BSS capacity increases with the size of the company's annual peak load. Here, the results show that the greater the peak shaving capacity of the company, the greater the profitability. Furthermore, a significant influence of two load indicators can be observed. The interpretation of these load indicators suggests that companies with daily balancing load peaks and valleys as well as companies with only single load peaks during the day can achieve higher BSS profitability.

Arbitrage trading has a negligible share in the revenues of BSS operations for all 50 companies. This is mainly because in most cases of the year under consideration, the price difference in the energy markets is too small to compensate for the costs incurred by battery ageing and charging and discharging losses of the BSS. However, the results of the study are sensitive to the change in the BSS price and the capital interest rate.

## 4.2 Publication B – Optimal PV and battery investment of market-participating industry facilities

The results from Publication A have already provided a deep insight into the economical dispatch and capacity of BSS. However, the discussion part of the study has also highlighted the uncertainties of the results, especially due to the deterministic formulation of the model. To address part of these uncertainties, Publication B develops the two-stage optimisation model *BSS-robust-model*, see 3.3.2.1, integrating intraday market behaviour as a sub-problem using robust optimisation. The results from Publication B shed light on the influence of uncertainty considerations on the investment and dispatch of the BSS. In addition, the paper uses 20 industrial load profiles to investigate the impact of aggregating industrial loads. The model is applied to the three market areas Germany, Denmark and Croatia, and investigates the possibility of installing a BSS together with a PV system in an industrial manufacturing plant.

The results show that the investment in a BSS is particularly refinanced by the returns on the FCR market. Furthermore, the results indicate that the PV system is especially used to reduce the amount of energy purchased on the energy markets through self-generation and to reduce the peak load. The dispatch of the BSS can be seen as complementary to the PV operation at many

[1] The provision of FCR power can also take place without the connection to an industrial company

time steps, as it supports the increase in self-consumption and the reduction of the peak load. In addition, BSS capacity is used to provide FCR. Without an FCR market, as in Croatia, the model results indicate the installation of only a PV system and no BSS. In a further comparison of the three countries, fees are the largest cost component in both Germany and Denmark, at around 70%. In Croatia, this component amounts to only just under 50%.

The consideration of uncertainties leads to the adjustment of the FCR offer to the uncertain load behaviour. Thus, the FCR offer is reduced in order not to jeopardise possible peak shaving targets. Furthermore, the risk of the bidding procedures on the intraday market is mapped via robust optimisation. The results represent different levels of risk affinity or market skill by varying an uncertainty budget between a minimum (high risk or skill) and a maximum value (low risk or skill). The consequence of the maximum uncertainty budget is a relative increase in energy market prices. In these cases, the model sizes the PV system and the BSS larger to increase self-consumption and reduce energy purchase costs.

However, this is only the case if the industrial companies are considered individually. If aggregation of the industrial loads is assumed, the size of the PV plant and the BSS remains constant despite an increasing uncertainty budget. Through aggregation, demand can be made more flexible. The combination of different load profiles already leads to a maximisation of the self-consumption rate of the self-generated PV electricity. Through aggregation, part of the economic success is therefore already secured against uncertainties on the intraday market.

All results of this publication can be considered robust after a sensitivity analysis and Monte Carlo simulation. The sensitivity analysis has shown that the results do not deviate strongly from each other for consideration of at least four typical weeks. The observations should include at least four scenarios per week. The Monte Carlo simulation proved the robustness of the results regarding the derived scenarios.

## 4.3 Publication C – Stochastic optimization of battery storage investment in industry – Comparing a two-stage and multi-stage approach

The investigations in Publication A and Publication B have already shown that the economic feasibility of a BSS particularly depends on the FCR market and peak shaving activities. In this context, the importance of the uncertain price and load behaviour for the investment decision was also highlighted. However, since the time sequence of decisions can only be represented to a limited extent in the two-stage approach from Publication B, a multi-stage stochastic optimisation programme is developed in Publication C. Using this *BSS-mult-stg-model* described in Section 3.3.2.2, the consecutive sequence of market decisions is examined in more detail. Stochastic

realisations of market prices and load patterns are considered, and operational constraints due to battery ageing and cycle life are also integrated.

The study applies the *BSS-mult-stg-model* to the annual load profile of a German company from the steel industry and investigates the investment and dispatch of a BSS in the context of the revenue streams peak shaving, FCR and energy arbitrage. The results are compared with the results from the *BSS-two-stg-model* and calculated for up to three typical days and two typical weeks. Different modes of operation are analysed by varying capacity prices and price spreads in the energy markets.

The results show that the two-stage formulation neglects the operational risk because, from its basic principle, it only replicates the consecutive sequence of decisions to a limited extent. However, this limitation already leads to significant differences in the optimal size of the BSS. These differences are primarily due to the dependency of FCR and peak shaving activities, as well as the methodologically different considerations of ageing and cyclical lifetime.

The economic FCR potential is lower in the multi-stage case than in the two-stage case because at the time of the FCR decision it is not known which load behaviour will be realised. Accordingly, in the multi-stage case, an FCR decision must be made that takes all possible load patterns into account and keeps enough BSS capacity free to meet the peak shaving targets. This means that if the realisation of high peak loads is possible in the associated subsequent stage, the FCR amount offered is kept as low as possible to shift this peak load. This happens regardless of whether low loads are indicated in the other realisation scenarios. This connection has already been indicated in the results from Publication B. If, on the other hand, the FCR and the BSS dispatch decision are made deterministically at the same level, as in the *BSS-two-stg-model*, an FCR decision is only associated with one realisation scenario for the load profile, which means that the FCR amount offered is larger on average.

Furthermore, the results show that the consideration of BSS ageing and cycle life of the two models also has an influence on the optimal investment and dispatch of the BSS. Thus, in the two-stage approach, the ageing and the charging cycles are included in the optimisation problem as a weighted average value over all time periods. This can lead to dispatch scenarios that are at odds with reality and overestimate the economic dispatch potential. In the multi-stage case, the problem formulation considers the charging behaviour of complete multi-stage scenarios. These scenarios include the consecutive sequence of events of each stage and thus each time step.

However, the degree of accuracy gained for the multi-stage problem is accompanied by a relatively high degree of model complexity and computational intensity. This degree, as known from the theory in Section 3.2, increases exponentially with the number of stages considered. This leads to the fact that the problem can only be solved for a relatively small number of typical time periods and realisation scenarios. A variation of the number of typical time periods that are computationally tractable reveals a considerable deviation of results. Thus, the results lack

robustness regarding the derived scenarios. Also, in contrast to the sensitivity analysis from Publication B, the number of time periods can be regarded as too small. Although this weakens the practical statement of the case study, theoretical consecutive dependencies of FCR and load activities, or BSS charging cycles on profitability, are highlighted that are important for future scenarios and model design.

## 4.4 Publication D – Comparing empirical and model-based approaches for calculating dynamic grid emission factors: An application to CO2-minimizing storage dispatch in Germany

Building on the findings from Publication A, Publication D investigates how the optimised use of a BSS in an industrial plant can reduce the $CO_2$-emissions associated with the electricity drawn from the grid. Especially in the transition phase from a conventional energy system to a predominantly "renewable" energy system, the $CO_2$-emissions of grid electricity can change significantly from hour to hour. By shifting demand over time, a BSS can make a significant contribution here, charging at a favourable time for low $CO_2$-emissions and discharging at an unfavourable time. However, determining a signal for such a favourable time is a complex task in a pan-European energy system. Therefore, Publication D investigates different emission factors that can serve as a signal and the influence that a BSS could have on the mitigation of a manufacturing plant's $CO_2$-emissions.

For this investigation, two optimisation models are applied. First, following the *BSS-Opt model* described in Section 3.3.1, the investment and dispatch of a BSS are economically optimised, considering only peak shaving as a revenue stream. In the second step, the ecological dispatch is optimised using the BSS-$CO_2$-model from Section 3.3.3. The avoided amount of $CO_2$ is determined from the comparison between the economic and $CO_2$-minimal dispatch.

To determine the $CO_2$-minimal dispatch, it is first important to define the $CO_2$ load of the grid electricity. For this purpose, four dynamic emission factors (*EF*) are determined, as described in Section 3.3.3. The three empirical EFs and one model-based EF differ both in terms of magnitude and volatility, and also show opposite signals at some points in time. All four EFs have advantages and disadvantages to serve as a reliable signal for a $CO_2$-minimal dispatch of a BSS. For example, the *marginal system response* EF has the largest spread between the maximum and minimum values and thus also stimulates the highest $CO_2$-reduction in a storage operation. However, the negative values of this EF cannot be interpreted intuitively. The EF taken from the literature *marginal power mix* by Hawkes (2010), on the other hand, no longer seems appropriate for the current energy system and the high share of RES because of the periodic behaviour.

The *average emission factor* shows the smallest deviations over the course of the year, which in turn makes the $CO_2$-minimisation incentive low. For the study, the largest share of RES in the energy system is not directly included in the EF, as these energy sources are considered as currently not dispatchable and thus would not respond to a change in demand. This puts the *average emission factor* in stark contrast to existing average EFs from other scientific publications. However, for most time steps, the signal direction (relatively high or low EF values) coincides with that of the model-based *marginal power plant* EF. Especially in magnitude, however, the two values differ, since the *average emission factor* considers the entire system and the *marginal power plant* EF addresses the individual marginal power plant. Even though the *average emission factor* and the *marginal power plant* EF seem to be the most suitable to serve as $CO_2$-emission signals, the quality of the publicly available databases should be greatly improved to obtain reliable EFs.

First, the study investigates the $CO_2$-reduction potential of a generic storage system to obtain a general statement on flexibility measures for $CO_2$-reduction and then applies the optimisation model to the specific characteristics of a BSS. Here, it becomes clear that the EF in the case of a generic storage can indeed stimulate a $CO_2$-reduction, but a clear trade-off between the economic goal of peak-shaving and the ecological goal of $CO_2$-minimisation can be seen. Thus, the $CO_2$-reduction potential strongly depends on the individual load profile. This potential can be estimated as relatively high if the load profile and the EF profile correlate with each other.

Second, the specific characteristics of a BSS are studied, which diminish the reduced $CO_2$-emission amounts significantly. The observations of the storage dispatch for $CO_2$-minimisation are very similar to the observations on energy arbitrage from Publication A. For example, the BSS cycle life severely limits the number of daily charging cycles and only accounts for the largest differences in emissions. At the same time, the charging and discharging losses ensure that there must be a minimum difference in the EF value between periods of high and low $CO_2$-emissions to stimulate load shifting by the BSS. Although ageing effects are not considered in this study, a high load on the BSS due to high C-rates and depths of discharge can be observed, as in arbitrage operation. This would have negative effects on battery life.

# 5 Discussion and critical review

The results of this thesis shed light on the optimal operation of a BSS in an industrial manufacturing plant and how the optimal size of such a BSS can be determined from different points of view. Furthermore, the results provide a good answer to the research questions posed in this thesis, which focus on the influence of different revenue streams, uncertainties and $CO_2$-minimal charging on the profitability of the BSS. Nevertheless, the answers to these research questions need to be critically examined and the limitations of this thesis need to be highlighted, which will be done in the following.

## 5.1 Different revenue streams

This thesis shows that for the economic evaluation of a BSS, different revenue streams should be considered simultaneously. Furthermore, it shows that the BSS operation with the objective of FCR marketing and peak shaving together achieves the highest economic efficiency. These two revenue streams are to be considered complementary. However, the economic performance depends strongly on the individual load profiles of the industrial companies.

Furthermore, the results show that operation according to an FCR and peak shaving business model is associated with a relatively low burden on the lifetime of the BSS. This means that these two revenue streams allow for a profitable operation within the technological boundary conditions of the BSS. Profitable operation is possible without exceeding the limited number of charging cycles defined by the BSS life and also results in relatively low C-rates and DoD. This advantage becomes particularly clear in comparison to arbitrage trading. In an economic comparison, the arbitrage trading revenue stream can only generate relatively low revenues on the energy markets. This is due, on the one hand, to the low price differences on the markets and, on the other hand, to the energy losses during charging and discharging as well as the ageing effects and limiting charging cycles considered in this thesis. In addition, the operation is associated with high C-rates and high DoD, which additionally burden BSS life. However, C-rate and DoD are not considered in the optimisation models used.

The economic analysis presents a different picture if additional “flexibility” is considered through the installation of a PV system and the associated self-generation or through the aggregation of industrial loads. In these cases, these flexibility measures can hedge against the uncertainties in

the energy markets by increasing the self-consumption rate. The higher self-consumption avoids fees, taxes, and high prices for energy purchases.

However, the results are subject to some uncertainty as they have been found to be sensitive to price changes. The prices assumed for a BSS in the studies of this thesis are still current for 2021, see Eble (2021), but advances and further developments are expected in the coming years, which might result in decreasing prices conducive to economic performance. Sections 2.4.3 show that the grid charges relevant for peak shaving are subject to large fluctuations regionally and depending on the voltage level, which has a direct influence on the operation and economic efficiency of the BSS. Even though the past has shown an increasing trend in grid charges, due to the difference between regional grid charges, a more reliable economic assessment should always be carried out for a specific business location.

In this study, only a capacity price and not an energy price is assumed for the grid charges to be paid. However, this only partially reflects the reality for Germany, as explained in 2.4.3, and is approximately only valid for a company operating with high annual full load hours and connected at higher voltage levels. Furthermore, 2.6 shows that in German regulation there is an “inflection point” in the quantitative relation between energy and capacity price, which has a great influence on the economic performance of a BSS. Thus, depending on the load profile, it might be economically more appropriate to optimise the annual full load hours so that the area above the “inflection point” of 2,500 annual full load hours is reached, see Weinand et al. (2021), or to give more weight to the energy price in the objective function than to the capacity price.

From a business perspective, the current regulatory framework is well suited to stimulate load flexibility. As mentioned in Section 2.4.3, however, it is questionable whether this “flexibility” can also be interpreted as such “flexibility” from an energy system perspective. For the energy system, a storage operation that relieves the stress on the grid could rather be given dynamic, regional, or even node-specific price signals instead of a fixed annual price stimulated load shifting. Additionally, after the CJEU’s ruling, the future regulations of network charges in Germany hold many uncertainties.

Uncertainties also affect the FCR market. For example, Section 2.4.4 has shown how the German FCR market has been subject to continuous changes recently, affecting both the FCR product and the market structure. This has resulted in considerable price differences within and between years. In addition, the demand for balancing reserves is limited, so that every new market participant, such as BSS operators, can have a direct influence on prices. It is also difficult to compare market prices from previous years. Thus, a statement about long-term price behaviour is risky.

This thesis considers a medium- to long-term investment period of 11 years and assumes for the economic analysis that the load behaviour and prices from the year under consideration can be extrapolated for the entire investment period of 11 years. As mentioned in the previous

paragraph, the results must therefore be viewed from the perspective that there is a high degree of ignorance about future developments. This of course also includes the assumption about the load behaviour of an industrial plant. In the long term, this is dependent on the economic situation as well as the sector-specific economic utilisation, and in the short term, it is exposed to company-specific shocks, which can affect, among other things, the personnel, the operational process or the supply chain.

Under the impression of constantly changing market conditions, it is essential for the operator of a BSS to continuously evaluate the operating model. It is helpful to note that a special feature of the BSS is its diverse range of applications. Thus, future markets for system services such as reactive power provision or flexibility at the distribution grid level should be investigated with a view to economic deployment. Site-specific services such as support for power quality or utilisation as a backup power generator also offer added value. However, the economic evaluation of these services is not trivial as they reduce equipment damages and production outages but are not unambiguously linked to a revenue stream such as energy trading. Regarding Li-ion technology, the focus in these cases is particularly on products that emphasise the properties of the Li-ion technology as power storage rather than as energy storage.

Finally, it should be noted that an implementability of the resulting optimal dispatch is assumed. For the implementation, a management system is necessary that ensures optimal operation and short-term scheduling. The costs incurred for this are not considered in the model. Furthermore, the meteorological control system must permit such operation. Moreover, the model neglects other fees that are incurred in energy trading and the provision of FCR power (see Section 2.4.1). These fees would increase more if the discrete minimum bid size in the markets is considered. In this thesis, a continuous bid size is assumed. It would be possible to move away from continuous bid sizes on the model side and integrate them as integer discrete bid size steps. However, this would be accompanied by a considerable increase in model complexity and computing time. However, one could also insert additional costs through fees for an aggregator, since the offer of a continuous bid size of energy or power is only possible if one participates in the markets via just such an aggregator. These additional costs would reduce the FCR revenue.

Additional costs for energy trading, on the other hand, are not so significant, since without self-generation the arbitrage business contributes only a small part to the profitability. At the same time, the price differences on the markets are particularly decisive for the revenue stream because of the storage losses. Accordingly, as long as only the time of power purchase shifts and not the amount of energy, the profit remains unaffected by additional costs. However, this is not the case when storage losses are considered, as shown in Publication B, and when energy is fed into the grid and then sold on the markets.

## 5.2 Uncertainties

This thesis has shown that a large part of the uncertainties affecting the medium- to long-term investment in a BSS can be addressed through stochastic and robust programming. Even if ignorance of future market changes cannot be covered, risk and uncertainty in price and load behaviour can be incorporated into the investment decision. The various methodological approaches of stochastic programming and robust optimisation have revealed fundamental relationships in the investment and dispatch planning of a BSS.

In two-stage stochastic optimisation, the integration of the bidding behaviour on the intraday market via robust optimisation has covered the risk in energy trading particularly well. This risk can be mitigated by investing in self-generation. However, the results also illustrate the problem that when considering several revenue streams in parallel, abstractions of reality are necessary and these usually lead to a higher economic valuation of a few individual revenue streams.

The results provide information that especially if the marketing opportunities of FCR and peak shaving are of high economic importance, these important decisions should be made at separate stochastic stages. Hence, this mainly concerns the FCR decision and the charging and discharging decision with the aim of reducing the peak load. The representation of these consecutive decision interdependencies can only be realised inadequately in a two-stage approach; in a multi-stage approach, however, it can. Nevertheless, the multi-stage formulation is accompanied by considerable computational expenses.

The multi-stage problem could also be solved for a larger number of time steps using approaches such as stochastic dynamic programming. However, the constraint of the cyclic lifetime would have to be relaxed, as this increases the model complexity due to the scenario path dependency. Therefore, scenario generation is of great importance. In particular, by reducing type weeks to four-hour time periods, which would correspond to the current FCR market conditions, an adequate scenario design is necessary to increase the accuracy of the stochastic programme but reduce the model complexity.

## 5.3 $CO_2$-minimal dispatch

The investigations have shown that the data basis for the preparation of emission factors is currently still insufficient. Nevertheless, insights can be drawn that are particularly relevant in a transition phase from a conventional energy system to an energy system largely determined by RES. Regarding ecological dispatch planning, it can be stated that storage technologies could certainly be suitable for reducing the $CO_2$-emissions of the energy system. A BSS, on the other hand, is not suitable for this because of technological constraints.

In the development of the emission factor, the average emission factor *AEF* and the emission factor *MPP* describing the marginal power plant have particularly stood out as plausible indicators. Here, the signalling effect of the AEF contrasts with the average emission factor used elsewhere in the literature. This illustrates that there should be agreement on the definition of system boundaries and system responses in the discussion on the determination of systemic emissions. In this thesis, it is assumed that the largest number of RES plants has a feed-in priority over conventional power plants and is thus assumed to be non-dispatchable. However, this also presumes that the marginal consumer can be clearly identified so that the marginal emissions can also be precisely assigned to one consumer.

The results show that the AEF and the MPP coincide in their signal direction at many points in time. However, the MPP has a larger deflection, as it represents explicit power plants. A model-based emission factor appears to be the most accurate instrument, but many of the existing model-based emission factors can be described with high model complexity and as non-transparent with numerous assumptions. Furthermore, many inaccuracies due to model assumptions on import power, CHP operation and must-run conditions are included in the calculation of the emission factor. This problem will increase if the number of dispatchable RES plants and the installed capacity of storage plants increase in the future.

The study has raised the question of the extent to which $CO_2$-minimal dispatch is compatible with other objective formulations. On the one hand, $CO_2$-minimal dispatch conflicts with the economic objective of minimum costs, as the dispatch bears great similarity to the dispatch in energy arbitrage trading. Thus, large C-rates and DoD can be observed, which would put a heavy strain on the lifetime of the BSS and thus also on the economic efficiency. On the other hand, the rigid peak shaving boundary conditions only allow a dynamic and “system-stabilising” storage use to a limited extent, since the flexibility incentive is set as an annual peak threshold. At the same time, the term “system-stabilising” depends on the perspective. Thus, it can be assumed that its signal for national $CO_2$-emissions differs from a signal that serves the grid. A coherent behaviour of these two objectives, grid-stabilizing and $CO_2$-minimal, can rather be assumed if the local level is considered, which better reflects grid nodes and decentralised RES plants.

# 6 Summary and conclusion

In the context of a changing energy system towards a system dominated by RES, this paper contributes to a better understanding of the business decision spectrum in the marketing of energy flexibility. In particular, it deals with the techno-economic investment decision in a battery storage system (BSS) from the perspective of an industrial company. The framework chapter shows that the need for flexible energy demand and supply will increase. In this context, the use of a BSS, especially to make industrial energy demand more flexible, can play an important role in the future. However, the scientific literature does not adequately answer how to make an economically optimal investment decision on the installation of a BSS in an industrial manufacturing plant. This thesis complements the scientific literature and shows under which circumstances an investment can be considered profitable and which risks and uncertainties have to be considered. In addition, this thesis discusses what contribution such a BSS can make to the transformation of the national energy system.

For this purpose, the technological and economic context for the use of a BSS in the industry is examined in the framework chapter. The studies published as part of this thesis analyse in detail the optimal investment and dispatch planning for a BSS. Publication A examines the economic profitability considering simultaneous revenue streams for electric flexibility, FCR provision, peak shaving and arbitrage trading on energy spot markets. Publication B extends the revenue streams by the possibility of PV self-generation and incorporates the uncertainties about market prices and load behaviour into the investment decision. Publication C further elaborates on this consideration of stochastic uncertainties and analyses in particular the effects of consecutive uncertain market decisions. Finally, Publication D compares the economically optimal storage use with an ecological $CO_2$-minimal storage use. In all decision models, not only the economic but also the technological constraints resulting from the operation of a BSS are taken into account, which particularly concerns the efficiency and the ageing behaviour of the systems.

A further addition to the scientific literature lies in the methodological extensions of the investment and dispatch planning problem. The problem considers different revenue streams simultaneously and is formulated both as a deterministic and a stochastic LP. The stochastic approach is implemented as both a two-stage and a multi-stage stochastic optimisation problem. In addition, the stochastic market behaviour is abstracted by a robust optimisation approach. For the overall system assessment, emission factors are generated, which are derived from a new data basis.

The results of this thesis show that especially the possibility of grid charge reduction, peak shaving, enables an economically feasible investment in a BSS. Peak shaving can be complemented by the marketing of FCR. In addition, self-generation through a PV system can act as a risk mitigant against uncertain market behaviour. It should be noted, however, that the economic viability must be assessed individually, as the grid charges differ depending on the region and voltage level, and the industrial load profiles can vary greatly. Furthermore, FCR shows strong price fluctuations due to changing market structures. At the same time, the FCR market volume is limited, which means that future valuation is associated with high uncertainties. Nevertheless, when making investment decisions, it is important to consider the consecutive order of uncertain market decisions to reduce economic risk. The decision sequence is also important to integrate the BSS ageing as accurately as possible into the economic evaluation. The BSS ageing, as well as its efficiency in charging and discharging, severely limits profitability, making arbitrage trading in particular unprofitable for a BSS. The same ageing constraints also restrict the use of a BSS for $CO_2$-emission reduction. Here, other flexibility technologies promise greater success.

The results show that the installation of a BSS in an industrial plant can be assessed as profitable. However, there is uncertainty regarding the assumed parameters, especially FCR and electricity market prices as well as the assumed battery price. Revenues from flexibility marketing need to compensate the price for a BSS. However, market studies show that longer lifetimes than assumed in this thesis can be expected, especially in the stationary sector, which would have a positive impact on profitability. In addition, a BSS as a technology can serve different flexibility products at the same time. Therefore, depending on future market developments, the profitability of a BSS should be re-evaluated. In particular, the regulation of grid charges might undergo severe changes, as the current regulation does not sufficiently consider the future demands of dynamic grid relief. This could result in new economic marketing opportunities for the operation of a BSS.

For future research, it is therefore important to evaluate the technological progress in battery technology and storage technology in general and to investigate it in new case studies. Other technologies, such as LTO battery cells or power-to-x solutions, coincide with different prices and technological constraints, which yield different revenue opportunities. The same applies to regulatory developments, which could enable new marketing concepts for BSSs. A broader database on industrial load profiles would allow more general conclusions to be drawn, which are interesting for both new business models and the political framework. Furthermore, this work highlights the importance of uncertainties for an optimal design of a BSS. Further research should aim at reducing the computational complexity of the multi-stage stochastic optimisation model through appropriate abstraction to produce more robust results. Advances in the decomposition of the problem and scenario generation of the input parameters can be used to improve the solution techniques. This work has outlined initial approaches for this.

# Bibliography


50Hertz Transmission GmbH. Archiv Netzfrequenz: Netzfrequenz 2016, 2022. URL https://www.50hertz.com/de/Transparenz/Kennzahlen/Regelenergie/ArchivNetzfrequenz, 2022-03-21.

Agora Energiewende. Flexibility in thermal power plants: With a focus on existing coal-fired power plants. 2017. URL https://static.agora-energiewende.de/fileadmin/Projekte/2017/Flexibility_in_thermal_plants/115_flexibility-report-WEB.pdf.

A.-C. Agricola, H. Seidl, and S. Mischinger. dena Ancillary Service Study 2030: Security and reliability of a power supply with a high percentage of renewable energy, Deutsche Energie-Agentur GmbH, 2014.

Y. M. Al-Humaid, K. A. Khan, M. A. Abdulgalil, and M. Khalid. Two-Stage Stochastic Optimization of Sodium-Sulfur Energy Storage Technology in Hybrid Renewable Power Systems. *IEEE Access*, 9:162962–162972, 2021. doi: 10.1109/ACCESS.2021.3133261.

M. I. Alizadeh, M. Parsa Moghaddam, N. Amjady, P. Siano, and M. K. Sheikh-El-Eslami. Flexibility in future power systems with high renewable penetration: A review. *Renewable and Sustainable Energy Reviews*, 57:1186–1193, 2016. ISSN 13640321. doi: 10.1016/j.rser.2015.12.200.

Ş. Y. Balaman. Uncertainty Issues in Biomass-Based Production Chains. In S. Y. Balaman, editor, *Decision-Making for Biomass-Based Production Chains*, pages 113–142. Elsevier Science & Technology, San Diego, 2018. ISBN 9780128142783. doi: 10.1016/B978-0-12-814278-3.00005-4.

A. Barré, B. Deguilhem, S. Grolleau, M. Gérard, F. Suard, and D. Riu. A review on lithium-ion battery ageing mechanisms and estimations for automotive applications. *Journal of Power Sources*, 241:680–689, 2013. ISSN 03787753. doi: 10.1016/j.jpowsour.2013.05.040.

R. Bathke. Bundestag bringt Netzbooster auf den Weg. *energate messenger*, 2021. URL https://www.energate-messenger.de/news/209300/bundestag-bringt-netzbooster-auf-den-weg.

BDEW. BDEW-Strompreisanalyse Januar 2022, BDEW Bundesverband der Energie- und Wasserwirtschaft e.V., 2022. URL https://www.bdew.de/media/documents/220124_BDEW-Strompreisanalyse_Januar_2022_24.01.2022_final.pdf.

BDEW Bundesverband der Energie- und Wasserwirtschaft e.V. Netzbetrieb 2.0: Grundsätze des zukünftigen Netzbetriebs und der Zusammenarbeit von Übertragungs- und Verteilnetzbetreibern, BDEW Bundesverband der Energie- und Wasserwirtschaft e.V., 2018. URL https://www.bdew.de/media/documents/20181128_Diskussionspapier_Netzbetrieb_2.0.pdf.

B.-A. Behrens, A. Brosius, W.-G. Drossel, W. Hintze, S. Ihlenfeldt, and P. Nyhuis. *Production at the Leading Edge of Technology*. Springer International Publishing, Cham, 2022. doi: 10.1007/978-3-030-78424-9.

A. Ben-Tal. *Robust Optimization*, volume 28 of *Princeton Series in Applied Mathematics Ser*. Princeton University Press, Princeton, 2009. ISBN 9781400831050.

Beschlusskammer 6. Beschluss BK6-20-298: In dem Festlegungsverfahren zu Ausnahmeentscheidungen von der marktgestützten Beschaffung von nicht frequenzgebundenen Systemdienstleistungen, Bundesnetzagentur, 2020. URL https://www.bundesnetzagentur.de/DE/Beschlusskammern/1_GZ/BK6-GZ/2020/BK6-20-298/BK6-20-298_beschluss_vom_18.12.2020.pdf?__blob=publicationFile&v=3.

Beschlusskammer 6. BK6-21-360: Einleitung eines Festlegungsverfahrens gem. §§ 12h Abs. 4, 29 Abs. 1 EnWG zur Ausnahme von der Verpflichtung der marktgestützten Beschaffung der nicht frequenzgebundenen Systemdienstleistung Schwarzstartfähigkeit durch die Betreiber von Elektrizitätsverteilernetzen nach § 12h Abs. 1 S. 1 Nr. 5 EnWG (BK6-21-360), 2021a. URL https://www.bundesnetzagentur.de/DE/Beschlusskammern/1_GZ/BK6-GZ/2021/BK6-21-360/BK6-21-360_Verfahrenseinleitung.html?nn=975644.

Beschlusskammer 6. BK6-21-023: Einleitung eines Festlegungsverfahrens gem. §§ 12h Abs. 5, 29 Abs. 1 EnWG zu den Spezifikationen und technischen Anforderungen der transparenten, diskriminierungsfreien und marktgestützten Beschaffung der nicht frequenzgebundenen Systemdienstleistung „Schwarzstartfähigkeit“ durch die deutschen regelzonenverantwortlichen Übertragungsnetzbetreiber (ÜNB) gem. § 12h Abs. 1 S. 1 Nr. 5 EnWG, 2021b. URL https://www.bundesnetzagentur.de/DE/Beschlusskammern/1_GZ/BK6-GZ/2021/BK6-21-023/BK6-21-023_Verfahrenseinleitung.html?nn=975644.

S. Beucker, C. Heyken, S. Hüttner, C. Over, M. Richter, M. Richter, F. Stein, and A. Weber. Best Practive Manuel: Flex identifizieren!, WindNODE-Verbundskoordination and 50Hertz Transmission GmbH, 2020. URL https://www.windnode.de/fileadmin/Daten/Downloads/Publikationen/WindNODE-BPM_FlexIdentifizieren-Online-Version.pdf.

S. Beucker, H. Doderer, A. Funke, C. Koch, H. Kondziella, J. Hartung, S. Maeding, H. Medert, G. Meyer-Braune, M. Rath, and N. Rogler. Flexibilität, Markt und Regulierung: Synthesebericht, WindNODE-Verbundskoordination and 50Hertz Transmission GmbH, 2021. URL https://www.windnode.de/fileadmin/Daten/Downloads/FMR_ES.pdf.

J. R. Birge and F. Louveaux. *Introduction to Stochastic Programming*. Springer New York, New York, NY, 2011. doi: 10.1007/978-1-4614-0237-4.

G. Blumberg, C. Wagner, W. Lehnert, M. Bucksteeg, and M. Greve. Marktgestützte Beschaffung von Blindleistung: Bericht im Vorhaben „SDL-Zukunft“, ef.Ruhr GmbH, 2021. URL https://stiftung-umweltenergierecht.de/wp-content/uploads/2021/04/Stiftung_Umweltenergierecht_WueStudien_20_Neues-Beschaffungsverfahren-fuer-Blindleistung-durch-%C2%A7-12h-EnWG.pdf.

E. Borgonovo and E. Plischke. Sensitivity analysis: A review of recent advances. *European Journal of Operational Research*, 248(3):869–887, 2016. ISSN 0377-2217. URL https://econpapers.repec.org/article/eeeejores/v_3a248_3ay_3a2016_3ai_3a3_3ap_3a869-887.htm.

K. Bradbury, L. Pratson, and D. Patiño-Echeverri. Economic viability of energy storage systems based on price arbitrage potential in real-time U.S. electricity markets. *Applied Energy*, 114: 512–519, 2014. ISSN 03062619. doi: 10.1016/j.apenergy.2013.10.010.

F. Braeuer, M. Kleinebrahm, and E. Naber. Effects of the tenants electricity law on energy system layout and landlord-tenant relationship in a multi-family building in Germany. *IOP Conference Series: Earth and Environmental Science*, 323:012168, 2019a. ISSN 1755-1315. doi: 10.1088/1755-1315/323/1/012168.

F. Braeuer, J. Rominger, R. McKenna, and W. Fichtner. Battery storage systems: An economic model-based analysis of parallel revenue streams and general implications for industry. *Applied Energy*, 239:1424–1440, 2019b. ISSN 03062619. doi: 10.1016/j.apenergy.2019.01.050.

F. Braeuer, R. Finck, and R. McKenna. Comparing empirical and model-based approaches for calculating dynamic grid emission factors: An application to CO2-minimizing storage dispatch in Germany. *Journal of Cleaner Production*, 266:121588, 2020. ISSN 09596526. doi: 10.1016/j.jclepro.2020.121588.

F. Braeuer, M. Kleinebrahm, E. Naber, F. Scheller, and R. McKenna. Optimal system design for energy communities in multi-family buildings: the case of the German Tenant Electricity Law. *Applied Energy*, 305:117884, 2022. ISSN 03062619. doi: 10.1016/j.apenergy.2021.117884.

R. Brealey, S. Myers, and F. Allen. *Principles of Corporate Finance*. McGraw-Hill/Irwin, 10 edition, 2011. ISBN 978-0-07-353073-4.

N. Brinkel, T. AlSkaif, and W. van Sark. Grid congestion mitigation in the era of shared electric vehicles. *Energy Storage*, 48:103806, 2022. ISSN 2352-152X. doi: 10.1016/j.est.2021.103806.

C. Brunner, G. Deac, S. Braun, and C. Zöphel. The future need for flexibility and the impact of fluctuating renewable power generation. *Renewable Energy*, 149:1314–1324, 2020. ISSN 09601481. doi: 10.1016/j.renene.2019.10.128.

A. Bublitz, D. Keles, F. Zimmermann, C. Fraunholz, and W. Fichtner. A survey on electricity market design: Insights from theory and real-world implementations of capacity remuneration mechanisms. *Energy Economics*, 80:1059–1078, 2019. ISSN 01409883. doi: 10.1016/j.eneco.2019.01.030.

I. Buchmann. BU-502: Discharging at High and Low Temperatures, Battery University, 2021. URL https://batteryuniversity.com/article/bu-502-discharging-at-high-and-low-temperatures, 2022-07-22.

M. Budt, D. Wolf, R. Span, and J. Yan. A review on compressed air energy storage: Basic principles, past milestones and recent developments. *Applied Energy*, 170:250–268, 2016. ISSN 03062619. doi: 10.1016/j.apenergy.2016.02.108.

M. Bulut and E. Özcan. Integration of Battery Energy Storage Systems into Natural Gas Combined Cycle Power Plants in Fuzzy Environment. *Energy Storage*, 36:102376, 2021. ISSN 2352-152X. doi: 10.1016/j.est.2021.102376.

Bundesnetzagentur. Stromnetzentgelte im Bundesschnitt 2021 weitgehend konstant, 2021-01-14. URL https://www.bundesnetzagentur.de/SharedDocs/Downloads/DE/Allgemeines/Presse/Pressemitteilungen/2021/20210114_Netzentgelte.pdf;jsessionid=DEA7C89596A53FFE7C1EF4DF6AB852E7?__blob=publicationFile&v=3.

Bundesnetzagentur. Bundesnetzagentur zur Entscheidung des Europäischen Gerichtshofs in Energiesachen: Pressemitteilung, 2021-09-02. URL https://www.bundesnetzagentur.de/SharedDocs/Downloads/DE/Allgemeines/Presse/Pressemitteilungen/2021/20210902_RegEnergieEugh.pdf?__blob=publicationFile&v=2.

Bundesnetzagentur and Bundeskartellamt. Monitoringbericht Energie 2020, Bundesnetzagentur, 2020. URL https://www.bundesnetzagentur.de/SharedDocs/Mediathek/Berichte/2020/Monitoringbericht_Energie2020.pdf?__blob=publicationFile&v=5.

Bundesnetzagentur and Bundeskartellamt. Monitoringbericht 2021, Bundesnetzagentur, 2022. URL https://www.bundesnetzagentur.de/SharedDocs/Mediathek/Monitoringberichte/Monitoringbericht_Energie2021.pdf?__blob=publicationFile&v=7.

T. Cai, M. Dong, H. Liu, and S. Nojavan. Integration of hydrogen storage system and wind generation in power systems under demand response program: A novel p-robust stochastic programming. *International Journal of Hydrogen Energy*, 47(1):443–458, 2022. ISSN 03603199. doi: 10.1016/j.ijhydene.2021.10.027.

P. E. Campana, L. Cioccolanti, B. François, J. Jurasz, Y. Zhang, M. Varini, B. Stridh, and J. Yan. Li-ion batteries for peak shaving, price arbitrage, and photovoltaic self-consumption in commercial buildings: A Monte Carlo Analysis. *Energy Conversion and Management*, 234: 113889, 2021. ISSN 01968904. doi: 10.1016/j.enconman.2021.113889.

C.A.R.M.E.N. e.V. Marktübersicht Batteriespeicher 2021 – Online Version, 2021a. URL `https://www.carmen-ev.de/service/marktueberblick/marktuebersicht-batteriespeicher/marktuebersicht-batteriespeicher-online-version/`, 2022-03-18.

C.A.R.M.E.N. e.V. Marktübersicht Batteriespeicher 2021: Informationsangebot, 2021b. URL `https://www.carmen-ev.de/wp-content/uploads/2021/09/Marktuebersicht-Batteriespeicher_2021-09-22.pdf`.

L. Chen, Q. Xu, Y. Yang, and J. Song. Optimal energy management of smart building for peak shaving considering multi-energy flexibility measures. *Energy and Buildings*, 241:110932, 2021. ISSN 03787788. doi: 10.1016/j.enbuild.2021.110932.

D. Choi, N. Shamim, A. Crawford, Q. Huang, C. K. Vartanian, V. V. Viswanathan, M. D. Paiss, M. J. E. Alam, D. M. Reed, and V. L. Sprenkle. Li-ion battery technology for grid application. *Journal of Power Sources*, 511:230419, 2021. ISSN 03787753. doi: 10.1016/j.jpowsour.2021.230419.

S. Choudhury. Flywheel energy storage systems: A critical review on technologies, applications, and future prospects. *International Transactions on Electrical Energy Systems*, 31(9), 2021. ISSN 2050-7038. doi: 10.1002/2050-7038.13024.

Connect Energy Economics GmbH, Consentec GmbH, and Fraunhofer-Institut für System- und Innovationsforschung. Leitstudie Strommarkt 2015: Studie im Auftrag des Bundesministeriums für Wirtschaft und Energie, Connect Energy Economics GmbH, 2015. URL `https://www.bmwi.de/Redaktion/DE/Publikationen/Studien/leitstudie-strommarkt-2015.pdf?__blob=publicationFile&v=9`.

M. Cossutta, S. Pholboon, J. McKechnie, and M. Sumner. Techno-economic and environmental analysis of community energy management for peak shaving. *Energy Conversion and Management*, 251:114900, 2022. ISSN 01968904. doi: 10.1016/j.enconman.2021.114900.

N. Covic, F. Braeuer, R. McKenna, and H. Pandzic. Optimal PV and Battery Investment of Market-Participating Industry Facilities. *IEEE Transactions on Power Systems*, 36(4):3441–3452, 2021. ISSN 0885-8950. doi: 10.1109/TPWRS.2020.3047260.

G. B. Dantzig. Linear Programming. *Operations Research*, 50(1):42–47, 2002. doi: 10.1287/opre.50.1.42.17798.

E. Delage and Y. Ye. Distributionally Robust Optimization Under Moment Uncertainty with Application to Data-Driven Problems. *Operations Research*, 58(3):595–612, 2010. doi: 10.1287/opre.1090.0741.

Der Gerichtshof der europäischen Union. Urteil des Gerichtshofs (Vierte Kammer) - ECLI:EU:C:2021:662: In der Rechtssache C-718/18. 2021. URL https://eur-lex.europa.eu/legal-content/DE/TXT/PDF/?uri=CELEX:62018CJ0718&from=de.

Die BBH-Gruppe. Dämpfer für deutsche Industrie: Europäisches Gericht sieht in Netzentgeltbefreiung eine Beihilfe, 2021. URL https://www.die-bbh-gruppe.de/de/aktuelles/news/daempfer-fuer-deutsche-industrie-europaeisches-gericht-sieht-in-netzentgeltbefreiung-eine-beihilfe, 2021-12-14.

Y. Ding and M. D. McCulloch. Distributionally robust optimization for networked microgrids considering contingencies and renewable uncertainty. In *60th IEEE Conference on Decision and Control*, pages 2330–2335, Piscataway, NJ, 2021. IEEE. ISBN 978-1-6654-3659-5. doi: 10.1109/CDC45484.2021.9683658.

M. Doppelbauer. *Grundlagen der Elektromobilität*. Springer Fachmedien Wiesbaden, Wiesbaden, 2020. doi: 10.1007/978-3-658-29730-5.

dpa. EuGH: Deutschland muss Energierecht ändern – neue Rolle für die Netzagentur: Urteil. *Handelsblatt*, 2021. URL https://www.handelsblatt.com/politik/deutschland/urteil-eugh-deutschland-muss-energierecht-aendern-neue-rolle-fuer-die-netzagentur/27573446.html?ticket=ST-615677-Y10ulf7uvRISUXs4jgYB-cas01.example.org.

M. Dreisbusch, S. Mang, S. Ried, F. Kellerer, and X. Pfab. Regulierung des netzdienlichen Ladens aus der Nutzerperspektive. *ATZelektronik*, 15(11):58–65, 2020. ISSN 2192-8878. doi: 10.1007/s35658-020-0281-4.

G. Eble. Kosten für Batteriespeicher ziehen an: Marktüberblick. *energate messenger*, 2021.

M. Ecker, N. Nieto, S. Käbitz, J. Schmalstieg, H. Blanke, A. Warnecke, and D. U. Sauer. Calendar and cycle life study of Li(NiMnCo)O2-based 18650 lithium-ion batteries. *Journal of Power Sources*, 248:839–851, 2014. ISSN 03787753. doi: 10.1016/j.jpowsour.2013.09.143.

E. Ela, M. Milligan, and B. Kirby. Operating Reserves and Variable Generation, National Renewable Energy Lab., 2011.

EnBW Energie Baden-Württemberg AG. EnBW AG: „Gegeneinanderregeln“ gehört in Deutschland der Vergangenheit an – Netzregelverbund seit 1. Mai 2010 bundesweit realisiert, 2010. URL https://web.archive.org/web/20120112080023/http://www.enbw.com/content/de/presse/pressemitteilungen/2010/05/PM_20100504_tng_mw01/index.jsp;jsessionid=3AFEC7A0C4952D2746AF47B80B638696.nbw05.

EPEX SPOT. Trading at EPEX SPOT: 2021, 2021. URL https://www.epexspot.com/sites/default/files/2021-05/21-03-15_Trading%20Brochure.pdf.

European Commission. Quarterly Report: on European Electricity Marktes. *Market Observation for Energy*, 14, 2021.

J. Figgener, P. Stenzel, K.-P. Kairies, J. Linßen, D. Haberschusz, O. Wessels, G. Angenendt, M. Robinius, D. Stolten, and D. U. Sauer. The development of stationary battery storage systems in Germany – A market review. *Energy Storage*, 29:101153, 2020. ISSN 2352-152X. doi: 10.1016/j.est.2019.101153.

S. Fischhaber, A. Regett, S. F. Schuster, and H. Hesse. Studie: Second-Life-Konzepte für Lithium-Ionen-Batterien aus Elektrofahrzeugen: Analyse von Nachnutzungsanwendungen, ökonomischen und ökologischen Potenzialen, Begleit- und Wirkungsforschung Schaufenster Elektromobilität, 2016. URL https://www.ffe.de/wp-content/uploads/2016/06/StudieSecondLifeKonzepte1.pdf.

G. Fitzgerald, J. Mandel, J. Morris, and H. Touati. The economics of battery energy storage: How multi-use, customer-sited batteries deliver the most servics and value to customers and the grid. *Rocky Mountain Institute*, 2015. URL https://rmi.org/wp-content/uploads/2017/03/RMI-TheEconomicsOfBatteryEnergyStorage-FullReport-FINAL.pdf.

Fraunhofer IFF. Prospektive Flexibiltätsoptionen in der produzierenden Industrie: Lastverschiebepotenziale erkennen, modellieren und vermarkten, Fraunhofer-Institut für Fabrikbetrieb und -automatisierung, 2020. URL https://www.iff.fraunhofer.de/content/dam/iff/de/dokumente/publikationen/prospektive-flexibiltaetsoptionen-in-der-produzierenden-industrie-fraunhofer-iff.pdf.

N. Friedrichsen. Verbrauchssteuerung. In M. Wietschel, S. J. Ullrich, P. Markewitz, F. Schulte, and F. Genoese, editors, *Energietechnologien der Zukunft*, pages 417–443. Springer Vieweg, Wiesbaden, 2015. ISBN 978-3-658-07128-8. doi: 10.1007/978-3-658-07129-5_20.

N. Friedrichsen, J. Hilpert, M. Klobasa, and F. Sailer. Anforderungen der Integration der erneuerbaren Energien an die Netzentgeltregulierung – Diskussion ausgewählter Vorschläge zur Weiterentwicklung des Netzentgelt- und Netznutzungssystems: Zusammenfassung für politische

Entscheidungsträger, Umweltbundesamt, 2016. URL https://www.umweltbundesamt.de/publikationen/anforderungen-der-integration-der-erneuerbaren.

W. Fritz, C. Maurer, and A. Jahn. Zukünftige Anforderungen an ein energiewendegrechte Netzkostenallokation: Impuls, Agora Energiewende, 2021.

M. Gargiulo and B. Ó. Gallachóir. Long-term energy models: Principles, characteristics, focus, and limitations. *WIREs Energy and Environment*, 2(2):158–177, 2013. ISSN 2041-8396. doi: 10.1002/wene.62.

H. C. Gils. Assessment of the theoretical demand response potential in Europe. *Energy*, 67: 1–18, 2014. ISSN 0360-5442. doi: 10.1016/j.energy.2014.02.019.

H. Golmohamadi. Demand-side management in industrial sector: A review of heavy industries. *Renewable and Sustainable Energy Reviews*, 156:111963, 2022. ISSN 13640321. doi: 10.1016/j.rser.2021.111963.

K. Graichen. Skriptum Methoden der Optimierung und optimalen Steuerung (WS 2016/2017), Universität Ulm, 2016.

A.-M. Gruber. *Zeitlich und regional aufgelöstes industrielles Lastflexibilisierungspotenzial als Beitrag zur Integration Erneuerbarer Energien.* Dissertation, TU München, Munich, 2017.

A. Halbig. Ein Neues Beschaffungsverfahren für Blindleistung durch § 12h EnWG: Blindleistung und Erneuerbare-Energien-Anlagen – ein Update. *Würzburger Studien zum Umweltenergierecht*, (20), 2021.

A. D. Hawkes. Estimating marginal CO2 emissions rates for national electricity systems. *Energy Policy*, 38(10):5977–5987, 2010. ISSN 0301-4215. doi: 10.1016/j.enpol.2010.05.053.

H. He, E. Du, N. Zhang, C. Kang, and X. Wang. Enhancing the power grid flexibility with battery energy storage transportation and transmission switching. *Applied Energy*, 290:116692, 2021. ISSN 03062619. doi: 10.1016/j.apenergy.2021.116692.

S. He, H. Gao, J. Liu, X. Zhang, and Z. Chen. Distribution system planning considering peak shaving of energy station. *Applied Energy*, 312:118692, 2022. ISSN 03062619. doi: 10.1016/j.apenergy.2022.118692.

R. Heffron, M.-F. Körner, J. Wagner, M. Weibelzahl, and G. Fridgen. Industrial demand-side flexibility: A key element of a just energy transition and industrial development. *Applied Energy*, 269:115026, 2020. ISSN 03062619. doi: 10.1016/j.apenergy.2020.115026.

H. Hesse, M. Schimpe, D. Kucevic, and A. Jossen. Lithium-Ion Battery Storage for the Grid—A Review of Stationary Battery Storage System Design Tailored for Applications in Modern Power Grids. *Energies*, 10(12):2107, 2017. ISSN 1996-1073. doi: 10.3390/en10122107.

L. Hirth and I. Ziegenhagen. Balancing power and variable renewables: Three links. *Renewable and Sustainable Energy Reviews*, 50:1035–1051, 2015. ISSN 13640321. doi: 10.1016/j.rser.2015.04.180.

IRENA. Electricity storage and renewables: Costs and markets to 2030. *International Renewable Energy Agency*, 2017. URL `https://www.irena.org/publications/2017/oct/electricity-storage-and-renewables-costs-and-markets`.

S. Jeddi and A. Sitzmann. Netzentgeltsystematik in Deutschland – Status-Quo, Alternativen und europäische Erfahrungen. *Zeitschrift für Energiewirtschaft*, 43(4):245–267, 2019. ISSN 0343-5377. doi: 10.1007/s12398-019-00265-6.

P. Jochem, S. Babrowski, and W. Fichtner. Assessing CO2 emissions of electric vehicles in Germany in 2030. *Transportation Research Part A: Policy and Practice*, 78:68–83, 2015. ISSN 09658564. doi: 10.1016/j.tra.2015.05.007.

C. R. Jones, P. Hilpert, J. Gaede, and I. H. Rowlands. Batteries, compressed air, flywheels, or pumped hydro? Exploring public attitudes towards grid-scale energy storage technologies in Canada and the United Kingdom. *Energy Research & Social Science*, 80:102228, 2021. ISSN 22146296. doi: 10.1016/j.erss.2021.102228.

A. Jossen and W. Weydanz. *Moderne Akkumulatoren richtig einsetzen*. Ubooks-Verlag, Neusäß, 1st edition, 2006. ISBN 3937536019.

C. Julien, K. Zaghib, Alain Mauger, and Ashok Vijh. *Lithium Batteries : Science and Technology*. Springer, Cham, 2016. ISBN 9783319191089. doi: 10.1007/978-3-319-19108-9.

P. Kall and S. W. Wallace. *Stochastic programming*. Wiley-Interscience series in systems and optimization. Wiley, Chichester, reprinted. edition, 1997. ISBN 0471951080.

J. Kallrath. *Gemischt-ganzzahlige Optimierung: Modellierung in der Praxis*. Springer Fachmedien Wiesbaden, Wiesbaden, 2013. doi: 10.1007/978-3-658-00690-7.

T. Kaschub. *Batteriespeicher in Haushalten unter Berücksichtigung von Photovoltaik, Elektrofahrzeugen und Nachfragesteuerung*. Dissertation, Karlsruher Institut für Technologie, Karlsruhe, 2017.

J. Kasnatscheew, U. Rodehorst, B. Streipert, S. Wiemers-Meyer, R. Jakelski, R. Wagner, I. C. Laskovic, and M. Winter. Learning from Overpotentials in Lithium Ion Batteries: A Case Study on the LiNi 1/3 Co 1/3 Mn 1/3 O 2 (NCM) Cathode. *Journal of The Electrochemical Society*, 163(14):A2943–A2950, 2016. ISSN 0013-4651. doi: 10.1149/2.0461614jes.

T. Kern. Primärregelleistungspreise im neuen Marktdesign: In welche Richtung werden sich die PRL-Preise zukünftig bewegen?, FfE München, 2021. URL

https://www.ffe.de/veroeffentlichungen/primaerregelleistungspreise-im-neuen-marktdesign-in-welche-richtung-werden-sich-die-prl-preise-zukuenftig-bewegen/.

H. Kondziella and T. Bruckner. Flexibility requirements of renewable energy based electricity systems – a review of research results and methodologies. *Renewable and Sustainable Energy Reviews*, 53:10–22, 2016. ISSN 13640321. doi: 10.1016/j.rser.2015.07.199.

R. Korthauer. *Handbuch Lithium-Ionen-Batterien*. Springer Berlin Heidelberg, Berlin, Heidelberg, 2013. doi: 10.1007/978-3-642-30653-2.

E. Kraft. *Decision-making under uncertainty in short-term electricity markets*. Dissertation, Karlsruher Institut für Technologie, Karlsruhe, 2022.

M. Kraiczy. *PV as an ancillary service provider: IEA PVPS Task 14*. 2021. ISBN 978-3-907281-24-6.

N. Kularatna and K. Gunawardane. *Energy Storage Devices for Renewable Energy-Based Systems : Rechargeable Batteries and Supercapacitors*, volume Second edition. Academic Press, London, 2021. ISBN 9780128207789.

P. Kurzweil. *Angewandte Elektrochemie*. Springer Fachmedien Wiesbaden, Wiesbaden, 2020. doi: 10.1007/978-3-658-32421-6.

M. Lang. *Degradationsmechanismen großformatiger Lithium-Ionen-Batterien für Elektrofahrzeuge*. Dissertation, Karlsruher Institut für Technologie, Karlsruhe, 2018.

C. Lange. *Energiesektoren-übergreifende Lastspitzenreduktion mit elektrischen und thermischen Energiespeichern*. Dissertation, Friedrich-Alexander-Universität Erlangen-Nürnberg, Nuremberg, 2021.

C. L. Lara, J. D. Siirola, and I. E. Grossmann. Electric power infrastructure planning under uncertainty: stochastic dual dynamic integer programming (SDDiP) and parallelization scheme. *Optimization and Engineering*, 21(4):1243–1281, 2019. ISSN 1389-4420. doi: 10.1007/s11081-019-09471-0.

M. T. Lawder, B. Suthar, P. W. C. Northrop, S. De, C. M. Hoff, O. Leitermann, M. L. Crow, S. Santhanagopalan, and V. R. Subramanian. Battery Energy Storage System (BESS) and Battery Management System (BMS) for Grid-Scale Applications. *Proceedings of the IEEE*, 102(6):1014–1030, 2014. ISSN 0018-9219. doi: 10.1109/JPROC.2014.2317451.

J. W. Lee, M. H. S. M. Haram, G. Ramasamy, S. P. Thiagarajah, E. E. Ngu, and Y. H. Lee. Technical feasibility and economics of repurposed electric vehicles batteries for power peak shaving. *Energy Storage*, 40:102752, 2021. ISSN 2352-152X. doi: 10.1016/j.est.2021.102752.

J. Li, D. Wang, and M. Pecht. An electrochemical model for high C-rate conditions in lithium-ion batteries. *Journal of Power Sources*, 436:226885, 2019. ISSN 03787753. doi: 10.1016/j.jpowsour.2019.226885.

Z. Li, L. Wu, Y. Xu, and X. Zheng. Stochastic-Weighted Robust Optimization Based Bilayer Operation of a Multi-Energy Building Microgrid Considering Practical Thermal Loads and Battery Degradation. *IEEE Transactions on Sustainable Energy*, 13(2):668–682, 2022. ISSN 1949-3029. doi: 10.1109/TSTE.2021.3126776.

G. Liu, Y. Xu, and K. Tomsovic. Bidding Strategy for Microgrid in Day-Ahead Market Based on Hybrid Stochastic/Robust Optimization. *IEEE Transactions on Smart Grid*, 7(1):227–237, 2016. ISSN 1949-3053. doi: 10.1109/TSG.2015.2476669.

S. Liu, J. Wang, H. Liu, Q. Liu, J. Tang, and Z. Li. Battery degradation model and multiple-indicators based lifetime estimator for energy storage system design and operation: Experimental analyses of cycling-induced aging. *Electrochimica Acta*, 384:138294, 2021. ISSN 00134686. doi: 10.1016/j.electacta.2021.138294.

P. D. Lund, J. Lindgren, J. Mikkola, and J. Salpakari. Review of energy system flexibility measures to enable high levels of variable renewable electricity. *Renewable and Sustainable Energy Reviews*, 45:785–807, 2015. ISSN 13640321. doi: 10.1016/j.rser.2015.01.057.

J. Ma, V. Silva, R. Belhomme, D. S. Kirschen, and L. F. Ochoa. Evaluating and Planning Flexibility in Sustainable Power Systems. *IEEE Transactions on Sustainable Energy*, 4(1): 200–209, 2013. ISSN 1949-3029. doi: 10.1109/TSTE.2012.2212471.

S. Ma, M. Jiang, P. Tao, C. Song, J. Wu, J. Wang, T. Deng, and W. Shang. Temperature effect and thermal impact in lithium-ion batteries: A review. *Progress in Natural Science: Materials International*, 28(6):653–666, 2018. ISSN 10020071. doi: 10.1016/j.pnsc.2018.11.002.

T. Maiyalagan and P. Elumalai. *Rechargeable Lithium-Ion Batteries : Trends and Progress in Electric Vehicles*. CRC Press, Boca Raton, FL, 2021. ISBN 9780367510138.

S. Materi, A. D'Angola, D. Enescu, and P. Renna. Reducing energy costs and CO2 emissions by production system energy flexibility through the integration of renewable energy. *Production Engineering*, 15(5):667–681, 2021. ISSN 0944-6524. doi: 10.1007/s11740-021-01051-5.

M. Mazidi, N. Rezaei, and A. Ghaderi. Simultaneous power and heat scheduling of microgrids considering operational uncertainties: A new stochastic p-robust optimization approach. *Energy*, 185:239–253, 2019. ISSN 0360-5442. doi: 10.1016/j.energy.2019.07.046.

E. Merkel. *Analyse und Bewertung des Elektrizitätssystems und des Wärmesystems der Wohngebäude in Deutschland*. Dissertation, Karlsruher Institut für Technologie, Karlsruhe, 2016.

J. Michaelis, T. Muller, U. Reiter, F. Fermi, A. Wyrwa, Y.-k. Chen, C. Zophel, N. Kronthaler, and R. Elsland. Comparison of the techno-economic characteristics of different flexibility options in the European energy system. In *2017 14th International Conference on the European Energy Market (EEM)*, pages 1–5, Piscataway, NJ, 2017. IEEE. ISBN 978-1-5090-5499-2. doi: 10.1109/EEM.2017.7981983.

D. Mietzner. *Strategische Vorausschau und Szenarioanalysen: Methodenevaluation und neue Ansätze*. Innovation und Technologie im modernen Management. 2010. ISBN 9783834983824. doi: 10.1007/978-3-8349-8382-4.

T. Müller and D. Möst. Demand Response Potential: Available when Needed? *Energy Policy*, 115:181–198, 2018. ISSN 0301-4215. doi: 10.1016/j.enpol.2017.12.025.

A. Najafi-Ghalelou, M. Khorasany, and R. Razzaghi. Risk-Constrained Scheduling of Energy Hubs: A Stochastic p-Robust Optimization Approach. *IEEE Systems Journal*, pages 1–12, 2022. ISSN 1932-8184. doi: 10.1109/JSYST.2022.3143517.

N. Nasiri, S. Zeynali, S. N. Ravadanegh, and M. Marzband. A hybrid robust-stochastic approach for strategic scheduling of a multi-energy system as a price-maker player in day-ahead wholesale market. *Energy*, 235:121398, 2021. ISSN 0360-5442. doi: 10.1016/j.energy.2021.121398.

N. Naval and J. M. Yusta. Virtual power plant models and electricity markets - A review. *Renewable and Sustainable Energy Reviews*, 149:111393, 2021. ISSN 13640321. doi: 10.1016/j.rser.2021.111393.

Next Kraftwerke GmbH. Was sind Systemdienstleistungen?, Next Kraftwerke GmbH, 2021a. URL `https://www.next-kraftwerke.de/wissen/systemdienstleistungen`, 2021-12-14.

Next Kraftwerke GmbH. Regelenergie & Regelleistung - was ist das?, Next Kraftwerke GmbH, 2021b. URL `https://www.next-kraftwerke.de/wissen/regelenergie`, 2021-12-14.

Next Kraftwerke GmbH. Abschaltverordnung, Next Kraftwerke GmbH, 2021c. URL `https://www.next-kraftwerke.de/wissen/abschaltverordnung`, 2021-12-27.

Next Kraftwerke GmbH. Was ist Arbitrage?, Next Kraftwerke GmbH, 2022. URL `https://www.next-kraftwerke.de/wissen/arbitrage`, 2022-04-12.

P. Nystrup, H. Madsen, E. M. Blomgren, and G. de Zotti. Clustering commercial and industrial load patterns for long-term energy planning. *Smart Energy*, 2:100010, 2021. ISSN 26669552. doi: 10.1016/j.segy.2021.100010.

J. Oehmen, G. Locatelli, M. Wied, and P. Willumsen. Risk, uncertainty, ignorance and myopia: Their managerial implications for B2B firms. *Industrial Marketing Management*, 88:330–338, 2020. ISSN 00198501. doi: 10.1016/j.indmarman.2020.05.018.

S. Paarmann. *How Non-Uniform Temperatures Influence the Performance and Ageing of Lithium-Ion Batteries*. Dissertation, Karlsruher Institut für Technologie, Karlsruhe, 2021.

S. S. Parvar and H. Nazaripouya. Optimal Operation of Battery Energy Storage Under Uncertainty Using Data-Driven Distributionally Robust Optimization. *Electric Power Systems Research*, 211:108180, 2022. ISSN 03787796. doi: 10.1016/j.epsr.2022.108180.

M. Paulus and F. Borggrefe. The potential of demand-side management in energy-intensive industries for electricity markets in Germany. *Applied Energy*, 88(2):432–441, 2011. ISSN 03062619. doi: 10.1016/j.apenergy.2010.03.017.

I. J. Perez-Arriaga, J. D. Jenkins, and C. Batlle. A regulatory framework for an evolving electricity sector: Highlights of the MIT utility of the future study. *Economics of Energy & Environmental Policy*, 6(1), 2017. ISSN 21605882. doi: 10.5547/2160-5890.6.1.iper.

S. Petrovic. *Battery Technology Crash Course*. Springer International Publishing, Cham, 2021. doi: 10.1007/978-3-030-57269-3.

S. Rebennack. *A unified state-space and scenario tree framework for multi-stage stochastic optimization: An application to emission-constrained hydro-thermal scheduling*. Dissertation, University of Florida, 2010.

Regelleistung.net. Abschaltbare Lasten, 2020. URL `https://www.regelleistung.net/ext/static/abla`, 2021-12-27.

Regelleistung.net. Information zum Netzregelverbund und der internationalen Weiterentwicklung: - Weitere ÜNBs treten dem IGCC (International Grid Control Cooperation) bei -, Regelleistung.net, 2021a. URL `https://www.regelleistung.net/ext/download/marktinformationenApg`, 2021-12-22.

Regelleistung.net. Ausschreibungsübersicht, 2021b. URL `https://www.regelleistung.net/ext/tender/`, 2021-12-22.

J. C. Richstein and S. S. Hosseinioun. Industrial demand response: How network tariffs and regulation (do not) impact flexibility provision in electricity markets and reserves. *Applied Energy*, 278:115431, 2020. ISSN 03062619. doi: 10.1016/j.apenergy.2020.115431.

J. Richter and J. Porst. Operational Strategies for Battery Energy Storage Systems for Corrective Congestion Management: PESS 2021 – Power and Energy Student Summit. *Conference Proceedings 25 – 26 November 2021, University of Kassel, Germany, Online Conference*, 2022. URL http://www.content-select.com/index.php?id=bib_view&ean=9783800757169.

H.-K. Ringkjøb, P. M. Haugan, and I. M. Solbrekke. A review of modelling tools for energy and electricity systems with large shares of variable renewables. *Renewable and Sustainable Energy Reviews*, 96:440–459, 2018. ISSN 13640321. doi: 10.1016/j.rser.2018.08.002.

J. Rominger. *Provision of Flexibility Services by Industrial Energy Systems*. Dissertation, Karlsruher Institut für Technologie, Karlsruhe, 2020.

H. M. Rouzbahani, H. Karimipour, and L. Lei. A review on virtual power plant for energy management. *Sustainable Energy Technologies and Assessments*, 47:101370, 2021. ISSN 22131388. doi: 10.1016/j.seta.2021.101370.

M. Ruppert, V. Slednev, R. Finck, A. Ardone, and W. Fichtner. Utilising Distributed Flexibilities in the European Transmission Grid. In V. Bertsch, A. Ardone, M. Suriyah, W. Fichtner, T. Leibfried, and V. Heuveline, editors, *Advances in Energy System Optimization*, Springer eBook Collection, pages 81–101, Cham, 2020. Springer International Publishing and Imprint Birkhäuser. ISBN 978-3-030-32156-7. doi: 10.1007/978-3-030-32157-4_6.

A. Sakti, K. G. Gallagher, N. Sepulveda, C. Uckun, C. Vergara, F. J. de Sisternes, D. W. Dees, and A. Botterud. Enhanced representations of lithium-ion batteries in power systems models and their effect on the valuation of energy arbitrage applications. *Journal of Power Sources*, 342:279–291, 2017. ISSN 03787753. doi: 10.1016/j.jpowsour.2016.12.063.

A. Saltelli, S. Tarantola, and F. Campolongo. Sensitivity Analysis as an Ingredient of Modeling. *Statistical Science*, 15(4):377–395, 2000. ISSN 08834237. URL http://www.jstor.org/stable/2676831.

Sandia National Laboratories. Statistics: Energy Storage Installations by Year, U.S. Department of Energy/National Nuclear Security Administration, 2022. URL https://sandia.gov/ess-ssl/gesdb/public/statistics.html, 2022-02-28.

W.-P. Schill. Residual load, renewable surplus generation and storage requirements in Germany. *Energy Policy*, 73:65–79, 2014. ISSN 0301-4215. doi: 10.1016/j.enpol.2014.05.032.

I. Schlecht, C. Wagner, W. Lehnert, M. Bucksteeg, A. Schinke-Nendza, and N. Voß. Effizienzprüfung marktgestützter Beschaffung von nicht-frequenzgebundenen Systemdienstleistungen (NF-SDL): Bericht im Vorhaben „SDL-Zukunft“, ef.Ruhr GmbH, 2020. URL https://www.bmwi.de/Redaktion/DE/Downloads/E/ergebnispapier-effizienzpr%C3%BCfung-nf-sdl.pdf?__blob=publicationFile&v=2.

H. Schwarz. *Optimierung der Investitions- und Einsatzplanung dezentraler Energiesysteme unter Unsicherheit*. Dissertation, Karlsruher Institut für Technologie, Karlsruhe, 2019.

H. Schwarz, H. Schermeyer, V. Bertsch, and W. Fichtner. Self-consumption through power-to-heat and storage for enhanced PV integration in decentralised energy systems. *Solar Energy*, 163:150–161, 2018. ISSN 0038092X. doi: 10.1016/j.solener.2018.01.076.

H. Seidl, C. Schenuit, M. Teichmann, E.-L. Limbacher, Mann Jakob, and A. Dünnwald. Impulse zur Weiterentwicklung der Netzentgeltsystematik: Industrielles Verbrauchsverhalten im Rahmen der Energiewende netzdienlich gestalten, Deutsche Energie-Agentur GmbH, 2018. URL `https://www.dena.de/fileadmin/dena/Dokumente/Pdf/9238_Ergebnispapier_der_Taskforce_Netzentgelte_Impulse_zur_Weiterentwicklung_der_Netzentgeltsyst.pdf`.

C. Shang and F. You. Process Scheduling under Ambiguity Uncertainty Probability Distribution. In A. Friedl, J. J. Klemeš, S. Radl, P. S. Varbanov, and T. Wallek, editors, *28th European Symposium on Computer Aided Process Engineering*, volume 43 of *Computer-aided chemical engineering*, pages 919–924. Elsevier, Amsterdam and Boston and Heidelberg, 2018. ISBN 9780444642356. doi: 10.1016/B978-0-444-64235-6.50162-5.

A. Shivakumar, C. Taliotis, P. Deane, J. Gottschling, R. Pattupara, R. Kannan, D. Jakšić, K. Stupin, R. V. Hemert, B. Normark, and A. Faure-Schuyer. Need for Flexibility and Potential Solutions. In M. Welsch, S. Pye, D. Keles, A. Faure-Schuyer, A. Dobbins, A. Shivakumar, P. Deane, and M. Howells, editors, *Europe's energy transition*, pages 149–172. Academic Press, London and San Diego, CA and Cambridge, MA and Oxford, 2017. ISBN 9780128098066. doi: 10.1016/B978-0-12-809806-6.00021-3.

R. Sioshansi, P. Denholm, T. Jenkin, and J. Weiss. Estimating the value of electricity storage in PJM: Arbitrage and some welfare effects. *Energy Economics*, 31(2):269–277, 2009. ISSN 01409883. doi: 10.1016/j.eneco.2008.10.005.

SMARD. Regelarbeitsmarkt gestartet, Bundesnetzagentur, 2020. URL `https://www.smard.de/page/home/topic-article/444/196354`, 2021-12-15.

L. V. Snyder and M. S. Daskin. Stochastic p-robust location problems. *IIE Transactions*, (38): 971–985, 2006. doi: 10.1080/07408170500469113.

T. Sriyakul and K. Jermsittiparsert. Optimal economic management of an electric vehicles aggregator by using a stochastic p-robust optimization technique. *Energy Storage*, 32:102006, 2020. ISSN 2352-152X. doi: 10.1016/j.est.2020.102006.

M. Stadler, M. Groissböck, G. Cardoso, and C. Marnay. Optimizing Distributed Energy Resources and building retrofits with the strategic DER-CAModel. *Applied Energy*, 132:557–567, 2014. ISSN 03062619. doi: 10.1016/j.apenergy.2014.07.041.

J. Stede, K. Arnold, C. Dufter, G. Holtz, S. von Roon, and J. C. Richstein. The role of aggregators in facilitating industrial demand response: Evidence from Germany. *Energy Policy*, 147: 111893, 2020. ISSN 0301-4215. doi: 10.1016/j.enpol.2020.111893.

O. Stein. *Grundzüge der globalen Optimierung*. Springer eBook Collection. Springer Spektrum, Berlin and Heidelberg, 2nd edition, 2021. ISBN 978-3-662-62533-0. doi: 10.1007/978-3-662-62534-7.

M. Sterner and I. Stadler. *Energiespeicher - Bedarf, Technologien, Integration*. Springer Berlin Heidelberg, Berlin, Heidelberg, 2014. doi: 10.1007/978-3-642-37380-0.

A. Stirling. Renewables, sustainability and precaution: Beyond Environmental Cost-benefit and Risk Analysis. In R. E. Hester and R. M. Harrison, editors, *Sustainability and Environmental Impact of Renewable Energy Sources*, volume 19, pages 113–134. The Royal Society of Chemistry, 2003. ISBN 978-0-85404-290-6. doi: 10.1039/9781847551986-00113.

K. Strauß. *Kraftwerkstechnik*. Springer Berlin Heidelberg, Berlin, Heidelberg, 2009. doi: 10.1007/978-3-642-01431-4.

E. Svetlova and H. van Elst. How Is Non-knowledge Represented in Economic Theory? *Voprosy Ekonomiki*, (8):82–105, 2013. ISSN 0042-8736. doi: 10.32609/0042-8736-2013-8-82-105.

L. Tang, Y. Han, P. Yang, C. Wang, and A. S. Zalhaf. A review of voltage sag control measures and equipment in power systems. *Energy Reports*, 8:207–216, 2022. ISSN 23524847. doi: 10.1016/j.egyr.2022.05.158.

Y. Tohidi and M. Gibescu. Stochastic optimisation for investment analysis of flow battery storage systems. *IET Renewable Power Generation*, 13(4):555–562, 2019. ISSN 1752-1416. doi: 10.1049/iet-rpg.2018.5788.

TransnetBW. Netzbooster-Pilotanlage Kupferzell: Projektvorstellung, TransnetBW, 2021. URL `https://www.transnetbw.de/files/pdf/netzentwicklung/projekte/netzbooster-pilotanlage/broschuere.pdf`.

M. Uddin, M. F. Romlie, M. F. Abdullah, S. Abd Halim, A. H. Abu Bakar, and T. Chia Kwang. A review on peak load shaving strategies. *Renewable and Sustainable Energy Reviews*, 82: 3323–3332, 2018. ISSN 13640321. doi: 10.1016/j.rser.2017.10.056.

C. Wagner, I. Schlecht, and M. Bucksteeg. Marktgestützte Beschaffung von Schwarzstartfähigkeit: Bericht im Vorhaben „SDL-Zukunft“, ef.Ruhr GmbH, 2020. URL `https://www.bmwi.de/Redaktion/DE/Downloads/E/ergebnispapier-beschaffungskonzept-schwarzstartfaehigkeit.pdf?__blob=publicationFile&v=4`.

R. Walawalkar, J. Apt, and R. Mancini. Economics of electric energy storage for energy arbitrage and regulation in New York. *Energy Policy*, 35(4):2558–2568, 2007. ISSN 0301-4215. doi: 10.1016/j.enpol.2006.09.005.

Z. Wang, S. Xu, X. Zhu, H. Wang, L. Huang, J. Yuan, and W. Yang. Effects of short-term over-discharge cycling on the performance of commercial 21,700 lithium-ion cells and the identification of degradation modes. *Energy Storage*, 35:102257, 2021. ISSN 2352-152X. doi: 10.1016/j.est.2021.102257.

J. E. Ward and R. E. Wendell. Approaches to sensitivity analysis in linear programming. *Annals of Operations Research*, 27(1):3–38, 1990. ISSN 0254-5330. doi: 10.1007/BF02055188.

K. Weinand, F. Braeuer, T. Geisert, M. Skoruppa, and P. Jochem. Atypische Netznutzung in Industriebetrieben – lohnt sich ein Batteriespeicher? *Energiewirtschaftliche Tagesfragen*, 2021(1/2):74–78, 2021. URL `https://emagazin.et-magazin.de/de/profiles/cb1a7fd451c4/editions/cc8dbb94a79db886ea57`.

M. Weiss. Impedanzgestützte Lebensdaueranalyse von Lithium-Ionen Batterien: Dissertation. *Schriften des Instituts für Angewandte Materialien – Werkstoffe der Elektrotechnik*, 40, 2019. doi: 10.5445/KSP/1000099243.

M. Wietschel, S. J. Ullrich, P. Markewitz, F. Schulte, and F. Genoese, editors. *Energietechnologien der Zukunft: Erzeugung, Speicherung, Effizienz und Netze*. Springer Vieweg, Wiesbaden, 2015. ISBN 978-3-658-07128-8. doi: 10.1007/978-3-658-07129-5.

J. Xie and Y.-C. Lu. A retrospective on lithium-ion batteries. *Nature communications*, 11(1): 2499, 2020. doi: 10.1038/s41467-020-16259-9.

B. Xu, W. Diao, G. Wen, S.-Y. Choe, J. Kim, and M. Pecht. Decoupling the thermal and non-thermal effects of discharge C-rate on the capacity fade of lithium-ion batteries. *Journal of Power Sources*, 510:230390, 2021. ISSN 03787753. doi: 10.1016/j.jpowsour.2021.230390.

X. Xu, W. Hu, Di Cao, Q. Huang, Z. Liu, W. Liu, Z. Chen, and F. Blaabjerg. Scheduling of wind-battery hybrid system in the electricity market using distributionally robust optimization. *Renewable Energy*, 156:47–56, 2020. ISSN 09601481. doi: 10.1016/j.renene.2020.04.057.

W. Zander, U. Rosen, A. Nolde, S. Patzack, S. Seier, M. Hübschmann, M. T. Piske, S. Lemkens, and K. V. Boesche. Gutachten Digitalisierung der Energiewende: Topthema 2: Regulierung, Flexibilisierung und Sektorkopplung, Ernest & Young and BET and WIK, 2018. URL `https://www.bmwi.de/Redaktion/DE/Publikationen/Studien/digitalisierung-der-energiewende-thema-2.pdf?__blob=publicationFile&v=8`.

M. Zare Oskouei, M. A. Mirzaei, B. Mohammadi-Ivatloo, M. Shafiee, M. Marzband, and A. Anvari-Moghaddam. A hybrid robust-stochastic approach to evaluate the profit of a multi-energy retailer in tri-layer energy markets. *Energy*, 214:118948, 2021. ISSN 0360-5442. doi: 10.1016/j.energy.2020.118948.

P. Zhao, C. Gu, Da Huo, Y. Shen, and I. Hernando-Gil. Two-Stage Distributionally Robust Optimization for Energy Hub Systems. *IEEE Transactions on Industrial Informatics*, 16(5): 3460–3469, 2020. ISSN 1551-3203. doi: 10.1109/TII.2019.2938444.

X. Zhao, H. Zhang, Z. Ni, and G. Liu. Development and Test of a UPS for Voltage Sag Immunity in IC Manufacturing. In *2021 IEEE 17th International Conference on Automation Science and Engineering (CASE)*, pages 738–741, Piscataway, NJ, 2021. IEEE. ISBN 978-1-6654-1873-7. doi: 10.1109/CASE49439.2021.9551458.

B. Zimmermann and B. Breuer. ELGEVOS - Studie zur Elektroenergieversorgung von Gewächshäusern aus einem volatilen Stromnetz mit hohem Anteil erneuerbarer Energien: Forschungsbericht Fraunhofer IEE, Fraunhofer-Institut für Energiewirtschaft und Energiesystemtechnik, 2019. URL `http://www.elgevos.de/img/media/ELGEVOS_Schlussbericht_HUB.pdf`.

H.-J. Zimmermann. *Operations Research: Methoden und Modelle. Für Wirtschaftsingenieure, Betriebswirte, Informatiker*. Vieweg, Wiesbaden, 2nd edition, 2008. ISBN 978-3-8348-0455-6.

# Part II

# Publications

# Publication A

## Battery storage systems: An economic model-based analysis of parallel revenue streams and general implications for industry

Fritz Braeuer[a], Julian Rominger[b], Russell McKenna[c], Wolf Fichtner[a]

[a]*Chair of Energy Economics, Institute for Industrial Production, Karlsruhe Institute of Technology, Karlsruhe, Germany*

[b]*FZI Forschungszentrum Informatik, Karlsruhe, Germany*

[c]*DTU Management Engineering, Technical University of Denmark (DTU), Kgs. Lyngby, Denmark*

Published in:

Applied Energy, Volume 239, 1st of April 2019, pages 1424-1440

https://doi.org/10.1016/j .apenergy.2019.01.050

Applied Energy 239 (2019) 1424–1440

Contents lists available at ScienceDirect

Applied Energy

journal homepage: www.elsevier.com/locate/apenergy

# Battery storage systems: An economic model-based analysis of parallel revenue streams and general implications for industry

Fritz Braeuer[a,*], Julian Rominger[b], Russell McKenna[c], Wolf Fichtner[a]

[a] Chair of Energy Economics, Institute for Industrial Production (IIP), Karlsruhe Institute of Technology (KIT), Karlsruhe, Germany
[b] FZI Forschungszentrum Informatik, Karlsruhe, Germany
[c] DTU Management Engineering, Technical University of Denmark (DTU), Kgs. Lyngby, Denmark

## HIGHLIGHTS

- Battery provides pseudo-flexibility by not affecting production processes.
- Optimize battery size for peak shaving, arbitrage trading, primary balancing power.
- Application to load profiles of 50 German SMEs.
- Profitably of revenue streams: not in isolation, but combined for some companies.
- Developed load indicators provide general profitability insights.

## ARTICLE INFO

*Keywords:*
Battery storage system
Industry
Primary control reserve
Energy market
Peak shaving
Load Indicator

## ABSTRACT

This paper evaluates the economic potential of energy flexibility in 50 different German small and medium sized enterprises (SMEs) through the installation of a battery storage system (BSS). The central innovation lies in the possibility of pursuing multiple revenue streams simultaneously: peak shaving, provision of primary control reserve (PCR) and energy-arbitrage-trading through intraday and day-ahead markets. The energy system of an industrial manufacturing plant is modelled as a linear program (LP) with a 15-min resolution. The model offers the option to invest in BSSs with different capacities, with the objective of minimizing the overall cost and identifying the optimal size of the BSS. The results show that none of these three revenue streams individually is economically attractive, but when combined, all three together can achieve profitability for some companies, whereby the majority of the cash flow comes from peak shaving and PCR. With a fixed BSS capacity of 500 kWh, the Net Present Value (NPV) varies from a minimum of −350,000 € for just arbitrage up to about 200,000 € for all three use cases in parallel. In the case of a variable BSS capacity, the capacity varies up to 1200 kWh and the Profitability Index (the ratio of investment to NPV) varies from 0.06 to 0.31. Under current German market conditions, arbitrage trading contributes only marginally to the profitability, as the price spreads are too small to justify stronger battery degradation. The paper also identifies various load indicators from the analysis of the demand profile that support the evaluation of a BSS in industry. A stepwise linear regression reveals a moderate dependency of the BSS profitability on two newly developed load indicators. Future work should focus on a more detailed depiction of the battery's technical behaviour and increasing the sample size to improve the statistical significance of the results.

## 1. Introduction

The growing share of volatile renewable electricity is increasing the stress on the German electricity grid: electricity producers are asked to balance sudden power shortfalls on the supply side and distribution grid operators need to overcome an increasing number of congestions. To counter these challenges and generate higher flexibilities on the demand side, different market measures have been implemented. The market for ancillary services has been opened to a growing number of prequalified suppliers of balancing power. The feed–in tariffs for renewable energy have also been drastically reduced, which alongside the achievement of grid parity for some technologies such as photovoltaics (PV) encourages a higher rate of energy self-sufficiency. Furthermore, through grid service charges or bilateral agreements, industrial

* Corresponding author.
*E-mail address:* fritz.braeuer@kit.edu (F. Braeuer).

https://doi.org/10.1016/j.apenergy.2019.01.050
Received 15 August 2018; Received in revised form 18 December 2018; Accepted 4 January 2019

**Nomenclature**

*Acronyms*

| | |
|---|---|
| BSS | battery storage system |
| PCR | primary control reserve |
| SME | small and medium sized enterprises |
| LP | linear program |
| NPV | net present value |
| PI | profitability index |
| PP | payback period |
| U1–U6 | use case, combination of revenue streams |
| DSM | demand side management |

*Sets and indices*

| | |
|---|---|
| q | quarter hour |
| h | hour |
| w | week |
| grid | electricity grid |
| BSS | battery storage system |
| prod | production process |
| arb | arbitrage trading |
| peak | peak shaving |
| PCR | primary control reserve |
| old | before installation of BSS |
| new | after installation of BSS |
| i | 15-min time step in a day |
| j | day per year |

*Load indicators*

| | |
|---|---|
| $P_{MD}$ | mean daily peak load |
| $P_{ToU}$ | most frequent peak load interval |
| $P_{LF}$ | daily peakyness |
| $P_{PoU}$ | yearly period of use |
| $P_{i,j}$ | mean production load |
| $E_{peak,i,j}$ | peak energy |
| $E_{above}$ | energy above peak threshold |
| $P_{interval,j}$ | number of peak intervals per day |
| $\text{Peak}_{\text{integral}}$ | peak integral |
| $\text{Peak}_{\text{above}}$ | peak above |
| $\text{Peak}_{\text{interval}}$ | peak interval |
| $\text{Peak}_{\text{density}}$ | peak density |
| $\text{peak}_{\text{abil}}$ | peak ability |

*Variables*

| | |
|---|---|
| $x_{grid}$ | electrical energy flow from and to grid [kWh] |
| $x_{x,y}$ | electrical energy flow from x to y [kWh] |
| $x_{BSS,tot}$ | energy in-flow in BSS per year [kWh] |
| $P^{w}_{PCR}$ | amount of provided for PCR per week [MW] |
| $P_{x,y}$ | electrical power flow from x to y [MW] |
| $P_{peak}$ | peak power from grid per year [MW] |
| $l^{q,h,w}_{BSS}$ | storage level of BSS [kWh] |
| $C^{h,w}_{el}$ | cost and revenue for electricity trading [€] |
| $R^{w}_{PCR}$ | revenue from PCR [€] |
| $C_{peak}$ | cost for power capacity [€] |
| $A_{BSS}$ | annuity payment for BSS [€] |
| $cap^{w}_{PCR}$ | capacity of BSS reserved for PCR [kWh] |
| $cap_{BSS}$ | installed capacity of BSS [kWh] |
| $cap_{BSS,aged}$ | invested capacity of BSS with battery degradation [kWh] |
| $cap_{add,l}$ | additional capacity invest due to storage level degradation [kWh] |
| $cap_{red,cycl}$ | reduced capacity invest due to unexploited cycle life [kWh] |
| $CF_{tot}$ | total cash flow per year [€] |
| $CF_{x}$ | cash flow from revenue stream x [€] |

*Parameters*

| | |
|---|---|
| $D_{x,prod}$ | electrical energy demand of production [kWh] |
| $D_{P,prod}$ | electrical power demand of production [MW] |
| $LT_{cal}$ | calendar lifetime [years] |
| $LT_{cycl}$ | cycle lifetime [cycles] |
| $p^{h,w}_{ahead}$ | electricity price on day-ahead market [€/kWh] |
| $p^{q,h,w}_{intra}$ | electricity price on intraday market [€/kWh] |
| $p_{peak}$ | grid charges [€/MW] |
| $p_{BSS}$ | price for BSS capacity [€/KWh] |
| $puff_{PCR}$ | puffer factor for PCR [–] |
| $T_{PCR,crit}$ | critical time threshold for PCR [h] |
| $T$ | number of annuities [a] |
| $i$ | discount rate [%] |

electricity consumers are motivated to shift their peak load [1,2].

Because of their high energy demand, industrial companies can profit from these novel flexibility measures. To provide these flexibilities, industrial energy consumers can choose to adapt their production processes to electricity or capacity prices with demand response measures. Especially individual energy intensive processes can be linked to energy prices [3]. In other cases electricity can be integrated as a time-dependent production factor into the production planning process [4,5]. On the other hand, for many producing companies these options offer no economic value, as their production systems are laid out to achieve the highest utilization of their machine capacities. Additionally, there are further regulatory and knowledge based hurdles for such demand response schemes [6].

An alternative to demand response is the installation of a battery storage system (BSS). A BSS provides a pseudo-flexibility: a flexible electricity demand can be offered to grid operators and electricity markets via different revenue streams while the production remains unaffected. Like self-sufficiency-optimization, peak shaving or the provision of ancillary services, various marketing schemes for the flexibility from BSSs in industries have been individually examined [7,8]. However, one unique attribute of BSSs is the ability to follow different business models simultaneously [9]. Many publications mention this possibility [10,11] but the potential has not yet been thoroughly studied.

Only a few authors focus their studies on the potential of BSS following different revenue streams in parallel. Stephan et al. [12] run an hourly dispatch algorithm in a two phase simulation and divide the dispatch into a primary and secondary application (hierarchical order), focus on peak shaving, self-consumption, investment deferral and control reserve. This hierarchical order of revenue streams might underestimate the economic success of a BSS because of the time variability and interdependency of these different revenue streams. Lombardi and Schwabe [13] apply a similar hierarchical prioritization of the peak shaving revenue stream. They simulate the BSS dispatch under a sharing economy principle for different customers but focus on PV-self-consumption and restrict BSS charging from the grid. Cho and Kleit [14] and Moreno et al. [15] apply similarly strict charging constraints. Cho and Kleit [14] analyse the BSS's operation with a three stage hotelling rent approach considering energy markets and ancillary services. Their model constrains battery charging and discharging to once a day. Moreno et al. [15] apply an MILP to study the battery dispatch from the energy utilities' point of view, whereby the peak shaving potential is

restricted through a fixed power limit. This reduced degree of freedom might severely diminish the economic potential of a peak shaving application. Instead the power limit should rather be a decision variable of the optimization model. Dowling et al. [16] optimize the battery dispatch for energy utilities in the U.S. They integrate different time layers in their model to expand their scope on intraday and day-ahead markets, ancillary services as well as virtual bidding products. Atabay [17] develop an open-source MILP model to optimize capacity planning and unit commitment of the multi-commodity system of an industrial company with time-sensitive commodity prices and peak demand charges.

The general conclusion is that combining different revenue streams increases the profitability of the BSS but there is "still an idle potential for even more applications" [13]. The following deficiencies in studies about multiple revenue streams for BSS can be identified in the literature:

- No combination of all three revenue streams of arbitrage trading, peak shaving and PCR.
- No actual parallelization of all revenue streams. In contrast, a hierarchical approach is used.
- No investigation of the influence of different industrial load profiles.
- No combination of battery dispatch and battery investment for parallel revenue streams.

Against this background, this paper evaluates the economic potential of energy flexibility in industrial companies through the installation of a BSS. The contribution of this paper is the modelling of three revenue streams, energy arbitrage trading, peak shaving and PCR, applied in parallel. Furthermore, through the study of 50 different German small and medium–sized enterprises (SMEs) the effect that the different revenue streams and different load profiles have on the profitability of a BSS-investment is shown. In addition, the paper identifies specific load indicators that explain the variation in profitability for different BSSs in industry. This paper focusses on the German energy and power markets applying current regulations and prices of the mentioned revenue streams. The two main research hypotheses are:

H1. Applying different use cases in parallel increases the profitability of a BSS in industry.
H2. Specific load indicators explain the variation in profitability of a BSS in industry.

To test these statements, we perform three analytical steps:

A1. Optimizing with fixed BSS capacity
A2. Optimizing with variable BSS capacity
A3. Stepwise linear regression of load indicators.

To optimize the operation and size of a BSS, we model the industrial manufacturing plant as a linear program (LP). The optimization model offers the option to invest in BSSs with different capacities, with the objective of minimizing the overall cost. In *A1*, the installed capacity of the BSS is an exogenous parameter and all 50 companies install identical BSSs. The model identifies the optimal operation of the BSS for different use cases. We study six different use cases, which represent different combinations of the different revenue streams providing primary control reserve, peak shaving and arbitrage trading respectively. Thereby we are able to answer *H1*. To test *H2* we perform *A2* and *A3*. For *A2*, the model identifies the optimal capacity endogenously. As the BSS's capacity differs for all the 50 companies, we derive a profitability index (PI) for the individual systems. In *A3*, we incorporate the *PI* as the dependent variable in a stepwise multi-linear regression model. The independent variables are the different load indicators that describe the load profile characteristics of the 50 industrial companies. The resulting linear regression model identifies the key load indicators that have a significant influence on explaining the variation of the profitability of BSSs.

The paper is structured as follows. In Section 2, we describe the different revenue streams and review related work. In Section 3, we present the methodology for our analysis, the optimization model, the economic evaluation, the load indicators and the stepwise multi-linear regression. Section 4 gives an overview of employed data. Next, the results of our analysis are presented in Section 5. The paper concludes in Section 6.

## 2. Revenue streams

This section describes the three revenue streams that we consider in our analysis and summarizes the state of the art in scientific publications. From this overview, we derive assumptions for our research hypothesis *H1* and *H2*. The three revenue streams are the following:

1. Arbitrage trading (arb): trading electricity on the day-ahead and intraday markets. Using the BSS to store electricity in times of low prices and using electricity in times of high prices or selling it on the market.
2. Providing power control reserve (PCR): providing frequency containment or restoration reserve.
3. Peak shaving (peak): considering capacity prices from grid operators as a fixed price on the maximum power consumption per year.

### 2.1. Arbitrage trading

Multiple publications discuss arbitrage trading as a revenue stream for BSSs. In arbitrage trading, the operator of a BSS can capitalize the time-dependent price differences on the electricity market. These price differences arise because of a deviation of the projected demand and supply of electricity. In such a case, the BSS-operator buys energy to charge its battery in times of low prices. Vice versa, he sells energy to discharge the BSS in times of high prices. In our study, we consider two German energy markets, the day-ahead auction and the intraday continuous market part of the EPEX-Spot market.

At the day-ahead auction at 12.00 pm, energy is mainly traded for hourly intervals of the next day. Energy is bought and sold at a market-clearing price. For the year 2017, this market-clearing price ranged between −83.06 €/MWh and 163.52 €/MWh. The day-ahead market is the biggest market on the EPEX with 233 TWh traded in 2017 [18] and covers roughly 39 percent of the total energy consumed in Germany.[1]

In December 2011, the intraday continuous market was introduced in Germany to mitigate the growing influence of intermittent renewable energy sources. On this market, energy is continuously traded up to five minutes before delivery for each 15-min interval. No uniform market-clearing price exists but instead a buy order is immediately executed if matched with a sell order and vice versa. This results in very volatile and dynamically changing prices, for 2017 ranging from −193.02 €/MWh and 329.8 €/MWh.[2] With 54 TWh in 2017 [19], the volume on this market is relatively small compared to the day-ahead market.

Many studies look at arbitrage trading as an applicable revenue stream for electrical storage systems. As arbitrage trading capitalizes on price differences, many authors emphasize the importance of large price spreads for a profitable use case [20–22]. Under current market conditions, the results of most studies show, that profitable arbitrage trading cannot be achieved yet [11]. Nonetheless, sinking battery cost and more volatile energy prices might drive the use of BSSs that follow

[1] The electricity consumption of Germany for the year 2017 accounted for 599 TWh [64].

[2] The maximum price occurred on the 23.01.2017 between 11.45 and 12.00 h. The minimum price occurred on the 30.04.2017 between 17.00 and 17.15 h.

an arbitrage trading scheme [23].

Heymans et al. [24] and Dowling et al. [16] concluded that the volatility of energy prices increases if energy is traded close to real-time. The price is less elastic in longer time intervals, which underestimates the real-time demand imbalances and therefore underestimates the revenue potential of the arbitrage trading. Additionally, Zheng et al. [25] and Sandoval and Leibundgut [22] conclude that the profitability depends strongly on the stochastic behaviour of load and price profiles.

Next to the strategic decision making, other authors focus on the real-time operation of BSS [14,26] and optimal bidding strategies on real-time energy markets [27] to evaluate the implementation of profitable arbitrage trading. Nevertheless, the large number of uncertainties makes the profitability of the revenue stream questionable.

In conclusion, arbitrage trading is an intensively discussed revenue stream for BSSs. Because of the increasing amounts of renewable energies, authors predict growing price spreads on electricity markets. Together with sinking battery cost, this will strengthen the profitability of an arbitrage use case.

### 2.2. Power control reserve (PCR)

In order to maintain the grid operation frequency at its nominal value and therefore guarantee safe operation of connected devices, transmission system operators (TSOs) generally procure power control reserve - the flexibility of power devices to adjust their operation point. In Central Europe, the European Network of Transmission System Operators for Electricity (ENTSO-E) is in charge of dimensioning and operating said reserve, while national TSOs are in charge of its allocation, supervision and deployment. Three different control reserve products exist: Frequency containment reserve (FCR) is activated first and is technically most difficult to provide, after which automatic frequency restoration reserve (aFRR) and manual frequency restoration reserve (mFRR) are deployed [28]. This paper focusses on the provision of FCR, as a regulatory framework for BSSs exist and it is the most profitable power control reserve. Currently, TSOs of six European country including Germany jointly procure FCR in a weekly auction. Remuneration is pay-as-bid, thus remuneration of bidders can vary for each auction.

FCR is provided proportional to the deviation of the current grid frequency from the nominal grid frequency. Traditionally, conventional power plants have provided FCR; however, generally only a small fraction of the rated power can be provided as fast response characteristics and symmetric provision of FCR is required. BSS inhibit transient response characteristics well suitable for the provision of FCR: the process of converting chemical into electrical energy and vice versa entails fast response times and high accuracy towards power signal resulting in little overshoot. While intermittent renewable energy sources already supply a great share of electricity supply, they hardly contribute to the provision of FCR [29]. Here, BSSs are a good alternative to reduce must-run capacities of fossil fuel power plants [30].

First ideas for BSSs to provide control reserve were published by [31] for the insular power system of West Berlin. The successful operation of a test facility including a battery with a rated power of 14.4 kW by the local utility and transmission operator resulted in the operation of a lead-acid BSS with rated power of 17 MW between 1987 and 1995 [32–34]. Due to high battery costs and short cycle lifetime only a limited number of mainly lead-acid BSS were built for the provision of FCR in the 1990s. Falling costs for lithium-ion BSS [35,36], high remuneration for the provision of FCR within Germany and specified operation criteria by the German TSOs [37,38] have resulted in a strong increase in the number of battery projects providing FCR [39,40]. This also led to an increase in publications concerning model-based approaches of BSS providing FCR. The majority of these models intend to decrease necessary schedule-based (dis-)charge events of battery systems providing FCR, which would result in higher operation costs [41–45].

From a technical standpoint, BSSs are well suited to provide FCR due to their power response characteristics.

To sum up, decreasing costs for batteries and a regulatory framework have led to a large number of realized projects within Germany in recent years. For simplicity reasons, this paper henceforth refers to the provision of power control reserve (PCR) specifically referring to the provision of FCR.

### 2.3. Peak shaving

Peak shaving describes the use case where the peak load from the grid is reduced by the provision of energy from the BSS. Thereby, the maximum power drawn from the grid decreases and additional charges and fees by grid operators can be avoided. In Germany, distribution grid operators generally bill yearly capacity demand charges in € per kW which account for the maximum power drawn from the grid over the course of one year in a 15-min interval. Additionally, they consider the individual voltage level and the specific consumption characteristics: In the south of Germany, demand charges on the medium-voltage level range from 10.02 €/kW for consumers with fewer full load hours ($< 2500$ h) until 78.89 €/kW for consumers with a high number of full load hours ($> 2500$ h).[3]

As peak shaving is a common use case for various real life applications [43,46,47] several studies have investigated the techno-economic feasibility of a BSS employing peak shaving. In most cases, peak shaving creates additional revenue for commercial and residential end-users [6,48,49]. Nonetheless, many researchers conclude that current battery prices are too high for BSSs to be cost effective when employing only peak shaving. Atabay [17] evaluated a multi–energy system of different energy intensive industries considering variable energy prices and demand charges. They concluded that “for all scenarios with regular investment costs for electrical storage, batteries were not economically efficient [17]”. Telaretti et al. [47] investigated how an electrochemical storage could help an Italian super market to profit from low price and high price periods and to lower its demand charges. They considered different electrochemical storage technologies but concluded that none of them is cost effective under current prices. In contrast, Zheng et al. [50] and Nottrott et al. [51] showed that for the specific application in a U.S. household, several BSSs can profitably provide peak shaving. Chua et al. [52] concluded through their simulation that integrating energy storage systems to avoid high peak demand can be beneficial for utility companies as well as industrial energy consumers. This is in line with the findings of Park and Lappas [53] for the Australian setting.

Atabay [17] identified the magnitude of demand charges to be the most influential factor on the capacity choice of the storage unit. On the other hand, Sandoval and Leibundgut [22] analyzed the energy system of a low-exergy building with stochastic PV-Profiles and stated as a result that the volatility of the profiles has the highest influence on the sizing of the BSS. Adding to the optimal sizing problem, Gitizadeh and Fakharzadegan [54] point out that the aging behavior of a BSS is an essential factor.

## 3. Methodology

In this section, we describe the methodology for our analytical steps *A1–A3*. The first subsection describes the optimization model needed for *A1* and *A2* that models a BSS in an industrial production. The description focuses on the essential mathematical expressions for the reader to understand the conclusions of the paper. The model is fully

[3] Mean demand charges for 2016 in Baden-Würtemberg, Germany, according the Landesregierungsbehörde Baden-Württemberg, https://www.versorger-bw.de/landesregulierungsbehoerde/stromnetze/netzentgelte.html, checked 08.08.18

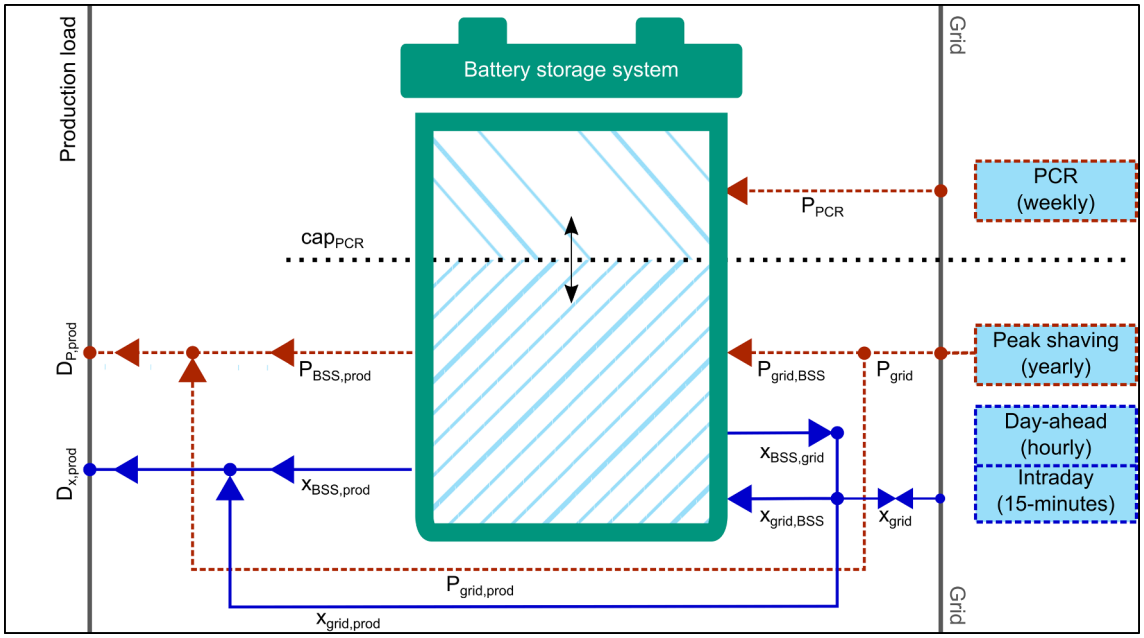


**Fig. 1.** Graphical model schematic (parts of the schematic are creative commons designed by Freepik).

explained in the Appendix A. The subsequent subsection further elaborates the economic evaluation techniques that we apply on the results, the load indicators and the stepwise multi-linear regression model we need for *A3*.

### 3.1. The linear optimization model

For the analytical steps *A1* and *A2*, we implemented a linear problem (LP) in GAMS. Fig. 1 shows graphically the structure of the energy model. In the schematic, $x$ indicates electrical energy flows and $P$ indicates electrical power flows. To investigate the economic benefits of a BSS, we consider the electrical energy and power demand ($D_{x,prod}$ and $D_{P,prod}$) of an industrial production as an exogenous input parameter that needs to be satisfied at all times. The demand can be covered by electricity either directly from the grid ($x_{grid,prod}$) or electricity previously stored in a BSS ($x_{BSS,prod}$). The BSS can either draw electricity from the grid ($x_{grid,BSS}$) or provide it to the grid ($x_{BSS,grid}$). The electricity from and to the grid ($x_{grid}$) can be traded on the hourly day-ahead market and the 15-min intraday market. In analogy to the electricity flows, $P_{BSS,prod}$, $P_{grid,BSS}$ and $P_{grid}$ describe the power flows affecting the peak shaving potential. Furthermore, every week a portion of the BSS's capacity can be blocked to provide only PCR ($cap_{PCR}$). The energy system is evaluated over the course of one year (52 weeks) in 15-min time intervals. The economic evaluation of the system is based on the year 2017. This year is considered as representative for all operating years. Furthermore, the authors assume perfect foresight for load profiles and price development on the day-ahead and control reserve markets, omitting the possibility of a bid rejection.

The model is divided into three time intervals that result from the market design of the different flexibility markets. $q$ describes the quarter hourly time level on the intraday market, $h$ describes the hourly time level on the day-ahead market and $w$ describes the weekly time level, as PCR has to be reserved continuously for a whole week. These time levels are added up to one year as the peak shaving potential considers the peak load of one year. The decision variables of the model are the electrical energy flows in every time step, the power offered for PCR every week and the installed capacity of the BSS.

Formulating the constraints of the optimization model, the authors' aim is to reduce the complexity of the energy model while maintaining the actual depiction of energy and power flows. Therefore, this paper employs an LP-approach consisting of 349,441 equations, 262,133 variables and 1,118,261 non-zeros using the CPLEX-solver. With an average run time of around 9 min and 40 s, 350 model runs[4] sum up to a total computation time of 2 days and 16 h.[5]

Table 1 presents additional model assumptions. The charging efficiency, $\eta_{in}$, and discharging efficiency, $\eta_{out}$, is assumed to be 90% where the self-discharge is set to 2%/month. Additional technical assumptions, further discussed in Section 3.1.3, are the end-of-life factor, $EoL = 80\%$, as well as a calendar lifetime, $LT_{cal}$, of 11 years and a cycle lifetime, $LT_{cycl}$, of 4000 cycles. Concerning PCR conditions, treated in Section 3.1.2, the critical time that PCR, $T_{PCR,crit}$, must be provided for is a half hour, the PCR puffer factor, $puff_{PCR}$, is 1.5 and mean weekly charge due to PCR provision, $E_{PCR,mean}$, is 4889.7 kWh/week. The discount rate is 2% and the number of years $T$ considered for the annuities is 11 years.

#### 3.1.1. Objective functions

The objective of the optimization problem is to minimize the overall system costs. This objective function is slightly modified for *A1* and *A2* as later described in Table 2. The nomenclature in the following section describes electricity flow with an $x$ in kWh, power with a $P$ in MW and the price with a small $p$. The expenditure as described in Eq. (1) is comprised of the cost and revenue from electricity trading, $C_{el}^{h,w}$, the revenue from the provision of PCR, $R_{PCR}^{w}$, the charges for the yearly power capacity, $C_{peak}$, and the annuity payment of the BSS, $A_{BSS}$.

$$min\ f,\quad f = \sum_{w=1}^{52}\left(\sum_{h=1}^{168}\left(C_{el}^{h,w}\right) - R_{PCR}^{w}\right) + C_{peak} + A_{BSS} \tag{1}$$

Electricity is traded on the day-ahead market in hourly intervals and on the intraday market in 15-min intervals. The first term in (2) multiplies the amount of electricity, $x_{ahead}^{h,w}$, traded on the day-ahead market with the price, $p_{ahead}^{h,w}$, on the day-ahead market for every hour in one year. $x_{ahead}^{h,w}$ can take positive values, implying electricity bought, or negative values, implying electricity sold. Accordingly, the second term in (2) describes the cost and revenue generated on the intraday market in one hour of the year. $x_{intra}^{q,h,w}$ represents the amount of electricity and

[4] For *A1*, 50 companies with 6 use cases add up to 300 model runs. Together with 50 model runs for *A2*, this sums up to 350 model runs in total.

[5] The machine used for the computations utilizes 2.66 GHz on 4 cores and 24 GB of RAM.

**Table 1**
Model assumptions.

| Parameter | Unit | | Parameter | Unit | Parameter |
|---|---|---|---|---|---|
| $\eta_{in}$ | % | 90 | $T_{PCR,crit}$ | Hours | 0.5 |
| $\eta_{out}$ | % | 90 | $puff_{PCR}$ | – | 1.5 |
| $dis_{BSS}$ | %/month | 2 | $E_{PCR,mean}$ | kWh/week | 4889.7 |
| $EoL$ | % | 80 | Discount rate $i$ | % | 2 |
| $LT_{cal}$ | years | 11 | Number of annuities $T$ | years | 11 |
| $LT_{cycl}$ | Cycles | 4000 | | | |

$p_{intra}^{q,h,w}$ the price on the intraday market for every 15-min time interval. The general assumption for the use case arbitrage is that only one trade for each 15-min product is executed on the intraday market.

$$C_{el}^{h,w} = x_{ahead}^{h,w} \cdot p_{ahead}^{h,w} + \sum_{q=1}^{4} (x_{intra}^{q,h,w} \cdot p_{intra}^{q,h,w}), \quad \forall\, h, w \tag{2}$$

The revenue from PCR is calculated by the amount of provided power $P_{PCR}^{w}$, multiplied by the weekly price for PCR $p_{PCR}^{w}$, in Eq. (3).

$$R_{PCR}^{w} = P_{PCR}^{w} \cdot p_{PCR}^{w}, \quad \forall\, w \tag{3}$$

The capacity charges for the yearly peak power, $C_{peak}$, is result of maximal power drawn from the grid over the course of one year, $P_{peak}$, times the capacity price, $p_{peak}$. This is shown by Eq. (4). Eq. (5) determines $P_{peak}$ that is at least equal to any electricity flow from the grid, $x_{grid}^{q,h,w}$, during all 15-min time intervals of the year. As capacity charges are priced in €/MWa, we multiply $x_{grid}^{q,h,w}$ with the term $^{4}/_{1000}$.

$$C_{peak} = P_{peak} \cdot p_{peak} \tag{4}$$

$$P_{peak} \geq x_{grid}^{q,h,w} \cdot \frac{4}{1000}, \quad \forall\, q, h, w \tag{5}$$

Eq. (6) calculates the annuity payment for the investment of the BSS, $A_{BSS}$. It is the product of the $cap_{BSS,aged}$, the battery capacity to account for battery degradation, and the battery price, $p_{BSS}$. For this study, we only consider the energy capacity in kWh. Finally, this term is multiplied by the annuity factor $AF$[6], $\frac{1}{i} - \frac{1}{i \cdot (1+i)^{T}}$.

$$A_{BSS} = cap_{BSS,aged} \cdot p_{BSS} \cdot \left( \frac{1}{i} - \frac{1}{i \cdot (1+i)^{T}} \right) \tag{6}$$

### 3.1.2. PCR specifics

The model accounts for the provision of PCR as one revenue stream but does not depict the actual electricity flow due to generally balanced reserve calls [55]. When the model chooses to provide PCR, one part of the BSS's capacity is blocked for any other BSS-application. Eqs. (7) and (8) describe this blocking. The model can only utilize residual parts of the BSS, the difference between the actual capacity of the BSS, $cap_{BSS}$, and the part of the capacity that is blocked for PCR, $cap_{PCR}^{w}$. $cap_{PCR}^{w}$ can be adapted weekly according to market prices for PCR. $cap_{PCR}^{w}$ is always smaller than $cap_{BSS}$, Eq. (9). Eq. (10)[7] defines $cap_{PCR}^{w}$ as it multiplies the offered amount of PCR, $P_{PCR}^{w}$, by a puffer factor, $puff_{PCR}$. The value of this puffer factor is determined by the regulatory standards to meet the criteria for qualification to offer PCR. The value is usually greater than one.

$$x_{BSS,in}^{q,h,w} \leq cap_{BSS} - cap_{PCR}^{w}, \quad \forall\, q, h, w \tag{7}$$

$$x_{BSS,out}^{q,h,w} \leq cap_{BSS} - cap_{PCR}^{w}, \quad \forall\, q, h, w \tag{8}$$

$$cap_{PCR}^{w} \leq cap_{BSS}, \quad \forall\, w \tag{9}$$

$$cap_{PCR} = puff_{PCR} \cdot P_{PCR}^{w} \cdot 1000, \quad \forall\, w \tag{10}$$

[6] $AF$ refers to the annuity factor [7], considering a constant discount rate $i$ and number of annuities $T$: $AF = \frac{1}{i} - \frac{1}{i \cdot (1+i)^{T}}$

[7] The term is multiplied by the factor 1000 to convert from MW to kW

Additionally, in order to qualify to provide PCR, the storage level, $l_{BSS}^{q,h,w}$, in the first period of the week must not be smaller than a critical lower bound, Eq. (11), and not be greater than a critical upper bound, Eq. (12). $l_{BSS}^{q,h,w}$ describes the storage level of the BSS for every time step in kWh. The critical threshold is defined by the amount of time measured in hours, $T_{PCR,crit}$, one needs to be able to continuously provide the maximum amount of PCR in one direction, positive or negative PCR [56]. We assume that an aggregator operates the BSS. Therefore, $P_{PCR}^{w}$ is modelled as a continuous variable.

$$l_{BSS}^{q,h,w} \leq cap_{BSS} - (P_{PCR}^{w} \cdot T_{PCR,crit}), \quad \forall\, q, h, w \tag{11}$$

$$l_{BSS}^{q,h,w} \geq P_{PCR}^{w} \cdot T_{PCR,crit}, \quad \forall\, q, h, w \tag{12}$$

### 3.1.3. Battery degradation

To incorporate battery degradation into the model, we follow the approach of Kaschub et al. [57]. They consider the end of life condition of the BSS as well the influence of the calendar and cycle life restrictions. In order to properly assess the economic performance of a BSS, Kaschub et al. [57] account for these different aging effects by oversizing the initial BSS capacity the model invests in. Thereby, they guarantee that the BSS dispatch plan can be fulfilled until the end of life of the BSS. In this current study, we refer to the aged and oversized capacity as $cap_{BSS,aged}$.

The basis of the degradation formulations is the assumption that the end of life is reached at the end of calendar life and that the cycle life is fully exploited. At the end of life, the BSS can only utilize a portion of its initial capacity. This portion is described by the end of life factor, $EoL$. We assume the risk of operating the BSS beyond this point in time is economically unacceptable. The full calendar life can be reached as long as the average storage level is low. Higher storage levels reduce the calendar life. In contrast, if the cycle life is not fully exploited, this prolongs the BSS's calendar life. Thus, to guarantee that the installed capacity $cap_{BSS}$ is fully accessible until the last day of operation, the invested BSS capacity $cap_{BSS,aged}$ needs to compensate the degradation effects. Eq. (13) describes $cap_{BSS,aged}$ and splits it into three terms. The first term considers the end of life condition of the BSS and the installed capacity, $cap_{BSS}$, needs to be oversized by $\frac{1}{EoL}$.

$$cap_{BSS,aged} = \frac{cap_{BSS}}{EoL} + cap_{add,l} - cap_{red,cycl} \tag{13}$$

The second term of Eq. (13) considers an additional capacity, $cap_{add,l}$, to compensate the BSS degradation due to high storage levels of the BSS. Eq. (14) states that $cap_{add,l}$ is $\frac{1}{3}$ of the average storage level, $l_{BSS}^{q,h,w}$, over the number of time intervals $N_{intervall}$.[8] The third term of Eq. (13), considers the fact that a not fully exploited cycle life results in a prolonged calendar life and $cap_{red,cycl}$ reduces $cap_{BSS,aged}$. $cap_{red,cycl}$ is calculated in Eq. (15). Here, $x_{BSS,tot}$ refers to the total amount of electricity that flows into the BSS over the course of one year. $x_{BSS,tot}$ is multiplied by $LT_{cal}$, the calendar lifetime, and divided by $LT_{cycl}$, the cycle lifetime, to show the average electricity in-flow per cycle. Finally, the difference between $cap_{BSS}$ and this average electricity in-flow per cycle is multiplied by the factor $\frac{1}{3}$[9]. $x_{BSS,tot}$ is calculated in Eq. (16) and is the sum of the electricity in-flow for every time interval, $x_{BSS,in}^{q,h,w}$, plus a weekly share of electricity in-flow due to PCR provision. As we do not model the actual electricity flow for PCR, we include a mean value $E_{PCR,mean}$ multiplied by the amount of power offered for PCR $P_{PCR}^{w}$.[10]

[8] "It is a linear function derived from Lunz et al. [68], which states that an always fully charged SBS reduces its whole lifetime by about one third." [57].

[9] The factor $\frac{1}{3}$ refers to Bloom et al. [65] and the result that the cycle life influences one third of the BSS's life time.

[10] $E_{PCR,mean}$ is the mean amount of energy that a BSS providing 1MW of PCR had to charge per week in the year 2016. We concluded this mean value from the frequency data of the year 2016. The unit is $kWh/MW$.

Finally, we consider Eq. (17) to guarantee that the amount of electricity over the calendar life, $x_{BSS,tot} \cdot TL_{cal}$, does not exceed the product of cycle life times BSS capacity.

**Table 2**
Name of the different use cases, the referred number and the modified objective function.

| Use case | Name of the use case | Objective function | |
|---|---|---|---|
| U1 | Arbitrage | $\min\ f,\quad f = \sum_{w=1}^{52} (\sum_{h=1}^{168} (C_{el}^{h,w})) + A_{BSS}$ | (18) |
| U2 | Peak shaving | $\min\ f,\quad f = C_{peak} + A_{BSS}$ | (19) |
| U3 | PCR | $\min\ f,\quad f = \sum_{w=1}^{52} (-R_{PCR}^{w}) + A_{BSS}$ | (20) |
| U4 | PCR and arbitrage | $\min\ f,\quad f = \sum_{w=1}^{52} (\sum_{h=1}^{168} (C_{el}^{h,w}) - R_{PCR}^{h,w}) + A_{BSS}$ | (21) |
| U5 | PCR and peak | $\min\ f,\quad f = \sum_{w=1}^{52} -R_{PCR}^{w} + C_{peak} + A_{BSS}$ | (22) |
| U6 | All of the above | $\min\ f,\quad f = \sum_{w=1}^{52} (\sum_{h=1}^{168} (C_{el}^{h,w}) - R_{PCR}^{h,w}) + C_{peak} + A_{BSS}$ | (23) |

$$cap_{add,l} = \frac{1}{3} \cdot \sum_{w=1}^{52} \sum_{h=1}^{168} \sum_{q=1}^{4} l_{BSS}^{q,h,w} \cdot \frac{1}{N_{intervall}} \tag{14}$$

$$cap_{red,cycl} = \frac{1}{3} \cdot \left( cap_{BSS} - \left( x_{BSS,tot} \cdot \frac{LT_{cal}}{LT_{cycl}} \right) \right) \tag{15}$$

$$x_{BSS,tot} = \sum_{w=1}^{52} \left( \left( \sum_{h=1}^{168} \sum_{q=1}^{4} x_{BSS,in}^{q,h,w} \right) + P_{PCR}^{w} \cdot E_{PCR,mean} \right) \tag{16}$$

$$x_{BSS,tot} \cdot TL_{cal} \leq TL_{cycl} \cdot cap_{BS} \tag{17}$$

With exemplary numbers, we illustrate the effect that the battery degradation constraints have on the annuity payment of the investment. For this example, the average storage level is assumed to be 100 kWh. This results in a $cap_{add,l}$ of 33 kWh. Furthermore, under the assumption that the installed BSS capacity is 500 kWh, the example case utilizes roughly half the available charging cycles. This would add up to $x_{BSS,tot}$ of around 90,000 kWh and in a $cap_{red,cycl}$ of 84 kWh. Consequently together with an EoL of 80%, $cap_{BSS,aged}$ would amount to 574 kWh. Thus, the installed capacity is oversized to compensate for the degradation effects. This increases the annuity payment, which is considered in the objective function, Eq. (1). It should be noted that a small number of utilized cycles leads to a $cap_{red,cycl}$, which overcompensates the other degradation effects resulting in a $cap_{BSS,aged}$ smaller than the installed $cap_{BSS}$. This translates into a fictive case where, because of the prolonged calendar life, the BSS is still usable after its end of life and the residual value of the BSS reduces the investment.

#### 3.1.4. Modifications for A1 and A2 and the different use cases

In the analytical step *A1* and *A2,* we investigate the economic potential of a BSS following different revenue streams in parallel. For this paper, we constructed six use cases, which represent either an individual revenue stream or a combination of different revenue streams in parallel. Considering the literature overview in this section and the current price level on the different markets, we assume that PCR will have the biggest effect on the profitability of the BSSs. Thus, for the parallel revenue stream cases PCR is the common option to generate revenue. Table 2 gives a detailed overview of the different use cases and their respective objective function. Eq. (18) refers to *U1*, where arbitrage trading generates the only revenue and expenses. *U2* utilizes the battery to profit from peak shaving, Eq. (19). Eq. (20) refers to *U3* where the model only provides PCR and therefore only considers the $R_{PCR}^{h,w}$. *U4* combines PCR and arbitrage trading and *U5* combines PCR and peak shaving. Finally, *U6* considers all three revenue streams, PCR, arbitrage trading and peak shaving.

As part of the overall cost, $A_{BSS}$ is considered for every objective function. For analytical step *A1,* we compare the same BSS for the different industrial companies. Here, the BSS's capacity is an exogenous parameter. Therefore, $A_{BSS}$ depends only on the battery degradation. The essential difference for the analytical step *A2* is that $cap_{BSS}$ is an endogenous variable. For *A2* we analyse only U6.

### 3.2. Economic evaluation

To evaluate the profitability of the BSS we calculate the net present value *NPV*, Eq. (24). From the total cash flow of the system $CF_{tot}$ of one year multiplied with the capital recovery factor [11], $\frac{(1+i)^T \cdot i}{(1+i)^T - 1}$, the investment for the BSS, $cap_{BSS,aged}$ multiplied with the battery price $p_{BSS}$ is substracted.

$$NPV = CF_{tot} \cdot \left( \frac{(1+i)^T \cdot i}{(1+i)^T - 1} \right) - cap_{BSS,aged} \cdot p_{BSS} \tag{24}$$

$CF_{tot}$ refers to the cash flow of the considered revenue stream. The cash flow for arbitrage trading, $CF_{arb}$, is the difference between the total cost for electricity without a BSS, $C_{el,old}$, and with a newly installed BSS, $C_{el,new}$.

$$CF_{arb} = \sum_{h,w} C_{el,old}^{h,w} - \sum_{h,w} C_{el,new}^{h,w} \tag{25}$$

The cash flow for peak shaving, $CF_{peak}$, describes the savings in capacity spending between the old peak, $P_{peak,old}$ without a BSS, and the new peak, $P_{peak,new}$, multiplied with the capacity price, $p_{peak}$.

$$CF_{peak} = (P_{\text{peak,old}} - P_{peak,\text{new}}) \cdot p_{peak} \tag{26}$$

The cash flow for PCR provision, $CF_{PCR}$, is the total revenue of PCR, $R_{PCR}$, over one year.

$$CF_{PCR} = \sum_{w=1}^{52} R_{PCR}^{w} \tag{27}$$

For the comparison of different investments, we calculate the profitability index *PI,* Eq. (18). The PI represents the NPV per invested Euro ([66], p. 115).

$$PI = \frac{NPV}{cap_{BSS,aged} \cdot p_{BSS}} \tag{28}$$

### 3.3. Load indicators

In *A3,* we want to identify the significant independent variables, the load indicators that influence the profitability of a BSS. These indicators illustrate the characteristics of the individual load profiles. McLoughlin et al. [58] introduced three electrical parameters to characterize the domestic electricity demand. They describe $P_{MD}$ as the mean daily peak load, $P_{ToU}$ as the maximum time of use and $P_{LF}$ as the "daily peakyness". We expand on these parameters to compare the peak shaving potential of the different industrial load profiles.

[11] The capital recovery factor refers to the capital recovery factor, the inversion of the present value calculation method with constant annuities [66], considering a constant discount rate $i$ and number of annuities $T$: $CRF = \frac{(1+i)^T \cdot i}{(1+i)^T - 1}$.

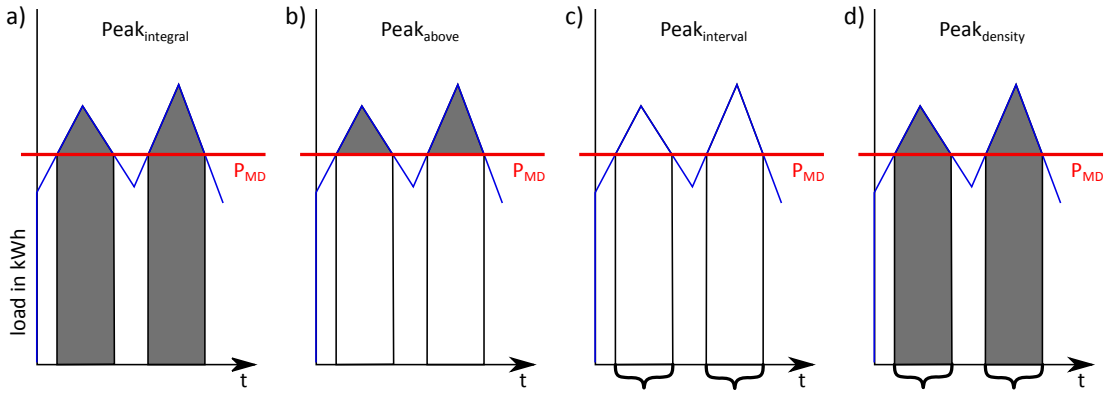


**Fig. 2.** Graphic explanation of load indicators. (a) displays $Peak_{integral}$, the energy consumed during a peak period, (b) displays $Peak_{above}$, the energy above a peak threshold, (c) with the brackets displays $Peak_{interval}$, the number of 15-min intervals in a peak period and (d) displays $Peak_{density}$, the amount of energy per $Peak_{interval}$. All the indicators are normalized to the daily energy consumption.

$P_{MD}$ describes the mean daily peak load in MW over the period of one year, see Eq. (29). $P_{i,j}$ is the mean production load over 15 min in MW and $n$ is the number of 15-min time periods in one day. $m$ is the number of days per year.

$$P_{MD} = \frac{1}{m}\sum_{j=1}^{m} \max\{P_{i,j},\ 1 \le i \le n\} \tag{29}$$

$P_{ToU}$ identifies the time interval of one day, $j_{max}$, during which the peak load occurs. Eq. (30) builds the mode over all days of one year. Thereby, $P_{ToU}$ shows the time interval where the peak load occurs most of the time.

$$P_{ToU} = mode\{j_{\max} | P_{j_{\max}} = \max\{P_{i,j},\ 1 + n(j-1) \le i \le n,\ 1 \le j \le m\}\} \tag{30}$$

The third indicator of McLoughlin et al. [58] is $P_{LF}$, which they refer to as the "daily peakyness", see Eq. (31). First, the equation compares the mean to the peak load of one day. Then, the mean of the sum of this daily ratio results in $P_{LF}$. This is a measure to describe the continuity of a load profile.

$$P_{LF} = \frac{1}{m}\sum_{j=1}^{m} \frac{\frac{1}{n}\sum_{i=1}^{n} P_{i,j}}{\max\{P_{i,j},\ 1 \le i \le n\}} \tag{31}$$

To describe the continuity, we use an additional load indicator that is already established in the field of energy economics: the yearly period of use, $P_{PoU}$, or full load hours, Eq. (32). It compares the yearly energy demand to the yearly peak power demand and illustrates how many hours one would continuously draw energy from the grid if the power were held constant at its maximum. To make it more tangible, we divide this ratio by the number of hours per year resulting in a percentage of a year.

$$P_{PoU} = \frac{\sum_{i=0}^{n\cdot m} \frac{P_i}{4}}{\max\{P_i,\ 1 \le i \le n\cdot m\}} \cdot \frac{1a}{8760h} \tag{32}$$

To display the peak shaving potential, we developed four indicators, $Peak_{integral}$, $Peak_{above}$, $Peak_{interval}$ and $Peak_{density}$. Fig. 2 gives a graphic explanation of these indicators. $Peak_{integral}$ describes the ratio of the energy amount that is consumed during a peak period to the total amount of energy consumed in one day as an average over the course of one year. Eq. (33) gives the definition of a peak energy, $E_{peak,i,j}$. It accounts for all intervals where the load is greater than a fixed peak threshold in our case $P_{MD}$. $E_{peak,i,j}$ takes the value of $P_{i,j}$, if $P_{i,j} \ge P_{MD}$, or else the value 0 for all intervals of the day $n$ and all days of the year $m$. Furthermore, $P_{i,j}$ is multiplied by the term $\frac{24}{n}$ to derive energy and devided by the total amount of energy consumed in one day. $E_{peaki,j}$ shows the percentage of the daily energy that is consumed during a peak interval.

$$E_{peak,i,j} = \begin{cases} \frac{P_{i,j}\cdot\frac{24}{n}}{\sum_i^n P_{i,j}},\ if P_{i,j} \ge P_{MD}, & 1 \le i \le n,\quad 1 \le j \le m \\ 0,\ if P_{i,j} < P_{MD} \end{cases} \tag{33}$$

Eq. (34) builds the mean of. $E_{peak,i,j}$ over one year to get the indicators $Peak_{integral}$, Fig. 2a.

$$Peak_{integral} = \frac{1}{m}\sum_{j}^{m}\sum_{i}^{n} E_{peak,i,j} \tag{34}$$

Accordingly, we get the indicator $Peak_{above}$, Fig. 2b. The only difference is that we consider the amount of energy that is above our threshold $P_{MD}$, see Eq. (35). In Eq. (36), $Peak_{above}$ resembles the mean percentage of the daily-consumed energy that is above the peak threshold.

$$E_{above,i,j} = \begin{cases} \frac{(P_{peak,i,j} - P_{MD})\cdot\frac{24}{n}}{\sum_i^n P_{i,j}},\ if \quad \sum_i^n P_{i,j} > 0, & 1 \le i \le n,\quad 1 \le j \le m \\ 0,\ if \quad \sum_i^n P_{i,j} = 0 \end{cases} \tag{35}$$

$$Peak_{above} = \frac{1}{m}\sum_{j}^{m}\sum_{i}^{n} E_{above,i,j} \tag{36}$$

$Peak_{interval}$, Fig. 2c, accounts for the mean number of peak intervals per day. Eq. (37) builds the cardinal number of intervals $i$, where the load is above the peak threshold for every day, $P_{interval,j}$. Eq. (38) calculates the mean of the percentage of $P_{interval,j}$ in one day ($n$ is number of time intervals per day) over the course of one year.

$$P_{interval,j} = card(\{i \in \mathbb{N} \mid P_{i,j} \ge P_{MD},\quad 1 \le i \le n\}) \tag{37}$$

$$Peak_{interval} = \frac{1}{m}\sum_{j}^{m} \frac{P_{interval,j}}{n} \tag{38}$$

Lastly, $Peak_{density}$, Fig. 2d, describes how daily peak energy, $\sum_i^n E_{peaki,j}$, is spread over the daily peak intervals, $P_{intertval,j}$, see Eq. (39). It is shown as the mean over one year.

$$Peak_{density} = \frac{1}{m}\sum_{j}^{m} \frac{\sum_i^n E_{peak,i,j}}{P_{interval,j}} \tag{39}$$

### 3.4. Stepwise multi-linear regression

A stepwise multi-linear regression method is employed, to identify the significant independent variables that influence the profitability of a BSS. For the implementation, *Matlab R2016a* and the function *stepwiselm*[12] us

[12] A more detailed explanation of the function can be found the Mathworks-homepage: https://de.mathworks.com/help/stats/stepwisefit.html#bq9x28h-1 (4th May 2018)

used. This function applies a bidirectional elimination algorithm. The selection criterion is the default p-value ($p - value < 0.05$ to enter, $p - value < 0.1$ to remove). The result of this method is a linear model, which includes all the significant independent variables $x_i$ to describe the dependent variable $y$. $\beta_o$ describes the y-intercept and $\beta_i$ the coefficient or the slope of the independent variable, see Eq. (40).

$$y = \beta_0 + \sum_j^n \beta_j \cdot x_j \tag{40}$$

## 4. Data

### 4.1. Load data

We evaluated the load profiles of 50 different companies. The focus of this study is on small-medium-sized companies (SMEs) in Germany. The data cover a variety of different sectors, such as hotels, metals refining or production of drop forgings, as indicated by the more detailed meta-data for 20 companies. The data cover the whole year of 2017 at 15 min resolution. We refer to the Appendix A for a detailed overview of the companies and their load indicators. The sample companies show a variety of different load behaviours. The annual peak load ranges from 34 kW to 4718 kW. From the mean of 570 kW, a standard deviation of 996 kW and a mode of 326 kW, we can observe that the distribution of the annual peak load of the 50 companies is skewed to the left. The same holds true for the annual energy consumption, $E_{total}$, and $P_{MD}$. Using the above introduced load indicators, we are able to compare the load profiles of the different companies. Fig. 3 illustrates the box plot of the load indicators. It shows that for the sample of 50 companies the distributions of the load indicators are slightly skewed.

### 4.2. Market data

We considered the market prices of the year 2017. For the continuous intraday market and the day-ahead market, we used the prices accessible over the *EPEX*-Database. The intraday price represents the mean average price and the day-ahead price the market-clearing price. For the PCR-prices, we used the maximum price bid that was accepted. We extract the prices from the homepage of *regelleistung.net*, a cooperation of the German transmission service operators. The capacity price $p_{peak}$ is the mean price on the medium-voltage level in the German federal state of Baden-Württemberg. The capacity prices are separated by the yearly period of use of 2500 h/a. Because of modelling restrictions we consider the average price of 44.46 €/kWha, but mention that the price range is significant.[13] The BSS price is assumed to be 800 €/kWh. In order to analyse the potential from a macroeconomic point of view and in the context of ongoing discussions about costs and potentials of flexibility, the applied discount rate is 2%.

## 5. Results and discussion

### 5.1. A1: optimizing with fixed capacity

For A1, we analysed the net present value (NPV) of the different use cases with a fixed BSS capacity of 500 kWh and a maximum power capability of 500 kW.[14] Fig. 4 depicts the NPVs of all 50 companies for the different use cases. The use cases are sorted from lowest to highest NPV. The graph shows that the BSS can only generate a positive NPV for the latter two use cases, *U5* and *U6*. Nonetheless, this is not the case for

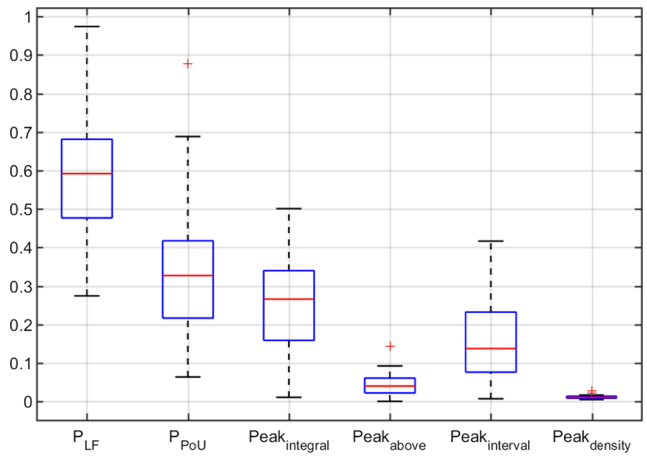


**Fig. 3.** Box plot of load indicators.

roughly half of the companies. The different load profiles influence the NPV of the use cases with peak shaving. In the other use cases, *U1, U3* and *U4,* the NPV is independent of the load profile. Table 4 gives on overview of the results for the different use cases with a fixed battery capacity. It shows the mean and standard deviation for the NPV, $cap_{aged}$, number of full cycle equivalents and the c-rate[15] for all charging activities.

The use case with the lowest NPV is arbitrage trading and is the same for all 50 companies. This implies that the BSS only profits from price spreads on the energy markets by buying and selling on these markets and is not used to cover any part of the production load. The annual cash flow that the BSS generates through arbitrage trading sums up to 2019 €. The BSS is charged during 144 time intervals and discharged during 181 intervals. This indicates that the BSS is utilized roughly 0.5% of the time. In contrast, the number of full cycle equivalents is 375 cycles, 9.3% of the cycle life of 4000 cycles, as the BSS charges and discharges with the maximum power capability to exploit the price spread on the market. The mean c-rate for all charging activities is 0.7542. The constraints for battery degradation encourage the optimization model to keep the number of cycles to a minimum as well as the number of intervals with a high storage level. Avoiding a high number of cycles prolongs calendar life and reduces the investment. For the *U1*, arbitrage trading, the low level of activity decreases the invested battery capacity, $cap_{aged} = 476$ kWh. The reduced battery capacity is a result of the battery degradation constraint in Eq. (13) in Section 3.1.3. For a profitable use case, the profit that can be generated on the energy market needs to be greater than the additional investment required to compensate battery degradation. For a battery price of 800 €/kWh, the price spread on the energy markets needs to be greater than 0.0759 €/kWh.[16] This threshold would rise by 0.0069 €/kWh for every time interval the storage level is not reduced. Additionally, the selling price needs to be at least 1.23 of the buying price to cover the electricity losses of the BSS.

The studies on the use cases with peak shaving, *U2*, show better NPVs, but a 500 kWh battery is not profitable even for the largest company. However, it is striking that the profitability of this use case

[13] *yearly period of use* $< 2500\frac{h}{a}$, $p_{peak} = 10.02\frac{€}{kWha}$ and *yearly period of use* $\geq 2500\frac{h}{a}$, $p_{peak} = 78, 89\frac{€}{kWha}$

[14] 500 kWh and 500 kW represent the rounded mean value of the peak load of all 50 companies.

[15] The c-rate describes the rate at which a BSS charges or discharges (in kW) in relation to its capacity (in kWh), so for example a c-rate of 1 will deliver 100% of the BSS' capacity in one hour, and a c-rate of 2 in 0.5 h etc.

[16] The derived price spreads are a result of the partial derivative of Eq. (13) shown below: $\frac{dInv_{BSS}}{dx_{BSSin}} = cost_{BSS} \cdot \frac{dcap_{aged}}{dx_{BSSin}} = cost_{BSS} \cdot \left( \frac{dTL_{redcal}}{dx_{BSSin}} - \frac{dTL_{redcycl}}{dx_{BSSin}} \right)$

$= cost_{BSS} \cdot \left( \frac{0.3}{\Delta t} + \left( \frac{1}{3} \cdot \frac{TL_{cal}}{TL_{cycl}} \right) \right) = \frac{0.0069}{\Delta t} \frac{€}{kWh} + 0.0759 \frac{€}{kWh}$

$\frac{\delta^2 Inv_{BSS}}{\delta x_{BSSin} \cdot \delta t} = \frac{\frac{0.0069}{\Delta t} \frac{€}{kWh} + 0.0759 \frac{€}{kWh}}{dt} = 0.0069 \cdot \frac{€}{kWh \cdot \text{time interval}}$

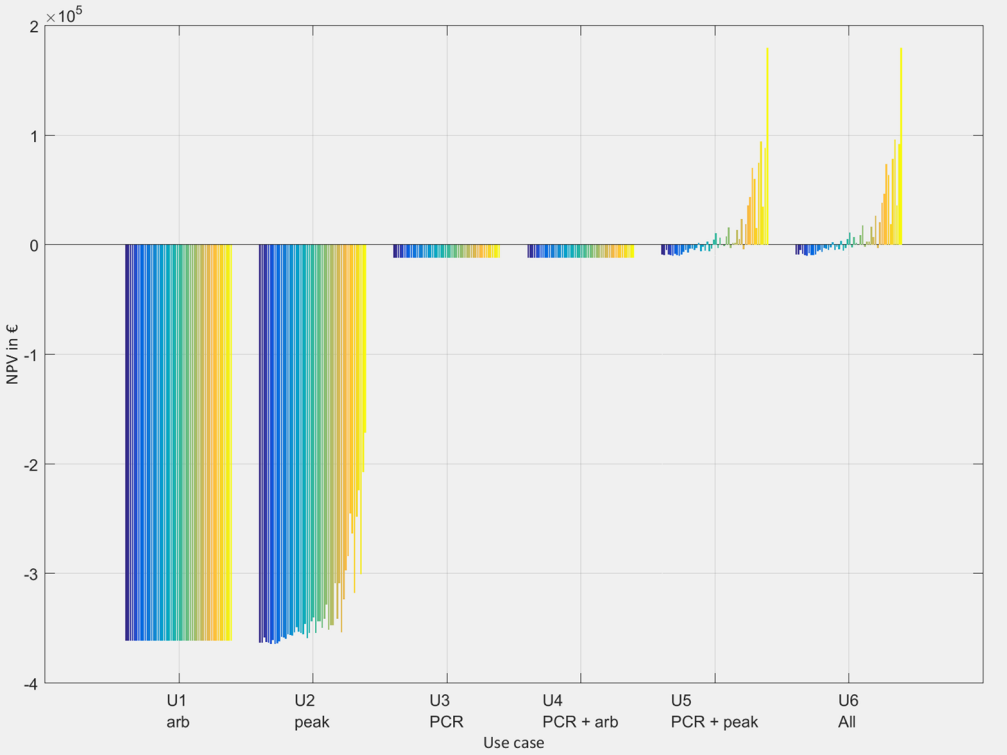


**Fig. 4.** Bar chart of NPV of the different use cases for the 50 companies. The companies are arranged in ascending order referring to the yearly peak load.

**Table 3**
Statistical overview of the load data.

| | Peak load kW | $E_{total}$ in MWh | $P_{MD}$ in kW | $P_{ToU}$ – | $P_{LF}$ – | $P_{PoU}$ – | $Peak_{integral}$ – | $Peak_{above}$ – | $Peak_{interval}$ – | $Peak_{density}$ – |
|---|---|---|---|---|---|---|---|---|---|---|
| min | 33.8 | 52 | 12.4 | 14 | 27.4% | 6.4% | 1.08% | 0.04% | 0.71% | 0.50% |
| max | 4717.6 | 22,375 | 2654.0 | 96 | 97.4% | 87.8% | 50.10% | 14.43% | 41.65% | 2.82% |
| mean | 570.1 | 2059 | 361.4 | 45 | 57.4% | 33.4% | 25.24% | 4.15% | 15.42% | 1.13% |
| std | 996.1 | 4462 | 658.9 | 18 | 14.9% | 16.5% | 12.88% | 2.92% | 9.28% | 0.42% |
| mode | 325.6 | 1252 | 215.4 | 35 | 71.1% | 44.0% | 34.07% | 5.17% | 23.37% | 0.99% |

**Table 4**
Results for the different use cases with a fixed BSS capacity.

| | NPV | | $cap_{aged}$ | | cycles | | c-rate | |
|---|---|---|---|---|---|---|---|---|
| | mean in € | mean in € | mean in kWh | std in kWh | mean – | std – | mean – | std – |
| *U1* | −361,225 | 0 | 476 | 0 | 375 | 0 | 0.7542 | 0.0000 |
| *U2* | −331,361 | 44,662 | 468 | 11 | 222 | 250 | 0.0722 | 0.0960 |
| *U3* | −11,674 | 0 | 586 | 0 | 9 | 0 | 0.0002 | 0.0000 |
| *U4* | −11,674 | 0 | 586 | 0 | 9 | 0 | 0.0002 | 0.0000 |
| *U5* | 13,378 | 35,532 | 588 | 2 | 100 | 98 | 0.0011 | 0.0011 |
| *U6* | 14,486 | 36,069 | 590 | 4 | 156 | 141 | 0.0067 | 0.0061 |

strongly depends on the individual load profile of the companies. Conclusively, companies with a high peak load usually also have higher NPVs. The economic potential of peak shaving increases with the absolute peak load. For most of the companies on the other hand, a battery capacity of 500 kWh is disproportionately large and the cash flow through peak shaving never exceeds the investment in the BSS. In all cases, however, the battery is also used so little that $cap_{aged}$ drops and has an average value of 468 kWh. The number of cycles and the c-rate can explain the great influence of the different load profiles on the profitability of the peak shaving use case. For example, the average number of cycles is 222 over the 11 years under consideration, but there is a large difference between the individual companies. Thus, Co50 has only 13 cycles, which is hardly more than 1 cycle per year, and a relatively high c-rate. Nevertheless, Co50 achieves the highest reduction in capacity prices. In contrast, the BSS of Co36 goes through 992 cycles over 11 years.

The values for the *U3* and *U4* are the same for all companies. This is because in both use cases the entire battery capacity is blocked for the provision of PCR. For all weeks in 2017, it is economically more attractive to offer PCR than to trade energy. Therefore, there is no possibility to use the battery for arbitrage trading. Of all revenue streams individually, PCR is the most profitable. However, on the PCR market, a 500 kWh battery at a price of 800 €/kWh will not produce a positive NPV. Even following two revenue streams in parallel, PCR and arbitrage, does not change the NPV. Overall, the battery is charged and discharged very lightly with regard to the number of cycles. Only nine additional full cycles are achieved in eleven years. Nevertheless, the battery capacity to be invested in has increased to 586 kWh, see Table 3, due to battery degradation, as the average charge level over the entire time is 50%.

Only for the last two use cases, *U5* and *U6*, can a positive NPV be observed, but not for all companies. Again, companies with relatively high peak load have higher NPVs than companies with a lower peak load. PCR is offered in all cases every week, but the amount of PCR offered varies weekly. This frees up battery capacity for either peak shaving, *U5*, or peak shaving and arbitrage trading, *U6*. Fig. 4 shows

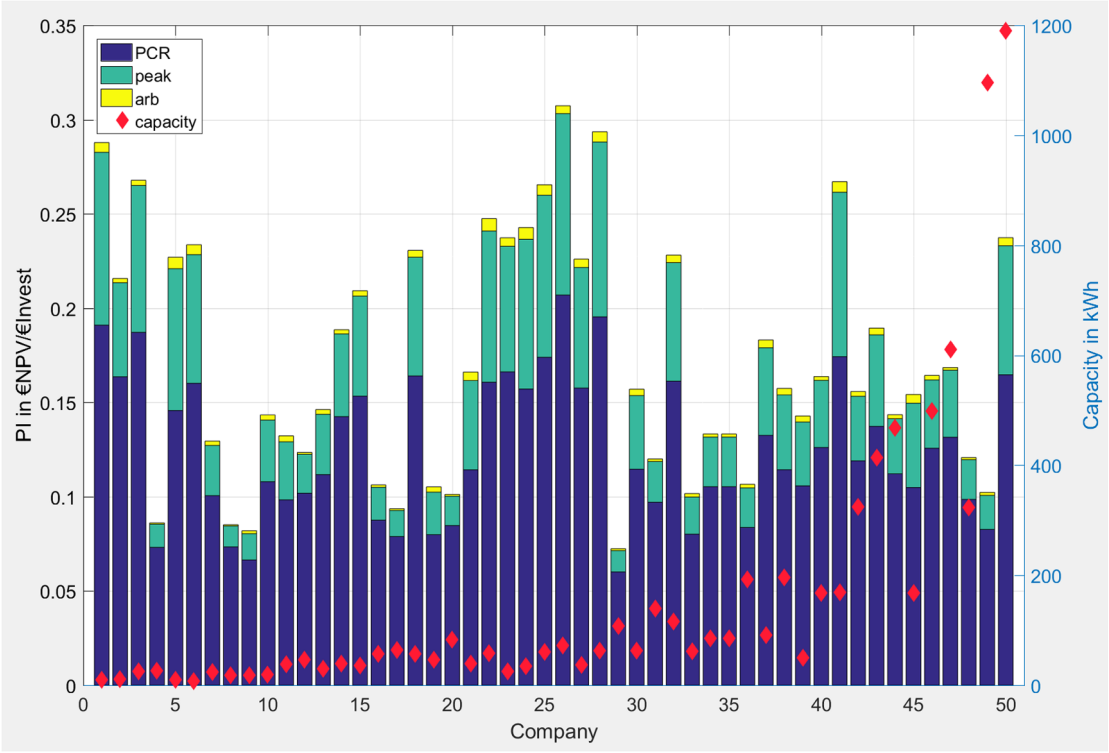


**Fig. 5.** Results of U6 with variable $BSS_{cap}$, PI for 50 companies ascending by peak load, divided into the share of the single revenue streams of the total cash flow.

that the combination of PCR and peak shaving has the greatest influence on the profitability of BSS. The addition of arbitrage trading can only positively influence the NPV in individual cases and only by a relatively small amount.

Considering the *cap_aged*, cycle number and c-rate, the observations for the single revenue stream use cases hold true for the parallel revenue streams as well. Combining peak shaving with PCR increases the average cycle number and average c-rate. Including arbitrage trading into the use cases increases these numbers even further. This in return leads to a higher degradation of the BSS and therefore in a higher $cap_{aged}$.

### 5.2. A2: optimizing with variable capacity

For *A2*, we run the model one more time for use case *U6*. This time we include the option to determine $BSS_{cap}$ endogenously. This allows us to consider the different production sizes of the 50 companies. Fig. 5 shows the results of the model run for *U6* as a bar chart. The different colours in the bars indicate the proportion of the total cash flow that can be attributed to one of the three revenue streams, PCR, peak shaving and arbitrage trading. Furthermore, the red diamonds show the installed capacity of the BSS and is orientated to the right y-axis.

One can observe that the installed $cap_{BSS}$ differs quite substantially, the lowest being around 8 kWh and the highest reaching close to 1200 kWh. For a better comparison, we show the profitability index, PI, of the installed BSS of the different companies. For illustration, for company 49 and company 50 the model installs two large BSSs of 1096 kWh and 1189 kWh respectively. Simultaneously, company 49 could reach with its BSS a PI of 0.1023 €/€, whereas company 50 reaches a PI of 0.2373 €/€. Applying this to the rest of the sample companies, we detect that the PI seems independent from $cap_{BSS}$. In general, with a mean value of 0.1717 the overall level of PI seems very low. This is even more evident, once we consider the payback period (PP). The mean PP is reached after 8.4 years with a standard deviation of 0.45 years. This translates into a breakeven point after more than 75% of the BSS lifetime.

When we take a close look at the share of the single revenue streams of the total cash flow, we observe that arbitrage trading plays a minor role determining the PI of the BSS. The highest share is on the PCR revenue stream, mean of roughly 75%, and then the peak shaving revenue stream, mean of roughly 24%. Furthermore, we observe that the PI is increasing with a growing peak-share.[17] Fig. 6 shows the scatter of PCR-share and peak-share to the PI. The least square fit lines indicate the trend of the relation between the revenue share and the PI. Both of the independent variable are highly correlated with the dependent variable PI. For the PCR-share the $R^2$ *is* 0.78 and for peak-share the $R^2$ *is* 0.83. Additionally, we detect that the trend is almost complementary to 1, which can be explained as arbitrage trading plays a minor role.

To explain the economic potential for peak shaving in the different companies, we calculate the peak ability of the BSS, $peak_{abil}$, shown in Eq. (41). This describes by how many kW every kWh of battery capacity installed reduces the original peak load. Fig. 7 shows the scatter plot of PI over $peak_{abil}$ with a least square fit curve and a $R^2$ *of* 0.88.

$$peak_{abil} = \frac{Peak_{max,old} - Peak_{max,new}}{cap_{BSS}} \tag{41}$$

This leads us to the conclusion that the profitability of a BSS mostly depends on the two revenue streams PCR and peak shaving. The higher the share of the total cash flow is due to peak shaving, the higher the overall profitability of the BSS investment. Therefore, the BSS that can utilize its capacity more efficiently than others to reduce the peak load is more likely to achieve a higher profitability. Still, the PCR and peak shaving revenue stream function complementarily. By itself under our assumed prices, one revenue stream cannot generate enough cash flow for the investment to break even. Our model finds for each company the optimal combination of how much capacity of the BSS to block for the

[17] The term peak-share refers to the share the peak shaving revenue stream provides to the cash flow. Respectively, PCR-share describes the share of the PCR revenue stream.

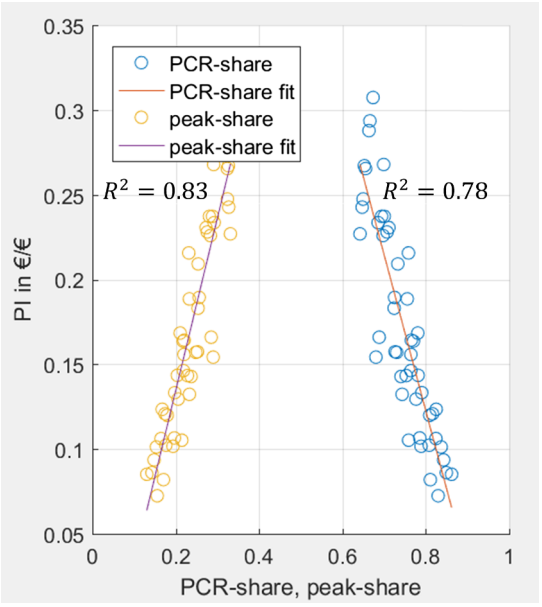


**Fig. 6.** Scatter plot of PCR-share and peak-share to Pi including a least square fit line.

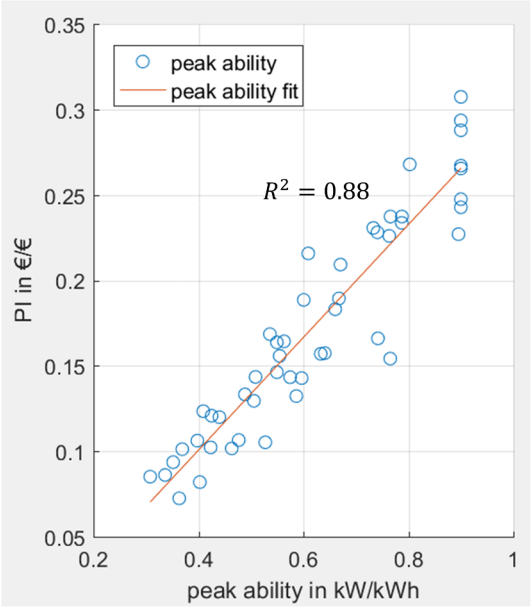


**Fig. 7.** Scatter plot of Pi over peak ability with least square fit.

PCR operation as to still generate enough revenue by peak shaving.

### 5.3. A3: stepwise linear regression of load characteristics

In the analysis *A3*, we develop a linear regression model to describe the relationship between load indicators and the model result, *PI*, for all 50 companies. The load indicators are described in Section 3.3.

Table 5 shows the steps of the stepwise linear regression analysis. The first variable that is added to describe the variance of *PI* is the load indicator $Peak_{density}$. In the second step, the variable $Peak_{above}$ is added to the linear model to further increase the $R^2$. The stepwise analyses identifies no other variables to be significant, hence no further steps are needed to further add or remove variables from the linear model.

Eq. (42) shows the derived linear regression model to describe the variation of *PI*. The ordinary $R^2$ of the model is 0.291 and the adjusted $R^2$ is 0.260. This shows that the linear model has a moderate ability to describe the variance of PI. Both variables have a *p-Value* below *0.01* and therefore correlate significantly with *PI*. For a better illustration, we multiplied the load indicators by 100 as to represent a percentage of the total daily energy consumption. The estimated coefficient for $Peak_{density}$ is 0.0809. If the other variable is held constant *PI* would increase by 0.0809 €/€ once $Peak_{density}$ is increased by 1 percentage point. $Peak_{density}$ is positively correlated with the dependent variable *PI*. On the contrary, if the other independent variable $Peak_{above}$ is increased by 1 percent *PI* decreases by 0.0156 €/€ as they are negatively correlated. Therefore, the contribution to the variance of *PI* is higher for $Peak_{density}$ but for $Peak_{above}$ it is more significant. The collinearity statistics in Table 6 show that the case of multi-collinearity does not need to be considered (*tolerance* > 0.25 and *VIF* < 5.0).

**Table 5**
The steps of the stepwise linear regression.

| Step | Adding/removing | Variable | FStat | pValue |
|---|---|---|---|---|
| 1 | Adding | $Peak_{density}$ | 7.14 | 0.0103 |
| 2 | Adding | $Peak_{above}$ | 10.68 | 0.0020 |

The results are in line with the expectations. A higher value for $Peak_{density}$ would imply that a greater amount of the daily energy consumption occurs during a peak period. Therefore, this could be an implication for a greater peak shifting potential where greater amounts of energy can be easily shifted to non-peak periods. On the other hand, a lower value for $Peak_{above}$ implies that the amount of energy above the peak threshold, $P_{MD}$, is smaller compared to the daily energy consumption. For example, this could occur in cases of single high peaks or regular smaller peaks. In either case, the amount of peak shaving energy would decrease and the peak shaving potential of a small BSS would rise.

$$PI = 0.1451^{***} + 0.0809^{***} Peak_{Density} \cdot 100 - 0.0156^{***} Peak_{above} \cdot 100 \quad (42)$$

$$*p < 0.1, \quad **p < 0.05, \quad ***p < 0.01$$

### 5.4. Sensitivities

The model results are considerably sensitive to variations in battery price, lifetime of the BSS and assumed discount rate. With decreasing battery prices the model choses to install larger BSS capacities. Below a certain battery price, around 780 €/kWh, the installed capacity abruptly increases from values smaller than 2 MWh to the maximum value possible of 10 MWh. This sudden increase also appears with decreasing discount rate, at about 1.5%, which can be seen in Fig. 8, and an increasing battery life, at around 5000 cycles.[18] Furthermore, the sudden increase indicates a state where the installation of a BSS for PCR by itself is already profitable. As the PCR revenue stream is independent of individual load profiles the model chooses for every company the maximum capacity. Simultaneously, Fig. 8 shows that the installed battery capacity drops exponentially with an increasing discount rate and approaches zero. Fig. 8 depicts model results for the installed battery capacity, $cap_{BSS}$, as a mean value over all companies with varying discount rate.

Considering the results, for many companies a BSS is barely profitable. Therefore, changes in the PCR-prices and the capacity prices have a strong effect on the installed BSS-capacity. Current price trends on the PCR-market imply a lower price level than in 2017 while capacity prices have been increasing over the past years. Additionally, capacity prices vary significantly among the different regions in Germany. On average, the northern parts of Germany have capacity

[18] The influence of varying calendar life cannot be assessed as the constraints in Eqs. (13) and (15) underestimate and overestimates the battery degradation respectively, in case the assumed technology life differs from the calendar life.

**Table 6**
Linear model statistics.

| | Estimate | SE | tStat | pValue | Colinearity statistics | |
|---|---|---|---|---|---|---|
| | | | | | tolerance | VIF |
| (*Intercept*) | 0.1451 | 0.0226 | 6.4281 | < 0.001 | | |
| $Peak_{density}$ | 0.0809 | 0.0248 | 3.2680 | 0.0020 | 0.8185 | 1.22 |
| $Peak_{above}$ | −0.0156 | 0.0036 | −4.3585 | < 0.001 | 0.8185 | 1.22 |

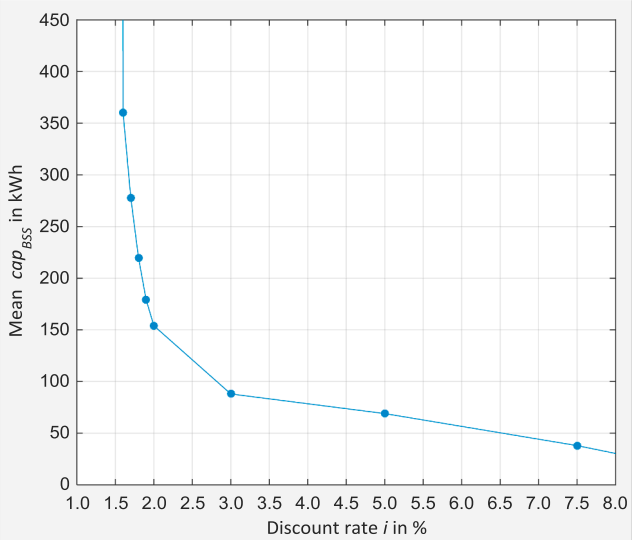


**Fig. 8.** Sensitivity analysis for varying discount rate. Shown are the results for the mean installed battery capacity, $cap_{BSS}$. (The line between the points is for graphical understanding only and does not refer to model results.)

prices three times as high as southern Germany. The local differences are even more extreme, as the highest price amounts to six times the lowest price [59]. For most companies, rising PCR-prices would lead to greater amounts of the capacity blocked for PCR-provision. Accordingly, rising capacity prices would lead to a higher peak-share and vice versa. Furthermore, with rising capacity prices one could observe a greater divergence between the PI of the different companies due to the load profile dependency. Eventually, how these price changes would vary the profitability of the BSS, still depends on the peak potential of the individual company, the correlation of the PCR-price-profile and the individual load-profile and the relationship of the PCR-price level and the capacity price-level.

### 5.5. Critical reflection

This section provides a brief critical reflection on the developed approach and assumptions. Attention is firstly turned to the developed model, which is a deterministic optimization under perfect foresight for a representative year. This approach furthermore assumes a predictable load and 100% acceptance of price bids on all three markets, and the year 2017 is assumed a representative year for the lifetime of the BSS. Hence, there is a significant level of uncertainty associated with future developments in load profiles and market prices, neither of which are well captured in the model. The load profiles are based on a sample with a limited amount of metadata, which makes it difficult to infer the importance of sample bias. In addition, the system boundary for the analysis is at the company level. Implicitly, we assume that an aggregator is able to pool the required BSS capacities to trade on the respective markets. The associated costs of which are neglected. Furthermore, the assumed discount rate of 2% depicts a macroeconomic social discount rate. The discount rate employed by the individual company might be much higher, which would further decrease the profitability of investment. Whilst the reported sensitivity analysis indeed goes some way to exploring the impacts of different assumptions on the profitability of different business cases, this uncertainty cannot be eliminated and the results should therefore be interpreted in this context.

The intraday market might hold higher potential for arbitrage trading than displayed in this paper as prices change dynamically. In this paper, only the weighted average and no order book price data have been applied. The model therefore limits the number of trades on the intraday market to one per product disregarding for reasons of long runtimes the potential that lies in dynamic asset-backed trading. Furthermore, the analysis neglects any feedback effects of the BSS optimisation: the PCR market has a total volume of 1378 MW,[19] so if the 50 SMEs were to install the maximum capacity of 10 MWh combined they would be able to offer around 333 MW of PCR. The ensuing market saturation would probably result in much lower prices and therefore less favourable economic conditions. Additionally, future market changes will have an influence on the potential of parallel revenue streams for the BESS. For example, the product duration of PCR will decrease from 7 days to 1 day in November 2018 and 4 h products in July 2020 [60], which will increase the flexibility for companies to switch between possible revenue streams.

Other weaknesses relate the technology of the BSS itself, especially the model constraints to depict battery degradation. Current studies from battery testing of electric vehicles indicate at least double the life duration than we considered [61]. Additionally, the influence of the c-rate, depth of discharge and the temperature on the degradation process [49,62,63] is not included in the model. On the other hand, the observed c-rates are low. Thus, the influence might be negligible. For our model, we assume a battery control system that is capable of implementing the advised dispatch plan. Additional cost for such a management system is not included. Finally, the reliability of the battery is not considered, which would have important implications for the production process. We have assumed that the BSS is a pseudo-flexibility, in that it does not interfere with the production process directly. But cost savings through peak shaving need to outweigh production uncertainties. Especially in SMEs, the production is more volatile and order-dependent than in energy-intensive industries. So analysing the implications of lower BSS reliabilities should be covered by future work.

Finally, future research needs to extend the linear regression model to make it more robust. Results from sensitivity analyses, like the variation of the ratio between the PCR and capacity price level, should be included. The choice of $P_{MD}$ as the threshold for peak definition is useful as it allows for comparability between different load profiles. For a better understanding of the peak shaving potential, the definition of a peak needs to be explored further and the scope of the load profile data extended.

## 6. Summary and conclusion

Increasing fractions of renewable electricity generation require more flexibility within the energy system, especially on the demand side. Against this background, this paper has developed and applied an optimization model to assess the profitability of different parallel revenue streams for a battery storage system (BSS) in industrial companies. By not interfering with the production process, the BSS provides a pseudo-flexibility with significant advantages compared to other intrusive DSM measures. The linear program (LP) with 15-min resolution optimizes the capacity of a BSS by maximising the Net Present Value (NPV) across the operational lifetime. In contrast to existing

[19] The mean value per week of the required primary control reserve in 2017 [67]

contributions, the BSS is employed for one or more revenue streams in parallel, including arbitrage trading, power control reserve (PCR) and peak shaving. The novelty of the approach lies in this combination of revenue streams, which especially due to the quite different market requirements and timeframes is challenging to model. A final step involves a stepwise linear regression of the profitability in relation to newly-defined load indicators.

The model is applied to a set of 50 German small and medium enterprises (SMEs), based on empirical data for these companies. The results show that, under the default assumptions, neither of these three business cases is economically attractive (i.e. negative NPVs) individually. When combined, the most profitable business model is achieved with all revenue streams (positive NPVs). Hence, with a fixed BSS capacity of 500 kWh, the Net Present Value (NPV) varies from a minimum of −350,000 € for just arbitrage up to about 200,000 € for all three use cases in parallel. In the case of a variable BSS capacity, this varies up to 1200 kWh and the Profitability Index (the ratio of investment to NPV) varies from 0.06 to 0.31. The profitability can be attributed mostly to the cash flow from peak shaving and PCR. Under current market conditions, arbitrage trading contributes marginally to the profitability as the price spreads on the energy markets are too small to justify stronger battery degradation. There is a large variation in profitability between the companies in terms of the profitability and the size of the battery installed, both of which are closely related to the characteristics of the electrical load profile. The stepwise linear regression reveals a moderate dependency of the BSS profitability on the two newly developed indicators $\text{Peak}_{\text{density}}$ and $\text{Peak}_{\text{above}}$. The profitability of the BSS is strongly affected by the techno-economic assumptions, for example the BSS capacity suddenly increases from below 2 MWh up to the maximum possible value of 10 MWh with battery prices below 780 €/kWh, interest rates below 1.5% and more than 5000 remaining cycles.

The developed approach is subject to considerable uncertainties relating to the future development of load profiles, market frameworks and technology costs, which should all be borne in mind when interpreting the results. Furthermore, the microeconomic perspective adopted in this work does not consider the feedback effects that individual SMEs investing in BSSs would have on the PCR markets. In the extreme case, these markets could become completely saturated, thereby negating any apparent economic potential shown here. Future work should therefore especially focus on a more detailed depiction of the BSS's technical behaviour, including degradation and reliability, as well on developing more robust statistical relationships between load indicators, based on larger samples, and profitability.

## Acknowledgements

The authors thank the Energie Consulting GmbH in Kehl-Goldscheuer, Germany, and its managing director Dr. Jürgen Joseph for the provision of the anonymized data of the 50 SMEs. The third author (RM) gratefully acknowledges the support of the Flex4RES project (http://www.nordicenergy.org/flagship/flex4res/) for enabling his contribution. Finally, the authors are grateful for the helpful comments of the three reviewers during earlier revisions of this manuscript. The usual disclaimer applies.

## Conflict of interest

The authors declare no competing interests.

## Appendix A

### A.1. Model description

In this section, we present the model equations. The essential equations are shown in section Methodology on page 8.

#### A.1.1. Electricity flow balance constraints

The production demand ($D_{prod}^{q,h,w}$) can be either satisfied through electricity directly from the grid ($x_{grid,prod}^{q,h,w}$) or electricity stored in the BSS ($x_{BSS,prod}^{q,h,w}$), Eq. (43). As shown in Eq. (44), the electricity from the grid, $x_{grid}^{q,h,w}$, flows either to the BSS, $x_{grid,BSS}^{q,h,w}$, directly to the production, $x_{grid,prod}^{q,h,w}$ or is fed into the grid from the BSS, $x_{BSS,grid}^{q,h,w}$. Furthermore, one part of $x_{grid}^{q,h,w}$ is traded on the dayhead market, $x_{ahead}^{h,w}$, the other on the intraday market, $x_{intra}^{q,h,w}$. Eq. (45) shows the electricity balance for one hour.

$$D_{prod}^{q,h,w} = x_{BSS,prod}^{q,h,w} + x_{grid,prod}^{q,h,w},\ x_{BSS,prod}^{q,h,w},\ x_{grid,prod}^{q,h,w} \geq 0 \tag{43}$$

$$x_{grid}^{q,h,w} = x_{grid,BSS}^{q,h,w} + x_{grid,prod}^{q,h,w} - x_{BSS,grid}^{q,h,w},\ x_{grid,prod}^{q,h,w},\ x_{grid,BSS}^{q,h,w},\ x_{BSS,grid}^{q,h,w} \geq 0 \tag{44}$$

$$\sum_{q=1}^{4} x_{grid}^{q,h,w} = x_{ahead}^{h,w} + \sum_{q=1}^{4} x_{intra}^{q,h,w} \tag{45}$$

$$x_{BSS,in}^{q,h,w} = \eta_{in} \cdot x_{grid,BSS}^{q,h,w} \tag{46}$$

$$x_{BSS,out}^{q,h,w} = \frac{1}{\eta_{out}} \cdot (x_{BSS,grid}^{q,h,w} + x_{BSS,prod}^{q,h,w}) \tag{47}$$

Eqs. (46) and (47) describe the electricity flow in, $x_{BSS,in}^{q,h,w}$, and out, $x_{BSS,out}^{q,h,w}$, of the BSS. $x_{BSS,in}^{q,h,w}$ multiplies $x_{grid,BSS}^{q,h,w}$ with an efficiency factor, $\eta_{in}$, which considers the electricity losses of the charging process of the BSS. $x_{BSS,out}^{q,h,w}$ flows either back into the grid or to the production. In this case, an inverse efficiency factor, $\eta_{out}$, is considered. Eq. (48) states that the maximum power capability of the BSS, $Pcap_{BSS}$[20], restricts the maximal electricity flow in and out of the BSS. The ratio between the power capability and the energy capacity of the BSS is set to 1.

$$x_{BSS,out}^{q,h,w} + x_{BSS,in}^{q,h,w} \leq \frac{Pcap_{BSS}}{4} \tag{48}$$

[20] The term $\frac{Pcap_{BSS}}{4}$ converts power in kW into energy in kWh.

### A.1.2. Battery constraints

Eqs. (49)–(52) describe the storage level of the BSS, $l_{BSS}^{q,h,w}$, for every time interval. The level of the next period, $l_{BSS}^{q+1,h,w}$, equals the storage level of the current period, $l_{BSS}^{q,h,w}$, adjusted for self-discharge losses, $(1 - dis_{BSS})$, combined with the electricity flowing in and out of the BSS until the next period. Eqs. (50)–(52) initialize the storage level for the beginning of every time level. Eq. (50) shows that $l_{BSS}^{1,h,w}$, the storage level of the first period of the time level $h$ and $w$, refers to the storage level of the last period ($q = 4$) of the previous hourly time level $(h - 1)$ for every $h \neq 1 \;\; and \;\; w \neq 1$. Accordingly (Eq. (51)), the first period of every week $w$ refers to the last period of the previous week $(w - 1)$. Finally, Eq. (52) defines the circular definition of the time levels. To define the storage level of the first time period of the year, $l_{BSS}^{1,1,1}$, we refer to the last period of the year, $l_{BSS}^{4,168,52}$.

$$l_{BSS}^{q+1,h,w} = (1 - dis_{BSS}) \cdot l_{BSS}^{q,h,w} + x_{BSS,in}^{q+1,h,w} - x_{BSS,out}^{q+1,h,w}, \;\; if \;\; q \neq 1, \; h \neq 1 \; and \; w \neq 1 \tag{49}$$

$$l_{BSS}^{1,h,w} = (1 - dis_{BSS}) \cdot l_{BSS}^{4,h-1,w} + x_{BSS,in}^{1,h,w} - x_{BSS,out}^{1,h,w}, \;\; if \;\; h \neq 1 \; and \; w \neq 1 \tag{50}$$

$$l_{BSS}^{1,1,w} = (1 - dis_{BSS}) \cdot l_{BSS}^{4,168,w-1} + x_{BSS,in}^{1,1,w} - x_{BSS,out}^{1,1,w}, \;\; if \;\; w \neq 1 \tag{51}$$

$$l_{BSS}^{1,1,1} = (1 - dis_{BSS}) \cdot l_{BSS}^{4,168,52} + x_{BSS,in}^{1,1,1} - x_{BSS,out}^{1,1,1} \tag{52}$$

## A.2. Detailed load data

| Company | Peak load kW | Energy consumption in MWh | $P_{MD}$ in kW | $P_{ToU}$ – | $P_{LF}$ – | $P_{PoU}$ – | $Peak_{integral}$ – | $Peak_{above}$ – | $Peak_{interval}$ – | $Peak_{density}$ – |
|---|---|---|---|---|---|---|---|---|---|---|
| 1 | 33.8 | 153.88 | 25.5 | 37 | 69.5% | 52.2% | 1.08% | 0.05% | 0.71% | 0.71% |
| 2 | 33.8 | 152.71 | 25.5 | 14 | 68.5% | 51.7% | 4.01% | 0.23% | 3.03% | 0.63% |
| 3 | 35.8 | 51.76 | 12.4 | 34 | 54.0% | 16.6% | 12.13% | 2.21% | 7.08% | 0.81% |
| 4 | 37.6 | 163.44 | 26.1 | 91 | 71.7% | 49.8% | 4.47% | 0.47% | 3.67% | 0.59% |
| 5 | 39.3 | 70.29 | 23.8 | 31 | 32.1% | 20.5% | 25.18% | 3.26% | 10.69% | 1.60% |
| 6 | 41.2 | 236.98 | 35.7 | 80 | 76.1% | 65.9% | 1.53% | 0.04% | 1.18% | 0.65% |
| 7 | 43.7 | 104.88 | 22.5 | 35 | 53.3% | 27.5% | 9.49% | 1.34% | 6.49% | 0.82% |
| 8 | 46.2 | 225.74 | 36.6 | 77 | 70.6% | 55.9% | 11.09% | 0.71% | 8.59% | 0.58% |
| 9 | 54.4 | 154.15 | 29.0 | 37 | 63.1% | 32.4% | 35.37% | 5.59% | 25.26% | 1.03% |
| 10 | 60.1 | 208.42 | 39.2 | 57 | 62.5% | 39.7% | 26.29% | 3.22% | 18.19% | 0.99% |
| 11 | 73.3 | 59.50 | 26.2 | 31 | 28.8% | 9.3% | 22.10% | 6.37% | 7.84% | 1.40% |
| 12 | 75.6 | 305.86 | 47.0 | 26 | 74.7% | 46.3% | 6.48% | 0.60% | 5.19% | 0.50% |
| 13 | 82.0 | 201.75 | 44.0 | 38 | 57.4% | 28.2% | 26.87% | 5.02% | 15.80% | 1.09% |
| 14 | 83.5 | 157.53 | 44.0 | 36 | 39.7% | 21.6% | 23.41% | 3.96% | 12.43% | 1.32% |
| 15 | 88.7 | 167.85 | 42.8 | 39 | 51.8% | 21.7% | 27.58% | 4.31% | 14.11% | 1.41% |
| 16 | 102.8 | 293.79 | 52.6 | 36 | 65.6% | 32.7% | 45.75% | 7.70% | 34.95% | 1.13% |
| 17 | 104.7 | 205.78 | 54.1 | 46 | 42.1% | 22.5% | 23.97% | 4.46% | 13.06% | 0.98% |
| 18 | 106.0 | 239.84 | 55.5 | 44 | 44.0% | 25.9% | 23.17% | 2.63% | 13.97% | 1.42% |
| 19 | 107.1 | 107.54 | 44.0 | 45 | 32.4% | 11.5% | 21.76% | 6.66% | 7.26% | 1.56% |
| 20 | 114.1 | 378.70 | 66.9 | 65 | 69.2% | 38.0% | 33.54% | 3.66% | 23.06% | 1.05% |
| 21 | 115.1 | 229.95 | 62.9 | 35 | 47.7% | 22.9% | 15.87% | 2.00% | 7.62% | 1.53% |
| 22 | 117.2 | 131.41 | 55.5 | 32 | 32.6% | 12.8% | 22.68% | 3.95% | 7.78% | 2.19% |
| 23 | 120.3 | 382.24 | 78.3 | 50 | 59.6% | 36.4% | 39.31% | 5.65% | 24.12% | 1.14% |
| 24 | 124.0 | 261.86 | 54.6 | 20 | 63.0% | 24.2% | 26.96% | 4.07% | 16.75% | 1.02% |
| 25 | 164.5 | 380.79 | 71.7 | 35 | 61.1% | 26.5% | 13.45% | 2.30% | 10.33% | 0.65% |

| Company | Peak load kW | Energy consumption in MWh | $P_{MD}$ in kW | $P_{ToU}$ – | $P_{LF}$ – | $P_{PoU}$ – | $Peak_{integral}$ – | $Peak_{above}$ – | $Peak_{interval}$ – | $Peak_{density}$ – |
|---|---|---|---|---|---|---|---|---|---|---|
| 26 | 175.0 | 555.24 | 118.4 | 71 | 53.8% | 36.3% | 3.94% | 0.14% | 2.14% | 1.23% |
| 27 | 181.0 | 582.75 | 116.6 | 34 | 58.6% | 36.9% | 30.25% | 3.89% | 20.17% | 1.13% |
| 28 | 206.8 | 754.17 | 128.0 | 24 | 68.1% | 41.7% | 9.13% | 0.52% | 6.68% | 0.95% |
| 29 | 208.4 | 178.30 | 70.3 | 47 | 30.3% | 9.8% | 18.97% | 6.08% | 7.43% | 1.37% |
| 30 | 239.6 | 432.74 | 134.6 | 49 | 47.2% | 20.7% | 33.69% | 7.26% | 13.37% | 1.65% |
| 31 | 252.0 | 811.47 | 152.2 | 44 | 61.5% | 36.9% | 33.98% | 4.47% | 24.01% | 0.97% |
| 32 | 259.3 | 302.70 | 105.9 | 37 | 46.3% | 13.4% | 32.26% | 6.66% | 13.54% | 1.68% |
| 33 | 291.0 | 620.54 | 149.8 | 33 | 55.2% | 24.4% | 34.84% | 7.41% | 18.15% | 1.26% |
| 34 | 325.6 | 1251.54 | 215.4 | 47 | 71.1% | 44.0% | 34.07% | 5.17% | 23.37% | 0.99% |
| 35 | 325.6 | 1251.54 | 215.4 | 47 | 71.1% | 44.0% | 34.07% | 5.17% | 23.37% | 0.99% |
| 36 | 362.9 | 201.85 | 64.8 | 46 | 45.2% | 6.4% | 16.46% | 7.44% | 6.71% | 0.85% |
| 37 | 369.0 | 1501.01 | 257.9 | 32 | 67.2% | 46.6% | 30.52% | 2.77% | 23.21% | 0.90% |
| 38 | 391.0 | 584.33 | 172.8 | 35 | 52.4% | 17.1% | 25.32% | 4.99% | 11.94% | 1.45% |
| 39 | 460.0 | 1552.15 | 319.5 | 36 | 61.6% | 38.6% | 46.00% | 8.04% | 26.68% | 1.23% |
| 40 | 522.6 | 1494.29 | 313.0 | 35 | 52.4% | 32.7% | 30.73% | 4.71% | 20.75% | 1.02% |
| 41 | 674.0 | 2106.19 | 414.1 | 39 | 58.8% | 35.8% | 20.50% | 2.30% | 15.16% | 1.11% |
| 42 | 1136.0 | 2720.36 | 665.7 | 54 | 52.8% | 27.4% | 43.64% | 8.88% | 22.49% | 1.36% |
| 43 | 1252.0 | 4516.04 | 834.6 | 96 | 59.8% | 41.3% | 11.80% | 1.01% | 8.70% | 1.10% |
| 44 | 1422.0 | 6342.18 | 961.5 | 96 | 74.1% | 51.1% | 27.25% | 2.34% | 24.46% | 0.77% |
| 45 | 1524.0 | 1686.27 | 911.4 | 41 | 27.4% | 12.7% | 50.04% | 14.43% | 11.91% | 2.82% |
| 46 | 1793.5 | 6309.87 | 1206.8 | 41 | 63.2% | 40.3% | 32.81% | 4.25% | 21.40% | 1.10% |
| 47 | 2797.6 | 16819.08 | 2156.4 | 61 | 88.8% | 68.8% | 43.36% | 2.87% | 41.65% | 0.74% |
| 48 | 2916.8 | 22375.17 | 2630.4 | 64 | 97.4% | 87.8% | 30.03% | 0.81% | 29.81% | 0.54% |

| | | | | | | | | | | |
|---|---|---|---|---|---|---|---|---|---|---|
| 49 | 3698.4 | 9171.24 | 2024.7 | 27 | 52.9% | 28.4% | 50.10% | 9.24% | 30.12% | 1.25% |
| 50 | 4717.6 | 13797.35 | 2654.0 | 37 | 62.1% | 33.5% | 34.75% | 6.07% | 24.73% | 1.03% |

## Appendix B. Supplementary material

Supplementary data to this article can be found online at https://doi.org/10.1016/j.apenergy.2019.01.050.

## References


[1] Bolay Sebastian, Bullmann Till, Hegner Miriam. Faktenpapier Energiespeicher. Rechtsrahmen, Geschäftsmodelle, Forderungen. Edited by BVES - Bundesverband Energiespeicher e.V. Berlin, DIHK - Deutscher Industrie- und Handelskammertag; 2016.

[2] Jochem Patrick, Kaschub Thomas, Fichtner Wolf. How to integrate electric vehicles in the future energy system? In: Hülsmann Michael, Fornahl Dirk, editors. Evolutionary paths towards the mobility patterns of the future. Berlin, Heidelberg: Springer Berlin Heidelberg; 2014. p. 243–63. [Lecture Notes in Mobility].

[3] Rodríguez-García Javier, Álvarez-Bel Carlos, Carbonell-Carretero José-Francisco, Alcázar-Ortega Manuel, Peñalvo-López Elisa. A novel tool for the evaluation and assessment of demand response activities in the industrial sector. Energy 2016;113:1136–46. https://doi.org/10.1016/j.energy.2016.07.146.

[4] Atabay Dennis, Dornmair Rita, Hamacher Thomas, Keller Fabian, Reinhart Gunter. Flexibilisierung des Stromverbrauchs in Fabriken. Graz/Austria (13. Symposium Energieinnovation); 2014.

[5] Schultz Cedric, Sellmaier Peter, Reinhart Gunther. An approach for energy-oriented production control using energy flexibility. Proc CIRP 2015;29:197–202. https://doi.org/10.1016/j.procir.2015.02.038.

[6] Shoreh Maryam H, Siano Pierluigi, Shafie-khah Miadreza, Loia Vincenzo, Catalão João PS. A survey of industrial applications of Demand Response. Electr Power Syst Res 2016;141:31–49. https://doi.org/10.1016/j.epsr.2016.07.008.

[7] Thielmann Axel, Sauer Andreas, Wietschel Martin. Produkt-Roadmap Stationäre Energiespeicher 2030. Fraunhofer-Institut für System- und Innovationsforsching ISI. Karlsruhe; 2015.

[8] Gallo AB, Simões-Moreira JR, Costa HKM, Santos MM, Moutinho dos Santos E. Energy storage in the energy transition context. A technology review. Renew Sustain Energy Rev 2016;65:800–22. https://doi.org/10.1016/j.rser.2016.07.028.

[9] Reid Gerard, Julve Javier. Second life-batteries as flexible storage for renewable energies. Bundesverband Eneuerbare Energien e.V.; 2016.

[10] Eyer James M, Schoenung Susan M. Benefit/cost framework for evaluating modular energy storage. A study for the DOE energy storage systems program. Albuquerque: Sandia National Laboratories; 2008 [checked on 10/10/2017].

[11] Shcherbakova Anastasia, Kleit Andrew, Cho Joohyun. The value of energy storage in South Korea's electricity market: a Hotelling approach. Appl Energy 2014;125:93–102. https://doi.org/10.1016/j.apenergy.2014.03.046.

[12] Stephan A, Battke B, Beuse MD, Clausdeinken JH, Schmidt TS. Limiting the public cost of stationary battery deployment by combing applications. Nat Energy 2016;1.

[13] Lombardi P, Schwabe F. Sharing economy as a new business model for energy storage systems. Appl Energy 2017;188:485–96. https://doi.org/10.1016/j.apenergy.2016.12.016.

[14] Cho Joohyun, Kleit Andrew N. Energy storage systems in energy and ancillary markets. A backwards induction approach. Appl Energy 2015;147:176–83. https://doi.org/10.1016/j.apenergy.2015.01.114.

[15] Moreno Rodrigo, Moreira Roberto, Strbac Goran. A MILP model for optimising multi-service portfolios of distributed energy storage. Appl Energy 2015;137:554–66. https://doi.org/10.1016/j.apenergy.2014.08.080.

[16] Dowling Alexander W, Kumar Ranjeet, Zavala Victor M. A multi-scale optimization framework for electricity market participation. Appl Energy 2017;190:147–64. https://doi.org/10.1016/j.apenergy.2016.12.081.

[17] Atabay Dennis. An open-source model for optimal design and operation of industrial energy systems. Energy 2017;121:803–21. https://doi.org/10.1016/j.energy.2017.01.030.

[18] EPEX SPOT. Market data day-ahead auction. For the year 2017. EPEX SPOT; 2018. Available online at < https://www.epexspot.com/de/marktdaten/dayaheadauktion/chart/auction-chart/2017-12-31/DE > [checked on 6/6/2018].

[19] EPEX SPOT. Market data intraday auction. For the year 2017. EPEX SPOT; 2018. Available online at < https://www.epexspot.com/de/marktdaten/intradaycontinuous/chart/intraday-chart/2017-12-31/DE > [checked on 6/6/2018].

[20] Graditi G, Ippolito MG, Telaretti E, Zizzo G. Technical and economical assessment of distributed electrochemical storages for load shifting applications. An Italian case study. Renew Sustain Energy Rev 2016;57:515–23. https://doi.org/10.1016/j.rser.2015.12.195.

[21] Lin Boqiang, Wu Wei. Economic viability of battery energy storage and grid strategy. A special case of China electricity market. Energy 2017;124:423–34. https://doi.org/10.1016/j.energy.2017.02.086.

[22] Sandoval Diego, Leibundgut Hansjürg. Introduction of electrical batteries in the operation of LowEx buildings. Energy Build 2014;81:105–14. https://doi.org/10.1016/j.enbuild.2014.06.012.

[23] Bradbury Kyle, Pratson Lincoln, Patiño-Echeverri Dalia. Economic viability of energy storage systems based on price arbitrage potential in real-time U.S. electricity markets. Appl Energy 2014;114:512–9. https://doi.org/10.1016/j.apenergy.2013.10.010.

[24] Heymans Catherine, Walker Sean B, Young Steven B, Fowler Michael. Economic analysis of second use electric vehicle batteries for residential energy storage and load-levelling. Energy Policy 2014;71:22–30. https://doi.org/10.1016/j.enpol.2014.04.016.

[25] Zheng Menglian, Meinrenken Christoph J, Lackner Klaus S. Agent-based model for electricity consumption and storage to evaluate economic viability of tariff arbitrage for residential sector demand response. Appl Energy 2014;126:297–306. https://doi.org/10.1016/j.apenergy.2014.04.022.

[26] Faessler B, Kepplinger P, Petrasch J. Decentralized price-driven grid balancing via repurposed electric vehicle batteries. Energy 2017;118:446–55. https://doi.org/10.1016/j.energy.2016.12.013.

[27] Jiang Daniel R, Powell Warren B. Optimal Hour-Ahead bidding in the real-time electricity market with battery storage using approximate dynamic programming. INFORMS J Comput 2015;27(3):525–43.

[28] Hollinger R, Cortés AM, Erge T, Engel B. Analysis of the minimum activation period of batteries in frequency containment reserve. In: 2017 14th International Conference on the European Energy Market (EEM); 2017, p. 1–6. https://doi.org/10.1109/EEM.2017.7981904.

[29] Deutsche ÜNB. Prequalified capacity in Germany; 2018. Available online at < https://www.regelleistung.net/ext/download/pq_capacity > [checked on 8/6/2018].

[30] Ding D, Li JL, Yang SL, Wu XG, Liu ZQ. Capacity Configuration of BESS as an Alternative to Coal-Fired Power Units for Frequency Control. Adv Mat Res 2014;953–954:743–7. https://doi.org/10.4028/www.scientific.net/AMR.953-954.743.

[31] Kunisch HJ, Kramer KG, Dominik H. Battery Energy Storage Another Option for Load-Frequency-Control and Instantaneous Reserve. IEEE T Energy Conver 1986;EC-1(3):41–6. https://doi.org/10.1109/TEC.1986.4765732.

[32] Taylor PA. Update on the Puerto Rico electric power authority's spinning reserve battery system. In: Proceedings of 11th Annual Battery Conference on Applications and Advances; 1996, p. 249–252. https://doi.org/10.1109/BCAA.1996.485003.

[33] Joseph A, Shahidehpour M. Battery storage systems in electric power systems. In: Power Engineering Society General Meeting, 2006. IEEE: IEEE; 2006, 8-pp. https://doi.org/10.1109/PES.2006.1709235.

[34] Doughty DH, Butler PC, Akhil AA, Clark NH, Boyes JD. Batteries for Large-Scale Stationary Electrical Energy Storage. Elec Soc Inter 2010, 19(3), pp. 49–53, https://doi.org/10.1149/2.F05103if.

[35] Anderson D. An evaluation of current and future costs for lithium-ion batteries for use in electrified vehicle powertrains 2009.

[36] Nykvist B, Nilsson M\ta. Rapidly falling costs of battery packs for electric vehicles. Nat Clim Change 2015;5(4):329–32. https://doi.org/10.1038/nclimate2564.

[37] Deutsche ÜNB. Anforderungen an die Speicherkapazität bei Batterien für die Primärregelleistung; 2015. Available online at < https://www.regelleistung.net/ext/download/anforderungBatterien > [checked on 8/7/2018].

[38] Deutsche ÜNB. Eckpunkte und Freiheitsgrade bei Erbringung von Primärregelleistung. Leitfaden für Anbieter von Primärregelleistung; 2014. Available online at < https://www.regelleistung.net/ext/download/eckpunktePRL > [checked on 8/7/2018].

[39] Haberschusz D, Kwiecien M, Badeda J, Schulte D, Jöris F. Zwischenbericht Projekt BSMS; 2016, https://doi.org/10.13140/RG.2.2.36259.25121.

[40] Senkel K. Wieviel Batteriegroßspeicher verträgt der Primärregelleistungsmarkt?; 2017; Available at < http://www.enervis.de/de/news-strommarkt/493-wieviel-batteriegrossspeicher-vertraegt-der-primaerregelleistungsmarkt > [checked on 1/3/2018].

[41] Swierczynski M, Stroe DI, Stan AI, Teodorescu R, Lærke R, Kjær PC. Field tests experience from 1.6MW/400kWh Li-ion battery energy storage system providing primary frequency regulation service. In: IEEE PES ISGT Europe 2013; 2013, p. 1–5. https://doi.org/10.1109/ISGTEurope.2013.6695277.

[42] Lei B, Li XR, Huang JY, Tan SJ. Droop Configuration and Operational Mode Setting of Battery Energy Storage System in Primary Frequency Regulation. Appl Mech Mater 2014;448–453:2235–8, https://doi.org/10.4028/www.scientific.net/AMM.448-453.2235.

[43] Koller Michael, Borsche Theodor, Ulbig Andreas, Andersson Göran. Review of grid applications with the Zurich 1MW battery energy storage system. Electr Power Syst Res 2015;120:128–35. https://doi.org/10.1016/j.epsr.2014.06.023.

[44] Fleer J, Stenzel P. Impact analysis of different operation strategies for battery energy storage systems providing primary control reserve. Energy Storage 2016;8:320–38. https://doi.org/10.1016/j.est.2016.02.003.

[45] Hollinger R, Diazgranados LM, Wittwer C, Engel B. Optimal Provision of Primary Frequency Control with Battery Systems by Exploiting All Degrees of Freedom within Regulation. Energy Proced 2016;99(Supplement C):204–14. https://doi.org/10.1016/j.egypro.2016.10.111.

[46] Malhotra Abhishek, Battke Benedikt, Beuse Martin, Stephan Annegret, Schmidt Tobias. Use cases for stationary battery technologies. A review of the literature and

existing projects. Renew Sustain Energy Rev 2016;56:705–21. https://doi.org/10.1016/j.rser.2015.11.085.
[47] Telaretti E, Graditi G, Ippolito MG, Zizzo G. Economic feasibility of stationary electrochemical storages for electric bill management applications. The Italian scenario. Energy Policy 2016;94:126–37. https://doi.org/10.1016/j.enpol.2016.04.002.
[48] Ceseña Martínez, Eduardo A, Good Nicholas, Mancarella Pierluigi. Electrical network capacity support from demand side response. Techno-economic assessment of potential business cases for small commercial and residential end-users. Energy Policy 2015;82:222–32. https://doi.org/10.1016/j.enpol.2015.03.012.
[49] Neubauer Jeremy S, Wood Eric, Pesaran Ahmad. A second life for electric vehicle batteries. Answering questions on battery degradation and value. SAE Int J Mater Manf 2015;8(2). https://doi.org/10.4271/2015-01-1306.
[50] Zheng Menglian, Meinrenken Christoph J, Lackner Klaus S. Smart households. Dispatch strategies and economic analysis of distributed energy storage for residential peak shaving. Appl Energy 2015;147:246–57. https://doi.org/10.1016/j.apenergy.2015.02.039.
[51] Nottrott A, Kleissl J, Washom B. Energy dispatch schedule optimization and cost benefit analysis for grid-connected, photovoltaic-battery storage systems. Renew Energy 2013;55:230–40. https://doi.org/10.1016/j.renene.2012.12.036.
[52] Chua Kein, Huat, Yun Seng Lim, Stella Morris. Cost-benefit assessment of energy storage for utility and customers. A case study in Malaysia. Energy Convers Manage 2015;106:1071–81. https://doi.org/10.1016/j.enconman.2015.10.041.
[53] Park Alex, Lappas Petros. Evaluating demand charge reduction for commercial-scale solar PV coupled with battery storage. Renew Energy 2017;108:523–32. https://doi.org/10.1016/j.renene.2017.02.060.
[54] Gitizadeh Mohsen, Fakharzadegan Hamid. Battery capacity determination with respect to optimized energy dispatch schedule in grid-connected photovoltaic (PV) systems. Energy 2014;65:665–74. https://doi.org/10.1016/j.energy.2013.12.018.
[55] Rominger Julian, Kern Fabian, Schmeck Hartmut. Provision of frequency containment reserve with an aggregate of air handling units. Comput Sci Res Dev 2018;33(1–2):215–21. https://doi.org/10.1007/s00450-017-0361-8.
[56] Deutsche ÜNB. Anforderungen an die Speicherkapazität beiBatterien für die Primärregelleistung; 2015. Available online at < https://www.regelleistung.net/ext/download/anforderungBatterien > [checked on 9/29/2015].
[57] Kaschub Thomas, Jochem Patrick, Fichtner Wolf. Solar energy storage in German households. Profitability, load changes and flexibility. Energy Policy 2016;98:520–32. https://doi.org/10.1016/j.enpol.2016.09.017.
[58] McLoughlin Fintan, Duffy Aidan, Conlon Michael. Evaluation of time series techniques to characterise domestic electricity demand. Energy 2013;50:120–30. https://doi.org/10.1016/j.energy.2012.11.048.
[59] Bundesnetzagentur. Monitoringbericht 2017. Edited by Bundesnetzagentur für Elektrizität, Gas, Telekommunikation, Post und Eisenbahn. Bonn; 2017 [checked on 7/6/2018].
[60] Deutsche ÜNB. TSOs' proposal for the establishment of common and harmonised rules and processes for the exchange and procurement of Balancing Capacity for Frequency Containment Reserves (FCR) in accordance with Article 33 of Commission Regulation (EU) 2017/2195 establishing a guideline on electricity balancing; 2018 [checked on 8/7/2018].
[61] Werwitzke Cora. Neue Erkenntnisse zu Akku-Degradation bei Tesla-Autos. electrive.net, 4/16/2018; 2018. Available online at < https://www.electrive.net/2018/04/16/neue-erkenntnisse-zu-akku-degradation-bei-tesla-autos/ > [checked on 7/12/2018].
[62] Han Xuebing, Ouyang Minggao, Lu Languang, Li Jianqiu. A comparative study of commercial lithium ion battery cycle life in electric vehicle. Capacity loss estimation. J Power Sources 2014;268:658–69. https://doi.org/10.1016/j.jpowsour.2014.06.111.
[63] Opitz A, Badami P, Shen L, Vignarooban K, Kannan AM. Can Li-ion batteries be the panacea for automotive applications? Renew Sustain Energy Rev 2017;68:685–92. https://doi.org/10.1016/j.rser.2016.10.019.
[64] AG Energiebilanz. Energy consumption in Germany in 2017. Edited by Hans-Joachim Ziesing. Berlin, Bergheim; 2018. Available online at < https://www.google.com/url?sa=t&rct=j&q=&esrc=s&source=web&cd=6&ved=0ahUKEwi9zcDs3b7bAhXEa1AKHY2rCrwQFghwMAU&url=https%3A%2F%2Fag-energiebilanzen.de%2Findex.php%3Farticle_id%3D29%26fileName%3Dageb_jahresbericht2017_20180420_englisch.pdf&usg=AOvVaw2OMenBmOX4HKDEMijrCQaG > [checked on 6/6/2018].
[65] Bloom Ira, Potter Benjamin G, Johnson Christopher S, Gering Kevin L, Christophersen Jon P. Effect of cathode composition on impedance rise in high-power lithium-ion cells. Long-term aging results. J Power Sources 2006;155(2):415–9. https://doi.org/10.1016/j.jpowsour.2005.05.008.
[66] Brealey Richard A, Myers Stewart C, Allen Franklin. Principles of corporate finance, 10th ed. McGraw-Hill/Irwin; 2011 [checked on 2/14/2018].
[67] Deutsche ÜNB. Tender overview; 2018. Available online at < https://www.regelleistung.net/ext/tender/?lang=en > [checked on 8/7/2018].
[68] Lunz Benedikt, Yan Zexiong, Gerschler Jochen, Sauer Bernhard, Uwe Dirk. Influence of plug-in hybrid electric vehicle charging strategies on charging and battery degradation costs. Energy Policy 2012;46:511–9. https://doi.org/10.1016/j.enpol.2012.04.017.

# Publication B

# Optimal PV and Battery Investment of Market-Participating Industry Facilities

Nikolina Čović[a], Fritz Braeuer[b], Russell McKenna[c], Hrvoje Pandžić[a]

[a]*Faculty of Electrical Engineering and Computing, University of Zagreb, Zagreb, Croatia*

[b]*Chair of Energy Economics, Institute for Industrial Production, Karlsruhe Institute of Technology, Karlsruhe, Germany*

[c]*Chair of Energy Transition, School of Engineering, University of Aberdeen, Aberdeen, United Kingdom*

Published in:

IEEE Transactions on Power Systems, Volume 36, 4th Issue, July 2021, pages 3441 – 3452

https://doi.org/10.1109/TPWRS.2020.3047260

# Optimal PV and Battery Investment of Market-Participating Industry Facilities

N. Čović, F. Braeuer, R. McKenna, and H. Pandžić, *Senior Member, IEEE*

***Abstract*—Introducing flexible consumers to electricity markets is beneficial to the power system and offers them potential economic savings. Industrial consumers are pioneer candidates due to their high energy demand and interest in reducing energy costs. This paper addresses the battery storage and photovoltaics investment problem, which includes five revenue streams for industrial consumers, such as participation in the day-ahead and intraday energy markets as well as the primary control reserve market peak shaving and optimized self-consumption. The uncertainty is considered using correlated scenarios of the local load, primary reserve market and day-ahead market prices, as well as generation from photovoltaics. The uncertainty of the pay-as-bid intraday market with continuous trading is modeled using robust optimization. Credibility and applicability of the model is achieved by using market settings and prices from three European countries (Germany, Denmark and Croatia) and comparing their suitability for encompassing the end-user flexibility. Results shed light on national energy-political and climatic differences, highlighting opportunities for active market participation through individual or aggregated industrial plants.**

***Index Terms*—Battery storage, clustering, industrial facilities, optimal investment, photovoltaics, robust optimization, stochastic optimization.**

## NOMENCLATURE

*Sets and Indices*

| | |
|---|---|
| $\Omega^H$ | Set of hours in a week, running from 1 to 168 |
| $\Omega^J$ | Set of breakpoints in linearized BSS charging curve, running from 1 to $N^j$ |
| $\Omega^M$ | Set of months in a year, running from 1 to 12 |
| $\Omega^S$ | Set of scenarios, running from 1 to $N^s$ |
| $\Omega^Q$ | Set of quarter-hour periods, running from 1 to 4 |
| $\Omega^W$ | Set of representative weeks, running from 1 to $N^w$ |

*Parameters*

| | |
|---|---|
| $C^{\text{fees}}$ | Fees and taxes for supplying electricity (€/kWh) |
| $C^{\text{peak}}$ | Peak power charges to end consumers (€/kW) |
| $D_{q,h,w,s}$ | Local electricity demand (kW) |
| $F_j$ | Maximum amount of energy that can be charged at specific battery state of energy breakpoint $R_j$ as a portion of installed BSS capacity |
| $i$ | Discount rate (%) |
| $I^{\text{pv}}$ | PV installation cost per kW (€/kW) |
| $I^{\text{BSSe}}$ | BSS installation cost per kWh (€/kWh) |
| $I^{\text{BSSp}}$ | BSS installation cost per kW (€/kW) |
| $k^{\text{s}}_{h,w,s}$ | Full load hours of PV plants (kWh/kW) |
| $k_\vartheta$ | Percentage of energy capacity for providing PCR lost due to battery cycling inefficiency (%) |
| $M$ | Big number |
| $n$ | Battery energy-to-power ratio in PCR market |
| $R_j$ | Capacity of each state of energy battery segment $j$ as a portion of the installed battery capacity |
| $T^{\text{BSS}}, T^{\text{PV}}$ | Number of BSS and PV annuities |
| $VoLL$ | Price for demand reduction (€/kW) |
| $\Gamma$ | Uncertainty budget |
| $\vartheta$ | Number of days |
| $\lambda^{\text{PCR}}_{w,s}$ | PCR price (€/kW) |
| $\lambda^{\text{DA}}_{h,w,s}$ | Day-ahead market price (€/kWh) |
| $\lambda^{\text{ID}}_{q,h,w,s}$ | Average intraday market price (€/kWh) |
| $\Delta\lambda^{\text{ID}}_{q,h,w,s}$ | Difference between minimum/maximum and average price in the intraday market (€/kWh) |
| $\pi_{w,s}$ | Probability of each scenario $s$ in week $w$ |
| $\rho_w$ | Number of weeks that week $w$ represents per year |

*Variables*

Positive continuous variables

| | |
|---|---|
| $b_{q,h,w,s}$ | Share of maximum price deviation for every time period in each week and scenario |
| $c^{\text{BSS}}$ | Annual cost of BSS installation (€) |
| $c^{\text{el}}_{h,w}$ | Cost of purchased electricity (€) |

Manuscript received June 25, 2020; revised November 17, 2020; accepted December 19, 2020. Date of publication December 24, 2020; date of current version June 18, 2021. The work of H. Pandžić was supported by the European Union through the European Regional Development Fund Operational Programme Competitiveness and Cohesion 2014-2020 of the Republic of Croatia under Project KK.01.1.1.04.0034 "Connected Stationary Battery Energy Storage". The work of N. Čović was supported by the Croatian Science Foundation under project DOK-2020-01-3911. This work was supported in part by the Croatian Science Foundation under project Active NeIghborhoods energy Markets pArTicipatION – ANIMATION (IP-2019-04-09164). Paper no. TPWRS-01049-2020. *(Corresponding author: Hrvoje Pandzic.)*

N. Čović and H. Pandžić are with the University of Zagreb Faculty of Electrical Engineering and Computing, Zagreb 10000, Croatia (e-mail: nikolina.covic@fer.hr; hrvoje.pandzic@ieee.org).

F. Braeuer is with the Karlsruhe Institute of Technology, Karlsruhe 76131, Germany (e-mail: fritz.braeuer@kit.edu).

R. McKenna is with the University of Aberdeen, Aberdeen AB24 3FX, U.K. (e-mail: russell.mckenna@abdn.ac.uk).

Color versions of one or more figures in this article are available at https://doi.org/10.1109/TPWRS.2020.3047260.

Digital Object Identifier 10.1109/TPWRS.2020.3047260

| | |
|---|---|
| $c^{\text{peak}}$ | Cost for peak power (€) |
| $c^{\text{PV}}$ | Annual cost of PV installation (€) |
| $d_{q,h,w,s}$ | Served demand (kW) |
| $e^{\text{DA}}_{h,w}$ | Electricity purchased in the day-ahead market (kWh) |
| $e^{\text{PCR}}_{q,h,w,s}$ | Electricity required to cover for battery cycling inefficiency when providing PCR (kWh) |
| $p^{\text{BSS}}$ | Installed BSS power (kW) |
| $p^{\text{PCR}}_{w}$ | Power provided for PCR per week (kW) |
| $p^{\text{peak}}$ | Annual peak power (kW) |
| $p^{\text{ch}}_{q,h,w,s}$ | BSS charging power (kW) |
| $p^{\text{dis}}_{q,h,w,s}$ | BSS discharging power (kW) |
| $p^{\text{pv}}_{h,w,s}$ | Utilized PV generation (kW) |
| $p^{\text{pv,cap}}$ | Installed capacity of PV generation (kW) |
| $r^{\text{PCR}}_{w}$ | Weekly revenue from PCR (€) |
| $soe^{\text{PCR}}_{w}$ | Capacity of BSS reserved for PCR auction (kWh) |
| $soe^{\max}$ | Installed BSS capacity (kWh) |
| $soe_{q,h,w,s}$ | BSS state of energy (kWh) |
| $soe_{q,h,w,s,j}$ | State of energy of battery segment $j$ (kWh) |
| $u_{q,h,w,s}$ | Unserved demand (kW) |
| $z_{w,s}, \omega_{q,h,w,s}$ | Dual variables associated with the constraints of the robust subproblem |
| Binary variables | |
| $x_{q,h,w,s}$ | 1 if BSS is charging and 0 otherwise |

## I. Introduction

In many countries, the transition process of the traditional towards highly-renewable energy systems results in an increasing volatility of energy supply. To account for this volatility, a more flexible demand side is needed. Due to high electricity needs and costs, industrial electricity consumers might play an important role in providing this flexibility. One way to increase flexibility of an industrial consumer is the installation of a battery storage system (BSS) [1], which provides multiple streams of revenue or savings, finally resulting in lower electricity costs [2]. Despite multiple BSS revenue streams, the initial investment is high, so accurate and robust investment models are required for favorable return on investment. To define the optimal BSS investment decision for an industrial plant (IP), one needs to carefully consider the country's specific market conditions. Furthermore, it is important to include the uncertainties of future cash flows that amortize the investment. These uncertainties cover energy market prices, volatility in the plant's operation as well as uncertainties affecting the generation from renewable energy sources (RES). In this paper, we consider photovoltaics (PV) as a potential local generation investment alongside BSS. The benefits of combining PV and BSS have been proven in the literature, e.g. [3].

### A. Literature Review

The majority of scientific literature on BSS and PV focuses on operation problems, while investment studies are more scarce. In the field of BSS investment in an industrial context, paper [4] proposes a two-stage optimization problem to identify the optimal size of a BSS in an industrial microgrid in Australia. The first stage describes the BSS investment decision and the second stage optimizes the BSS operation. The paper is focused on energy arbitrage and optimized self-consumption considering charging-power dependent efficiencies of the BSS. With more detail on the production process, [5] optimizes the size of a PV–BSS system incorporated into a semi-autogenous grinding mill plant. Their two-stage stochastic optimization model considers the uncertainty of the grindability of the rock and thus the energy demand of the plant as well as the uncertain RES production. While the first stage optimizes the investment along with the annual energy contracts, the second stage optimizes the operating cost that includes maintenance, replacement and the penalty paid for not matching the contracted energy supply. Paper [6] investigates the optimal BSS investment for an IP to lower its electricity costs. Decision theory is applied to identify optimal battery capacity from a predetermined set and schedule optimal dispatch for a variety of future scenarios. Finally, [7] includes an optimized production process of an industrial complex in the design of an industrial micro-grid. While uncertainty is not directly part of the optimization model, the results are tested for a variety of uncertain weather and production conditions.

Another interesting field of application is the residential and commercial sector. Here, [8] analyses the effects of uncertainty in electricity demand and prices for a commercial hotel building in Croatia. The study provides a comparison of the stochastic and robust optimization approaches to a deterministic optimization model. In contrast, [9] proposes a multi-stage stochastic optimization model to define the optimal size of a residential microgrid. The model formulates daily microgrid operation iteratively to determine the optimal size of the micro-grid. For a similar use case in a Dutch residential context, [10] analyzes revenue streams for a PV–BSS system. The system generates revenue in the day-ahead market, the imbalance market and through self-consumption. The proposed two-stage stochastic approach includes uncertainty on market prices, irradiation and demand profiles. Finally, [11] applies a (robust) data-driven dynamic programming approach to homes in Austin, Texas. They report that their approach outperforms the existing methods and significantly raises the break-even cost that incentivizes homeowners to invest in BSS.

Nonetheless, in an industrial context no study considers multiple revenue streams for a BSS–PV investment problem under uncertainty. Furthermore, no study compares market conditions in different countries.

### B. Research Questions and Contribution

In this paper, we study the BSS–PV investment decision in an IP under uncertainty. To find the optimal investment capacities, we formulate a two-stage stochastic optimization problem implemented as a mixed integer linear program (MILP). The BSS–PV system can be used to minimize the electricity costs

by altering the net load curve as seen from the grid side as well as by lowering the fees and peak power charges. In case an IP invests in a BSS, it can be used to provide primary control reserve (PCR).[1]

The considered uncertainties in the model are the load, PV production as well as market prices in the day-ahead, intraday and PCR markets. To represent the pay-as-bid nature of the continuous intraday market, the intraday trading is modeled using robust optimization. This is a suitable tool for considering the skillfulness (and luck) of the bidder. While robust optimization has been used for bidding in day-ahead markets, e.g. [13] and [14], its application to pay-as-bid continuous markets remains unexplored. *Pay-as-bid* means there is no single market clearing price, but multiple prices depending on the selling and purchasing bids. Furthermore, the term *continuous* means there is no gate closure time, instead the trading is performed continuously until the cut-off time, usually 15 or 30 minutes before the full hour. Therefore, it is not possible to derive any specific hour-by-hour scenario as there is no correlation between the prices in the consecutive hours (except for the highest and the lowest one). Robust formulation is a tool that enables us to model uncertain process (such as the one related to the success in trading in the intraday market) without knowing or assuming the distribution of uncertainty and only knowing the upper and lower bounds.

The model is applied to 20 IPs and a time horizon of one year is portrayed through representative weeks, each having its frequency of appearing in a year. We evaluate the profitability of a BSS–PV investment for each IP individually and together as one group and compare the results. Finally, an important value of this paper is its applicability as we compare the investment decisions under three diverse European market conditions in Germany, Denmark and Croatia, respectively. The following points summarize the contribution of the paper:

1) Formulation of the stochastic two-stage IP investment problem in a BSS and PV considering active participation in day-ahead, intraday and PCR markets.
2) Introduction of robust optimization to pay-as-bid intraday market allowing to control the expected success in bidding in such market.
3) A comprehensive comparison of optimal investments in different European countries, i.e. Germany, Denmark and Croatia, allowing us to assess the attractiveness of different market designs.

The rest of the paper is organized as follows. Section II. formulates the proposed mathematical model and provides its extensions for different market types. Section III. presents case studies for Germany, Denmark and Croatia and discusses the results. Verification of the results obtained in the case studies is demonstrated in Section IV. Finally, the relevant conclusions are provided in Section V.

[1]This setting is in line with Clean Energy for All Europeans Package [12] which supports activation of end consumers and instructs opening of the energy and reserve markets to flexible end consumers.

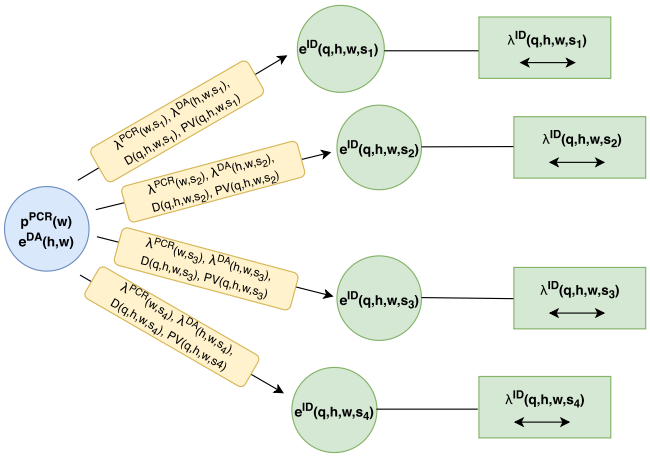


Fig. 1. In the first stage, the battery capacity and power for providing PCR are reserved and quantities in the day-ahead market for each day of the week are purchased. In the second stage, the intraday market volume is purchased for each scenario with knowledge of the day-ahead and PCR prices, along with the load and PV production.

## II. Mathematical Model

### A. Description

The operational model is a two-stage model, as shown in Fig. 1. In the first stage, two decisions are made (blue circle in Fig. 1): i) the battery power and capacity reserved for providing PCR, and ii) the quantities purchased in the day-ahead market for each day of the week. The uncertainties of the PCR prices, along with the day-ahead prices, are thus modelled as expected values. The stochastic model in this case degrades to a deterministic one with expected values of prices as input parameters, but differs from the deterministic problem posed for any particular scenario.

After these here-and-now decisions are made, the stochastic processes are realised depending on the scenario $s$. The day-ahead and PCR prices become known, along with the values of the load and the PV production (yellow "rectangles" in Fig. 1). Since the scenario generation process was performed considering the correlation of the above mentioned parameters, scenarios of the day-ahead and PCR prices match the scenarios of the load and PV output. Given these, we move to the second stage, which is closer to the realization of uncertainty.

The volume purchased in the intraday market is the decision made in the second stage (green circles in Fig. 1). Uncertainty of the intraday prices is not treated as a stochastic process, but using the robust framework with the associated price interval for each scenario.

### B. Assumptions

The described mathematical model is relevant for markets with the following rules:

- IPs with their assets (PV and BSS) can take part in the day-ahead and intraday energy markets. The day-ahead market is an hourly market with a uniform market clearing price, while the intraday market is pay-as-bid with 15-minute resolution.

- When consuming electricity, the IPs need to pay a fee, $C^{\text{fees}}$, for using the network, supporting renewables, and other levies.
- IPs can only purchase but not sell energy in the day-ahead and intraday markets. The first reason for disallowing energy selling is that any facility that injects energy into the grid (even very sporadically) needs to register as a power producer, thus incurring additional costs that depend on the prequalification procedure that includes an analysis of the surrounding network to determine if any upgrades are needed. The second reason is purely economical. Since the network fees constitute a huge portion of the consumers' energy cost, it is not viable to sell energy and increase the overall amount of energy later extracted from the grid, as that energy comes at high collateral cost in the form of grid fees and renewable support fees. The final reason is related to the modelling issues. Allowing $e^{\text{DA}}$ and $e^{\text{ID}}$ to become negative would enable arbitrage between the day-ahead and intraday markets without any actual energy flow. The result would be an indefinitely large BSS allowing the IP to obtain indefinite profit.
- Beside energy markets, IPs can take part in the PCR market with weekly resolution. Taking part in this market reserves a portion of the BSS power and energy capacity.
- Peak power charges of an IP are based on maximum 15-minute-average load throughout the year.
- Due to their relatively low capacity, IPs are price takers in all markets.
- Sources of uncertainty in the model are day-ahead market prices, PCR prices, PV output, IP load and intraday prices. The first four are defined by $\Omega^{\text{S}}$ scenarios per representative week at an appropriate resolution. Uncertainty of intraday prices is modeled using upper and lower price bounds, without considering the distribution of uncertainty.

### C. Base Formulation

#### 1) Objective Function:

$$\min_{\Psi} \sum_{w\in\Omega^{\text{W}}} \rho_w \cdot \left( \sum_{h=1}^{168} c^{\text{el}}_{h,w} - r^{\text{PCR}}_w \right) + c^{\text{peak}} + c^{\text{BSS}} + c^{\text{PV}} + \sum_{h=1}^{168}\sum_{q=1}^{4}\sum_{s\in\Omega^{\text{S}}} \pi_{w,s}\cdot u_{q,h,w,s}\cdot VoLL + \max_{b_{q,h,w,s}} \sum_{w\in\Omega^{\text{W}}} \rho_w \cdot \left( \sum_{h=1}^{168}\sum_{q=1}^{4}\sum_{s\in\Omega^{\text{S}}} \pi_{w,s}\cdot \Delta\lambda^{\text{ID}}_{q,h,w,s}\cdot\cdot e^{\text{ID}}_{q,h,w,s} \cdot b_{q,h,w,s} \right) \tag{1}$$

$$c^{\text{el}}_{h,w} = e^{\text{DA}}_{h,w}\cdot\left( C^{\text{fees}} + \sum_{s\in\Omega^{\text{S}}} \pi_{w,s}\cdot\lambda^{\text{DA}}_{h,w,s}\right) + \sum_{q=1}^{4}\sum_{s\in\Omega^{\text{S}}} \pi_{w,s}\cdot e^{\text{ID}}_{q,h,w,s}\cdot(\lambda^{\text{ID}}_{q,h,w,s} + C^{\text{fees}}), \quad \forall h,w \tag{2}$$

$$\sum_{h=1}^{168}\sum_{q=1}^{4} b_{q,h,w,s} \le \Gamma, \quad \forall w,s \tag{3}$$

$$0 \le b_{q,h,w,s} \le 1, \quad \forall q,h,w,s \tag{4}$$

$$r^{\text{PCR}}_w = p^{\text{PCR}}_w \cdot \sum_{s\in\Omega^{\text{S}}} \pi_{w,s}\cdot\lambda^{\text{PCR}}_{w,s}, \quad \forall w \tag{5}$$

$$c^{\text{peak}} = p^{\text{peak}}\cdot C^{\text{peak}} \tag{6}$$

$$p^{\text{peak}} \ge e^{\text{DA}}_{h,w} + e^{\text{ID}}_{q,h,w,s}\cdot 4, \quad \forall q,h,w,s \tag{7}$$

$$c^{\text{BSS}} = (soe^{\max}\cdot I^{\text{BSSe}} + p^{\text{BSS}}\cdot I^{\text{BSSp}})\cdot\frac{i\cdot(i+1)^{T^{\text{BSS}}}}{(1+i)^{T^{\text{BSS}}}-1} \tag{8}$$

$$c^{\text{PV}} = p^{\text{pv,cap}}\cdot I^{\text{pv}}\cdot\frac{i\cdot(i+1)^{T^{\text{pv}}}}{(1+i)^{T^{\text{pv}}}-1} \tag{9}$$

Objective function (1) minimizes the IP operating cost over the set of variables $\Psi = \{e^{\text{DA}}_{h,w},\ e^{\text{ID}}_{q,h,w,s},\ p^{\text{PCR}}_w,\ p^{\text{peak}},\ soe^{\max},\ p^{\text{BSS}},\ p^{\text{pv,cap}}\}$, consisting of the cost of purchased energy, $c^{\text{el}}_{h,w}$, weekly revenue from providing PCR, $r^{\text{PCR}}_w$, annual peak power payment, $c^{\text{peak}}$, and annuity payment for BSS and PV installations, $c^{\text{BSS}}$ and $c^{\text{PV}}$. Since we observe the IP's annual operating costs, parameter $\rho_w$ is introduced to represent the "weight" of each representative week, which is explained in more detail in Section III-B. Eq. (2) breaks down the energy costs into electricity trading in the day-ahead market, $e^{\text{DA}}_{h,w}\cdot\lambda^{\text{DA}}_{h,w,s}$, and the intraday market, $e^{\text{ID}}_{q,h,w,s}\cdot\lambda^{\text{ID}}_{q,h,w,s}$. An additional fee, $C^{\text{fees}}$, is imposed to aggregate the fees and taxes to be payed by any end consumer. Price uncertainty in the day-ahead market is considered using price scenarios $s$, each expanding to a specific range of intraday prices whose uncertainty is modeled using robust optimization. Since the intraday market does not have a unique price for each time period, there is an uncertain range limited by the minimum and maximum price, $[\lambda^{\text{ID}}_{q,h,w,s} - \Delta\lambda^{\text{ID}}_{q,h,w,s}, \lambda^{\text{ID}}_{q,h,w,s} + \Delta\lambda^{\text{ID}}_{q,h,w,s}]$. As a result, the third part of objective function (1) maximizes the damage suffered when purchasing energy in the intraday market. The damage is inflicted by reaching the maximum price in a specific time period, which is achieved by adding $\Delta\lambda^{\text{ID}}_{q,h,w,s}$ to the average intraday price, $\lambda^{\text{ID}}_{q,h,w,s}$. Relaxed binary variable $b_{q,h,w,s}$ defines in which time periods the prices take their maximum values. Constraints (3) and (4) define the behaviour of $b_{q,h,w,s}$. The number of periods in which the price can be altered to inflict the most damage to the objective function is controlled with parameter $\Gamma$. It can take values from the interval $[0,\ \Omega^{Q}\cdot\Omega^{H}]$ and presents the budget of uncertainty. For $\Gamma = 0$, the average prices in intraday market, $\lambda^{\text{ID}}_{q,h,w,s}$, are considered. As $\Gamma$ increases, the number of time periods affected by the price alteration increases as well and the model is protecting against those deviations. Consequently, when $\Gamma$ is maximum, i.e. equal to $\Omega^{Q}\cdot\Omega^{H}$, the maximum prices are considered as they cause the most damage to the objective function when the IP is purchasing energy. Since the objective function consists of two parts that need to be optimized in different directions (minimizing vs. maximizing), the robust

subproblem is modeled in its dual form, whose formulation and transformation are provided in Appendix A.

Eq. (5) defines weekly PCR revenue based on the weekly BSS power capacity reserved for PCR and scenario-based PCR price, $p_w^{\mathrm{PCR}} \cdot \lambda_{w,s}^{\mathrm{PCR}}$. Eq. (6) calculates the annual peak power payments, $p^{\mathrm{peak}} \cdot C^{\mathrm{peak}}$. Constraint (7) defines annual peak power as the maximum power purchased from the markets. Intraday energy is multiplied by 4 because of its 15-minute resolution. Finally, eqs. (8) and (9) define the annual cost of BSS and PV installations taking into account the value of money in the future and lifetime of the assets.

*2) Constraints:*

$$soe_w^{\mathrm{PCR}} = n \cdot p_w^{\mathrm{PCR}}, \quad \forall w \tag{10}$$

$$soe_w^{\mathrm{PCR}} \leq soe^{\max}, \quad \forall w \tag{11}$$

$$p_w^{\mathrm{PCR}} \leq p^{\mathrm{BSS}}, \quad \forall w \tag{12}$$

$$soe_{q,h,w,s} \leq soe^{\max} - soe_w^{\mathrm{PCR}}, \quad \forall q,h,w,s \tag{13}$$

$$p_{q,h,w,s}^{\mathrm{ch}} \leq p^{\mathrm{BSS}} - p_w^{\mathrm{PCR}}, \quad \forall q,h,w,s \tag{14}$$

$$p_{q,h,w,s}^{\mathrm{dis}} \leq p^{\mathrm{BSS}} - p_w^{\mathrm{PCR}}, \quad \forall q,h,w,s \tag{15}$$

$$\sum_{h=1+24\cdot(\vartheta-1)}^{24+24\cdot(\vartheta-1)} \sum_{q=1}^{4} e_{q,h,w,s}^{\mathrm{PCR}} \geq k_\vartheta \cdot soe_w^{\mathrm{PCR}}, \quad \forall w,s,\vartheta \in [1,7] \tag{16}$$

$$soe_{q,h,w,s} + soe_w^{\mathrm{PCR}} = \sum_{j=1}^{N^j-1} soe_{q,h,w,s,j}, \quad \forall q,h,w,s \tag{17}$$

$$soe_{q,h,w,s,j} \leq (R_{j+1} - R_j) \cdot soe^{\max}, \quad \forall q,h,w,s,j \tag{18}$$

$$\Delta soe_{q,h,w,s} = F_1 \cdot soe^{\max} + \sum_{j=1}^{N^j-1} \frac{F_{j+1}-F_j}{R_{j+1}-R_j} \cdot soe_{q-1,h,w,s,j}, \quad \forall q,h,w,s \setminus q_1 \tag{19}$$

$$\Delta soe_{q_1,h,w,s} = F_1 \cdot soe^{\max} + \sum_{j=1}^{J-1} \frac{F_{j+1}-F_j}{R_{j+1}-R_j} \cdot soe_{q_4,h-1,w,s,j}, \quad \forall h,w,s \setminus h_1 \tag{20}$$

$$p_{q,h,w,s}^{\mathrm{ch}} \leq \frac{\Delta soe_{q,h,w,s}}{\eta^{\mathrm{ch}}} \cdot 4, \quad \forall q,h,w,s \tag{21}$$

$$soe_{q,h,w,s} = soe_{q-1,h,w,s} + p_{q,h,w,s}^{\mathrm{ch}} \cdot \eta^{\mathrm{ch}} - p_{q,h,w,s}^{\mathrm{dis}} \cdot \frac{1}{\eta^{\mathrm{dis}}}, \quad \forall q,h,w,s \setminus q_1 \tag{22}$$

$$soe_{q_1,h,w,s} = soe_{q_4,h-1,w,s} + p_{q_1,h,w,s}^{\mathrm{ch}} \cdot \eta^{\mathrm{ch}} - p_{q_1,h,w,s}^{\mathrm{dis}} \cdot \frac{1}{\eta^{\mathrm{dis}}}, \quad \forall h,w,s \tag{23}$$

$$\sum_{s=1}^{4} soe_{q_4,h_{168},w,s} \cdot \pi_{w,s} \geq soe_0, \quad \forall w,s \tag{24}$$

$$p_{q,h,w,s}^{\mathrm{ch}} \leq x_{q,h,w,s} \cdot M, \quad \forall q,h,w,s \tag{25}$$

$$p_{q,h,w,s}^{\mathrm{dis}} \leq (1 - x_{q,h,w,s}) \cdot M, \quad \forall q,h,w,s \tag{26}$$

$$e_{h,w}^{\mathrm{DA}} \cdot 1 + e_{q,h,w,s}^{\mathrm{ID}} \cdot 4 = p_{q,h,w,s}^{\mathrm{ch}} + d_{q,h,w,s} - p_{q,h,w,s}^{\mathrm{dis}} - p_{h,w,s}^{\mathrm{pv}} - e_{q,h,w,s}^{\mathrm{PCR}} \cdot 4, \quad \forall q,h,w,s \tag{27}$$

$$d_{q,h,w,s} + u_{q,h,w,s} = D_{q,h,w,s}, \forall q,h,w,s \tag{28}$$

$$p_{h,w,s}^{\mathrm{pv}} \leq k_{h,w,s}^{\mathrm{s}} \cdot p^{\mathrm{pv,cap}} \quad \forall h,w,s \tag{29}$$

Eq. (10) relates battery energy capacity reserved for providing PCR and weekly amounts of PCR provided to the system operator using factor $n$. Constraints (11) and (12) restrict the battery energy and power capacity occupied for PCR, while (13)–(15) define the remaining BSS energy, charging and discharging capacities for other purposes.

When performing PCR, the BSS performs shallow charging/discharging cycles. Due to inefficiencies, it needs to be charged to sustain such operation and does not slowly deplete the accumulated energy (symmetrical provision is assumed). Therefore, a portion of the state of energy devoted to PCR, $k_\vartheta$, needs to be charged on a daily basis, as defined in eq. (16).

Constraints (17)–(21) describe the accurate battery charging model where the battery charging power reduces with its state of energy. Eq. (17) divides the used state of energy range at all time periods into $N^j - 1$ segments. Each segment's energy capacity is determined in (18), which is used in (19) and (20) to derive the maximum energy charging ability of the battery at each time period. The maximum energy charging ability is translated into the power charging limit in constraint (21). A more detailed explanation of this accurate battery charging model can be found in [15].

Eq. (22) calculates the battery state of energy in 15-minute intervals, considering the charging and discharging efficiencies, while eq. (23) calculates the state of energy on the transition between the hours considering the last 15-minute period of the previous hour. Constraint (24) is the state of energy level preservation constraint, while constraints (25) and (26) disable simultaneous charging and discharging of the battery that would otherwise occur at negative market prices.

Eq. (27) is a power balance constraint on a 15-minute basis, where the local demand, battery charging and discharging power, power purchased to support the PCR provision, and PV output power are balanced with the power purchased in the day-ahead and intraday markets. Variables $e_{h,w}^{\mathrm{DA}}$ and $e_{q,h,w,s}^{\mathrm{ID}}$ represent energy, not power, so they are multiplied with a corresponding time constant, i.e. variable $e_{h,w}^{\mathrm{DA}}$ is multiplied by 1 and variable $e_{q,h,w,s}^{\mathrm{ID}}$ is multiplied by 4. To enable demand flexibility, not all demand needs to be satisfied at all time periods. The unserved demand $u_{q,h,w,s}$ is penalized at price $VoLL$, which is added to the objective function. Constraint (28) ensures that the sum of the served and unserved energy is equal to the expected demand. Finally, constraint (29) limits the PV generation to the available power.

### *D. Formulation Extensions for Different Market Settings*

Model (1)–(29) defined above is valid under the assumptions from Section II-A. However, different countries may have

different market rules and resolution of services and products. The required changes to formulation (1)–(29) in case of different market rules are described below.

*1) Peak Power Charges:* Peak power charges are not necessarily on an annual basis. For example, in Croatia consumers above 20 kW are charged peak power prices on a monthly basis [16]. Since model (1)–(29) is based on representative weeks, it is necessary to keep track of which representative weeks constitute each month of the year. After that, the peak power for each month is calculated as the highest power over all representative weeks appearing in a specific month. Constraint (7) is thus replaced by the following one:

$$p_m^{\text{peak}} \geq e_{h,w}^{\text{DA}} + e_{h,w,s}^{\text{ID}}, \quad \forall h, w, m; w \in m \tag{30}$$

On the other hand, if there are no peak power charges, constraints (6) and (7) and variable $c^{\text{peak}}$ from (1) need to be removed.

*2) Intraday Market Resolution:* In case of intraday market operation on an hourly basis, eq. (27) is replaced by eq. (31), while the summation of the intraday cost over all quarters in eq. (2) is eliminated.

$$e_{h,w}^{\text{DA}} + e_{h,w,s}^{\text{ID}} = 0.25 \cdot \sum_{q=1}^{4} (p_{q,h,w,s}^{\text{ch}} + d_{q,h,w,s} - p_{q,h,w,s}^{\text{dis}}) - k_{h,w,s}^{\text{s}} \cdot p^{\text{pv,cap}} - e_{h,w,s}^{\text{PCR}}, \quad \forall h, w, s \tag{31}$$

As opposed to eq. (27), which balances power on a 15-minute resolution, eq. (31) balances power on a 1-hour resolution. For this reason, $e_{h,w,s}^{\text{ID}}$ on the left-hand side is no longer multiplied by 4 and the 15-minute power values on the right-hand side, i.e. $p_{q,h,w,s}^{\text{ch}}$, $d_{q,h,w,s}$ and $p_{q,h,w,s}^{\text{dis}}$, are averaged over one hour.

*3) PCR Market Resolution:* PCR capacity can be decided on a higher resolution than a week. For example, if PCR bids are at a 4-hour resolution, as in Denmark [17], the variables in eq. (5) need to be expanded to hourly dimension and eqs. (32), (33) and (34) need to be added to the model.

$$soe_{h,w}^{\text{PCR}} = soe_{h+l,w}^{\text{PCR}}, \quad \forall h, w, l; \text{ if}(h\%4 = 1 \wedge l \in \{1, 2, 3\}) \tag{32}$$

$$p_{h,w}^{\text{PCR}} = p_{h+l,w}^{\text{PCR}}, \quad \forall h, w, l; \text{ if } (h\%4 = 1 \wedge l \in \{1, 2, 3\}) \tag{33}$$

$$\sum_{h=1+24\cdot(\vartheta-1)}^{24+24\cdot(\vartheta-1)} e_{h,w,s}^{\text{PCR}} \geq k_\vartheta \cdot \sum_{h'=1}^{168} soe_{h,'w}^{PCR}, \quad \forall w, s, \vartheta \in [1, 7], \text{ if } (h'\%4 = 1) \tag{34}$$

If no PCR market is available in a country, variables $r_w^{\text{PCR}}$, $p_w^{\text{PCR}}$ and $soe_w^{\text{PCR}}$ are eliminated from the objective function (1) and constraints (14), (15) and (17), and constraints (10)–(12) are completely eliminated.

TABLE I
KEY SETTINGS AND CONSTRAINTS FOR THE THREE COUNTRIES

| | Germany | Denmark | Croatia |
|---|---|---|---|
| ID market | quarterly | hourly | hourly |
| PCR market | weekly | 4 hour blocks | – |
| Peak power | yearly | – | monthly |
| $C^{\text{peak}}$, €/kW | 44.5 | – | 5.07 |
| $C^{\text{fees}}$, €/kWh | 0.15 | 0.08 | 0.06 |
| $\Gamma^{\max}$ | 672 | 168 | 168 |
| PV full load hours, [kWh/kW] | 1092 | 1079 | 1293 |
| Constraints | (1)–(29) | (1)–(5), (8)–(15), (17)–(26), (28)–(29), (31)–(34) | (1)–(4), (6), (8), (9), (13)–(15), (17)–(26), (29)–(31) |

## III. CASE STUDY

### A. Description

The case study is performed for three European countries, Germany, Denmark and Croatia. These countries differ in the organization of the intraday market, PCR market, peak power payments for the consumers, market prices, energy delivery fees, as well as the number of annual full load hours (PV production). An overview of specific rules and prices for each country is presented in Table I. Germany generally has the highest energy costs for end consumers, foremost due to high energy delivery fees, 0.15 €/kWh [18], [19]. Annual peak power price used in this paper is calculated as a mean price of all German distribution grid operators. Energy delivery fees for industrial consumers are much lower in Denmark [20] and the lowest in Croatia [21]. Peak power prices are the highest in Croatia, where they are paid on a monthly basis, while in Germany the peak power payments are annual. In both countries they are based on the highest average consumed power over all 15-minute periods. On the other hand, in Denmark there are no peak power charges.

Energy market prices are taken from the local wholesale markets. Day-ahead markets operate in the same way in all three countries. However, the intraday market in Germany is on a 15-minute basis (hence $\Gamma^{\max}$ in Table I is 672), while in Denmark and Croatia it is operated on an hourly basis resulting in 168 bidding periods in a week. PCR market rules for Germany are based on the German market rules from [22],[2] which is based on weekly tenders [23]. On the other hand, PCR market resolution in Denmark DK1 zone is four hours [24], while in Croatia the PCR provision is mandatory for hydro power plants with capacity over 10 MW and thermal power plants with capacity over 30 MW without remuneration [25]. The energy-to-power ratio for BSS when providing PCR is $n = 2$, which should allow the BSS to enter the PCR provision service with SOE in between the 25% and 75% [26] and preserve the low battery cycling rate [27]. Due to their specifics, Table I contains a list of constraints used in the problem formulation for all three countries. It also shows the amount of PV generation in each country based on data obtained from [28]. Croatia, as

[2]Since July 2019, the German PCR market moved from weekly to daily resolution [23] However, due to insufficient historical data, our model is based on the weekly tendering.

the south-most country, provides the most full load hours, while Denmark is the least generous in PV production.

Battery and PV prices are the same for all three countries. The lifetime of the batteries and the PV panels is estimated at 15 and 20 years, respectively. Battery investment is $I^{\mathrm{BSSp}} =$ 400 €/kW and $I^{\mathrm{BSSe}} =$ 400 €/kWh [29]. Both charging and discharging efficiencies are set to 93%. The battery starts each week at 50% of its energy capacity, which needs to be fulfilled at the end of the week. This choice is primarily related to the PCR requirements. As indicated in [26], the centerfold value of state of energy maximizes the PCR provision. Since the model assumes high energy-to-power ratio of 2, and considering the current European regulation that dictates full PCR activation only after the frequency deviation has reached 200 mHz [30], the expected degradation due to cycling when providing PCR should be quite low [27]. Thus, no additional BSS degradation penalty is assigned to PCR provision. However, we acknowledge that the battery cycling occurs when providing PCR and assign PCR energy losses to $k = 10.32\%$ based on frequency deviation data analysis obtained from the Croatian Transmission System Operator and rules on PCR activation in Europe [30]. The PV investment is 1750 €/kW [31] and interest rate is set to 3%.

The case study considers IPs [32] looking to invest in PV and BSS to reduce their operating costs. One of the goals of the study is to compare the benefits of aggregating the IPs, which is performed by running the optimization model for each of the 20 IPs individually and comparing their summed investments and overall operating costs to a setting where all IPs act as a single entity, both as investors and market participants, virtually forming a balancing group of their own.

Using robust optimization to model the intraday market prices enables us to observe how the factor $\Gamma$ impacts the overall expected cost, as well as the amount of energy purchased in the intraday versus the day-ahead market.

### *B. Input Data Preparation*

The presented planning model is subject to uncertainty of input parameters, which include load, day-ahead prices, intraday prices, PCR prices and PV generation. The available data for 52 weeks during year 2016 were clustered into five representative ones to reduce the complexity of the model as shown in Fig. 2. Each week has its corresponding weight that denotes how many times it appears in a year. This technique is commonly used in investment studies, e.g. [33], however, instead of using a well-adopted time span of characteristic days, we expand it to a week for two reasons. First, the PCR market in Germany is organized on a weekly basis and, furthermore, peak power payments in Croatia are on a monthly basis. Therefore, representative weeks can be considered as a golden middle between the day-ahead market, weekly PCR market and monthly peak power payments. Second, the purpose of this setting is to assess the market interaction throughout each representative week, considering the related uncertainties, in order to derive the optimal investment plan. This setting is not applicable to the operation models, where the day-ahead bidding is performed for each day individually, considering the historic data (including

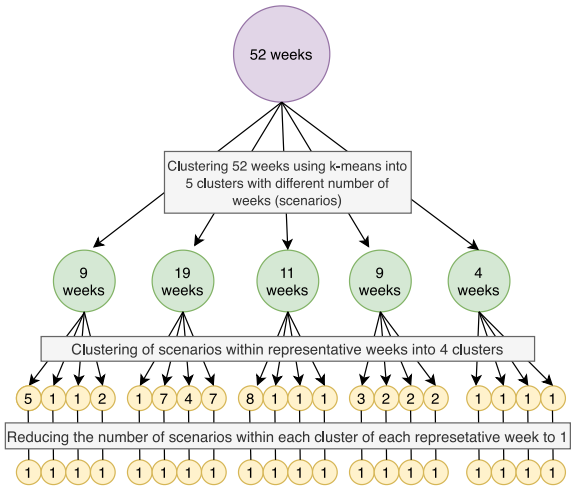


Fig. 2. Preparation of input data using k-means clustering.

the previous day), the most recent load forecast and the most recent PV output forecast. However, we do not develop an operating model of the industrial facilities, we merely replicate its operation in order to derive the optimal investment in battery and PV. In other words, the entire day-by-day bidding process is replaced by a weekly scenario. The clusterization was conducted using the k-means method that groups the most similar data from a dataset [34]. It was performed measuring the similarities in the load, the PV production, the day-ahead prices and the PCR prices data between the weeks (listed data were concatenated in order to obtain a single data series and to consider correlation between them). After clustering the data into five clusters (representative weeks), the clusters contained a different number of members, as shown in Fig. 2 (green circles). The cluster members represent scenarios in each representative week and, in reality, those are the weeks of the year that are the most similar in terms of the load, the PV production, the day-ahead prices and the PCR prices. In order to reduce the complexity of the model by reducing the number of weeks (that represent scenarios), each representative week was clustered once again using the k-means algorithm (second step in Fig. 2, first row of yellow circles) into 4 clusters. That number was chosen as a minimum number of scenarios over all representative weeks (green circles). To obtain only one representative of the four clusters in each representative week, the scenario with the lowest distance from the mean of a specific cluster was chosen (or the mean in the case of two scenarios), which is shown as the final step in Fig. 2. The procedure resulted in five representative weeks, each containing four scenarios. A uniform distribution of weeks is assumed to calculate probabilities of each representative week and scenario. For example, in the second representative week (representing 19 actual weeks): $\pi_{w=2,s=1} = 1/19$, $\pi_{w=2,s=2} = 7/19$, $\pi_{w=2,s=3} = 4/19$, $\pi_{w=2,s=4} = 7/19$, while this representative week occurs 19 times per year. For the three analyzed countries, the calculation was performed for each IP individually (I) and for all of them aggregated and acting as a single subject (A). Furthermore, we compare two cases: Business as Usual (BaU), where no investments are made, and Flexible Investment (FlexI),

TABLE II
ANNUAL COST PER OBJECTIVE FUNCTION SEGMENT FOR ALL THREE COUNTRIES FOR BUSINESS-AS-USUAL (BAU) AND FLEXIBLE INVESTMENT (FLEXI) CASES (I: INDIVIDUAL IPS, A: AGGREGATED IPS)

| | Business-as-Usual (in 1000 €) | | | | | Flexible Investment (in 1000 €) | | | | | | | |
|---|---|---|---|---|---|---|---|---|---|---|---|---|---|
| GERMANY | Energy DA | Energy ID | Fees | Peak power | Overall cost | Energy DA | Energy ID | Fees | Peak power | BSS cost | PCR revenue | PV cost | Overall cost |
| $\Gamma = 0$ (I) | 1,347 | 2,416 | 13,592 | 1,004 | 18,361 | 1,199 (-11.0%) | 2,198 (-9.0%) | 12,570 (-7.5%) | 946 (-5.8%) | 199 | 89 | 756 | 17,781 (-3.2%) |
| $\Gamma = 0$ (A) | 1,541 | 2,187 | 13,592 | 836 | 18,158 | 1,315 (-14.7%) | 1,890 (-13.6%) | 12,158 (-10.6%) | 720 (-13.9%) | 620 | 348 | 1,074 | 17,433 (-4.0%) |
| $\Gamma = 10$ (I) | 1,467 | 2,468 | 13,592 | 1,004 | 18,531 | 1,314 (-10.4%) | 2,263 (-8.3%) | 12,557 (-7.6%) | 943 (-6.1%) | 212 | 93 | 762 | 17,960 (-3.1%) |
| $\Gamma = 10$ (A) | 1,667 | 2,202 | 13,592 | 836 | 18,299 | 1,438 (-13.7%) | 1,938 (-12.0%) | 12,192 (-10.3%) | 725 (-13.3%) | 549 | 309 | 1,042 | 17,576 (-4.0%) |
| $\Gamma = 100$ (I) | 2,476 | 1,877 | 13,592 | 1,004 | 18,950 | 2,215 (-10.5%) | 1,741 (-7.2%) | 12,543 (-7.7%) | 940 (-6.4%) | 245 | 108 | 775 | 18,353 (-3.2%) |
| $\Gamma = 100$ (A) | 2,805 | 1,402 | 13,592 | 836 | 18,638 | 2,431 (-13.3%) | 1,233 (-12.1%) | 12,147 (-10.6%) | 720 (-13.9%) | 630 | 357 | 1,077 | 17,883 (-4.1%) |
| $\Gamma = 672$ (I) | 2,877 | 1,783 | 13,592 | 1,004 | 19,257 | 2,695 (-6.3%) | 1,474 (-17.3%) | 12,501 (-8.0%) | 936 (-6.8%) | 346 | 154 | 813 | 18,613 (-3.3%) |
| $\Gamma = 672$ (A) | 3,301 | 1,135 | 13,592 | 836 | 18,866 | 2,992 (-9.4%) | 847 (-25.4%) | 12,144 (-10.7%) | 719 (-14.0%) | 640 | 360 | 1,082 | 18,066 (-4.2%) |
| DENMARK | | | | | | | | | | | | | |
| $\Gamma = 0$ (I) | 694 | 2,870 | 7,249 | - | 10,814 | 611 (-12.0%) | 2,672 (-6.9%) | 6,752 (-6.9%) | - | 197 | 250 | 747 | 10,731 (-0.8%) |
| $\Gamma = 0$ (A) | 777 | 2,782 | 7,249 | - | 10,809 | 663 (-14.7%) | 2,474 (-11.1%) | 6,534 (-9.9%) | - | 434 | 551 | 1,130 | 10,685 (-1.1%) |
| $\Gamma = 10$ (I) | 807 | 2,831 | 7,249 | - | 10,888 | 718 (-11.0%) | 2,635 (-6.9%) | 6,751 (-6.9%) | - | 196 | 248 | 748 | 10,802 (-0.8%) |
| $\Gamma = 10$ (A) | 890 | 2,735 | 7,249 | - | 10,874 | 779 (-12.5%) | 2,416 (-11.7%) | 6,530 (-9.9%) | - | 420 | 533 | 1,130 | 10,745 (-1.2%) |
| $\Gamma = 100$ (I) | 1,634 | 2,124 | 7,249 | - | 11,008 | 1,431 (-12.4%) | 2,035 (-4.2%) | 6,750 (-6.9%) | - | 199 | 252 | 750 | 10,916 (-0.8%) |
| $\Gamma = 100$ (A) | 1,820 | 1,924 | 7,249 | - | 10,993 | 1,537 (-15.5%) | 1,768 (-8.1%) | 6,530 (-9.9%) | - | 420 | 532 | 1,130 | 10,854 (-1.3%) |
| $\Gamma = 168$ (I) | 1,678 | 2,081 | 7,249 | - | 11,009 | 1,429 (-14.8%) | 1,967 (-5.5%) | 6,706 (-7.5%) | - | 614 | 776 | 960 | 10,901 (-1.0%) |
| $\Gamma = 168$ (A) | 1,862 | 1,883 | 7,249 | - | 10,995 | 1,589 (-14.7%) | 1,719 (-8.7%) | 6,530 (-9.9%) | - | 420 | 532 | 1,130 | 10,857 (-1.3%) |
| CROATIA | | | | | | | | | | | | | |
| $\Gamma = 0$ (I) | 1,295 | 3,182 | 5,437 | 1,301 | 11,216 | 1,149 (-11.3%) | 2,975 (-6.5%) | 5,036 (-7.4%) | 1,275 (-2.0%) | - | - | 607 | 11,054 (-1.4%) |
| $\Gamma = 0$ (A) | 1,427 | 3,041 | 5,437 | 1,106 | 11,013 | 1,282 (-10.2%) | 2,800 (-7.9%) | 4,987 (-8.3%) | 1,025 (-7.3%) | - | - | 680 | 10,777 (-2.1%) |
| $\Gamma \geq 10$ (I) | 1,310 | 3,170 | 5,437 | 1,301 | 11,219 | 1,161 (-11.4%) | 2,975 (-6.2%) | 5,036 (-7.4%) | 1,275 (-2.0%) | - | - | 607 | 11,057 (-1.4%) |
| $\Gamma \geq 10$ (A) | 1,444 | 3,027 | 5,437 | 1,106 | 11,015 | 1,296 (-10.2%) | 2,789 (-7.9%) | 4,987 (-8.3%) | 1,025 (-7.3%) | - | - | 680 | 10,779 (-2.1%) |

where investments in the flexible assets (PV and BSS) are available. The models are run for various values of $\Gamma$ to assess the effects of the intraday trading uncertainty on the objective function.

### C. Results

*1) Germany:* The first case study was run using the German market rules. Table II shows the results. For $\Gamma = 0$ in the BaU case, the sum of individual IPs' electricity costs is € 18,361, which is 1.1% higher than € 18,158 (the overall electricity cost when the IPs act as a single entity). Over 70% of these costs are various fees, while energy purchases and peak power costs are much lower. In the FlexI case with individual IPs, the traded quantities are significantly reduced, by 11.0% in the day-ahead market and 9.0% in the intraday market for $\Gamma = 0$, and fees and peak power costs are reduced by 7.5% and 5.8%, respectively. All the reductions are a direct consequence of the BSS and PV investments, where the PV investment directly reduces the purchased energy quantities and, consequently, fees and peak power charges. The BSS, on top of its role in peak shaving and energy purchases during the high-price periods, accumulates revenue from the PCR market. The PCR market revenue makes up for roughly half of the BSS annual investment cost. As the intraday market trading becomes less favorable for higher values of $\Gamma$, the traded energy moves to the day-ahead market. In case of individual investments (I), the BSS investments increase with $\Gamma$ to counteract the unfavorable intraday prices, while the PV installations only slightly increase. On the other hand, when acting as an aggregation (A), the BSS and PV investment costs do not significantly change with $\Gamma$ due to the possibility of internal redispatch among the IPs. This means the aggregation provides the IPs additional protection against uncertainty.

TABLE III
BSS AND PV INVESTMENTS AS WELL AS ANNUAL PEAK POWER BEFORE AND AFTER THE INVESTMENTS FOR GERMANY

| | $soe^{\max}$ [kWh] | $p^{\mathrm{BSS}}$ [kW] | $p^{\mathrm{pv,cap}}$ [kW] | $p^{\mathrm{peak}}$, BaU [kW] | $p^{\mathrm{peak}}$, FlexI [kW] |
|---|---|---|---|---|---|
| $\Gamma = 0$ (I) | 4,025 | 1,918 | 6,433 | 22,562 | 21,261 |
| $\Gamma = 0$ (A) | 13,555 | 4,965 | 9,136 | 18,806 | 16,201 |
| $\Gamma = 10$ (I) | 4,271 | 2,081 | 6,483 | 22,562 | 21,204 |
| $\Gamma = 10$ (A) | 12,039 | 4,348 | 8,864 | 18,806 | 16,300 |
| $\Gamma = 100$ (I) | 4,953 | 2,382 | 6,593 | 22,562 | 21,133 |
| $\Gamma = 100$ (A) | 13,908 | 4,916 | 9,164 | 18,806 | 16,180 |
| $\Gamma = 672$ (I) | 6,967 | 3,371 | 6,919 | 22,562 | 21,040 |
| $\Gamma = 672$ (A) | 14,024 | 5,083 | 9,207 | 18,806 | 16,171 |

Another insight in the results is provided in Table III, which shows the installed BSS and PV capacity as well as peak power in the BaU and FlexI cases for Germany. The installed BSS and PV capacities increase for higher values of $\Gamma$ when considering IPs as individual investors (I). The increasing self-consumption is directly related to higher expected intraday costs. On the other hand, when IPs act jointly (A), the installed BSS and PV capacities are constant regardless of the $\Gamma$ (however, a drop is observed for $\Gamma = 10$). This is because the flexibility arises

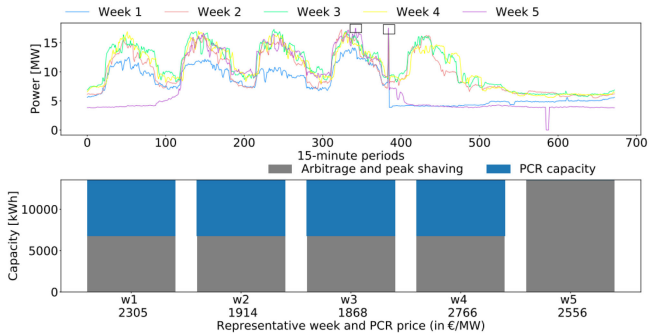


Fig. 3. Expected load profile for representative weeks (upper graph) and battery capacity reserved for arbitrage and peak shaving and PCR services in Germany for $\Gamma = 0$ (lower graph) for the aggregated case.

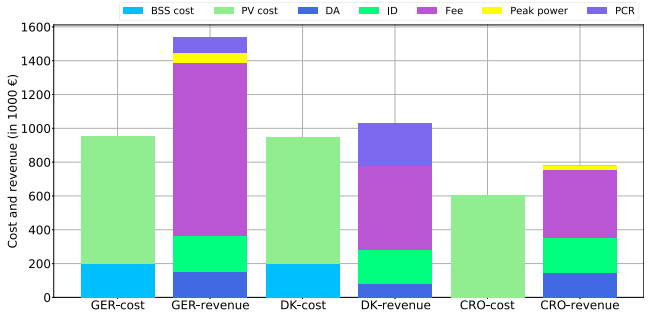


Fig. 4. Comparison of investment and revenue for the three countries for $\Gamma = 0$ (I).

from the heterogeneous IP load curves, which enable a steady self-consumption level. The drop in installed capacities for $\Gamma = 10$ occurs because the model finds it difficult to use BSS and PV to counteract such sporadic but time-period-wise uncertain increase in intraday prices. Instead of fighting uncertainty, it relies on reduced investment costs. The reduction through peak shaving is much higher for the aggregated IPs than individual ones. When acting as a group, the IPs manage to reduce the peak power by over 13%, while when acting individually this reduction is only 5.8–6.8%.

Fig. 3 shows the BSS capacity used for PCR for aggregated IPs' investments in all representative weeks for $\Gamma = 0$. Weeks 1–4 are attractive to provide PCR service. The BSS energy capacity devoted to PCR is at most 50% due to the selected energy-to-power factor $n = 2$. However, week 5 has higher expected PCR price than most of the weeks, but the battery is used only for the optimized self-consumption. This is because week 5 has the highest expected load (upper graph in Fig. 3) and BSS is thus used for peak shaving.

*2) Denmark:* Similar to Germany, in Denmark around 70% of expenses are dedicated to fees (€ 7,249 in all BaU cases, both (I) and (A)). The remaining costs are divided among the day-ahead and intraday energy markets as there are no peak-load payments. As $\Gamma$ increases, again the energy purchases move from the intraday to the day-ahead market. The FlexI case results in the BSS and PV investments of the same order of magnitude as in Germany. The BSS investment is entirely retrieved in the PCR market (PCR revenue is higher than the BSS cost), while the optimized self-consumption merely brings an added value. This indicates that the PCR prices in Denmark DK1 zone are highly favorable for the assumed battery costs. However, the required level of PCR in Denmark DK1 area in 2020 is only $\pm 21$ MW [35], thus such overinvestment in BSS capacity would greatly reduce the market prices rendering the investment infeasible. A much deeper analysis is required to understand if such high prices were a result of a large player exercising market power or not. On the other hand, BSSs' impact on the day-ahead and intraday energy quantities and fees is negligible.

*3) Croatia:* Results of the Croatian case study are shown in the last section of Table II. In the BaU case, all the fees are € 5,437, which is less than 50% of overall electricity cost. The model does not invest in BSS as there is no PCR market to spur the investment on top of optimized self-consumption and peak shaving. On the other hand, favorable PV production makes this investment attractive. Individual IPs invest in 5161 kW of PV at € 607 regardless of $\Gamma$, while the aggregated IPs install even more PV, 5787 kW at € 680, also regardless of $\Gamma$. The peak power cost is reduced by 2.0% for (I) and by 7.3% for (A), regardless of $\Gamma$. The overall cost reduction is 1.4% for the individual IPs and 2.1% for aggregated IPs.

### D. Discussion

The results in all three countries show that, with the employed assumptions, BSS, PV or a combination of both can reduce overall electricity costs for IPs, see Fig. 4. Generally, the highest cost reductions are achieved for Germany, due to high electricity fees for end consumers and an operational PCR market. In Denmark in absence of peak power charges and low solar production, BSSs are primarily installed to provide PCR. In contrast, Croatia does not have a PCR market, so BSS investments will probably not be profitable there until the PCR market is introduced. Thus, the IPs only invest in PV to profit from the high solar production. This indicates that developed PCR markets make the BSS investment attractive. Nonetheless, the PCR markets are quite small in terms of the power quantities and overinvestment in PCR-providing assets could drastically reduce the price, which is deemed to occur in Denmark and Germany.

In general and as expected, the aggregation of industrial loads leads to higher relative cost savings, due to a smoothing of the profile and economies of scale.

In Germany and Denmark the bidding behavior in the intraday market influences the investment decision. Higher values for $\Gamma$ lead to lower profits in the intraday market, thus higher cost of recourse for the investment and initial market decisions. The model answers the higher cost with an increased BSS and PV investment. This results in a higher self-consumption rate and, consequently, a higher security of supply of fix-priced solar electricity.

Nonetheless, with this study we compare national energy markets. To investigate the profitability of the proposed systems in more detail, one needs to take regional and even local market conditions into account. For example in Germany, local peak power charges vary from 17.22 €/kW [36] to 189.77 €/kW [37]. Additionally, PV output highly depends on the local climate.

TABLE IV
OBJECTIVE FUNCTION VALUE AND COMPUTATIONAL TIME FOR GERMANY (A)

| | | Cost (in € 1000) | Time (s) | Difference from base case (w5s4)(%) |
|---|---|---|---|---|
| Γ = 0 | **w5s4** | **17,433** | **31.4** | - |
| | w5s3 | 17,521 | 21.2 | 0.50 |
| | w5s2 | 17,497 | 139.7 | 0.36 |
| | w4s4 | 17,471 | 11.9 | 0.22 |
| | w3s4 | 16,934 | 0.36 | -2.86 |
| Γ = 10 | **w5s4** | **17,577** | **57.7** | - |
| | w5s3 | 17,648 | 32.4 | 0.41 |
| | w5s2 | 17,618 | 106.9 | 0.24 |
| | w4s4 | 17,627 | 14.9 | 0.29 |
| | w3s4 | 17,093 | 0.6 | -2.75 |
| Γ = 100 | **w5s4** | **17,884** | **298.3** | - |
| | w5s3 | 17,917 | 509.2 | 0.19 |
| | w5s2 | 18,041 | 272.2 | 0.88 |
| | w4s4 | 17,953 | 38.2 | 0.39 |
| | w3s4 | 17,464 | 0.6 | -2.35 |
| Γ = 672 | **w5s4** | **18,066** | **671.3** | - |
| | w5s3 | 18,060 | 2079.2 | -0.03 |
| | w5s2 | 18,943 | 259.1 | 4.85 |
| | w4s4 | 18,215 | 413.8 | 0.82 |
| | w3s4 | 17,942 | 0.5 | -0.69 |

The overall situation is likely to change in the near future as the cost of stationary BSS continues to decline. The regulatory frameworks are also likely to change, as flexibility becomes more incentivized for industrial consumers [12]. Finally, the development of electricity prices, grid charges and fees play an important role. Drivers exist in both directions; for example in Germany the levies and fees for RES should reduce in the coming years, but the carbon-related fees should increase. On a European level, there should be increased harmonization and integration of electricity markets, which will probably also alleviate some of the differences in profitability between the three settings analyzed here.

## IV. SOLUTION VERIFICATION

In this section we perform two studies to verify the quality of the obtained solutions. The first one is a sensitivity analysis on the number of representative days and scenarios used in the case studies, while the second one is an out-of-sample analysis of the obtained solutions. Both are conducted for the Germany case study and the aggregated market participation of the IPs.

### A. Sensitivity Analysis on the Number of Representative Days and Scenarios

In order to analyze the sufficiency of the number of representative days and scenarios for each representative day, we performed an appropriate sensitivity analysis on the overall cost and computational time for the German case study, whose results are available in Table IV. The aim of this analysis is to assess if the number of representative days and scenarios is sufficient to accurately capture the characteristics of the entire year. The analysis is performed for four different values of Γ, ranging from zero to 672. When only three representative weeks are used, but still preserving four scenarios per week (w3s4), the difference in the objective function value, i.e. the overall annual cost, toward the w5s4 case used throughout the study ranges from -2.86% for $\Gamma = 0$ to $-0.69\%$ for $\Gamma = 672$, which is a significant difference.

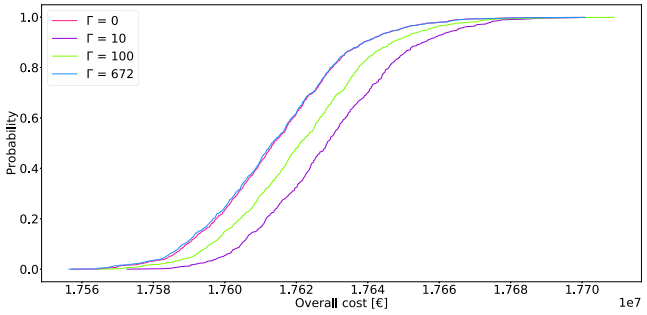


Fig. 5. CDF of the overall system cost for the German case (A) for $\Gamma = 0$, 10, 100 and 672.

Increasing the number of representative weeks to four shows much lower oscillations toward the w4s4 case as the difference in objective function values are at most 0.82% for $\Gamma = 672$. Thus the objective function value saturates when moving from four to five representative weeks (four scenarios in both cases).

Next we observe the objective function behavior for five representative weeks and variable number of scenarios. When the number of scenarios is only two (w5s2), the objective function value differs up to 4.85% as compared to the w5s4 case for $\Gamma = 672$. The maximum difference greatly reduces when the number of scenarios is increased to three (maximum difference is 0.5%), so we conclude that no significant loss on the solution quality is achieved for using four scenarios with five representative weeks.

Finally, we compare the computation times. Generally, it increases with the value of Γ and the number of representative weeks. On the other hand, the number of scenarios per representative weeks does not have a straightforward effect on the computational time.

### B. Out-of-Sample Analysis

To verify the quality of the obtained solutions, an out-of-sample analysis was conducted for Germany on 1000 different scenarios of the day-ahead prices, the intraday prices, the PCR prices, the load and the PV generation. Average intraday prices were considered to analyse the robustness of the solutions obtained using different Γ values. Instead of using representative weeks and corresponding weights, in this analysis we used all 52 unique weeks. First we calculated the mean and standard deviation for each uncertain dataset (e.g. day-ahead prices). Then, we sampled the error ($\varepsilon$) out of the normal distribution with calculated parameters ( $\varepsilon \sim \mathcal{N}(\mu, \sigma^2)$ ) and added it to the original dataset. This procedure resulted in 1000 scenarios of possible uncertainty realizations used in the Monte Carlo simulation.

Fig. 5 shows the cumulative probability distribution functions (CDF) of the expected operating cost as calculated using Monte Carlo simulations for $\Gamma = 0$, 10, 100 and 672. The best performance is achieved for Γ values 0 and 672. These CDFs both have a mean € 1,761 thousands, while the standard deviation is € 19,828 for $\Gamma = 0$ and € 20,177 for $\Gamma = 672$ (both slightly above 0.1%). The worst results are achieved for $\Gamma = 10$, which has mean value € 1,763 thousands with standard deviation €

19,986. All the CDFs have quite low standard deviation, which indicates that the solution is robust to the actual realization of uncertainty. Also, the extreme values of the uncertainty budget $\Gamma$ perform better than the ones in between, emphasizing the importance of its proper selection based on the prior bidding experience.

## V. Conclusion

This contribution presents a stochastic two-stage optimization model for IP participation in parallel revenue streams, namely day-ahead, intraday, PCR market participation as well as peak shaving and optimized self-consumption. The model is applied in a case study to three countries, Denmark, Germany and Croatia, allowing the implications of differences in market frameworks and climates to be evaluated.

The results show that investment in BSS and/or PV systems can lead to relatively small economic savings for the considered IPs, with equally small advantages through aggregated market participation. The presented case studies for each country indicate that the developed PCR markets make the BSS investment attractive at 400€/kW and 400€/kWh cost, while the absence of such markets (and low end-consumer fees) will deter the BSS investment. On the other hand, the PCR markets are quite small in terms of the power quantities and over-investment in PCR-providing assets could drastically reduce the price, which is deemed to occur in Denmark. BSS is a powerful ally for PV to increase the level of self-consumption. However, the cost of BSS needs to be further reduced to make the BSS-PV joint investment profitable under the current low electricity consumption fees. At this point, the high PV output in Croatia makes only the PV investment attractive. Generally, the highest cost reductions are achieved in Germany, due to high electricity fees for end consumers and operational PCR market.

This overall situation is expected to change in the near future, as both BSS costs and energy-political frameworks develop. On the one hand, industrial flexibility should benefit from additional incentives, on the other hand future electricity prices are highly uncertain.

## Appendix

Objective function (1) consists of two parts – the first two lines minimize the system's cost, while the third line maximizes the damage caused by the volatile intraday prices and acts as a robust subproblem with the following objective function:

$$\max_{b_{q,h,w,s}} \sum_{w\in\Omega^{\mathrm{W}}} \rho_w \cdot \left( \sum_{h=1}^{168} \sum_{q=1}^{4} \sum_{s\in\Omega^{\mathrm{S}}} \pi_{w,s} \cdot \Delta\lambda^{\mathrm{ID}}_{q,h,w,s} \cdot e^{\mathrm{ID}}_{q,h,w,s} \cdot b_{q,h,w,s} \right) \quad \text{(A-1)}$$

The robust subproblem takes average values of the intraday prices and has a possibility to add $\Delta\lambda^{\mathrm{ID}}_{q,h,w,s}$ value in order to deteriorate the objective function value. In equation (A-1), variable $b_{q,h,w,s}$ decides in which time periods the price is going to take its highest value to inflict the most damage to the objective function. $b_{q,h,w,s}$ is a relaxed binary variable and behaves under the following constraints:

$$\sum_{h=1}^{168} \sum_{q=1}^{4} b_{q,h,w,s} \le \Gamma, \quad \forall w, s \quad \text{(A-2)}$$

$$0 \le b_{q,h,w,s} \le 1, \quad \forall q, h, w, s \quad \text{(A-3)}$$

Thus, the relaxed binary variable can take value above 0 in any time period, but the sum of those values can be at most equal to $\Gamma$, which is a user-controlled parameter that represents the uncertainty budget.

Since the objective function consists of two parts that have different optimization directions (the first part aims at minimizing the objective value, while the second parts wants to maximize it), the robust subproblem (A-1)–(A-3) is converted to its dual form to change the direction of its objective function. Minimizing the dual will achieve the same optimal solution as when maximizing the primal and can then be directly integrated in objective function (1). Based on the rules for converting a primal problem to its dual form [38], the part of objective function that maximizes the inflicted damage is formulated as its dual subproblem minimizing over the set $\Upsilon = \{z_{w,s}, \omega_{q,h,w,s}, y_{q,h,w,s}\}$ as follows:

$$\min_{\Upsilon} \sum_{w\in\Omega^{\mathrm{W}}} \rho_w \cdot \left( \sum_{h=1}^{168} \sum_{q=1}^{4} \sum_{s\in\Omega^{\mathrm{S}}} \pi_{w,s} \cdot \omega_{q,h,w,s} + \sum_{s\in\Omega^{\mathrm{S}}} \pi_{w,s} \cdot z_{w,s} \cdot \Gamma \right) \quad \text{(A-4)}$$

$$z_{w,s} + \omega_{q,h,w,s} \ge \Delta\lambda^{\mathrm{ID}}_{q,h,w,s} \cdot e^{\mathrm{ID}}_{q,h,w,s}, \quad \forall q, h, w, s \quad \text{(A-5)}$$

Since each constraint of the primal problem has a corresponding dual variable, the robust subproblem has two dual variables. Variable $z_{w,s}$ represents the sensitivity of the model to changing the parameter $\Gamma$. This parameter can take values from 0 to the number of considered time periods and it represents the number of time periods in which the price may be altered from its average value to inflict damage to the objective function. The worst case is when $\Gamma$ takes the maximum value allowing the prices in all time periods to take their highest value.

In the primal problem there is variable $b_{q,h,w,s}$, which indicates if the price in specific time period was altered. Dual variable $\omega_{q,h,w,s}$ takes value greater than 0 when $b_{q,h,w,s}$ is greater than 0.

To conclude, both $z_{w,s}$ and $\omega_{q,h,w,s}$ represent sensitivity of the model to the number of intervals in which the price was altered to inflict the most damage to the objective function.

## References


[1] A. Masoumzadeh, E. Nekouei, and T. Alpcan, "Wind versus storage allocation for price management in wholesale electricity markets," *IEEE Trans. Sust. Energy*, vol. 11, no. 2, pp. 817–827, Apr. 2020.

[2] F. Braeuer *et al.*, "Battery storage systems: An economic model-based analysis of parallel revenue streams and general implications for industry," *Appl. Energy*, vol. 239, pp. 1424–1440, 2019. [Online]. Avialable: https://www.sciencedirect.com/science/article/abs/pii/S0306261919300479

[3] Q. Yan *et al.*, "Optimized operational cost reduction for an EV charging station integrated with battery energy storage and PV generation," *IEEE Trans. Smart Grid*, vol. 10, no. 2, pp. 2096–2106, Mar. 2019.

[4] G. Mohy-ud-din, D. H. Vu, K. M. Muttaqi, and D. Sutanto, "An integrated energy management approach for the economic operation of industrial microgrids under uncertainty of renewable energy," *IEEE Trans. Ind. Appl.*, vol. 56, no. 2, pp. 1062–1073, Mar./Apr. 2020.

[5] J. M. Ortiz, W. Kracht, G. Pamparana, and J. Haas, "Optimization of a SAG mill energy system: Integrating rock hardness, solar irradiation, climate change, and demand-side management," *Math. Geosci.*, vol. 52, no. 3, pp. 355–379, 2020.

[6] G. Carpinelli, A. Di Fazio, S. Khormali, and F. Mottola, "Optimal sizing of battery storage systems for industrial applications when uncertainties exist," *Energies*, vol. 7, no. 1, pp. 130–149, 2014.

[7] V. Subramanyam, T. Jin, and C. Novoa, "Sizing a renewable microgrid for flow shop manufacturing using climate analytics," *J. Cleaner Prod.*, vol. 252, pp. 1–15, 2020. [Online]. Available: https://www.sciencedirect.com/science/article/abs/pii/S0959652619346992

[8] H. Pandžić, "Optimal battery energy storage investment in buildings," *Energy Buildings*, vol. 175, pp. 189–198, 2018. [Online]. Available: https://www.sciencedirect.com/science/article/abs/pii/S0378778818307795

[9] F. Hafiz, A. Rodrigo de Queiroz, P. Fajri, and I. Husain, "Energy management and optimal storage sizing for a shared community: A multi-stage stochastic programming approach, *Appl. Energy*, vol. 236, pp. 42–54, 2019. [Online]. Available: https://www.sciencedirect.com/science/article/abs/pii/S0306261918317963

[10] Y. Tohidi and M. Gibescu, "Stochastic optimisation for investment analysis of flow battery storage systems," *IET Renewable Power Gener.*, vol. 13, no. 4, pp. 555–562, 2019.

[11] N. Zhang, B. D. Leibowicz, and G. A. Hanasusanto, "Optimal residential battery storage operations using robust data-driven dynamic programming," *IEEE Trans. Smart Grid*, vol. 11, no. 2, pp. 1771–1780, Mar. 2020.

[12] Directorate-General for Energy, "Clean energy for all europeans," European Commission. Jul. 2019. [Online]. Available: tinyurl.com/yb4morv9

[13] M. Rahimiyan and L. Baringo, "Strategic bidding for a virtual powerplant in the day-ahead and real-time markets: A. price-taker robust optimization approach," *IEEE Trans. Power Syst.*, vol. 31, no. 4, pp. 2676–2687, Jul. 2016.

[14] G. Liu, Y. Xu, and K. Tomsovic, "Bidding strategy for microgrid in day-ahead market based on hybrid stochastic/robust optimization," *IEEE Trans. Smart Grid*, vol. 7, no. 1, pp. 227–237, Jan. 2016.

[15] H. Pandžić and V. Bobanac, "An accurate charging model of battery energy storage," *IEEE Trans. Power Syst.*, vol. 34, no. 2, pp. 1416–1426, Mar. 2019.

[16] Croatian Energy Regulatory Agency - HERA, Official Gazette (*in Croatian*). "General conditions for the use of the network and the supply of electricity," Tech. Rep. NN 85/2015-1666, May 2015. [Online]. Available: narodne-novine.nn.hr/clanci/sluzbeni/2015_08_85_1666.html

[17] Energinet, "Ancillary Services to Be Delivered in Denmark Tender Conditions," Tech. Rep. 13/80940-115, Oct. 2019. [Online]. Available: en.energinet.dk

[18] Tennet, "German Regulation," Accessed: May 2020. [Online]. Available: www.tennet.eu/e-insights/regulation/german-regulation/

[19] Retail Energy Price Data, "Electricity Prices," Accessed: May 2020. [Online]. Available: www.globalpetrolprices.com/electricity_prices

[20] Nordic Energy Regulators, "Tariffs in Nordic countries – survey of load tariffs in DSO grids," NordREG, Tech. Rep. 3/2015, Nov. 2015. [Online]. Available: tinyurl.com/ybxakbft

[21] HEP Elektra, "Tariffitems (prices)," Accessed: Mar. 2020. [Online]. Available: www.hep.hr/elektra/kucanstvo/tarifne-stavke-cijene/1547

[22] METIS Technical Note T4. "Overview of european electricity markets," European Commission, Feb. 2016. [Online]. Available: ec.europa.eu/energy/sites/ener/files/documents/metistechnical\notet4-overviewofeuropeanelectricitymarket.pdf

[23] Reserve prices in Germany, "Common tendering for primary control reserve." Accessed: Mar. 2020. [Online]. Available: www.regelleistung.net/ext/static/prl?lang=en

[24] NERGI DATASERVICE, "FCR, frequency containment reserves, DK1," Accessed: Mar. 2020. [Online]. Available: https://www.energidataservice.dk/tso-electricity/fcrreservesdk1

[25] Grid Code of the Croatian Transmission System Operator - HOPS (In Croatian), "Grid codeof the transmission system," Tech. Rep. NN 67/2017-1585, Jul. 2017. [Online]. Available: narodne-novine.nn.hr/clanci/sluzbeni/2017_07_67_1585.html

[26] A. Zeh *et al.*, "Fundamentals of using battery energy storage systems to provide primary control reserves in Germany," *Batteries*, vol. 2, no. 29, pp. 1–21, 2016.

[27] Battery University, "BU-808: How to prolong lithium-based batteries," Accessed: Nov. 2020. [Online]. Available: https://batteryuniversity.com/learn/article/howtoprolonglithiumbasedbatteries

[28] S. Pfenninger and I. Staffell, "Renewables.ninja," Accessed: Mar. 2020. [Online]. Available: www.renewables.ninja

[29] W. Cole and A. W. Frazier, "Cost projections for utility-scale battery storage," National Renewable Energy Laboratory (NREL), Tech. Rep. NREL/TP-6A20-73222, Jun. 2019. [Online]. Available: www.nrel.gov/docs/fy19osti/73222.pdf

[30] EUR-Lex, "Commission Regulation (EU) 2017/1485 of 2 August 2017 establishing a guideline on electricity transmission system operation," Tech. Rep. 32017R1485, Aug. 2017. Accessed: Mar. 2020. [Online]. Available: https://eur-lex.europa.eu/eli/reg/2017/1485/oj#d1e11013-1-1

[31] Energysage, "How much do solar panels cost in the U.S. in 2020?," Accessed: Mar. 2020. [Online]. Available: tinyurl.com/yb4px3fy

[32] F. Braeuer, "Load profile data of 50 industrial plants in Germany for oneyear: (Version 1.0), Jun. 2020. [Online]. Available: https://doi.org/10.5281/zenodo.3899018

[33] Y. Dvorkin *et al.*, "Ensuring profitability of energy storage," *IEEE Trans. Power Syst.*, vol. 32, no. 1, pp. 611–623, Jan. 2017.

[34] H. Teichgraeber and A. R. Brandt, "Clustering methods to find representative periods for the optimization of energy systems: An initial framework and comparison," *Appl. Energy*, vol. 239, pp. 1283–1293, 2019.

[35] Rambøll Danmark A/S, "Ancillary services from new technologies - technical potentials and market integration," Tech. Rep. 1191289-2/Version 3, Dec. 2019. [Online]. Available: energinet.dk

[36] eneREGIO GmbH, "Price sheet for electricity grid usage," (in German), Nov. 2019. [Online]. Available: https://tinyurl.com/yawm4emo

[37] Energie- und Wasserversorgung Kirchzarten GbmbH, 2019. "Network access fees for electricity. Accessed: May 2020. [Online]. Available: https://tinyurl.com/y7wxd7kh

[38] K. Šepetanc and H. Pandžić, "A cluster-based model for charging a fleet of electric vehicles," *PSCC*, Porto, Portugal, Jun. 2020.

# Publication C

## Stochastic Optimization of Battery Storage Investment in Industry – Comparing a Two-stage and Multi-Stage Approach

Fritz Braeuer[a], Manuel Ruppert[a], Wolf Fichtner[a]

[a]*Chair of Energy Economics, Institute for Industrial Production, Karlsruhe Institute of Technology, Karlsruhe, Germany*

Submitted to:

Annals of Operations Research, 4th of May 2022, currently under review with editor, 2022

# Stochastic Optimization of Battery Storage Investment in Industry – Comparing a Two-stage and Multi-Stage Approach

Fritz Braeuer[a], Manuel Ruppert[a], Wolf Fichtner[a]

[a]*Institute for Industrial Production (IIP), Karlsruhe Institute of Technology (KIT), Karlsruhe, Germany,*

**Abstract**

The provision of electric flexibility through the integration of battery storage systems plays a vital role in the stability of the future energy system. Significantly, the integration into an industrial context offers multiple electricity marketing opportunities. Nevertheless, the investment decision for a battery storage system is challenging due to uncertainties such as future energy prices and load behavior. In this paper, we develop a multi-stage stochastic optimization model for battery storage investment planning in industry to consider these uncertainties. We include uncertainty from frequency containment market prices, electricity spot market prices, as well as load behavior and apply it to a case study representing a German manufacturing company. Finally, we compare the multi-stage model to a conventional two-stage model and show that the two-stage formulation overestimates the profitability as it neglects the consecutive order of market and dispatch decisions. The two-stage model yields larger battery capacities for two typical weeks than the multi-stage model. Simultaneously, the multi-stage model requires a significantly larger amount of computational resources due to the large number of scenarios and state variables and the resulting model complexity.

*Keywords:* battery energy storage, demand flexibility, multi-stage investment model, stochastic optimization, industrial demand response
*PACS:* 0000, 1111
*2000 MSC:* 0000, 1111

## 1. Introduction

The transition of the electricity generation towards a decarbonized system based on renewable fuels poses both challenges and opportunities for industrial electricity consumers. The subsequently increasing dependency of the power generation on volatile power sources such as wind and solar leads to increasing volatility in wholesale electricity prices and rising relevance of load shifting abilities of large consumers from both a microeconomic and macroeconomic point of view. For industrial consumers, these changes in their environment make the investment into additional flexibility provided by an on-site battery storage system (BSS) a potentially attractive option. While the improvement in the environmental balance and increased security of supply might already be a strong positive driver for the investment, cost-effectiveness of the measure remains the most important factor in the microeconomic decision-making process. Evaluating the economic feasibility of such an investment is challenging due to the various uncertainties involved in the process. Especially for the case of adding a BSS to the energy system of an

**Nomenclature**

| ***Parameters and Symbols*** | | ***Indices*** | |
|---|---|---|---|
| $\pi$ | Probability | *BSS* | Battery storage system |
| $c$ | Specific cost | *peak* | Peak load |
| $\rho$ | Weighting factor | *BSaged* | Battery aging component |
| $d$ | Electricity demand in $kWh$ | *in* | Electricity flow into system |
| *puff* | Puffer factor for FCR bidding | *out* | Electricity flow out of system |
| $\eta$ | Efficiency | *sell* | Sold on market |
| *Pcap* | Power capacity | *buy* | Bought on market |
| *CRF* | Capital recovery factor | *ID* | Intraday market |
| *Eol* | End of life factor | *DA* | Day-ahead market |
| $LT_{cal}$ | Battery calendar lifetime in years | *FCR* | Primary control reserve |
| $LT_{cycl}$ | Battery cycle lifetime in number of cycles | *grid* | Electricity grid |
| $r^{Pcap}$ | Power capacity ratio | *prod* | Production |
| $r^{FCRmin}$ | Minimum FCR capacity ratio | *ch* | Charging |
| $E^{FCR,mean}$ | Mean energy demand due to FCR provision in $kWh$ | *dis* | Discharging |
| $time_{tot}$ | Number of time steps per year | *sdis* | Self-discharging |
| $T_{inv}$ | Investment period in years | *max* | Maximum allowed |
| $r^{cal}$ | Calendar aging factor | *tot* | Total amount per year |
| *NoT* | Number of typical time frames | *cal* | Calendar life |
| | | *cycl* | Cycle life |

industrial site, different revenue streams with uncertain economic viabilities over the course of the operation period are required to offset a significant up-front investment. Thus, a high level of accuracy when modelling the uncertainties is a key factor for evaluating the feasibility of an industrial BSS investment decision.

### *1.1. Literature review*

The methodological approaches to consider uncertainty in capacity planning of energy systems with a BSS are manifold [1]. Among others, a prominent solution is stochastic programming, where the field differentiates between two-stage and multi-stage approaches. Within this field, the majority of studies optimize the operation and dispatch decision under uncertainty, e.g. Vahid-Pakdel et al. [2]. Studies that investigate the optimal investment and planning decision implement a two-stage model in most of the cases, e.g. Go et al. [3].

Another branch of research utilizing a two-stage stochastic optimization approach investigates the optimal residential energy system. Tohidi and Gibescu [4] optimize the PV-BSS revenue stream considering day-ahead markets, imbalance markets and self-consumption for a Dutch residential complex. For a redox flow BSS, the BSS's capacity is exogenous while the optimal grid connection category, in terms of power capacity, is a decision variable. Pandžić [5] compare a two-stage and a robust modelling approach to solve the investment problem for the energy system with a PV-BSS of a Croatian hotel. They consider uncertain electricity demand and prices. Schwarz et al. [6] and Schwarz et al. [7] evaluate the optimal energy system investment for a residential quarter with a multitude of yearly scenarios coinciding with a high model complexity. The model of Chatterji and Bazilian [8] optimizes the investment in a residential energy system with PV, a BSS and EV charging under time-of-use prices. Nevertheless, battery

**Nomenclature continued**

| | | | |
|---|---|---|---|
| ***Indices and ordered sets*** | | ***Variables*** | |
| $q \in Q$ | Quarter hour | $C$ | Cost in € |
| $h \in H$ | Hour | $R$ | Revenue in € |
| $w \in W$ | Week | $x$ | Electricity flow in $kWh$ |
| $n \in N$ | Node | $P$ | Power in $MW$ |
| $\gamma \in \Gamma$ | Stage | $Ann$ | Annuity payment in € |
| $P(n) \subseteq N$ | Parent node of node $n$ | $cap$ | Capacity in $kWh$ |
| $\gamma arb \subseteq \gamma$ | Set of arbitrage stages or odd stages | $soc$ | State of charge in $kWh$ |
| $\gamma fcr \subseteq \gamma$ | Set of arbitrage stages or odd stages | $f$ | Primary objective function in € |
| $Qend$ | Final element of ordered set $Q$ | $cap^{FCR,lim}$ | Limiting available capacity due to FCR bidding in $kWh$ |
| $Hend$ | Final element of ordered set $H$ | | |
| $\Gamma end$ | Final element of ordered set $\Gamma$ | | |
| $\|X\|$ | Cardinality of set $X$ | ***Acronyms*** | |
| ***Indices and sets*** | | BSS | Battery storage system |
| $l \in L$ | Technology | FCR | Frequency containment reserve |
| $n \in N$ | Node | NPV | Net present value |
| $S_x \subseteq N$ | Set of nodes of stage $x$ or scenario $x$ | PV | Photovoltaic |
| $s \in S$ | Scenario of two-stage model | RES | Renewable energy sources |
| $\xi \in \Xi$ | Scenario per stage in multi-stage model | TF | Time frame |
| $sc \in SC$ | Scenario of multi-stage model | VPP | Virtual power plant |
| ***Sample nomenclature of electricity flows*** | | | |
| $x^{grid,BSS}$ | Electricity flow from grid to BSS | | |
| $x^{BSS,grid}$ | Electricity flow from BSS to grid | | |

degradation is not considered. For a residential PV-BSS, Zheng et al. [9] assume an exogenous yearly battery degradation factor without any additional cycle life restrictions.

Next to the residential sector, other applications are energy hubs or energy communities as well the industrial context. Shen et al. [10] present a planning model for a hybrid energy storage system for an energy community without the consideration of battery degradation or cycle limits. In contrast, Chen et al. [11] incorporate a battery degradation model into their two-stage robust planning and operation model for an energy hub with a BSS and thermal storage. A little differently, Alharbi and Bhattacharya [12] include a battery degradation matrix in their investment planning model for a BSS in an isolated micro grid. In the industrial context, Ortiz et al. [13] optimize the investment for a PV-BSS in a grinding mill. They consider the influence of uncertainties in the production process on the energy demand and energy system size. Mohy-ud din et al. [14] propose a two-stage optimization model to identify the optimal BSS size for an industrial microgrid, considering energy arbitrage and self-consumption. Here, peak shaving is achieved through an exogenous peak limit. Finally, Covic et al. [15] optimize the investment of a PV-BSS-system in an industrial complex considering multiple revenue streams. On the second stage, they combine stochastic optimization for the day-ahead market with a robust optimization approach for the intraday market.

Scientific publications in the field of multi-stage optimization are scarcer than those dealing with two-stage optimization models. Rebennack [16], Kaut et al. [17] and Lara et al. [18] develop a multi-stage stochastic optimization model to derive optimal decisions for national infrastruc-

ture investment planning. Next to their research, they present a well drafted overview of the theoretical background of multi-stage optimization and its scenario trees and present a variety of solutions techniques. Additionally, concerning infrastructure planning, Agrali et al. [19] present a three-stage investment planning model. The model includes the initial investment decision on the first stage, a second stage after five years and a final investment decision stage after 10 years. Bhattacharya et al. [20] solve the investment problem for a micro grid where distributed storage investment decision on the initial stage and the storage operation on the following stages is the main concern.

Other studies focus not on the investment, but on the operation of residential energy systems or virtual power plants (VPP). [21] develop a residential demand response model with various appliances. With PV-generation, they minimize the electricity cost for 24 hours under uncertain weather conditions. Hafiz et al. [22] optimize the energy management of residential PV-BSS. The model depicts the operation of 24 hours, with a stage for every consecutive hour. For VPP applications, Keles and Dehler-Holland [23] analyse the operation of a large-scale PV-BSS with uncertain spot and reserve market prices as well as uncertain PV-generation. They translate the operation into a Markov decision process. Wu et al. [24] present a multi-stage offering strategy. They consider the operation of a hydrogen fuelling station with uncertain electricity and reserve markets, as well as uncertain hydrogen demand. Badanjak and Pandzic [25] draft a three-stage problem for BSS market participation. They optimize the operation on existing markets and new flexibility markets. Abbasi et al. [26] formulate a three-stage risk constrained approach for the optimal operation of a VPP with wind power and EV charging active on different markets. With the same number of stages, Khaloie et al. [27] publish an optimization model for a wind-thermal-energy-storage system, where the storage decision is followed by the markets bids and, eventually, by the imbalance cost optimization. Finally, Heredia et al. [28] present a bidding and dispatch model for a virtual power plant (VPP) with wind power and a BSS. The model considers the uncertainty on the day-ahead, intraday and secondary reserve market with a detailed BSS operation constraints and a simplified cycle life constraint. The cycle life limits the expected value of full cycles over all scenarios.

In conclusion, the literature review shows the following deficiencies in the field of multi-stage stochastic programming:

- No study evaluates the BSS investment planning
- No study focuses on the industry sector
- No study considers revenue streams from peak shaving and reserve markets simultaneously
- Studies reveal insufficient cycle life constraints and BSS aging constraints.

### *1.2. Hypothesis and key contribution*

This paper makes the following hypothesis: The simplification of a two-stage model formulation compared to a multi-stage approach neglects operational risks of a BSS in industry. Thus, the two-stage approach overestimates the operational profitability of a BSS, which leads to higher investments. When optimizing the battery dispatch for different markets and consecutive, time-dependent market activities, the two-stage approach naturally limits a thorough consideration of stochastic processes. Similarly, the battery aging process depends on the consecutive order of dispatch decisions and is more realistically reflected by a multi-stage formulation. These stochastic risks need to be considered.

In this paper, to prove this hypothesis, we develop a multi-stage stochastic optimization approach to determine the optimal BSS investment considering the uncertainty of the on-site electricity load, wholesale electricity prices, and reserve market prices. We further present the results of our approach for a case study based on real-world industrial load profiles and compare the findings to a two-stage formulation to highlight the improvement of accuracy in the investment decision due to the increased consideration of uncertainty.

The considered wholesale markets for electricity trading are the day-ahead market with hourly electricity packages and the continuous intraday market with quarter-hourly electricity packages. The depicted reserve market is the frequency containment reserve (FCR) market. Here, market participants offer a certain amount of FCR power in a given timeframe. This reserve power is automatically activated as it reacts to frequency deviation of the electricity grid. FCR bids must provide positive and negative reserve power symmetrically. For a BSS, positive FCR means discharging and feeding power into the electricity grid and negative FCR means charging and drawing power from the grid.

The following points describe the key contributions of this paper:

- Development of a multi-stage stochastic optimization model for the BSS investment in industry
- Inclusion of BSS aging and cycle life constraints
- Consideration of a multi-use case with peak shaving, FCR market bids and energy arbitrage
- Comparing a two-stage and multi-stage stochastic optimization approach.

The paper is structured as follows. Section 2 describes the problem statement, outlines the two optimization approaches and presents the mathematical formulation of objective function and constraints for both methods. Section 3 depicts the case study and shows the results of the model comparison. Section 4 critically reviews these results, and Section 5 concludes this paper and gives an outlook on future research.

## 2. Methodology

This section describes the overall investment and dispatch problem for a BSS in an industrial application. The investment and dispatch problem can be optimized in a deterministic [29] or stochastic manner [15]. This paper further studies the stochastic optimization by proposing a novel multi-stage approach addressing the need to consider uncertainty in a more realistic manner and comparing the approach to a conventional two-stage approach. Both approaches for the same investment decision in an industrial application are explained in Section 2.2 to Section 2.4, including the necessary set of mathematical formulations.

### *2.1. Problem statement*

In this section, we describe the overall investment problem and the general assumptions. The setting is derived from Braeuer et al. [29]. The presented optimization models solve the investment and dispatch problem for a BSS installed at an industrial complex. The industrial complex has a given electricity load of the production. The industrial company has the option

to invest in a battery storage system and to profit from different revenue streams, energy market participation, FCR market participation and peak shaving.

We assume typical days or weeks to represent the behavior for one year over the course of the BSS's lifetime. This study refers to typical days or typical weeks as the considered time frame.

The considered revenue streams or business cases are peak shaving, FCR biding and arbitrage trading. Peak shaving is remunerated by the savings in peak load charges between grid load with and without a BSS. The peak load charges are paid on the maximum load for the whole year. On the FCR market, the industrial company has the option to offer a continuous amount of FCR in $MW$. In order to offer FCR, the company must reserve a certain amount of the BSS's capacity, which cannot be used for other revenue streams. For a weekly time frame, we assume weekly prices and weekly FCR offers. For the daily consideration, the weekly FCR prices are divided by the number of weekdays and, thus, the FCR offer counts for one day. We assume that FCR market always accepts the company's FCR offer. Finally, we assume energy arbitrage to take place on the day-ahead hourly market and the intraday quarter-hourly market. The industrial company can profit from price differences on these markets. Electricity is charged into the battery in times of low prices and discharged in times of high prices. The discharged energy either satisfies the electricity load of the production or is fed into the grid and sold on the respective electricity market. The time steps are quarter hours. In every time step, the electricity demand of the production must be satisfied either by electricity from the grid or additional electricity from the BSS.

### *2.2. The two-stage and multi-stage approach*

Both approaches, the two-stage model and the multi-stage model, consider the stochastic behavior of prices and electricity demand. In both cases, the model has to make a decision about the BSS investment without knowing the realization $\xi$ of the stochastic processes. The stochastic processes are the market prices on the FCR market, the day-ahead market as well as the intraday market as well as the electricity demand of the industrial production process. Together with the investment decision, the yearly peak load limit is set before knowing the actual load behavior.

Results from Braeuer et al. [29] indicate the most influential factor of the BSS investment decision is the FCR and peak shaving business case. Arbitrage trading yields relatively small profits. Furthermore, the consideration of multiple markets' stochastic separately would result in relatively high complexity of the multi-stage formulation. Therefore, this study groups the possible realizations $\xi$ of electricity market prices and load behavior together. For example, assuming $|\Xi| = 4$, this would result in four possible realizations of FCR prices and four realizations of a set of electricity market prices and load profiles.

Figure 1 illustrates the decision stages of the two-stage-model. The model makes a decision on the first stage without knowing the realization on the second stage. The second stage decision is made with the knowledge of the first stage's decision and the knowledge about the realization $\xi$ of the stochastic process on the second stage. The stochastic process is described by the scenario $s$ for every time frame $w$. The set of scenarios per time frame $S$ describes the combination of all FCR realization ($\xi^{FCR}$) and arbitrage realizations ($\xi^{arb}$), electricity market and load behavior. This means $|S| = |\Xi^{FCR}| \cdot |\Xi^{arb}|$.

- On stage 1, the decision about the BSS investment and sizing is made as well as the decision on the peak limit.

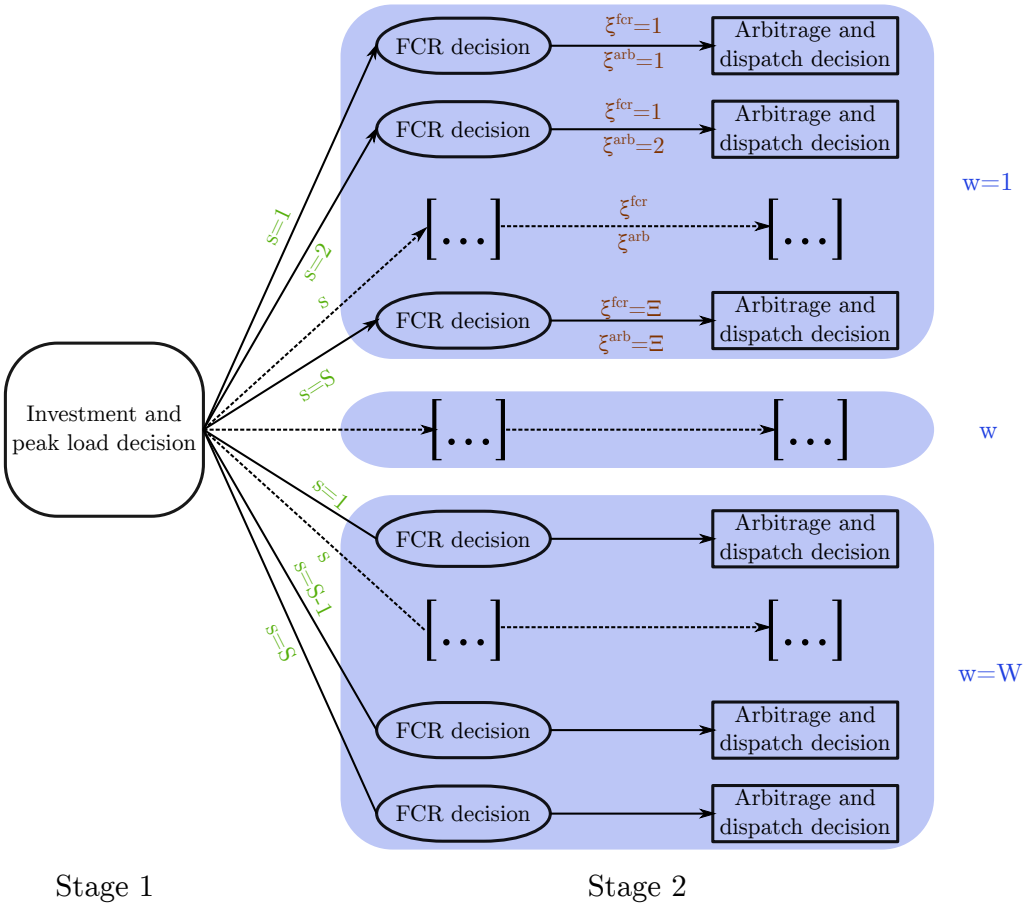


Figure 1: Two-stage model structure

- On stage 2, the decision about the FCR bid, the energy arbitrage activities as well as the BSS dispatch is made simultaneously. This has a recursive effect on the first stage decision as the market activities are bound by the BSS capacity and peak load limit.

Figure 2 shows the scenario tree of the multi-stage model. Similar to the two-stage model, the first stage decision is made without knowing the realization of the stochastic processes. Every consecutive stage knows about the realization on its current stage and the decision on its previous stage but does not to the realization of the stochastic processes of the following stages. The final stage has knowledge about the decisions on all previous stages. Additionally, the model considers the consecutive order of decisions such that every decision knows only of a single decision of it previous stage (path dependency).

- On stage 1, the decision about the BSS investment and sizing is made as well as the decision on the peak limit.

- On stage 2 and every even numbered stage (FCR stage), FCR prices are known and the decision about the FCR bid is made. This has a recursive effect on the first stage as the BSS capacity limits the FCR potential.
- On stage 3 and every odd numbered stage except stage 1 (arbitrage stage), electricity prices are known and the decision about the energy arbitrage and BSS dispatch is made. This has a recursive effect on the first stage decision as the market activities are bound by the BSS capacity and peak load limit. The previous FCR decisions limits the idle BSS capacity.

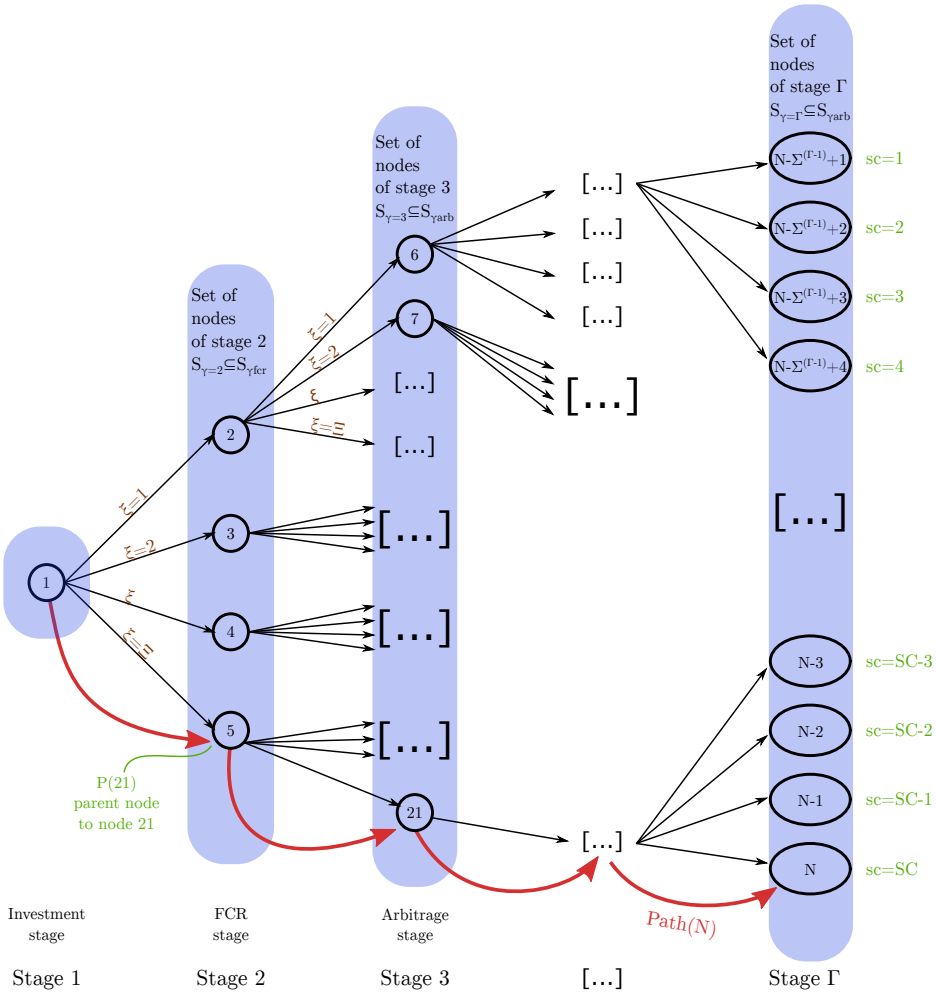


Figure 2: Scenario tree of multi-stage model

Figure 2 describes the decisions of the multi-stage model as nodes and the arrows describe the consecutive order of decision nodes. For a clearer understanding, we introduce the following list of sets and subsets to illustrate the scenario tree. These definitions are oriented on Lara et al. [18].

- $n \in N$ and $n = \sum_{\gamma} |\Xi|^{\gamma-1}$– set of decision nodes
- $\xi \in \Xi$ – set of uncertainty realizations of every stochastic process
- $\gamma \in \Gamma$ – set of stages
- $\gamma fcr \subseteq \gamma,\ \gamma fcr \notin \gamma arb,\ \gamma fcr \in \{2, 4, ..., \Gamma end - 1\}$ – set of FCR stages or even stages
- $\gamma arb \subseteq \gamma,\ \gamma arb \in \{3, 5, ..., \Gamma end\}$ – set of arbitrage stages or odd stages
- $sc \in SC$ and $|SC| = |\Xi|^{\Gamma end-1}$ – set of multi-stage scenarios
- $S_x$ – Set of nodes of stage $x$ or multi-stage scenario $x$
- $S_{sc} := Path(n), \quad \forall n \in S_{\Gamma end}$ – Set of nodes of scenario $sc$, which is defined as the unique scenario path that connects all nodes from the first stage node to node $n$ on the final stage $\gamma_{|\Gamma|}$ on the scenario tree
- $P(n)$ – Parent node to node $n$ for $\gamma > 1$, such that for every $n \in S_{\gamma}$ there exist a node $m$ with $m \in P(n)$ and $m \in S_{\gamma-1}$

### *2.3. Objective function*

In the following subsections, we describe the two stochastic model approaches. All equations are written as the deterministic equivalent to the extensive form. All variables are defined as positive continuous variables except for the variables named in Table 1.

| | Continuous variable $\in \mathbb{R}$ |
|---|---|
| Two-stage | $x^{grid}_{q,h,w,s}$, $x^{ID}_{q,h,w,s}$, $x^{DA}_{h,w,s}$, $C^{ID}_{q,h,w,s}$, $C^{DA}_{h,w,s}$ |
| Multi-stage | $x^{grid}_{q,h,n}$, $x^{ID}_{q,h,n}$, $x^{DA}_{h,n}$, $C^{ID}_{q,h,n}$, $C^{DA}_{h,n}$ |

Table 1: List of continuous variables.

Equation 1 describes the objective function of the two-stage model. The first stage decision includes the battery annuity payment ($Ann^{BSS}$), the yearly peak load charges as the product of the yearly peak load ($P^{peak}$) and the specific peak price ($c^{peak}$) as well as the additional annuity payment due to battery aging ($Ann^{BS\,aged}$). The recourse decisions are made in every time frame $w$ that coincides with a weighting factor $\rho$ and a probability factor $\pi$ for every scenario $s$. The objective function considers the expected value of the cost and revenue of electricity trading and the FCR revenue for every time frame. Cost and revenue of electricity trading are defined as the probability-weighted average of the sum of intraday electricity cost ($C^{ID}$) for every quarter-hour $q$ in hour $h$ of time frame $w$, the sum of day-ahead electricity cost ($C^{DA}$) for every hour of the time frame as well as the FCR revenue. The latter is defined as the product of offered FCR power ($P^{FCR}$) and the FCR price ($c^{FCR}$) per time frame. The average is weighted by the probability factor $\pi$ defined for every scenario and time frame. $\pi$ is introduced under the condition that the sum of the probability factor over all scenarios in one time frame equals 1. Finally, the sum of the weighting factor over all time frames equals to the number of time frames per year.

$$\min f = Ann^{BSS} + P^{peak} \cdot c^{peak} + Ann^{BS\,aged} + \sum_{w} \left( \rho_w \sum_{s} \pi_{w,s} \cdot \left( \sum_{h} \left( \sum_{q} (x^{ID}_{q,h,w,s} \cdot c^{ID}_{q,h,w,s}) + x^{DA}_{h,w,s} \cdot c^{DA}_{h,w,s} \right) - P^{FCR}_{w,s} \cdot c^{FCR}_{w,s} \right) \right) \quad (1)$$

Equation 2 describes the objective function of the multi-stage model. Like the two-stage model, the first stage decision is on the battery annuity payment and yearly peak charges. In contrast, the BSS aging cost is considered for every multi-stage scenario *sc* and included as the expected value, the product of the probability factor ($\pi$), and the annuity payment due to battery aging ($Ann^{BSS,aged}$). Except for the first stage, the decisions on the other stages depend on a stochastic process. Therefore, the objective function considers the expected value of electricity cost and FCR revenue on its respective stage. Every arbitrage stage $\gamma arb$ includes the sum of electricity cost on the intraday and day-ahead market multiplied by the probability factor $\pi$ and the weighting factor $\rho$ defined for every node on the respective arbitrage stage. In parallel, on every FCR stage $\gamma fcr$, the expected value is derived from the product of the FCR bid, the FCR price and the probability and weighting factor. Finally, the sum of all probabilities on one stage equals 1. The weighting factor is equal for all nodes in one stage. The sum of the weighting factor for all arbitrage or FCR stages on one scenario path equals the number of time frames per year.

$$\begin{aligned} \min f = & Ann^{BSS} + P^{peak} \cdot c^{peak} + \\ & \sum_{sc} \left( \pi_{sc} \cdot Ann^{BS\,aged}_{sc} \right) + \\ & \sum_{n \in S_{\gamma arb}} \left( \pi_n \cdot \rho_n \cdot \sum_{h} \left( \sum_{q} \left( x^{ID}_{q,h,n} \cdot c^{ID}_{q,h,n} \right) + x^{DA}_{h,n} \cdot c^{DA}_{h,n} \right) \right) + \\ & \sum_{n \in S_{\gamma fcr}} \left( \pi_n \cdot \rho_n \cdot (-P^{FCR}_{n}) \cdot c^{FCR}_{n} \right) \end{aligned} \quad (2)$$

### *2.4. Model constraints*

In this subsection, we describe the constraints of the two model approaches. Table 2, Table 3 and Table 4 list and compare the model constraints, the two-stage model on the left and the multi-stage model on the right of the table. Table 2 shows the electricity balance and market balance constraints. Table 3 lists constraints describing the battery operation. Finally, Table 4 defines battery capacity, battery annuity and battery aging.

First, Equation 3 until Equation 6 show the electricity balance of the industrial complex. The electricity balance constraints are similar for both models. In the two-stage model, they are defined for all time steps and scenarios and, in the multi-stage model, they are defined for all time steps on the arbitrage stage. Equation 3 states that the grid electricity flow ($x_{grid}$), which can take both positive and negative values, is the difference between the electricity flow from the grid into the industrial complex ($x_{grid,in}$) and the electricity flow into the grid ($x_{grid,out}$). Electricity that flows into the industrial complex is either directed to the BSS ($x_{grid,BSS}$) or to the production process ($x_{grid,prod}$), see Equation 4. Equation 5 states that the only electricity grid feed-in ($x_{grid,out}$)

| Two-stage model | | Multi-stage model | | Ref |
|---|---|---|---|---|
| *Electricity balance constraints* | | | | |
| $x^{grid}_{q,h,w,s} = x^{grid,in}_{q,h,w,s} - x^{grid,out}_{q,h,w,s}$ | $\forall q,h,w,s$ | $x^{grid}_{q,h,n} = x^{grid,in}_{q,h,n} - x^{grid,out}_{q,h,n}$ | $\forall q,h,n \in S_{\gamma arb}$ | (3) |
| $x^{grid,in}_{q,h,w,s} = x^{grid,BSS}_{q,h,w,s} + x^{grid,prod}_{q,h,w,s}$ | $\forall q,h,w,s$ | $x^{grid,in}_{q,h,n} = x^{grid,BSS}_{q,h,n} + x^{grid,prod}_{q,h,n}$ | $\forall q,h,n \in S_{\gamma arb}$ | (4) |
| $x^{grid,out}_{q,h,w,s} = x^{BSS,grid}_{q,h,w,s}$ | $\forall q,h,w,s$ | $x^{grid,out}_{q,h,n} = x^{BSS,grid}_{q,h,n}$ | $\forall q,h,n \in S_{\gamma arb}$ | (5) |
| $d_{q,h,w,s} = x^{BSS,prod}_{q,h,w,s} + x^{grid,prod}_{q,h,w,s}$ | $\forall q,h,w,s$ | $d_{q,h,n} = x^{BSS,prod}_{q,h,n} + x^{grid,prod}_{q,h,n}$ | $\forall q,h,n \in S_{\gamma arb}$ | (6) |
| *Electricity market constraints* | | | | |
| $x^{DA}_{h,w,s} = x^{DA,buy}_{h,w,s} - x^{DA,sell}_{h,w,s}$ | $\forall h,w,s$ | $x^{DA}_{h,n} = x^{DA,in}_{h,n} - x^{DA,sell}_{h,n}$ | $\forall h,n \in S_{\gamma arb}$ | (7) |
| $x^{ID}_{q,h,w,s} = x^{ID,buy}_{q,h,w,s} - x^{ID,sell}_{q,h,w,s}$ | $\forall q,h,w,s$ | $x^{ID}_{q,h,n} = x^{ID,buy}_{q,h,n} - x^{ID,sell}_{q,h,n}$ | $\forall q,h,n \in S_{\gamma arb}$ | (8) |
| $x^{DA,buy}_{h,w,s} + \sum_q x^{ID,buy}_{q,h,w,s} = \sum_q x^{grid,in}_{q,h,w,s}$ | $\forall h,w,s$ | $x^{DA,buy}_{h,n} + \sum_q x^{ID,buy}_{q,h,n} = \sum_q x^{grid,in}_{q,h,n}$ | $\forall h,n \in S_{\gamma arb}$ | (9) |
| $x^{ID,buy}_{q,h,w,s} \leq x^{grid,in}_{q,h,w,s}$ | $\forall q,h,w,s$ | $x^{ID,buy}_{q,h,n} \leq x^{grid,in}_{q,h,n}$ | $\forall q,h,n \in S_{\gamma arb}$ | (10) |
| $x^{DA,sell}_{h,w,s} + \sum_q x^{ID,sell}_{q,h,w,s} = \sum_q x^{grid,out}_{q,h,w,s}$ | $\forall h,w,s$ | $x^{DA,sell}_{h,n} + \sum_q x^{ID,sell}_{q,h,n} = \sum_q x^{grid,out}_{q,h,n}$ | $\forall h,n \in S_{\gamma arb}$ | (11) |
| $x^{ID,sell}_{q,h,w,s} \leq x^{grid,out}_{q,h,w,s}$ | $\forall q,h,w,s$ | $x^{ID,sell}_{q,h,n} \leq x^{grid,out}_{q,h,n}$ | $\forall q,h,n \in S_{\gamma arb}$ | (12) |
| *FCR constraints* | | | | |
| $cap^{FCR}_{w,s} = puff^{FCR} \cdot P^{FCR}_{w,s}$ | $\forall w,s$ | $cap^{FCR}_{n} = puff^{FCR} \cdot P^{FCR}_{n}$ | $\forall n \in S_{\gamma fcr}$ | (13) |
| $cap^{FCR}_{w,s} \leq cap^{BSS}$ | $\forall w,s$ | $cap^{FCR}_{n} \leq cap^{BSS}$ | $\forall n \in S_{\gamma fcr}$ | (14) |
| $--$ | | $cap^{FCR,lim}_{n} = cap^{FCR}_{P(n)}$ | $\forall n \in S_{\gamma arb}$ | (15) |
| *Peak shaving constraint* | | | | |
| $P^{peak} \geq x^{grid}_{q,h,w,s} \cdot 4/1000$ | $\forall q,h,w,s$ | $P^{peak} \geq x^{grid}_{q,h,n} \cdot 4/1000$ | $\forall q,h,n \in S_{\gamma arb}$ | (16) |

Table 2: Electricity balance and market constraints

| Two-stage model | Multi-stage model | Ref |
|---|---|---|
| *Battery operation constraints* | | |
| $x^{BSS,in}_{q,h,w,s} = \eta^{ch} \cdot x^{grid,BSS}_{q,h,w,s} \quad \forall q,h,w,s$ | $x^{BSS,in}_{q,h,n} = \eta^{ch} \cdot x^{grid,BSS}_{q,h,n} \quad \forall q,h,n \in S_{\gamma arb}$ | (17) |
| $x^{BSS,out}_{q,h,w,s} = 1/\eta^{dis} \cdot (x^{BSS,prod}_{q,h,w,s} + x^{BSS,grid}_{q,h,w,s}) \quad \forall q,h,w,s$ | $x^{BSS,out}_{q,h,n} = 1/\eta^{dis} \cdot (x^{BSS,prod}_{q,h,n} + x^{BSS,grid}_{q,h,n}) \quad \forall q,h,n \in S_{\gamma arb}$ | (18) |
| $soc_{q,h,w,s} = \frac{soc_{q+1,h,w,s} - x^{BSS,in}_{q+1,h,w,s} + x^{BSS,out}_{q+,h,w,s}}{1-\eta^{sdis}}$ $\forall q < Qend,h,w,s$ | $soc_{q,h,n} = \frac{soc_{q+1,h,n} - x^{BSS,in}_{q+1,h,n} + x^{BSS,out}_{q+1,h,n}}{1-\eta^{sdis}}$ $\forall q < Qend,h,n \in S_{\gamma arb}$ | (19) |
| $soc_{Qend,h,w,s} = \frac{soc_{1,h+1,w,s} + x^{BSS,in}_{1,h+1,w,s} + x^{BSS,out}_{1,h+1,w,s}}{1-\eta^{sdis}}$ $\forall h < Hend,w,s$ | $soc_{Qend,h,n} = \frac{soc_{1,h+1,n} + x^{BSS,in}_{1,h+1,n} + x^{BSS,out}_{1,h+1,n}}{1-\eta^{sdis}}$ $\forall h < Hend,n \in S_{\gamma arb}$ | (20) |
| $soc_{Qend,Hend,w,s} = \frac{soc_{1,1,w,s} - x^{BSS,in}_{1,1,w,s} + x^{BSS,out}_{1,1,w,s}}{1-\eta^{sdis}}$ $\forall w,s$ | $soc_{Qend,Hend,P(P(n))} = \frac{soc_{1,1,n} - x^{BSS,in}_{1,1,n} + x^{BSS,out}_{1,1,n}}{1-\eta^{sdis}}$ $\forall n \in S_{\gamma arb} \setminus S_{\Gamma end} \wedge S_{\gamma arb} \setminus S_{\gamma=3}$ | (21) |
| – | $soc_{Qend,Hend,n} = \frac{soc_{1,1,m} - x^{BSS,in}_{1,1,m} + x^{BSS,out}_{1,1,m}}{1-\eta^{sdis}}$ $\forall n \in S_{\Gamma end}, \forall m \in S_{\gamma=3}$ | (22) |
| *Charge and discharge limit* | | |
| $soc_{q,h,w,s} \leq cap^{BSS} - r^{FCRmin} \cdot cap^{FCR}_{w,s} \quad \forall q,h,w,s$ | $soc_{q,h,n} \leq cap^{BSS} - r^{FCRmin} \cdot cap^{FCR,lim}_{n} \quad \forall q,h,n \in S_{\gamma arb}$ | (23) |
| $soc_{q,h,w,s} \geq r^{FCRmin} \cdot cap^{FCR}_{w,s} \quad \forall q,h,w,s$ | $soc_{q,h,n} \geq r^{FCRmin} \cdot cap^{FCR,lim}_{n} \quad \forall q,h,n \in S_{\gamma arb}$ | (24) |
| $x^{BSS,in}_{q,h,w,s} \leq cap^{BSS} - cap^{FCR}_{w,s} \quad \forall q,h,w,s$ | $x^{BSS,in}_{q,h,n} \leq cap^{BSS} - cap^{FCR,lim}_{n} \quad \forall q,h,n \in S_{\gamma arb}$ | (25) |
| $x^{BSS,out}_{q,h,w,s} \leq cap^{BSS} - cap^{FCR}_{w,s} \quad \forall q,h,w,s$ | $x^{BSS,out}_{q,h,n} \leq cap^{BSS} - cap^{FCR,lim}_{n} \quad \forall q,h,n \in S_{\gamma arb}$ | (26) |
| $x^{BSS,out}_{q,h,w,s} + x^{BSS,in}_{q,h,w,s} \leq Pcap^{BSS} \cdot \frac{1}{4} \quad \forall q,h,w,s$ | $x^{BSS,out}_{q,h,n} + x^{BSS,in}_{q,h,n} \leq Pcap^{BSS} \cdot \frac{1}{4} \quad \forall q,h,n \in S_{\gamma arb}$ | (27) |

Table 3: Battery operation constraints

| Two-stage model | Multi-stage model | | Ref |
|---|---|---|---|
| *Battery capacity and annuity constraints* | | | |
| $Pcap^{BSS} = cap^{BSS} \cdot r^{Pcap}$ | $Pcap^{BSS} = cap^{BSS} \cdot r^{Pcap}$ | | (28) |
| $cap^{BSS} \leq cap^{BSS,max}$ | $cap^{BSS} \leq cap^{BSS,max}$ | | (29) |
| $Ann^{BSS} = cap^{BSS} \cdot c^{BSS} \cdot CRF$ | $Ann^{BSS} = cap^{BSS} \cdot c^{BSS} \cdot CRF$ | | (30) |
| $Ann^{BSS,aged} = cap^{BSS,aged} \cdot c^{BSS} \cdot CRF$ | $Ann^{BSS,aged}_{sc} = cap^{BSS,aged}_{sc} \cdot c^{BSS} \cdot CRF$ | $\forall sc$ | (31) |
| *Battery aging constraints* | | | |
| $x^{BSS,ch,tot} = \sum_w \rho_w \cdot \sum_s \pi_{w,s} \cdot \left( \sum_{q,h} (x^{BSS,in}_{q,h,w,s}) + x^{BSS,ch,FCR,tot}_{w,s} \right)$ | $x^{BSS,ch,tot}_{sc} = \sum_{n \in S_{sc}} \left( \rho_n \cdot \left( \sum_{q,h} x^{BSS,in}_{q,h,n} + x^{BSS,ch,FCR,tot}_{sc} \right) \right)$ | $\forall sc$ | (32) |
| $x^{BSS,ch,FCR,tot}_{w,s} = P^{FCR}_{w,s} \cdot E^{FCR,mean}$ | $x^{BSS,ch,FCR,tot}_{n} = P^{FCR}_{n} \cdot E^{FCR,mean}$ | $\forall n \in S_{\gamma fcr}$ | (33) |
| $x^{BSS,ch,tot} \cdot \frac{LT^{cal}}{cap^{BSS}} \leq LT^{cycl}$ | $x^{BSS,ch,tot}_{sc} \cdot \frac{LT^{cal}}{cap^{BSS}} \leq LT^{cycl}$ | $\forall sc$ | (34) |
| $cap^{BSS,aged,cal} = \sum_w \left( \rho_w \cdot \sum_{q,h,s} \pi_{w,s} \cdot \left( soc^{BSS}_{q,h,s} \right) \right) \cdot \frac{1}{time^{tot}} \cdot r^{cal}$ | $cap^{BSS,aged,cal}_{sc} = \sum_{n \in S_{sc}} \left( \rho_n \cdot \sum_{q,h} \left( soc^{BSS}_{q,h,n} \right) \right) \cdot \frac{1}{time^{tot}} \cdot r^{cal}$ | $\forall sc$ | (35) |
| $cap^{BSS,aged} = cap^{BSS} \cdot \frac{1}{EoL} + cap^{BSS,aged,cal}$ | $cap^{BSS,aged}_{sc} = cap^{BSS} \cdot \frac{1}{EoL} + cap^{BSS,aged,cal}_{sc}$ | $\forall sc$ | (36) |

Table 4: Battery capacity, annuity and aging constraints

comes from the BSS ($x_{BSS,grid}$). Finally, Equation 6 defines that the exogenous electricity demand of the production process ($d$) must always be satisfied. The electricity for the production process comes either from the BSS ($x_{BSS,prod}$) or the grid ($x_{grid,prod}$).

In Table 2, Equation 8 until Equation 12 constrain the arbitrage trading activities of the model. In the two-stage model, the equations are defined for all time frames and scenarios and, in the multi-stage model, for all nodes on the arbitrage stages. Equation 7 defines the electricity traded on the day-ahead market ($x_{DA}$) for every hour $h$. It takes positive values if the amount of electricity bought on the day-ahead market($x_{DA,buy}$) is greater than the amounts sold ($x_{DA,sell}$) and vice-versa. In analogy, Equation 8 defines the electricity traded on the intraday market for every quarter-hour $q$ and hour $h$. In either case, the electricity amount bought on the markets must not surpass the amounts drawn from the grid ($x_{grid,in}$). This shows Equation 9, which is defined for every hour and therefore considers the sum of all quarter-hourly electricity flows per hour. Additionally, Equation 10 states that, in every quarter-hour, the electricity bought on the intraday market ($x_{ID,buy}$) must not exceed the electricity drawn from the grid. Similarly, Equation 11 and Equation 12 restrict the electricity amounts sold on the electricity markets. Finally, Equations 9 until 12 allow only for physical arbitrage trading utilizing the BSS.

Equations 13 until 15 describe the FCR constraints. In the two-stage model, the FCR constraints are defined for every time frame and every scenario and, in the two-stage model, they are defined for every node on the FCR stage ($S_{\gamma fcr}$). Equation 13 states that the FCR bid ($P^{FCR}$) multiplied by a puffer factor ($puff^{FCR}$) equals to the BSS's capacity that is reserved for FCR activities ($cap^{FCR}$). $cap^{FCR}$ limits the BSS's capacity for other uses, explained in Equation 23 and following. Equation 14 bounds $cap^{FCR}$ not to exceed the BSS capacity ($cap^{BSS}$). Equation 15 is defined only for the multi-stage model. It introduces the state variable $cap^{FCR,lim}$ that links the FCR stage and its consecutive arbitrage stage. For the set of nodes on the arbitrage stage, Equation 15 defines an FCR capacity limit ($cap^{FCR,lim}$) that is equal to the FCR capacity of the parent node $P(n)$ on the FCR stage. $cap^{FCR,lim}$ is later used in Equation 23 and following.

Table 3 shows the constraints of the BSS operation. Equation 17 and Equation 18 show the

charge and discharge electricity flow of the battery for every time step of the two-stage scenarios and the arbitrage stage nodes of the multi-stage model. Equation 17 defines the charge electricity flow of the BSS ($x^{BSS,in}$) as the electricity flow from the grid to the BSS ($x^{grid,BSS}$) multiplied by the charging efficiency ($\eta^{ch}$). In Equation 18, the discharge electricity flow ($x^{BSS,out}$) is the inverse discharge efficiency ($\eta^{dis}$) times the sum of electricity flowing to the production process ($x^{BSS,prod}$) and electricity fed into the grid ($x^{BSS,grid}$).

Equations 19 until 22 define the state of charge (SOC) of every time step and connects the consecutive time steps. Equation 19 shows the principle that the SOC of a time step $q$ is equal to the SOC of the following time step $q+1$ minus the electricity charged in $q+1$ plus the electricity discharged in $q+1$. The sum of the three terms is divided by $(1-\eta^{sdis})$, the self-discharge rate. Equation 19 is defined for every time step except for the final time step of the set of $Q$. In the two-stage model, the equation accounts for every time frame $w$ and every scenario; in the multi-stage model, it accounts for every node on the arbitrage stage. Equation 20 and Equation 21 and Equation 22 define the SOC in analogy to Equation 19. Hereby, Equation 20 defines the SOC of the final quarter-hour $q = Q$ for every full hour $h$. In this case, the consecutive time step is defined as the first quarter-hour of the next full hour $h+1$. In the two-stage model, Equation 21 defines circular behavior of the SOC such that for the last quarter-hour of the last full hour in time frame $w$ the consecutive time step is the first quarter-hour of the first full hour of the same time frame $w$. In this case, the multi-stage formulation differs due to the consecutive order of stages and the use of state variables. Thus, for every arbitrage stage except the final stage($\gamma_{|\Gamma|}$) and the first stage ($\gamma = 3$), the first time step on an arbitrage stage is preceded by the last time step of its Parent's Parent node $P(P(n))$. The parent node would be on the proceeding FCR stage and its parent node would again be on its proceeding arbitrage stage. Equation 22 defines the circular behavior of the SOC for the multi-stage model. It states that the final time step of node $n$ on the final stage is succeeded by the first time step of node $m$ on the first arbitrage stage that is belongs to the same scenario path as $n$ ($m \in Path(m)$).

Finally, in Table 3, Equation 23 until Equation 27 define the charge and discharge limits for every time step of every time frame and every scenario or every arbitrage node respectively. Equation 23 sets the maximum SOC to be always smaller or equal to the difference of the installed BSS capacity and FCR capacity reserved for that time frame ($cap^{FCR}$) multiplied by a minimum FCR capacity ratio ($r^{FCRmin}$). For the multi-stage formulation, the variable $cap^{FCR,lim}$ resembles the reserved FCR capacity decision of the proceeding FCR stage, defined in Equation 15. Similarly to the upper bound, Equation 24 sets the SOC's lower bound to be greater or equal to the reserved FCR capacity multiplied by $r^{FCRmin}$. Additionally, Equation 25 and 26 limit the charge and discharge electricity to be less or equal to the difference between the installed capacity and the for FCR reserved capacity ($cap^{BSS}$ or $cap^{FCR}$ respectively). Finally, Equation 27 defines the sum of charge and discharge electricity to always be less or equal to the power capacity of the BSS ($Pcap^{BSS}$). To convert from the unit power to energy, $Pcap^{BSS}$ is divided by four.

The final table of constraints, Table 4, defines the capacity and annuity constraints, Equations 28 until 31, as well as the battery aging consideration, Equations 32 until 34. In both models, battery investment and capacity decisions are made on first stage. Thus, Equations 28, 29 and 30 are formulated equally for both models. In Equation 28, the power capacity is equal to the product of the BSS capacity and the power capacity ratio ($r^{Pcap}$). In Equation 29, the model formulation defines an upper bound ($cap^{BSS,max}$) for the battery capacity and Equation 30 derives the Annuity payment for the BSS investment ($Ann^{BSS}$). $Ann^{BSS}$ is the product of the battery capacity, the specific battery price ($c^{BSS}$) and the capital recovery factor ($CRF$). Next to the BSS annuity, both model formulations consider the annuity payment due to battery aging effects ($Ann^{BSS,aged}$)

defined in Equation 31. $Ann^{BSS,aged}$ considers the additional battery capacity that needs to be installed to compensate for the battery aging ($cap^{BSS,aged}$) further explained in Equation 35 and following. In the two stage model, $Ann^{BSS,aged}$ is defined singularly; in the multi-stage model, $Ann^{BSS,aged}$ is defined for every multi-stage scenario $sc$.

Equation 33 until Equation 36 represents the battery aging constraints. In both model formulations, battery aging is divided into two components, the cycle lifetime and the calendar lifetime of the battery. In case of the cycle lifetime, the number of full charging cycles must not surpass the cycle life of the battery. The key variable is the total amount of electricity charged ($x^{BS,ch,tot}$), in Equation 32. In the two-stage model, $x^{BS,ch,tot}$ is defined as the probability-weighted average of the sum of electricity charged ($x^{BSS,in}$) and the total amount of electricity charged for FCR activities ($x^{BSS,ch,FCR,tot}$) for every scenario per time frame with probability $\pi$. The expected values per time frame are summed up and multiplied with the respective weighting factor ($\rho$). In contrast, the multi-stage formulation defines $x^{BS,ch,tot}$ not as a single expected value but as multiple total amounts of electricity charged for every multi-stage scenario $sc$. In the multi-stage model, Equation 32 defines $x^{BS,ch,tot}$ as a state variable and considers the sum of electricity charged for every node in the same set of scenario nodes $S_{sc}$ multiplied by the respective weighting factor. Added to this is the total amount of electricity charged for FCR activities for the respective multi-stage scenario ($x_{sc}^{BSS,ch,FCR,tot}$).

In both formulations, $x^{BSS,ch,FCR,tot}$ is derived from the FCR bid multiplied by the mean amount of electricity needed for every $MW$ of FCR offered ($E^{FCR,mean}$), see Equation 33. To complete the cycle life component, Equation 34 converts the total amount of electricity charged into full load cycles by multiplying it with the ratio of calendar lifetime ($LT^{cal}$) and installed battery capacity. The number of full load cycles must always be smaller than the cycle lifetime ($LT^{cycl}$). In the two-stage model, Equation 34 refers to the expected value of full load cycles and, in the multi-stage model, it states that the full load cycle of every multi-stage scenario must not exceed the cycle life. The multi-stage formulation differs from Heredia et al. [28] who use the expected value of the full load cycle over all multi-stage scenarios.

In order to complete the assumed calendar lifetime of the battery, the model is able to compensate the calendar capacity loss by over-sizing the BSS. The additional installed capacity ($cap^{BSS,aged,cal}$) is defined in Equation 35 and refers to calendar aging due to high storage levels. In the two-stage model, $cap^{BSS,aged,cal}$ is declared as the expected value of the sum of the SOC for all time steps per time frame, summed up over all time frames considering the weighting factor. This summation is divided by the total number of time steps per year ($time^{tot}$) to derive the weighted average SOC per time step. To account for the calendar aging effect, the last term is multiplied by the calendar aging factor $r^{cal}$ concluded from Lunz et al. [30] and Kaschub et al. [31]. $r^{cal}$ describes the capacity loss if the SOC is at its maximum level over the whole lifetime. In the multi-stage model, the additional calendar capacity is defined as a state variable for every multi-stage scenario $sc$. Thus, Equation 35 calculates the average SOC for every time step of every node in the set of nodes of the respective scenario $S_{sc}$. Finally, Equation 36 considers the end-of-life condition and defines the additionally installed capacity to compensate battery aging ($cap^{BSS,aged}$) as the sum of the BSS capacity divided by the end-of-life-factor ($EoL$) and $cap^{BSS,aged,cal}$.

## 3. Case study results

In order to investigate the utility of the developed approach on a realistic industrial application, we develop a case study using data of a manufacturing company. This section splits into

three subsections. The first subsection 3.1 describes the case study. The subsections 3.2 and 3.3 present results of the case study. Additionally, it evaluates the plausibility of the two models as it identifies the most influential differences between the two model-formulations. Finally, subsection 3.4 quantifies the difference in profitably of the BSS for the two models and for a variation of the number of time frames, two or three, or the type, days or weeks.

### *3.1. Case study description*

The case study applies the method from section 2 to the load profile of a German manufacturing company for the production of die forgings from steel. The load profile data were recorded in 2016 and published inter alia in [32]. The other stochastic processes, next to the load profile, for this case study are the FCR market prices as well as the intraday and day-ahead market prices from the year 2017. For the FCR price, the case study considers the maximum price, for the intraday market the weighted-average price and for the day-ahead market the market clearing price. The assumed peak charges are in line with the listed charges in Baden-Württemberg, Germany, for the year 2016 on the medium voltage level. The minimum and maximum charges[1] are $35,470\,€/kW$ until $184,530\,€/kW$. The mean value among 100 grid operators is $44,460\,€/kW$[2].

| | *NoT* | |
|---|---|---|
| | 2 | 3 |
| $\Gamma$ | $\{1, 2, \ldots, 5\}$ | $\{1, 2, \ldots, 7\}$ |
| $SC$ | $\{1, 2, \ldots, 256\}$ | $\{1, 2, \ldots, 4096\}$ |
| $N$ | $\{1, 2, \ldots, 341\}$ | $\{1, 2, \ldots, 5461\}$ |

Table 5: Multi-stage input parameters

The case study considers different time frames ($TF$), either days or weeks, and a varying number of typical time frames ($NoT$), two days/weeks or three days/weeks. Table 5 presents the multi-stage sets that coincide with varying $NoT$. Additionally, Table 6 lists the input parameters and sets. Finally, the case study is evaluated for different set-ups, shown in the first three columns of Table 7. For nine different set-ups, either the input parameter peak charges or price factor are altered. The price factor describes the multiplicative factor for the intraday and day-ahead prices.

A k-means clustering approach derived from Covic et al. [15] attains the uncertainty realizations $\xi$ for the different stochastic processes. The case study considers different time frames ($TF$), either days or weeks, and a varying number of typical time frames ($NoT$), two days/weeks or three days/weeks. Therefore, the price and load profiles are divided into time frames for one year, either 365 or 52 profiles[3]. From the total number of time frames per year ($\#TF_{year}$) a k-means clustering algorithm concludes separate clusters for every time frame $w$. Every cluster is assorted a weighting factor $\rho_w$, which coincides with the number of time frames per cluster. From the first cluster, the k-means algorithm derives a second set of clusters for every realization $\xi \in \Xi$. Every realization is assorted a probability $\pi_{w,\xi}$, such that $\sum_{\xi} \pi_{w,\xi} = 1$. The chosen load profile for the case study is the median load profile of a realization cluster.

[1] These charges apply to consumers with more than 2,500 full load hours.

[2] These mean value is derived from charges of consumers with more and less than 2,500 full load hours.

[3] The FCR price clusters are constructed from weekly prices. Thus, for FCR, the considered time frame is weekly. For the daily consideration, the FCR price is divided by the number of weekdays.

| Parameter and sets | Unit | Value |
|---|---|---|
| $\Xi$ | | $\{1, 2, 3, 4\}$ |
| $S$ | | $\{1, 2, \ldots, 16\}$ |
| $c^{BSS}$ | $€/kWh$ | 650 |
| $\eta^{ch}$ | | 0.9 |
| $\eta^{dis}$ | | 0.9 |
| $\eta^{sdis}$ | | 0.02 |
| $EoL$ | | 0.8 |
| $cap^{BSS,fix}$ | $kWh$ | 1500 |
| $cap^{BSS,max}$ | $kWh$ | 10000 |
| $r^{Pcap}$ | | 1 |
| $r^{FCRmin}$ | | 0.5 |
| $r^{cal}$ | | 1/3 |
| $LT^{cal}$ | a | 11 |
| $LT^{cycl}$ | #cycles | 4000 |
| $puff^{FCR}$ | | 1.5 |
| $E^{FCR,mea}$ | $kWh$ | 4889.7 |
| $i$ | | 0.04 |
| $T^{inv}$ | a | 11 |

Table 6: Input parameter and sets

### *3.2. Model plausibility – FCR and arbitrage stage interdependencies*

This section discusses the results for the two-stage and multi-stage model runs and its plausibility for two typical days. The set-up of performing the optimization with only two typical days allows for low computational times. Additionally, it grants tractable overview of the results revealing the most important conclusions of the model comparison. This subsection elaborates on the effect of the interdependencies between the FCR stage and the arbitrage stage, while subsection 3.3 focuses on the effect of the cycle limitations.

Table 7 shows the results for model runs where the battery capacity is fixed at $1500\,kWh$ endogenously. Thus, the model is forced to install a BSS and the endogenous decision is only about peak load, FCR bidding, arbitrage trading and quarter-hourly dispatch. This allows for an easier understanding of the difference between the models' behavior. Table 7 column 6 shows the difference in the net present value (NPV) between the two-stage and multi-stage model in column 4 and 5. Furthermore, it shows the mean amount of FCR offered for all scenarios and typical days, column 7 and 8. For a fixed capacity of $1500\,kWh$, the maximum FCR bid is $1000\,MW$. Finally, the last two columns present the peak load the model chooses in the first stage.

For all set-ups, the NPV of the two-stage model is always greater than the NPV of the multi-stage model. For most of the set-ups, the mean FCR amount that is offered on the market is lower for the two-stage model than for the multi-stage model. Simultaneously, in most cases, the two-stage model achieves a greater peak load reduction than the multi-stage model. For one part, this can be explained by model-specific dependencies of the FCR bidding decision and the peak shaving decision. Both models choose the peak demand on the first stage. Nonetheless, the peak demand decision depends on the quarter hourly dispatch decision, which strongly depends on the load demand of the industrial process. In the two-stage model, this dispatch decision is made on the same stage as the FCR bidding decision. On this stage, the model can make a deterministic decision for both FCR, arbitrage trading and battery dispatch. In the multi-stage

model, the FCR decision is made on a stage prior to the arbitrage and dispatch decision. Thus, it is still stochastic in nature, as the model on the FCR stage only knows of the expected value resulting of the following stages.

Considering set-up 1 until 5 in Table 7, the parameter for the peak charges is increased from $10,000 €/kW$ until $100,000 €/kW$. Subsequently, the profitability of peak shaving increases as well. This results in higher values for $\Delta$peak for both models. Furthermore, the resulting values of $\text{FCR}_{\text{mean}}$ for set-ups 1 until 4 indicate a decreasing trend. Nonetheless, from set-up 4 to set-up 5 with the highest peak charges, the trend changes and the multi-stage value decreases rapidly. In this set-up, the two-stage model bids a mean value of $0.83\,MW$ and the multi-stage model a mean value of $0.65\,MW$, which indicates a reduction of 3% and almost 23% respectively. In case of the multi-stage model, one might assume a greater availability of idle resources of the BSS to reduce the peak demand. Nevertheless, the $\Delta$peak value for the two-stage model is still more than 40% larger than the multi-stage model value. The interdependence of the FCR decision and the uncertain arbitrage and dispatch decision lowers the profitability of the multi-stage model compared with two-stage approach.

Figure 3 illustrates this interdependence further. Figure 3 depicts the grid load profile of the energy system for one day and three different realizations. The grid load includes electricity drawn from the grid and fed into the grid. The dotted, horizontal lines indicate the FCR amount offered on that day corresponding to the respective color of the grid load profile. Furthermore, the upper graph shows the two-stage model results and the lower graph the multi-stage model results. Both results refer to the same FCR price realization as well as the same four load and arbitrage price realizations.

In the two-stage model, realizations 1 represent the load with the highest load shift. To achieve this high amount of shiftable load, the FCR bid in this scenario is minimal around 250 $kW$. Thus, a greater amount of idle capacity is available for peak shaving. Considering the load of realization 2, less load needs to be shifted to reach the same peak limit as in scenario s1. This results in a greater amount of capacity available for FCR activities, leading to a higher FCR bid around 800 $kW$. Finally, the load in realization 3 is below the peak limit. Thus, the maximum FCR bid, 1000 $kW$, is chosen in this scenario.

In the multi-stage model, the FCR decision is made on a stage prior to the arbitrage and dispatch stage. Therefore, the model chooses one single FCR bid indicated by one single horizontal FCR line in the multi-stage graph in Figure 3. The model chooses the FCR amount in such a way to leave enough of the BSS's capacity idle to allow for a successful peak shaving for either of the possible load demand profiles on the following stage. The multi-stage graph shows that the FCR level is chosen at roughly 700 $kW$. Compared to the two-stage results, the relatively high FCR bid reduces the peak shaving potential for grid load 1. In turn, this sets the overall peak limit. Therefore, for grid load 2, the peak reduction is smaller than in the two-stage scenario although the respective FCR-bid in the two-stage scenario is greater than the multi-stage bid and potentially greater amounts of idle BSS capacity in the multi-stage case is available. Because of the uncertainty consideration in the multi-stage model, the market potential is not fully exploited.

### *3.3. Model plausibility – Cycle limitations*

In Table 7, the results for set-up 6 until 9 reveal a second influential effect that results in a diverging profitability and dispatch decision for the two considered model approaches. This effects results from the way the two models consider the BSS's cycle limitations.

Set-ups 6 until 9 vary the price factor of the intraday and day-ahead prices. Thus, the price gap between low and high prices increases with an increasing price factor raising the profitability

| Set-up | $c_{peak}$ | Price factor | NPV two-stg | NPV mult-stg | ΔNPV | $FCR_{mean}$ two-stg | $FCR_{mean}$ mult-stg | Δpeak two-stg | Δpeak mult-stg |
|---|---|---|---|---|---|---|---|---|---|
| # | €/kW | - | k€ | k€ | k€ | MW | MW | kW | kW |
| 1 | 10000 | 1 | -13 | -80 | 67 | 0.95 | 0.92 | 107.1 | 170.24 |
| 2 | 20000 | 1 | -2 | -65 | 63 | 0.95 | 0.92 | 141.34 | 170.24 |
| 3 | 44460 | 1 | 47 | -25 | 72 | 0.9 | 0.88 | 344.0 | 195.08 |
| 4 | 70000 | 1 | 143 | 20 | 123 | 0.86 | 0.84 | 479.34 | 223.47 |
| 5 | 100000 | 1 | 278 | 94 | 184 | 0.83 | 0.65 | 546.97 | 347.97 |
| 6 | 44460 | 1 | 47 | -25 | 72 | 0.9 | 0.88 | 344.0 | 195.08 |
| 7 | 44460 | 2 | 315 | 174 | 141 | 0.85 | 0.83 | 262.0 | 233.0 |
| 8 | 44460 | 4 | 1082 | 619 | 463 | 0.72 | 0.66 | 107.12 | 325.0 |
| 9 | 44460 | 6 | 1899 | 1264 | 635 | 0.66 | 0.01 | 0.0 | -1.47 |

Table 7: Results for a fixed capacity of 1500 *kWh* and 2 typical days.

of the arbitrage business case. The effect of a more attractive arbitrage business case can be observed by considering the mean value of FCR bids. $FCR_{mean}$ decreases with an increasing price factor for both models. In the extreme case in set-up 9 with a price factor of 6, the multi-stage model does barely participate in the FCR market with a value of 0.01 $MW$, while the two-stage model still offers 0.66 $MW$. Additionally, the reduced peak load changes drastically with a rising price factor. Here, the two-stage model indicates different behavior than the multi-stage model. For the two-stage model, Δpeak reduces with an increasing price factor. With a rising price factor, the arbitrage business case appears more attractive than peak shaving. With a price factor of 6 no peak shaving is achieved, for the two-stage model, and, for the multi-stage model, Δpeak is slightly negative, with $-1.47$ $kW$. Thus, for the latter, the model exploits the price peaks and valleys, which results in a slight load increase. For the multi-stage model, the results indicate a rise in Δpeak at first. The model chooses to reduce the FCR bid as it is more profitable to pursue higher arbitrage peak shaving activities. Nonetheless, similar to the two-stage model, with a price factor of 6, Δpeak drops to near negative near zero and the FCR bid is close to zero.

| | Scenario | | | | | | | | | | | | | | | |
|---|---|---|---|---|---|---|---|---|---|---|---|---|---|---|---|---|
| | 1 | 2 | 3 | 4 | 5 | 6 | 7 | 8 | 9 | 10 | 11 | 12 | 13 | 14 | 15 | 16 |
| Day1 | 1 | 4000 | 649 | 1 | 1 | 4000 | 548 | 1 | 1 | 4000 | 548 | 1 | 1 | 4000 | 548 | 1 |
| Day2 | 1 | 4000 | 1258 | 1954 | 1 | 4000 | 1258 | 1887 | 1 | 4000 | 1258 | 1887 | 1 | 4000 | 1258 | 1887 |

Table 8: Rounded number of daily cycles in two-stage model for a fixed capacity of 1500 *kWh*, 2 typical days and set-up 9 with a price factor of 6.

As shown in Section 2 and more precisely in Equation 32 and Equation 34, the two-stage model uses the expected value of full cycles for all considered scenarios. Additionally, by definition, the two-stage model does not consider a consecutive order of the typical days. Thus, the two-stage formulation tents to overestimate the number of full cycles. As an example, Table 8 shows the results of full cycles per typical day and scenario of the two-stage model and set-up 12 with a price factor 6. Along with the probability of the scenario, the weighting factor of the typical day and the considered calendar life of 11 years, the total amount of full cycles is 4000, which is the maximum number of possible cycles [4]. Nonetheless, considering Table 8 and scenario 2, the number of cycles for both day 1 and day 2 is 4000. This effect overestimates the

[4] In both models and in every set-up, the maximum number of possible full cycles is always fully exploited.

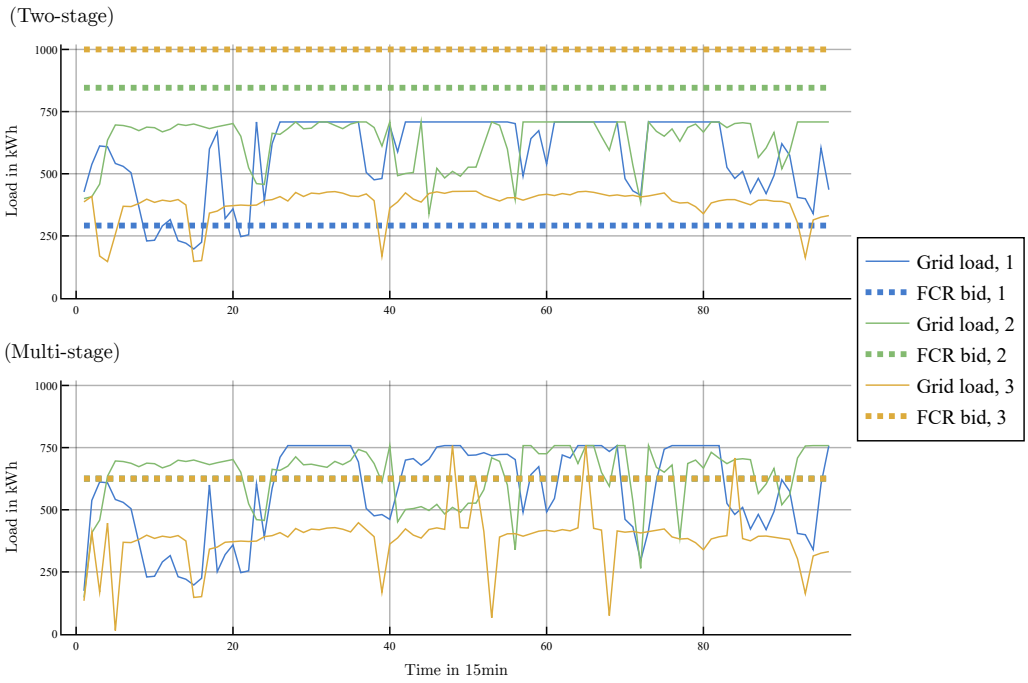


Figure 3: Results of grid load and FCR bid for one day with a fixed BSS capacity of 1500 $kWh$ for three exemplary realizations.

potential of the BSS as this specific dispatch for scenario 2 for both days would not hold up to reality. Nevertheless, these extreme values even out over all scenarios.

The multi-stage approach considers the consecutive order of scenarios and days and, set by Equation 34, the number of cycles for one scenario path cannot be greater than the maximum number of possible cycles. Figure 4 gives a visual illustration of this effect. It shows the SOC, shaded area, and the BSS charge and discharge as number of cycles over the lifetime, bar graph. Figure 4 shows the results for set-up 12 with a price factor of 6 where the highest dispatch activities are observable. The two-stage model fully exploits the maximum number of possible cycles in both days, which leads to 8000 cycles in this specific scenario. The multi-stage model exploits the maximum number of possible cycles over the whole time span of the 2 typical days. Figure 4 indicate a similar dispatch for both models on day 2. Nonetheless, the first day reveals less activity for the multi-stage model than for the two-stage model. This overestimation of the BSS's potential caused by the two-stage formulation is another explanation why the two-stage model calculates a higher NPV than the multi-stage model.

### *3.4. Quantifying the benefit of the multi-stage formulation*

This section investigates the influence of varying the number of typical days. The previous section used two typical days to allow for an easily accessible interpretation of model formulation differences. Nonetheless, the focus on only two typical days goes along with a high degree of uncertainties. Thus, this section expands the observations to three typical days and seven stages

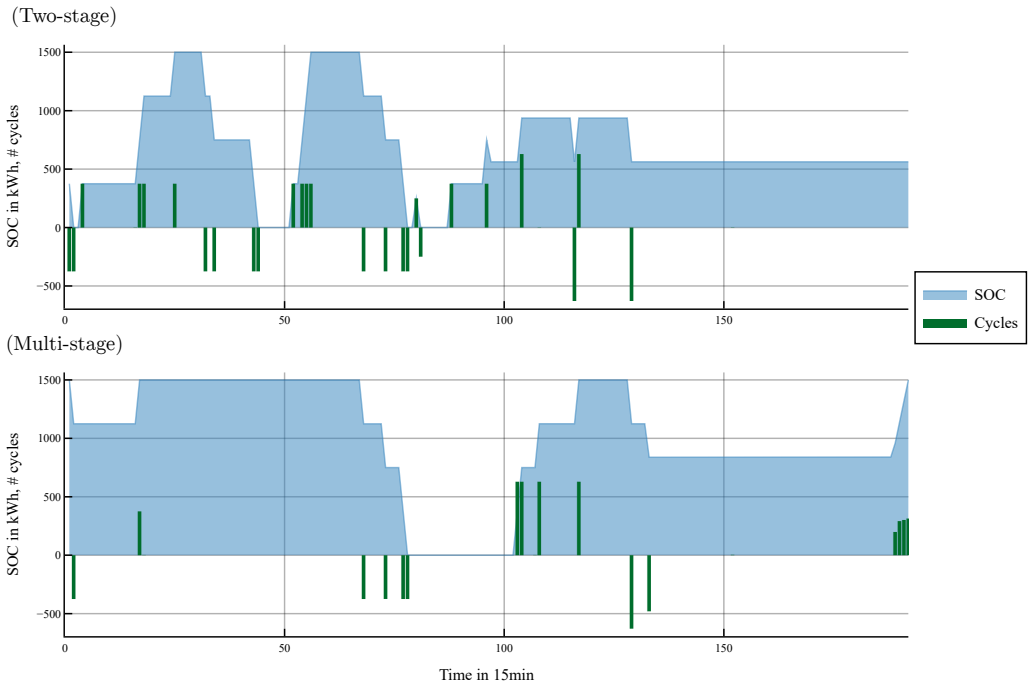


Figure 4: Results of SOC and full load cycles with a fixed BSS capacity of 1500 $kWh$ and set-up 9 with the maximum price factor 6 for the same FCR price and load realizations.

respective stages as well as two typical days with five stages. The varying considerations coincide with different load and price scenarios, for intraday, day-ahead and FCR market prices.

Figure A.6 shows the load profiles for the two-day, three-day and two-week observations and the respective four realizations in every time frame. Similarly, Figure A.7 presents the intraday price profiles. In Figure A.6 graphs 6 and 7, the considered industrial load profile represents, for most of the days, a weekday daylight production with high electricity demand during the day and low demand during nighttime and on the weekend. Additionally, it shows high demand volatility during the day and between the different weekdays. The weekly load behavior shows a high number of possible daily demand profiles that creates an under-representation of certain daily profiles when trying to fit the behavior into two typical days. This under-representation creates uncertainties, which are reduced when considering three typical days. Nevertheless, expanding to three days expands the complexity of the multi-stage model as it introduces two additional stages. From two days to three days, the number of multi-scenarios increases from 256 to 4096 and the number of nodes from 341 to 5461.

Figure 5 shows the results for varying time frames, two days and five stages, three days and seven stages as well as two weeks and five stages. It shows the NPV of the first seven case study set-ups where set-up 1-5 varies the peak charges and set-up 6-7 varies the price factor of arbitrage prices. The results indicate that the two-stage model always estimates a higher profit than the multi-stage model. Nonetheless, the NPV difference between the two model formulations appears smaller for the two-week consideration than for the daily consideration.

Overall, the results of the two-week time frame yield the lowest profitability compared to the other daily perspective. Comparing the two-day and three-day results, the considered three-day load realizations offer a higher peak shaving potential than the two-day profiles. Simultaneously, the combination of assumed price and load realization in the two-day framework offer higher revenues for arbitrage trading than the three-day perspective.

The above described observations are confirmed in Table 9 where, instead of an exogenous parameter, the BSS capacity is an endogenous decision variable for both models. Table 9 shows the results for installed BSS capacity and the NPV. For all time frames, the two-stage model yields higher profits than the multi-stage model while installing a larger BSS. The depicted set-up 3 considers mean peak charges and a price factor of 1. The greater peak shaving potential of the assumed three-day realization profiles results in the largest BSS capacity for the time frame. The smallest BSS is installed in the two-day framework for the multi-stage model. The difference between the two-stage and the multi-stage results varies for the capacity and the NPV. For the two-day perspective, the two-stage model installs a BSS that is more than three times as large as the multi-stage model's BSS. For the two-week case, the BSS is only 1.7 times as large. Nevertheless, it is the other way around for the NPV. Considering the two-day values, the two-stage model's NPV is roughly 1.9 times a large as the multi-stage NPV. For the two-week consideration, this factor is greater than 4.8.

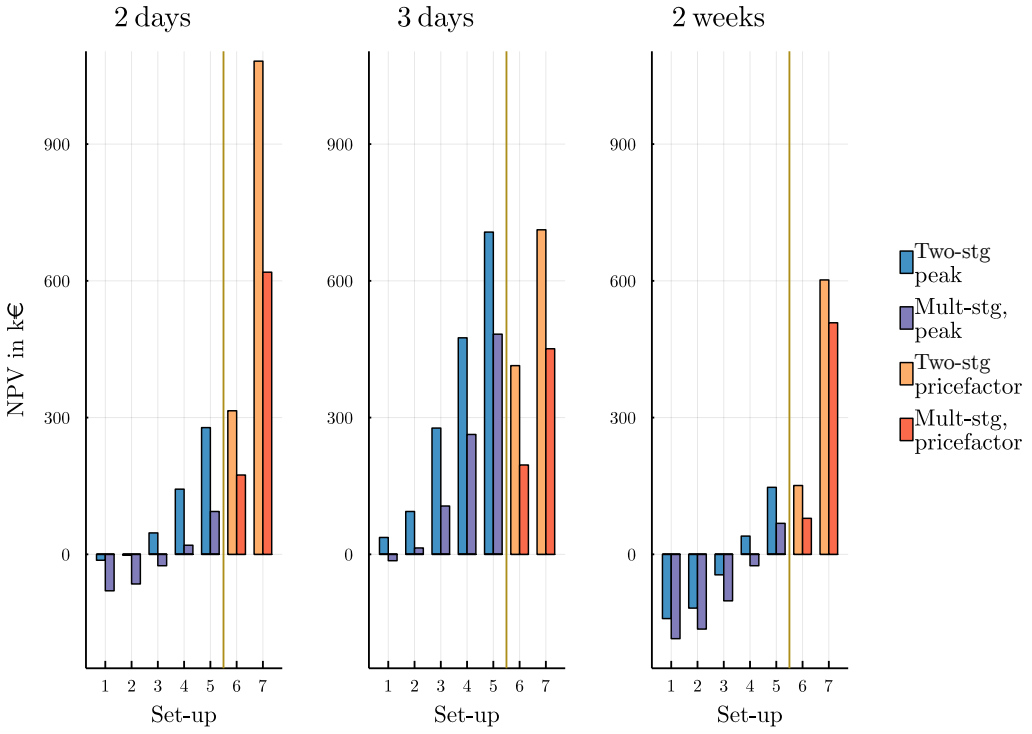


Figure 5: Comparing results for 2 days, 3 days and 2 weeks.

| | 2days | | 3days | | 2weeks | |
|---|---|---|---|---|---|---|
| | two-stg | mult-stg | two-stg | mult-stg | two-stg | mult-stg |
| Capacity in kWh | 525 | 157 | 5209 | 628 | 317 | 183 |
| NPV in k€ | 58 | 31 | 287 | 112 | 53 | 11 |

Table 9: Comparing results with variable BSS capacity for 2 days, 3 days and 2 weeks for set-up 3.

### *3.5. Computational expenses*

The case study was calculated on a Windows 64-bit machine with an Intel Xeon Gold CPU with 3.00$GHz$, 48 Kernels, 96 logical processors and 256$GB$ of RAM. The optimization models were implemented in Julia with the Julia specific optimization language JuMP and solved with the Gurobi solver.

Table 10 describes the computational expenses of the two model approaches. It shows the matrix dimensions of the respective optimization problem after the pre-solve operations of the Gurobi solver, which eliminates redundant equations and variables. Additionally, Table 10 shows the results for case studies of two days, three days and two weeks each with endogenous model decision on the BSS capacity and for set-up 3 as described in section 3.1.

Table 10 shows that the solving time of the two-stage model is much faster than the respective multi-stage solving time, which can be explained when looking at the respective problem size, which appears relatively small. The smallest two-stage problem is derived from the two-day use case, where 16 scenarios (see $S$ in Table 6) for every day and its 96 time steps leads to 28 321 equations with a solving time of 1.6 seconds. The second-largest two-stage problem is for the 3 days use case; here the model is expanded by an additional day with 16 scenarios. Although the two-week case study considers fewer scenarios than the three-day use case, the number of time steps per scenario increases by factor seven compared to the weekly consideration. Thus, the largest two-stage problem appears for the two-week use case with 197 921 equations and a solving time of 35.06 seconds.

The results for the multi-stage model formulation in Table 10 are ordered differently due to the exponential behavior of multi-stage scenario trees also known as the *curse of dimensionality* [33]. Here, the 2 days use case yields the smallest problem with 240 756 equations and a solving time of 18.55 seconds. Nevertheless, the number of equations is almost five times as large as the number of equations for the respective two-stage problem. This is due to the fact, that the multi-stage model considers the two days on five stages resulting in 256 scenarios (see Table 5) compared to 16 scenarios for 2 days of the two-stage model. The 2 weeks use case considers the same amount of stages extended by the number of weekly time steps. Considering the multi-stage formulation of the 3 days use case, Table 10 reveals an exponential jump in solving time from 443.04 seconds for 2 weeks to approximately 10.48 hours. This is a result of the basic multi-stage scenario tree characteristic that the number of scenarios grows with every stage exponentially[5].

## 4. Critical review

This study divides the industrial load behavior into typical days or weeks. While the division into typical days allows for an approachable illustration of the interdependencies of consecutive

[5]Considering a 3 weeks use case would expand the multi-stage problem further, leading to a solving time of around 65 hours

| | | 2 days | 2 weeks | 3 days |
|---|---|---|---|---|
| Two-stage | Equations | 28 321 | 197 921 | 42 481 |
| | Variables | 17 538 | 122 610 | 26 306 |
| | Non-zeros | 135 393 | 946 049 | 203 089 |
| | Solving time | 1.6 *sec* | 35.06 *sec* | 3.55 *sec* |
| Multi-stage | Stages | 5 stages | 5 stages | 7 stages |
| | Equations | 240 756 | 1 681 700 | 3 866 228 |
| | Variables | 148 870 | 1 041 590 | 2 390 406 |
| | Non-zeros | 1 147 144 | 8 018 536 | 18 818 568 |
| | Solving time | 18.55 *sec* | 443.04 *sec* | $\approx$ 10.48 *h* |

Table 10: Computational expenses of the two-stage and multi-stage model with variable BSS capacity for set-up 3.

market decisions, a daily depiction might not be suitable for most industrial processes to account for the load profile's heterogeneity. Here, a weekly representation or a consideration of a large variety of typical days might be more accurate. In this context, the analysis of the computational expenses reveals the multi-stage formulation's downside to incorporate large number of possible realizations per stage. If the heterogeneity of random realizations is important, the two-stage-approach might be more feasible; if the effect of consecutive decisions needs to be studied, the multi-stage formulation might be more appropriate.

The consideration of the BSS degradation and the BSS cycle limitations in a multi-stage problem is the key contribution of this study. Nevertheless, the BSS degradation model is still a simplification of reality. A more accurate model such as the consideration of the c-rate's effect[6] on BSS aging usually coincides with a higher model complexity due to non-linear constraints. Additionally, the scenario path dependency of the dispatch decisions due to the cycle limitations already introduces additional complexity to the model. Therefore, a quantification of such degradation effects is needed to better approximate the aging effect in order to reduce the solving time of the multi-stage model. Such an approximation might allow for an efficient decomposition of the scenario tree.

The case study results indicate that the economic performance of the two models depends on the chosen stochastic price and load scenarios. The interaction of peak prices, peak load and general load behavior, has a strong influence on the profitability of the BSS. These observations emphasize the importance of scenario generation. Especially for long term investment decisions with high yearly fluctuations of load profiles as in industry and volatile prices and market schemes, the scenarios need to be carefully considered.

Considering the real life application to a German manufacturing company, this study focuses on the economically most relevant uncertainties, FCR bidding and peak shaving with FCR prices and load behavior considered uncertain. Previous studies showed that these two business models yield the highest potential revenues and allow for a profitable BSS operation that is less demanding on the BSS degradation. Nevertheless, other uncertainties and inaccuracies exist that were not part of the model formulations but need to be kept in mind when evaluating the results. Inter alia, the case study's typical time frames are considered as representative over the whole life span. Furthermore, the random realizations of the load profile and spot market prices are sampled together, although being independent in reality. Finally, the sizes of FCR market bids

[6]The c-rate describes the charging rate of a battery cell and the higher the c-rate the faster a BSS charges. High c-rates reduce the BSS lifetime.

are modelled as continuous variables assuming an aggregator pooling bids of different suppliers, although the current market regulation only allow for discrete bid sizes.

## 5. Conclusion

This study develops a multi-stage stochastic optimization model to investigate the optimal investment decision for a BSS in industry and compares it to a two-stage model approach. We consider the stochastic behavior of FCR, day-ahead and intraday market prices, as well as the electrical load of an industrial manufacturing process in Germany. The chosen objective function results in a maximization of the revenue through peak shaving, FCR market participation and energy arbitrage through the BSS and is applied to time periods of either two or three typical days or two typical weeks.

The results of the developed multi-stage formulation show, that investment in a BSS is an economically feasible option for the manufacturing company investigated in this paper's case study. While the results vary with the choice of the number of representative days or weeks, the longest investigated period of two weeks shows a positive NPV for the default set-up 7, resulting in an optimal BSS investment of 183 kWh.

The results of the comparison with the two-stage formulation prove the hypothesis for a stochastic BSS investment problem in industry that the two-stage stochastic optimization approach neglects operational risks. Compared to the multi-stage model, the two-stage formulation overestimates the profitability of the BSS. The two-stage model needs to abstract from the consecutive order of operational decisions, thus, neglects the outcome of subsequent uncertainty realizations. In the considered case study, this is true for the interaction between the FCR bid and the consequent BSS dispatch decisions for peak shaving or arbitrage trading. Additionally, the two-stage formulation reduces the limiting effects of battery degradation and cycle life constraints.

Future research should focus on applying this study's observations to different industrial load profiles to assess the effect of different input parameters on the model results. Additional, studies should incorporate more advanced scenario generation techniques to derive real life implications. Finally, it is an exciting field to investigate various solving methods for this study's multi-stage problem. The large number of state variables creates a relatively complex problem. Appropriate solving techniques would allow for the consideration of additional scenarios and market decision stages.

## Declaration of competing interest

The authors declare that they have no known competing financial interests or personal relationships that could have appeared to influence the work reported in this paper.

## Appendix A. Input load profiles and price profiles

## References

[1] A. Alqurashi, A. H. Etemadi, A. Khodaei, Treatment of uncertainty for next generation power systems: State-of-the-art in stochastic optimization, Electric Power Systems Research 141 (2016) 233–245. doi:10.1016/j.epsr.2016.08.009.

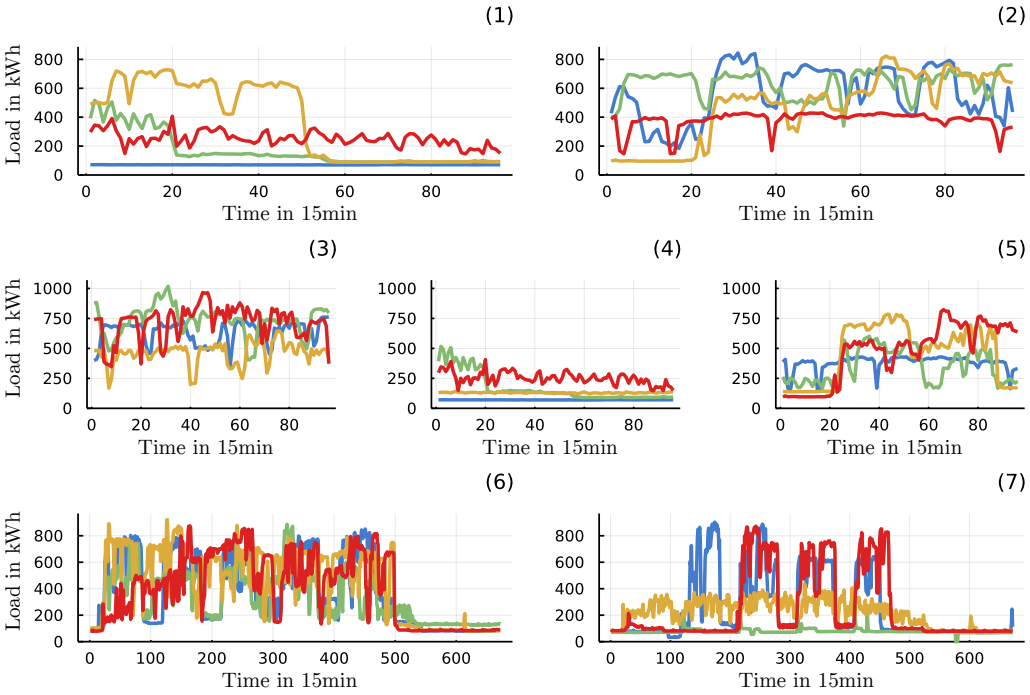


Figure A.6: Load profiles for 2 days (numbers 1 and 2), 3 days (numbers 3, 4 and 5) and 2 weeks (numbers 6 and 7) showing the four considered realizations.


[2] M. J. Vahid-Pakdel, S. Nojavan, B. Mohammadi-ivatloo, K. Zare, Stochastic optimization of energy hub operation with consideration of thermal energy market and demand response, Energy Conversion and Management 145 (2017) 117–128. doi:10.1016/j.enconman.2017.04.074.

[3] R. S. Go, F. D. Munoz, J.-P. Watson, Assessing the economic value of co-optimized grid-scale energy storage investments in supporting high renewable portfolio standards, Applied Energy 183 (2016) 902–913. doi:10.1016/j.apenergy.2016.08.134.

[4] Y. Tohidi, M. Gibescu, Stochastic optimisation for investment analysis of flow battery storage systems, IET Renewable Power Generation 13 (2019) 555–562. doi:10.1049/iet-rpg.2018.5788.

[5] H. Pandžić, Optimal battery energy storage investment in buildings, Energy and Buildings 175 (2018) 189–198. doi:10.1016/j.enbuild.2018.07.032.

[6] H. Schwarz, H. Schermeyer, V. Bertsch, W. Fichtner, Self-consumption through power-to-heat and storage for enhanced pv integration in decentralised energy systems, Solar Energy 163 (2018) 150–161. doi:10.1016/j.solener.2018.01.076.

[7] H. Schwarz, V. Bertsch, W. Fichtner, Two-stage stochastic, large-scale optimization of a decentralized energy system: a case study focusing on solar pv, heat pumps and storage in a residential quarter, OR Spectrum 40 (2017) 265–310. doi:10.1007/s00291-017-0500-4.

[8] E. Chatterji, M. D. Bazilian, Smart meter data to optimize combined roof-top solar and battery systems using a stochastic mixed integer programming model, IEEE Access 8 (2020) 133843–133853. doi:10.1109/ACCESS.2020.3010919.

[9] Z. Zheng, X. Li, J. Pan, X. Luo, A multi-year two-stage stochastic programming model for optimal design and operation of residential photovoltaic-battery systems, Energy and Buildings 239 (2021) 110835. doi:10.1016/j.enbuild.2021.110835.

[10] X. Shen, Z. Luo, J. Xiong, H. Liu, X. Lv, T. Tan, J. Zhang, Y. Wang, Y. Dai, Optimal hybrid energy storage system planning of community multi-energy system based on two-stage stochastic programming, IEEE Access 9 (2021) 61035–61047. doi:10.1109/ACCESS.2021.3074151.

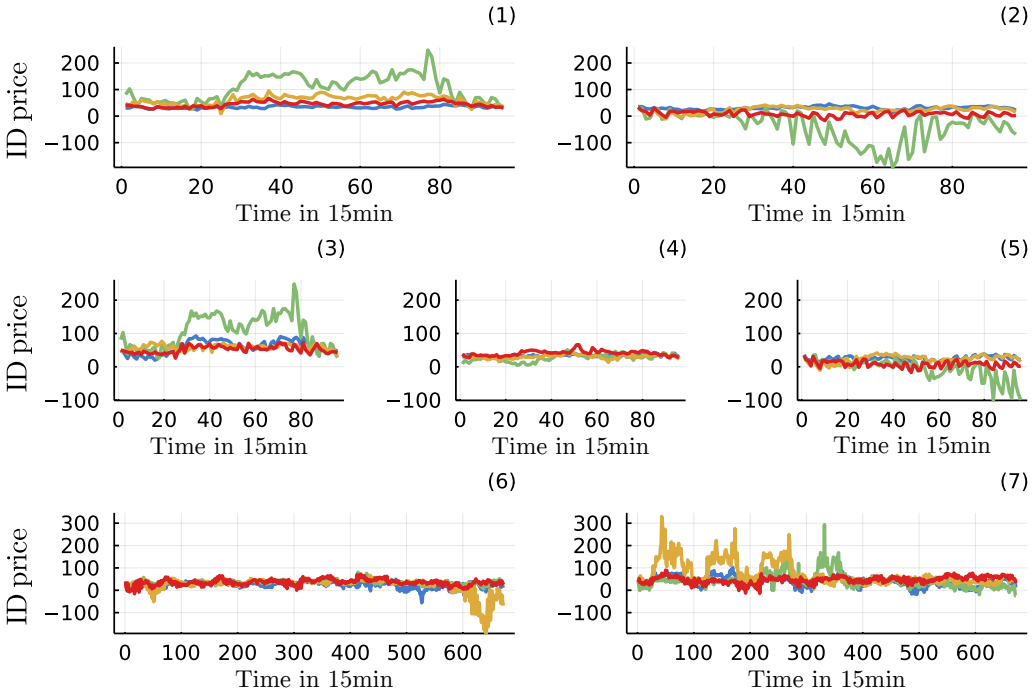


Figure A.7: Price profiles for 2 days (numbers 1 and 2), 3 days (numbers 3, 4 and 5) and 2 weeks (numbers 6 and 7) showing the four considered realizations.


[11] C. Chen, H. Sun, X. Shen, Y. Guo, Q. Guo, T. Xia, Two-stage robust planning-operation co-optimization of energy hub considering precise energy storage economic model, Applied Energy 252 (2019) 113372. doi:10.1016/j.apenergy.2019.113372.

[12] H. Alharbi, K. Bhattacharya, Stochastic optimal planning of battery energy storage systems for isolated microgrids, IEEE Transactions on Sustainable Energy 9 (2018) 211–227. doi:10.1109/TSTE.2017.2724514.

[13] J. M. Ortiz, W. Kracht, G. Pamparana, J. Haas, Optimization of a sag mill energy system: Integrating rock hardness, solar irradiation, climate change, and demand-side management, Mathematical Geosciences 52 (2020) 355–379. doi:10.1007/s11004-019-09816-6.

[14] G. Mohy-ud din, D. H. Vu, K. M. Muttaqi, D. Sutanto, An integrated energy management approach for the economic operation of industrial microgrids under uncertainty of renewable energy, IEEE Transactions on Industry Applications 56 (2020) 1062–1073. doi:10.1109/TIA.2020.2964635.

[15] N. Covic, F. Braeuer, R. McKenna, H. Pandzic, Optimal pv and battery investment of market-participating industry facilities, IEEE Transactions on Power Systems 36 (2021) 3441–3452. doi:10.1109/TPWRS.2020.3047260.

[16] S. Rebennack, A unified state-space and scenario tree framework for multi-stage stochastic optimization: An application to emission-constrained hydro-thermal scheduling, Dissertation at the University of Florida (2010).

[17] M. Kaut, K. T. Midthun, A. S. Werner, A. Tomasgard, L. Hellemo, M. Fodstad, Multi-horizon stochastic programming, Computational Management Science 11 (2014) 179–193. doi:10.1007/s10287-013-0182-6.

[18] C. L. Lara, J. D. Siirola, I. E. Grossmann, Electric power infrastructure planning under uncertainty: stochastic dual dynamic integer programming (sddip) and parallelization scheme, Optimization and Engineering 21 (2019) 1243–1281. doi:10.1007/s11081-019-09471-0.

[19] S. Agrali, F. Terzi, E. Canakoglu, E. Adiyeke, Y. Arikan, Energy investment planning at a private company: A mathematical programming-based model and its application in turkey, IEEE Transactions on Power Systems 32 (2017) 4180–4187. doi:10.1109/TPWRS.2017.2676819.

[20] A. Bhattacharya, J. P. Kharoufeh, B. Zeng, Managing energy storage in microgrids: A multistage stochastic programming approach, IEEE Transactions on Smart Grid 9 (2018) 483–496. doi:10.1109/TSG.2016.2618621.

[21] M. K. Şahin, Ö. Çavuş, H. Yaman, Multi-stage stochastic programming for demand response optimization, Computers & Operations Research 118 (2020) 104928. doi:10.1016/j.cor.2020.104928.

[22] F. Hafiz, A. Rodrigo de Queiroz, P. Fajri, I. Husain, Energy management and optimal storage sizing for a shared community: A multi-stage stochastic programming approach, Applied Energy 236 (2019) 42–54. doi:10.1016/j.apenergy.2018.11.080.

[23] D. Keles, J. Dehler-Holland, Evaluation of photovoltaic storage systems on energy markets under uncertainty using stochastic dynamic programming, Energy Economics 106 (2022) 105800. doi:10.1016/j.eneco.2021.105800.

[24] X. Wu, W. Zhao, H. Li, B. Liu, Z. Zhang, X. Wang, Multi-stage stochastic programming based offering strategy for hydrogen fueling station in joint energy, reserve markets, Renewable Energy 180 (2021) 605–615. doi:10.1016/j.renene.2021.08.076.

[25] D. Badanjak, H. Pandzic, Battery storage participation in reactive and proactive distribution-level flexibility markets, IEEE Access 9 (2021) 122322–122334. doi:10.1109/ACCESS.2021.3109108.

[26] M. H. Abbasi, M. Taki, A. Rajabi, L. Li, J. Zhang, Coordinated operation of electric vehicle charging and wind power generation as a virtual power plant: A multi-stage risk constrained approach, Applied Energy 239 (2019) 1294–1307. doi:10.1016/j.apenergy.2019.01.238.

[27] H. Khaloie, A. Abdollahi, M. Shafie-khah, A. Anvari-Moghaddam, S. Nojavan, P. Siano, J. P. Catalão, Coordinated wind-thermal-energy storage offering strategy in energy and spinning reserve markets using a multi-stage model, Applied Energy 259 (2020) 114168. doi:10.1016/j.apenergy.2019.114168.

[28] F.-J. Heredia, M. D. Cuadrado, C. Corchero, On optimal participation in the electricity markets of wind power plants with battery energy storage systems, Computers & Operations Research 96 (2018) 316–329. doi:10.1016/j.cor.2018.03.004.

[29] F. Braeuer, J. Rominger, R. McKenna, W. Fichtner, Battery storage systems: An economic model-based analysis of parallel revenue streams and general implications for industry, Applied Energy 239 (2019) 1424–1440. doi:10.1016/j.apenergy.2019.01.050.

[30] B. Lunz, Z. Yan, J. B. Gerschler, D. U. Sauer, Influence of plug-in hybrid electric vehicle charging strategies on charging and battery degradation costs, Energy Policy 46 (2012) 511–519. doi:10.1016/j.enpol.2012.04.017.

[31] T. Kaschub, P. Jochem, W. Fichtner, Solar energy storage in german households: profitability, load changes and flexibility, Energy Policy 98 (2016) 520–532. doi:10.1016/j.enpol.2016.09.017.

[32] F. Braeuer, Load profile data of 50 industrial plants in germany for one year: (version 1.0), zenodo dataset (2020). doi:10.5281/zenodo.3899018.

[33] W. B. Powell, Approximate dynamic programming: Solving the curses of dimensionality, Wiley series in probability and statistics, 2nd ed. ed., Wiley, Hoboken, N.J, 2011. URL: https://onlinelibrary.wiley.com/doi/book/10.1002/9781118029176. doi:10.1002/9781118029176.

# Publication D

## Comparing empirical and model-based approaches for dynamic grid emission factors: an application to $CO_2$-minimizing storage dispatch in Germany

Fritz Braeuer[a], Rafael Finck[a], Russell McKenna[b]

[a]*Chair of Energy Economics, Institute for Industrial Production, Karlsruhe Institute of Technology, Karlsruhe, Germany*

[b]*DTU Management Engineering, Technical University of Denmark (DTU), Kgs. Lyngby, Denmark*

Published in:

Journal of Cleaner Production, Volume 266, 1st of September 2020, 121588

https://doi.org/10.1016/j .jclepro.2020.121588

Journal of Cleaner Production 266 (2020) 121588

Contents lists available at ScienceDirect

Journal of Cleaner Production

journal homepage: www.elsevier.com/locate/jclepro

# Comparing empirical and model-based approaches for calculating dynamic grid emission factors: An application to $CO_2$-minimizing storage dispatch in Germany

Fritz Braeuer [a, *], Rafael Finck [a], Russell McKenna [b]

[a] Chair of Energy Economics, Institute for Industrial Production (IIP), Karlsruhe Institute of Technology (KIT), Karlsruhe, Germany
[b] Energy Systems Analysis, DTU Management, Technical University of Denmark (DTU), Kgs. Lyngby, Denmark

ARTICLE INFO

*Article history:*
Received 9 January 2020
Received in revised form
6 April 2020
Accepted 8 April 2020
Available online 26 April 2020

Handling editor: Jin Yang

*Keywords:*
Dynamic emission factors
Empirical emission factors
$CO_2$-minimizing dispatch
Energy storage system
German industry
$CO_2$ emissions

ABSTRACT

As one possibility to increase flexibility, battery storage systems (BSS) will play a key role in the decarbonization of the energy system. The emissions-intensity of grid electricity becomes more important as these BSSs are more widely employed. In this paper, we introduce a novel data basis for the determination of the energy system's $CO_2$ emissions, which is a match between the ENTSO-E database and the EUTL databases. We further postulate four different dynamic emission factors (EF) to determine the hourly $CO_2$ emissions caused through a change in electricity demand: the average emission factor (AEF), the marginal power mix (MPM), the marginal system response (MSR) and an energy-model-derived marginal power plant (MPP). For generic and battery storage systems, a linear optimization on two levels optimizes the economic and environmental storage dispatch for a set of 50 small and medium enterprises in Germany. The four different emission factors have different signaling effects. The AEF leads to the lowest $CO_2$ reduction and allows for roughly two daily cycles. The other EFs show a higher volatility, which leads to a higher utilization of the storage system from 3.4 to 5.4 daily cycles. The minimum mean value for $CO_2$ abatement costs over all 50 companies is 14.13 €/$t_{CO_2}$.



## 1. Introduction

In light of global decarbonization efforts, flexibility becomes increasingly important in energy systems (Ruppert et al., 2020). Energy storage systems (ESSs) in industry can contribute to the needed flexibility in two ways: First, they allow for a time variable consumption of electricity in good adaptation to volatile supply of renewable energies (Guney, 2017; Rashid et al., 2020). Thus, they ensure both security of supply and price stability for consumers. Second, they enable consumers to reduce their carbon footprint with respect to electricity drawn from the grid, if the carbon intensity is sufficiently signalled. The high and volatile load profile in industry is a key premise for a profitable utilization of flexible storage systems (Lund et al., 2015). Simultaneously, in energy systems where the power plant fleet comprises a variety of technologies, the $CO_2$ emissions change considerably over the course of one day (Rashid et al., 2019; Alsema, 2012). This holds true for average system emissions in one hour as well as for the marginal power plant, which responds to an incremental increase in electricity demand. ESSs offer a great potential to reduce the $CO_2$ footprint of energy intensive industry and $CO_2$ emissions of the energy system as they can charge/discharge in hours of low/high emissions.

Identifying these hours and incentivizing storage providers to utilize their flexibility potential to reduce greenhouse gas (GHG) emissions is no trivial task. Due to the missing internalization of cost, which are related to GHG emissions, market prices in most power markets do not reflect GHG intensity of the respective marginal technology. Hence a clear price signal is missing to incentivize $CO_2$-reducing charging or discharging behaviour. This problem can be solved by hourly emission factors (EFs), which signal $CO_2$ intensity to storage operators.

A number of researchers study dynamic $CO_2$ EFs. Most researchers apply dynamic EFs to evaluate charging strategies of electric vehicles (EVs). Axsen et al. (2011) consider the owner's behavior on $CO_2$ emissions in California. Jansen et al. (2010) extend their study on EV-emissions onto the western grid of the U.S. Kintner-Meyer et al. (2007) assess the technological load shifting

* Corresponding author.
*E-mail address:* fritz.braeuer@kit.edu (F. Braeuer).

https://doi.org/10.1016/j.jclepro.2020.121588
0959-6526/

**Nomenclature**

*Acronyms*

| | |
|---|---|
| AEF | average emission factor |
| BSS | battery storage systems |
| CHP | combined heat and power |
| EEMM | European electricity market model |
| EF | emission factor |
| ESM | energy storage model |
| ESS | energy storage system |
| ETS | emission trading system |
| EUTL | European Union Transaction Log |
| GHG | greenhouse gas |
| LCPD | Large Combustion Plants Directive |
| MEF | marginal emission factor |
| MPM | marginal power mix |
| MPP | marginal power plant |
| MSR | marginal system response |
| RES | renewable energy sources |
| SME | small and medium sized enterprises |

*Variables and parameters*

| | |
|---|---|
| $A_{ESS}$ | annuity for ESS [€] |
| $cap_{ESS,econ}$ | capacity of ESS of economic dispatch [kWh] |
| $cap_{ESS,envir}$ | capacity of ESS of environmental dispatch |
| $P_{peak}$ | peak power from grid per year [MW] |
| $p_{peak}$ | peak price [ €/*kWa*] |
| $x_{el,t}$ | electrical energy flow [kWh] |

*Symbols*

| | |
|---|---|
| $\Delta CO_2$ | avoided $CO_2$ emissions |
| $C_{abat}$ | $CO_2$ abatement cost |
| $C_{el}$ | cost for electricity |
| $cap_{stg}$ | capacity of storage |
| $charg_{stg}$ | energy charged in storage per year |
| $cycle_{day}$ | full daily cycles |
| $E$ | energy |
| $EF$ | emission factor |
| $L$ | load |
| $LT$ | life time |
| $m_{CO_2}$ | mass of $CO_2$ |
| $u_{cap}$ | utilization factor |

*Indices*

| | |
|---|---|
| exp | export |
| h | hour of a day |
| i | company |
| imp | import |
| j | power Plant |
| k | emission factor |
| Res | residual |
| RES | renewable energy sources |
| t | hour of the year |
| tot | total amount per year |

potential of EVs in the U.S. while Stephan and Sullivan (2008) study the impact of night time charging and Tamayao et al. (2015) analyse the life cycle emissions for EVs on the U.S. market. In contrast, Jochem et al. (2015) focus on the impact of EVs on the German energy system. One important result of these studies is that considering times of low emissions for the charging strategies reduces the overall $CO_2$-emissions substantially. The applied average and marginal EFs are results of different energy system models, which study the reaction of the energy system to different scenarios. Few studies consider the dynamic influence of emissions on the operation of stationary storage technologies. Hittinger and Azevedo (2015) studied the impact of bulk central energy storage systems on the emissions of the U.S. energy system; Arciniegas and Hittinger (2018) build up on this research and implement a multi-objective optimization of the storage operation considering economic and ecologic factors. Section 2 presents an extensive discussion on existing literature and identifies the following deficiencies in the literature on dynamic EFs and energy storage systems:

- No study derives dynamic EFs for the German energy system based on empirical data.
- No study investigates the environmental dispatch of ESS in industry.

In this study, we develop four different EFs, three based on empirical data and one model-based, to understand the average and marginal emissions of an energy system. The application to the German energy system is a novelty in the literature. We use these EFs to analyse the $CO_2$ emission abatement potential for 50 small to medium sized companies. An additional novel contribution is the development of a two-step approach based on Braeuer et al. (2019a), in which we first identify the optimal investment and dispatch of an EES from an economic perspective (*economic dispatch*) followed by the second step, in which the storage system is utilized to minimize the $CO_2$ intensity of the electricity drawn from the grid (*environmental dispatch*). This energy storage model (ESM) is formulated as a linear optimization model with perfect foresight. Thus, $CO_2$ abatement costs for the different companies can be formalized and used by decision-makers to compare the ESS to other reduction measures at their disposal.

This paper formulates four different EFs in hourly resolution. The main focus is on $CO_2$ emissions. The empirical $CO_2$ EFs are derived by joining the transparency platform of the European Network of Transmission System Operators for Electricity (ENTSO-E) with the European Union Transaction Log (EUTL) database, linking power output to reported emissions. This is the final novel contribution to the literature. Additionally, EFs for other emissions, $SO_2$, $NO_x$ and Dust, are derived from combining the ENTSO-E-database and the large combustion plants directive (LCPD) and shown in the Supplementary Information SI E. The empirical EFs are the average EF (*AEF*), the marginal system response (*MSR*) and the EF based on Hawkes (2010) (*MPM*). These EFs are compared to a model-based marginal power plant (*MPP*). It is result of a European electricity market model (EEMM).

The key objectives of this paper are the following:

1. Derive dynamic EFs for the German energy system from empirical and model data
2. Investigate the effect of four different EFs on the environmental dispatch of the ESS

3. Evaluate the $CO_2$ reduction potential of ESSs for different industrial load profiles.

## 2. Literature review

No standardized method to assess the EF of a country's or region's power mix has been presented in the scientific literature. Yang (2013) and Ryan et al. (2018) give an overview of the different dimensions to consider when calculating EFs. Yang (2013) divides these dimensions into scenario based (prospective) vs. system based (retrospective), aggregated vs. temporally explicit and average vs. marginal. Ryan et al. (2018) present an algorithm to guide the practitioner's selection of the appropriate EF fitting to their specific use case. For this study, we only consider dynamic EFs. Static and aggregated EFs are not further investigated. To assess dynamic EFS, we identify three approaches mentioned in recent scientific publications:

1. Marginal power mix (MPM)
2. Marginal power plant (MPP)
3. Average power mix (AEF).

For MPM, a linear regression model and historical data are used to compare the change in the generation to the change in $CO_2$ emissions of the electricity mix. The base definition of the MPM was first presented by Hawkes (2010) and Holland and Mansur (2008). The MPP approach determines the marginal power plant, which reacts to a marginal change in demand. Usually, it is a simulation or optimization model based approach. Tamayao et al. (2015) differentiates between these two approaches as top-down respectively bottom-up methods. The AEF relates the total $CO_2$ emissions to the total energy generated. Spork et al. (2015) present the method for a dynamic AEF applied to the Spanish electricity system. All three EFs can be disaggregated in different temporal resolutions. Furthermore, these approaches can be differentiated by their system boundaries. Tamayao et al. (2015) divides them into consumption based EFs, which consider exchange over the system boundaries and production based EFs, which take only the inner system production units into account. Table A4 summarizes the reviewed literature and SI A further reviews literature on MPM and MPP.

The MPM is based on empirical data. It depends strongly on the quality and accessibility of the data. The advantage of the MPM is that it does not need further assumptions regarding the pricing strategy of the power plants. A disadvantage is the lack of informative value for future scenarios. For the MPP, a variety of assumptions regarding inputs enable the incorporation of future developments into the model. At the same time, this makes the comparability of different model results difficult. For both approaches, the system boundaries need to be considered and it should be distinguished between a consumption based and a production based approach. Furthermore, many studies compare either EF to the AEF. While the AEF is seen as the intuitive approach, commonly applied to formulate political implications, Axsen et al. (2011) raise the question if a marginal emission factor (MEF) or an AEF is the appropriate measure. They conclude, the appropriateness depends on how "new and existing electricity demand" is valued (Axsen et al., 2011, p.1621). Yang (2013) consider the AEF suitable to "assign the emissions to all electricity load" while MEF help "understand the change in total electricity emissions" with the increase in demand (Yang, 2013, p.724). Tamayao et al. (2015) explicitly deem the AEF as "conceptually inappropriate for assessing" additional demand technologies. Ryan et al. (2018) propose that the appropriate method to evaluate additional, dynamic electricity demand is the MPP. For all studies considered, the MPP or MPM always surpasses the AEF. Regett et al. (2018) find "even hours for which the two methods show significantly opposing results." They advice that the appropriateness of the different methods depends strongly on the applications and research question.

## 3. Methodology

The methodological approach consists of three sections, as shown in Fig. 1. Section 3.1, data preparation, matches two different databases to derive individual EFs per power plant for the $CO_2$ emissions. Section 3.2 calculates the four dynamic EFs to describe the hourly behaviour of the German electricity system. In section 3.3, the final step is the ESM-model to determine an economic and environmental dispatch for an ESS in industry. Section 3.4 defines the performance indicators used for the analysis.

### 3.1. Data preparation

To derive hourly emission profiles of the German energy system, we combined information of two databases: The ENTSO-E transparency platform (ENTSO-E, 2019) and the EU Transaction Log (EUTL) (European Comission, 2019). The first offers data on hourly generation profiles"per generation unit" in MWh. EUTL contains data from the European Emissions Trading System (ETS). It lists the verified emissions per year for every installation in the ETS in tonnes of $CO_2$.

The data preparation is threefold. First step, we match the ENTSO-E-generation units to the EUTL-installation IDs. The matching table is shown in Braeuer et al. (2019). Second step, the total generation per year per power plant $j$ is derived from the ENTSO-E-data and divided by the respective emissions per year per power plant derived from the EUTL-data. This results in the yearly average EF per power plant ($EFj$), shown in equation (1). Last step, the $EFj$ is used to calculate the hourly emissions per power plant and eventually the hourly emissions of the German conventional energy mix ($m_{CO2,t,j}$).

$$EF_j = \frac{m_{CO_2,j}}{E_{tot,j}} \tag{1}$$

$$L_{Res,t} = L_t - E_{RES,t} - E_{imp,t} + E_{exp,t} \tag{2}$$

Hourly load data is provided by ENTSO-E (ENTSO-E, 2019), as well as the generation of renewable energy sources (RES) and import/export balance. Equation (2) describes the resulting residual load without import and export ($L_{Res,t}$). Import and export is excluded due to a lack of data availability.

The matching of the two databases produce certain data inaccuracies. These are explained in the following paragraphs. First, it is not possible to match all generation units from ENTSO-E to an installation listed in EUTL. 6 out of 207 (2.9 %) of the generation units are not matched, which represents roughly 3 % of the total conventional energy generation in 2017. Furthermore, multiple generation units in ENTSO-E are listed under one single installation name in EUTL. In these cases, we estimate the theoretical share one generation unit has of the total $CO_2$ emissions of the entire power plant listed in EUTL. SI B further illustrates this approach. It concerns almost half of the generation units representing up to 60 % of the total conventional energy generation.

Additionally, there is a divergence between the hourly profiles listed in ENTSO-E (2019) and the monthly domestic values for the generation per fuel type (ENTSO-E, 2019). For fuel types with a high number of smaller generation units like waste and run-of-river

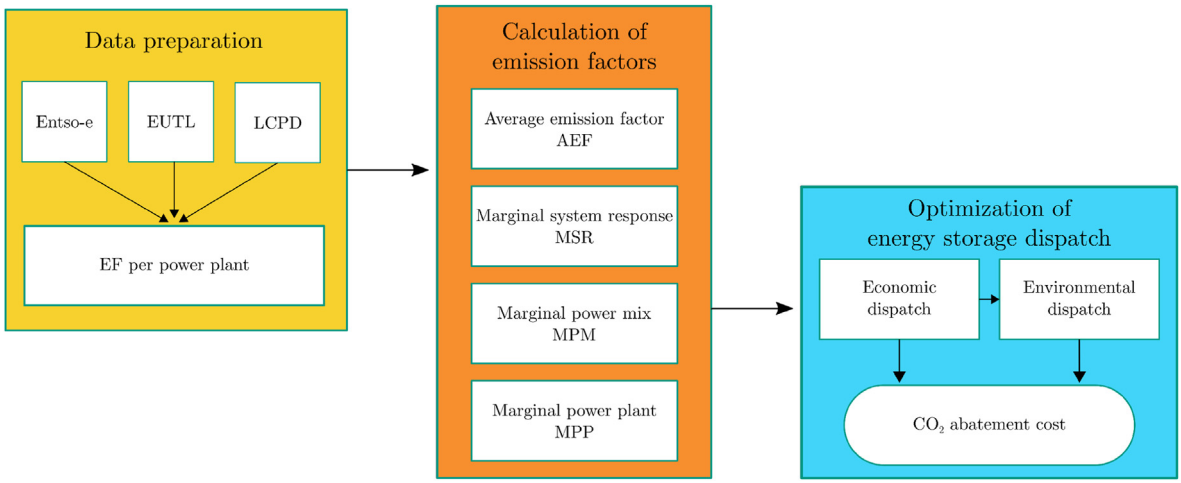


**Fig. 1.** Illustration of the methodological approach.

plants, it can be explained by the fact that the hourly profiles list only large generation units. Nonetheless, the values for electricity generation from lignite and nuclear power plants differ in average over the year between 2 % and 4 % and for fossil hard coal with 13 %. Finally, missing values for verified emissions as well as unreasonable high EFs per power plant greater than 2 t/MWh diminish the data quality further.[1] For compensation, these values are manually adapted, see SI B.

### 3.2. Calculation of EFs

For the analysis in this study, we apply four different emissions factors.

1. Average EF (AEF)
2. Marginal system response (MSR)
3. Marginal power mix after (Hawkes, 2010) (MPM)
4. Marginal power plant (MPP)

The AEF is described in equation (3) (Spork et al., 2015, equation (2)) as the sum of the $CO_2$ emissions of all power plants $j$ over the total energy production of all power plants in period $t$. Therefore, $AEF_t$ represents the average emissions in period $t$.

$$AEF_t = \frac{\sum_j m_{CO_2,t,j}}{\sum_j E_{t,j}}, \forall j \in J, t \in T \tag{3}$$

$$MSR_t = \frac{\sum_j m_{CO_2,t+1,j} - \sum_j m_{CO_2,t,j}}{L_{Res,t+1} - L_{Res,t}}, \forall j \in J, t \in T \tag{4}$$

The second factor is the *MSR*. It describes the reaction of the energy system in $CO_2$ emissions as the sum of emissions of all power plants ($m_{CO_{2,j,t}}$) to a change in the residual load ($LRes$) from hour $t$ to hour $t+1$, see equation (4). The *MPM* is derived from the work of Hawkes (2010). Over the course of one year, he assumes that the energy system reacts similar in every hour of the day. Analogous to Hawkes (2010) for every hour of the day $h$, we build a linear regression model consisting of 365 samples. The slope of the hourly regression line is defined as the *MPM*.[2] Finally, the *MPP* results from a European electricity market model (Ardone et al., 2002) and resembles the EF of the last accepted power plant on the wholesale market. To replicate the historic dispatch, generation availability and load levels have been scaled to match the values reported by ENTSO-E monthly domestic values. Additionally, outages for generation units and transmission elements have been implemented as reported by the e-transparency platform. Efficiencies are derived by age and technology of the power plants and for EF calculation we distinguish between full-load and part load operation. For part-load operation, efficiencies are reduced according to the regression formula reported in Brouwer et al. (2015). Thus, we obtain an effective EF depending on the ratio of power output and installed capacity for each marginal power plant in every hour.

For this study and the case of Germany, we only consider dispatchable production units as part of the power mix that actively react to changes in energy demand. Based on Graf and Marcantonini (2017) as well as Spork et al. (2015), we describe these units in Table 1. Thus, we exclude the output of the majority of RES. The German energy system prioritizes the dispatch of renewable energy sources. The only reason to curtail renewable energies is due to grid congestion. Therefore, RES are (in the given system) rarely the marginal production unit.

### 3.3. Energy storage model

The ESM is based on Braeuer et al. (2019a). The model identifies the optimal investment in an ESS for an industrial company to minimize cost for electricity. In line with the key findings of Braeuer et al. (2019a), this study only considers peak shaving as the most profitable business case for industry. Additionally, this study extends the model to minimize the $CO_2$ emissions.

The optimization is divided into two steps. The first step identifies the economic optimum for the ESS capacity and dispatch. The objective function $f$ in equation (5) (Braeuer et al., 2019a) minimizes the grid charges, the product of the yearly peak load ($P_{peak}$) and the price for the peak power ($p_{peak}$), along with annuity payment for the ESS ($A_{ES}$). For further explanation see SI C.

The second step of the optimization identifies the optimal environmental dispatch. A few equations from the economic optimization in Braeuer et al. (2019a) need to be altered. The objective $g$

[1] The issue might partly result from the fact that, for combined heat and power (CHP) units, all emissions for heat and power generation are accounted to the electricity sector as well as possible start-up procedures, where the power plant is not yet connected to the grid.

[2] For further elaboration see SI F.

**Table 1**
Dispatchable production units by fuel type.

| Fuel type |
|---|
| Nuclear |
| Fossil Brown coal/Lignite |
| Biomass |
| Other |
| Waste |
| Fossil Hard coal |
| Fossil Oil |
| Fossil Coal-derived gas |
| Fossil Gas |

in equation (6) minimizes the total $CO_2$ emissions for one year in hourly resolution due to the resolution of the emissions data basis. The total $CO_2$ emissions are the sum of the product of the electricity from the grid ($x_{el,t}$) and the respective EF ($EF_t$). We fix the capacity of the ESS to the size in the economic optimization, equation (7) to allow for a direct comparison of the ESS's utilization between the economic and environmental dispatch. Moreover, the yearly peak load in the environmental dispatch cannot be greater than in the economic dispatch, equation (8). This constraint is needed to answer the question if idle capacity of the ESS could be utilized to lower the $CO_2$ emissions without infringing the economic goals of the peak shaving business case.

$$min\, f,\ f = P_{peak} \cdot p_{peak} + A_{ESS} \tag{5}$$

$$min\, g,\ g = \sum_{t=1}^{8760} (x_{el,t} \cdot EF_t) \tag{6}$$

$$cap_{ESS,econ} = cap_{ESS,envir} \tag{7}$$

$$P_{peak,econ} \geq P_{peak,envir} \geq x_{el,t} \tag{8}$$

### 3.4. Performance indicators for the environmental dispatch

For the evaluation of the environmental dispatch, we consider a variety of indicators. Equation (9) defines the amount of avoided $CO_2$ emissions between the economic and environmental dispatch ($\Delta CO_{2,i,k}$). It is the sum of the consumed electricity ($x_{el}$) for an economic dispatch (*econ*) minus the electricity for an environmental dispatch (*envir*) multiplied by the respective $EF_k$ over all time steps $t$. It is calculated for all companies $i$ and all EFs $k$. Equation (10) describes the utilization factor $u_{cap}$, which is a measure for how much $CO_2$ emissions can be avoided by a storage system with a capacity of 1 *kWh*. Equation (11) describes the $CO_2$ abatement cost as the fraction of additional costs for electricity consumption compared to the economic dispatch and the avoided $CO_2$ emissions. Finally, equation (12) describes the number of full cycles per day.

$$\Delta CO_{2,i,k} = \sum_{t=1}^{T} \left( \left( x_{el,i,t,econ} - x_{el,i,t,envir} \right) \cdot EF_{t,k} \right),\ \forall i \in I, k \in K, t \in T \tag{9}$$

$$u_{cap,i,k} = \frac{\Delta CO_{2,i,k}}{cap_{stg,i,k}} \tag{10}$$

$$C_{abat,i,k} = \frac{C_{el,i,envir} - C_{el,i,econ}}{\Delta CO_{2,i,k}} \tag{11}$$

$$cycle_{day,i,k} = \frac{charg_{stg,i,k}}{cap_{stg,i,k}} \cdot \frac{1}{LT \cdot 365} \tag{12}$$

## 4. Application of the method

The evaluation is divided into 3 analytical steps. First in section 4.1, we compare the four different EFs. Second in section 4.2, we evaluate the dispatch of a generic storage system (GSS). The GSS is used to investigate the $CO_2$ reduction potential of a storage system without restricting cycle life conditions and a high efficiency of 98 %. Third in section 4.3, we analyse the optimal dispatch of a battery storage system (BSS) with constraining cycling conditions, 4000 cycles and 90 % efficiency.

### 4.1. Emission factors

As discussed in previous works, the four EFs differ significantly in both magnitude and volatility and thus produce different at times contrasting signals about the $CO_2$ intensity of the energy mix. Fig. 2 shows the EFs for the week from July 10 to July 16, 2017, in the German electricity mix. Also shown is the electricity generated per timestep and fuel type. AEF, MSR and MPM are derived using empirical data from ENTSO-E (ENTSO-E, 2019), while the MPP is the result of the EEMM.

The depicted week is a good example to illustrate the qualitative differences between the considered factors. The AEF ranges between 0.46 $kgCO_2/kWh$ and 0.86 $kgCO_2/kWh$, being the lowest when the share of technologies with low emissions is the highest. For the German power system, this is the case when a large amount of generators are dispatched and the cheap lignite power plants are complemented by relatively low emission technologies like hard coal and gas. The AEF gets larger when the share of technologies with high emissions increases. This is the case when either the amount of lignite increases in almost-all-renewable hours or when the residual load decreases and gas and hard coal fired power plants cease operation. It can be observed in Fig. 2 that the AEF is the lowest when total generation reaches its peak illustrating the described connection. With respect to a signaling effect for $CO_2$ reduction, the AEF provides a clear signal for hours of a high EF and hours of a low EF. However, as discussed in the literature review, it is questionable if the AEF is suited to indicate the additional emissions caused by an incremental increase in the electricity demand. Naturally, such an increase will not be answered by the power plant mixture but by an individual plant or a small group of plants.

The MPM shows by definition a periodical behaviour. It is notably lower than the AEF at all times. The MPM is based on a linear regression of the system response to shifts in generation and load and thus it represents a typical response. Therefore, this factor is most appropriate in hours which are least impacted by volatile renewable in-feed. This becomes more clear when looking at the value of the measure of determination ($R^2$) for the different hours of the day. Here, the MPM performs best in the night hours, when generation is at minimum load of many power plants and each shift in load is matched by a classic reaction of the power system. Nonetheless in hours where more flexible power plants are utilized, only the residual load has to be matched. Thus, the reaction of the power system is highly dependant on renewable in-feed. This

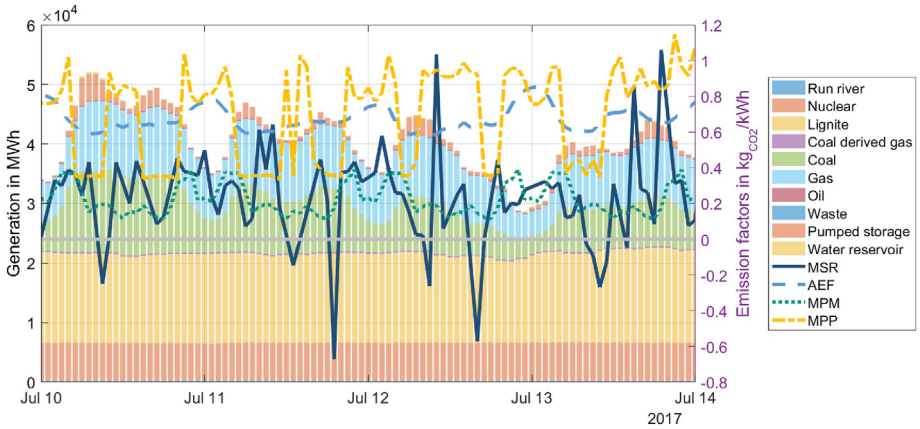


**Fig. 2.** Hourly generation and EFs in week 28, 2017.

**Table 2**
Characteristics of the EFs.

| | $CO_2$ in $kg_{CO_2}/MWh$ | | | |
|---|---|---|---|---|
| | AEF | MSR | MPM | MPP |
| Min | 486.5 | −679.1 | 114.2 | 0.0 |
| Max | 915.6 | 1190.3 | 390.1 | 1189.8 |
| Mean | 707.5 | 268.1 | 224.1 | 840.2 |
| Std | 76.1 | 304.1 | 90.4 | 267.0 |
| Varcoef | 0.1 | 1.1 | 0.4 | 0.3 |

results in very low $R^2$-values in the middle of the day (see Figure F3 in SI F). Moreover, the MPM reaches a local minimum when the AEF is at a local maximum. This can be observed regularly at the change of day. Due to its periodic behaviour it offers a well foreseeable potential for the use of flexibility, because the $CO_2$ EF for each time step is known in advance.

Similarly, the profile of the MPP implies a periodical behaviour. The MPP is not derived from empirical data since the data are insufficient to determine which power plant is marginal in each time step. Therefore, the EEMM determines the MPP, which represents the $CO_2$ EF of the marginal generation unit. The individual $CO_2$ EF of the marginal generation unit depends on the commissioning year and the technology. In many hours of high loads, the MPP is low as the marginal generation units are gas-fired power plants. In these hours, power plants with higher $CO_2$ emissions like lignite and coal are fully dispatched. These hours of low MPP-values coincide in many cases with low AEF-values. Simultaneously, hours of high MPP-values indicate low load in the system or a high share of renewable generators. The incremental energy demand increase is answered by a lignite-driven or coal-driven power plant. Again in many cases, hours of a high MPP coincide with hours of a high AEF. Exemptions can be observed in hours of relatively high renewable in-feed and relatively low loads. In these hours, most generators reduce their electricity output to their minimum must-run condition. In these cases, the MPP jumps between very high values, when lignite is the marginal fuel type, and values equals to zero when nuclear power plants or run-of-river plants answer the incremental increase in energy demand.

The MSR on the other hand is the most extreme factor by all means. With a standard deviation of 304.1 $kgCO_2/kWh$ it is by far the most volatile EF also reaching the global maximum and global minimum of all factors. Most striking are the negative values, which are not trivial to explain. Taking a closer look at the formulation, this can only occur when either the residual load is reduced but system emissions increase or vice versa, which seems not intuitive. We attribute this to the effect of ramping constraints, when slower power plants power up or down for the next/last hour without necessarily being directly connected to the change in residual load. However, the MSR offers the largest potential for $CO_2$ reduction due to the number and magnitude of peaks and valleys, which allow many adjustments within on day. Table 2 shows the mean, minimum, maximum and standard deviation of the four EFs considered for the whole year.

### 4.2. Generic storage system

Table 3 shows the statistical values of the performance indicators. These are the statistical results of the optimization runs for the 50 companies. One can observe significant differences between the possible $CO_2$ reductions ($\Delta\Delta CO_{CO2}$) of the four EFs. Hence, the mean values for $\Delta\Delta CO_{CO2}$ range between 6.81 $t$ for the AEF and 86.25 $t$ for the MSR, which is 12 times as much. One explanation for different mean values, is the number of daily cycles. The number of daily cycles is very different for the considered EF and the respective company. In average, the AEF allows for 2 full cycles per day with only minor variation between the companies, the coefficient of variation is 7 %. The values for MSR, MPM and MPP are considerably higher with a mean value for the number of daily cycles of up to 5.41 and the coefficient of variation ranging between roughly 19 % and 21 %. This indicates that the MSR, the MPM and the MPP have a higher frequency of peaks and valleys compared to the AEF. Simultaneously, the companies have deviating potentials to exploit these spreads in the hourly EF. The coefficient of variation of $\Delta\Delta CO_{CO2}$ is similar for all applied EFs. Therefore, the deviation in reduced $CO_2$ emissions for the different companies is similar for all EFs. To get a better understanding how the different EFs influence the environmental dispatch of the individual companies, we consider the utilization factor of the installed storage capacity ($u_{\text{cap}}$). In line with $\Delta\Delta CO_{CO2}$, it shows that the level of possible $CO_2$-reductions per installed capacity vary widely. Nonetheless, the coefficient of variation presents different values for the respective EF. The coefficient of variation is the lowest for the AEF and the highest for the MSR. This shows that the dependency of the utilization factor on the individual load profile is low for the AEF, coefficient of variation is 10 %, higher for the MPP, MPM and MSR, 15 % to 22 %.

Considering the $CO_2$-abatement costs ($C_{\text{abat}}$), the MPP shows mean values in the range of current ETS prices of around 25 €/$tCO_2$ (September 2019) and the MSR shows considerably lower mean values. With values around 62 €/$tCO_2$, the AEF and MPM present

**Table 3**
Statistical overview of results.

| | | Unit | GSS | | | | BSS | |
|---|---|---|---|---|---|---|---|---|
| | | | AEF | MSR | MPM | MPP | MSR | MPP |
| $\Delta CO_2$ | Min | t | 0.29 | 4.33 | 0.76 | 1.43 | 1.88 | 0.82 |
| | Max | t | 82.75 | 1038.37 | 201.72 | 371.68 | 344.98 | 153.49 |
| | Mean | t | 6.81 | 86.25 | 16.58 | 30.99 | 32.92 | 14.78 |
| | Varcoef | % | 187 | 188 | 189 | 186 | 2 | 2 |
| $u_{cap}$ | Min | kg/kWh | 45.54 | 372.58 | 86.51 | 182.26 | 341.91 | 154.99 |
| | Max | kg/kWh | 74.99 | 1109.66 | 194.47 | 366.27 | 443.01 | 194.32 |
| | Mean | kg/kWh | 68.08 | 861.89 | 165.39 | 310.76 | 411.65 | 185.61 |
| | Varcoef | % | 10 | 22 | 16 | 15 | 0 | 0 |
| $C_{abat}$ | Min | $€/t_{CO_2}$ | 53.33 | 11.86 | 46.61 | 16.73 | 26.38 | 58.48 |
| | Max | $€/t_{CO_2}$ | 65.05 | 14.60 | 72.33 | 27.23 | 34.20 | 75.44 |
| | Mean | $€/t_{CO_2}$ | 61.77 | 14.13 | 63.55 | 24.26 | 28.26 | 62.63 |
| | Varcoef | % | 4 | 4 | 10 | 11 | 0 | 0 |
| $cycle_{day}$ | Min | # | 1.59 | 2.57 | 2.32 | 1.88 | 1.00 | 1.00 |
| | Max | # | 2.23 | 6.80 | 5.99 | 4.25 | 1.00 | 1.00 |
| | Mean | # | 2.00 | 5.41 | 4.73 | 3.46 | 1.00 | 1.00 |
| | Varcoef | % | 7 | 21 | 20 | 19 | 0 | 0 |

notably higher results. With fixed electricity prices, the additional costs for $CO_2$-abatement are a result of efficiency losses during charging and discharging processes.

Concerning the coefficient of variation with values around 4 %, $C_{abat}$ of the sample companies are fairly concentrated for the AEF and the MSR compared to the other EFs. This implies a weaker dependency of $C_{abat}$ on individual load profiles. For the AEF, this can be explained by the low frequency of peaks in the EF and the resulting low number of cycles. In addition to a comparably small spread between the minimum and maximum value of the AEF, this does not allow for a high divergence among the companies. The low coefficient of variation for the MSR is somehow surprising as one can observe high variation among the companies considering the other three indicators. This might be a result of the extreme outliers of the MSR. The values of the $C_{abat}$ following the MPP deviate the most, which implies a stronger dependency on the individual load profiles.

To further illustrate the above mentioned effects, Fig. 3 compares the company 45 and company 46 showing the storage dispatch for the MSR. The figures show the load profile, the charging and discharging profile as well as the SoC on the left axis. The right axis indicates the respective EF. The horizontal dashed-dot lines indicate the maximum peak load that has to be achieved through peak shaving. All for two consecutive sample days, February 15th (Wednesday) till 17th (Friday) 2017.

While the two sample companies have a similar peak load level (translated into maximum energy per 15-min interval, company 45 with 327 *kWh* and company 46 with 370 *kWh*) as well as comparable optimized storage capacities (company 45 with 219 *kWh* and company 46 with 319 *kWh*), the load profiles are fairly different. Company 45, an iron casting company, shows very high singular peaks of more than 300 *kWh* followed by periods of low energy demand, not more than 20 *kWh*. Sample company 46, a manufacturer of mixed spices, shows five peaks per day of up to 400 *kWh*. The lowest load during these sample days is around 80 *kWh*. Thus, the load profile of company 46 allows for discharge of the storage system in low load periods. Compared to company 45, this leads to $CO_2$-shifting during these periods. Thus, company 46 has a higher utilization factor than 45. This has no strong effect in case of the AEF, see Figure D.2 in SI D, where the low frequency of the EF peaks results in two daily cycles. In Fig. 3, one can observe a high correlation between the MSR and the load profile of company 46, which allows for a high utilization of the storage system. Still, for example between 6 a.m. and noon on the 15th, the full $CO_2$-reduction potential cannot be reached as hours of a low MSR and a high load overlap. During these hours, charging is restricted due to peak shaving. Considering MSR, MPM and MPP, the GSS of company 46 is charged two times more than the GSS of company 45.

For further illustration of the environmental dispatch for all four EFs, we refer to Figures D.1 and D. 2 in SI D.

### 4.3. Battery storage system

In this subsection, the model constraints were adapted to fit the real life setting of a BSS. The BSS cycle life is restricted to 4000 cycles over 11 years, which is equivalent to one cycle per day. Additionally, the charging and discharging efficiency is reduced to 90 %. This affects the environmental dispatch substantially compared to the GSS. Table 3 shows in the two BSS-columns on the right the statistical evaluation of the optimization results for an environmental dispatch following the MSR and the MPP. The table indicates that the possible $\Delta CO_2$ is much lower for a BSS than for a GSS. The mean value of all 50 companies for a BSS is around 38 % of the mean value for the GSS following the MSR. Following the MPP, it is around 48 % of the GSS value. Partly, this great reduction is the result of the restricted cycle life. For both EFs, all 50 companies fully exploit the cycle life and reach 1 cycle per day. Next to the reduced cycle life, the lower efficiency of the charging process lowers the utilization factor of the BSS. A round-trip efficiency of 81 % results in a spread in an EF of more than 29 % that is needed for the model to choose a $CO_2$-shifting dispatch. Fig. 4 further illustrates these effects. The figure shows the environmental dispatch of a BSS for the MSR and the MPP for company 46. Compared to the GSS, the optimal peak load increases by roughly 6 % and the optimal BSS capacity is with 205 *kWh* around 21 % smaller than the GSS capacity. Considering Fig. 4, only the highest spreads are utilized for $CO_2$-shifting due to the restricted life time. In the MSR-graph, the BSS is charged during a period of a negative MSR value and discharged during hours of an MSR around 1 $t_{CO_2/kWh}$. During the next charging phase, noon of February the 16th, the spread between the low MSR and the high MSR is not large enough for the BSS to be charged. For the MPP, the BSS is charged while a nuclear power plant is the marginal generation unit with a MPP-value of 0 $t_{CO_2/kWh}$ and discharged while a lignite driven power plant is marginal. As such occurrences of spreads larger than 1 $t_{CO_2/kWh}$ are fairly rare, the model chooses to charge the BSS in hours of a coal-driven marginal power plant, around 0.7 $t_{CO_2/kWh}$.

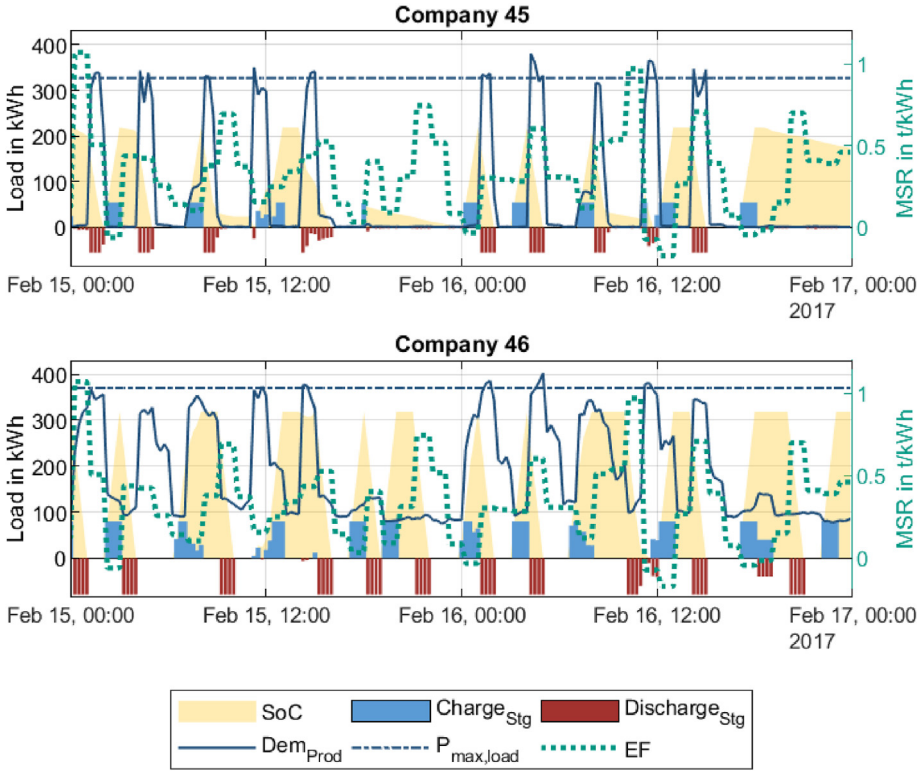


**Fig. 3.** Comparing load and charging profile of company 45 and company 46 for 2 days, showing the MSR.

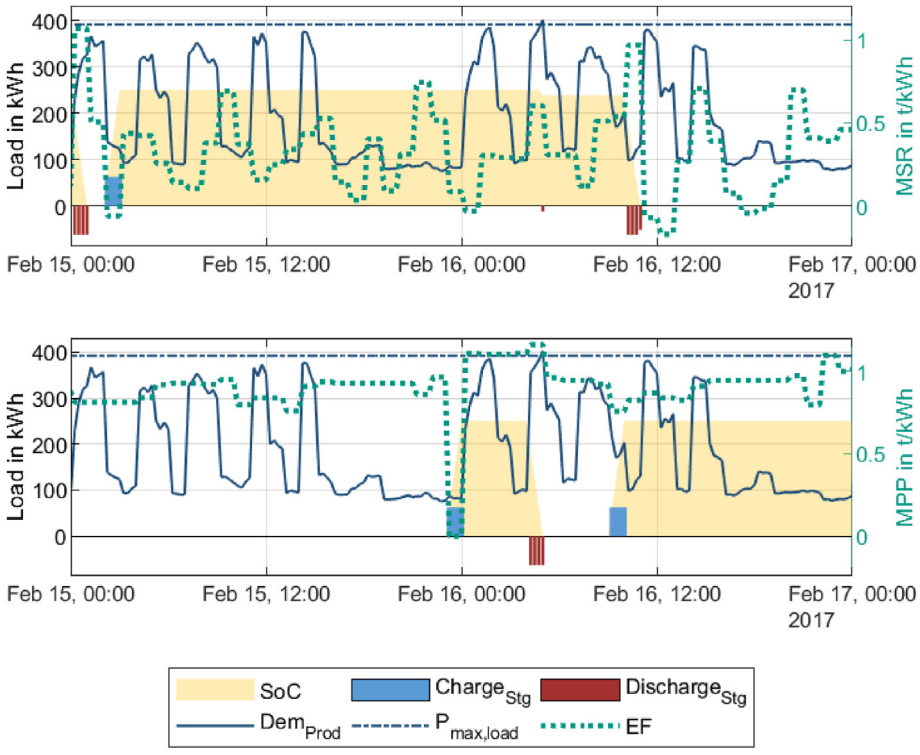


**Fig. 4.** Load and charging profile of a BSS for company 46 for 2 days.

In case of the environmental dispatch no additional degradation effects are considered. Nonetheless, results show that $CO_2$-shifting coincides with very high c-rates. Additionally, to fully exploit the $CO_2$-reduction potential, the results indicate very high depths of discharge

for a $CO_2$-reducing dispatch. Both effects have a strong influence on the premature aging of a BSS resulting in premature capacity losses.

## 5. Discussion

### 5.1. General methodology

This contribution employs two energy system models based on linear programming, one taking a micro-economic perspective for an individual company (ESM) and one taking a macro-economic perspective for Germany and surrounding countries (EEMM). Both of these models suffer from common limitations of linear optimization models, which for these particular instances are discussed elsewhere (Braeuer et al., 2019a) and (Ardone et al., 2002). The remainder of this subsection therefore concentrates on the methodological focus of this paper, namely on the definition and analysis of different emissions factors for integrated electricity systems.

*Data input.* As described in the section Data Preparation, this study introduces a novel data basis to allocate $CO_2$-emissions to the respective hourly energy generation of power plants. We provide a solution to overcome the missing matches between EUTL account holders and generation units in the ENTSO-E database. Yet, the deduction of hourly $CO_2$-emissions factors from the yearly verified $CO_2$-emissions remains a source of inaccuracies. To increase the robustness of the data, a larger number of years could be used. Additionally, with information about the individual part-load behavior of the generation units, it would be possible to estimate a part-load dependent EF. Without detailed knowledge about CHP units and their respective dispatch logic, how much heat is generated and sold, the data accuracy remains weakened.

*General EF-approach.* The results indicate that the four different EFs considered have different signaling effects for an environmentally-oriented dispatch.

In addition to Table 2, based on the annual sorted duration curve for the four EF approaches in Fig. 5, it is possible to reach some general insights. Firstly, the overall range of the factors is comparable for all methods, with the exception of the MPM, which is much lower than the others. This is due to the fact, that the hourly linear-regression model insufficiently approximates hourly $CO_2$-emissions changes. In addition, the differences in the extrema of the different factors are clearly visible.

AEF and MPM show an averaging effect, the AEF due to the large number of different technologies, the MPM due to the large number of hours per time-step. Both duration curves show a smaller range between the extrema then the MSR and MPP, which aim to describe the marginal reaction of the system and are more responsive to the $CO_2$-intensity of single technologies.

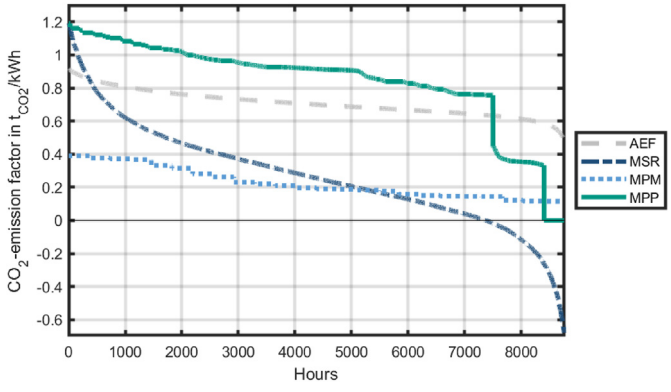


**Fig. 5.** Annual sorted duration curve of the EFs.

Furthermore, the number of hours with high and low $CO_2$-intensity are clearly visible in contrast to the weekly graph in Figs. 3 and 4 where the focus lies on volatility. The MSR and the MPP present a relative high number of extreme hours compared to the other two EFs. This high number together with high volatility strongly impacts storage dispatch decisions. Finally, the "drops" between marginal technologies are only visible in the MPP as this EF is technology specific. In contrast, the other EFs resemble the system's reaction.

Concerning the four different EF, we follow a production-based approach. For an energy system the size of Germany's, we assume a negligible influence of imported and exported energy flows. This is in line with the findings of Pareschi et al. (2017), but this simplification can still be challenged. An exception is the MPP, where market coupling is explicitly included in the model and the selection of the MPP thus also depends on the level of exchange with neighbouring countries.

Related to the above point, the marginal approach adopted for all of the EFs is only valid for small samples at the margin. In the case that a large number of consumers adopt electrical storages and implement the business models analyzed here, they will cease to be marginal. In other words, they will cease to be price takers and will become price setters, in this context affecting the marginal emissions factors that they are employing. This therefore needs to be borne in mind when analysing these dynamic emissions factors for a large number of distributed consumers. If all 50 companies would apply the optimized environmental dispatch the maximum load change would range around 5 *MW*.

*AEF.* This study analyzes the dynamic change in load and the energy system's reaction based on four EF approaches, which only consider the dispatchable generation units. In other words, the non-dispatchable generation is exogeneously fixed and defined by historical generation and feed-in profiles for renewables. This leads to an AEF that deviates from existing studies, whereby the AEF shows two peaks per day. However, the exclusion of RES as non-dispatchable units results in high values for the AEF in hours with a large share of RES in the system and vice versa. This is contrary to existing studies, which include RES into the AEF and indicate low values during periods of high RES share.

*MSR.* To identify the system's reaction, we postulate the EF MSR, which is oriented towards Hawkes (2010). This approach has obvious shortcomings, as it yields negative values in some hours, which is due to changes of load and emissions in opposite directions. This is counter-intuitive for the energy system in the year 2017 and as long as renewable energy sources are considered as non-dispatchable. An explanation could be a high share of CHP-units with uncertain heat production and ramp-up processes in hard-coal and lignite power plants. Additionally, a reaction of the generation units too small to be listed in the ENTSO-E data base is not accounted for by the MSR.

*MPM.* The evaluation of the MPM, the approach by Hawkes (2010), might not be fit to describe the German energy system in 2017. Hawkes (2010) focuses on the British energy system until 2009. With a higher share of volatile RESs, it seems no longer suitable to assume a reoccurring behavior of the electricity mix for one representative day over one year. In Figure F.3 in SI F, this study does not show sufficient values for the coefficient of determination for the hourly resolution. Thus except for three hours in the morning, the load change during one hour of the day (independent variable) is not sufficient to approximate the change in $CO_2$-emissions (dependent variable).

*MPP.* The model-based EF MPP appears to be most suitable to evaluate the effect of an increase in electricity demand. Nonetheless, because of the conformity issues of model results it lacks comparability to other energy models and possibly to reality. In

reality, there might be additional operational constraints not fully implemented in the EEMM. Moreover, the dispatch of power plants might be subject to portfolio optimization of the owner's fleet with different or even changing objectives. In return, this makes it very hard to identify an individual power plants, which would react market-wise to the change in demand implied by the flexibility provider.

### 5.2. Comparison with other studies

In this section, we briefly compare our results with the literature. Near-real time and historic EFs for Germany are available from Agora Energiewende (2019). The data on power generation is also based on ENTSO-E publications, while EFs are fuel specific based on Icha (2019). Emissions are only accounted for the generated power in Germany ignoring imports but also accounting for exported energy. This assumption is in line with our presented approach. However, Agora Energiewende (2019) include renewable energy sources in the calculation. Nonetheless, our presented approach is more detailed as we provide a mapping table for actual emissions reported to EUTL and power generation reported by ENTSO-E.

In contrast to our approach, Wörner et al. (2019) consider the life cycle emissions of each technology and Tranberg et al. (2019) include $CO_2$-emissions of the complete fuel chain. The former base the technology specific emissions on the ProBas database, the later base the fuel specific emissions on ecoinvent database; calculations outside the scope of our article, as we consider generation-based EFs. However, the results in Wörner et al. (2019) show that the inclusion of life cycle aspects only produce an offset in the $CO_2$-factor and have little qualitative impact on the dynamic EFs.

Furthermore, Wörner et al. (2019) present a representative winter and summer week for which the EFs of our current article compare as follows: in the characterized winter week our methodology leads to more volatile factors following more closely the load patterns of the day and also quantitatively higher than described by Wörner et al. (2019). We find the same effect of the summer week having significantly lower EFs than the winter weeks. We attribute this to the lower amount of residual load because of higher solar intensity. Apart from the two weeks a comparison is unfortunately not possible.

Tranberg et al. (2019) present a real-time carbon accounting method for the European electricity markets. The average $CO_2$-intensities are specific for each generation technology, thus neglecting the merit order within fuel types as well as must-run or part-load operation. The analysis is based on commercial data from electricitymap (Tomorrow, 2020), so we were not able to compare the results.

Deetjen and Azevedo (2019) chose a different approach, by developing a simplified merit order model. The data sources are specific to some US power markets. They address ramping constraints by explicitly modelling constraints in the dispatch model. While their definition of dynamic emissions is similar to our MEF, their proposed moving average approach is a deviation to our methodology. A comparison to our results is not possible due to the different geographic scope of the articles.

### 5.3. Outlook

The results of the study implicate that rewarding environmental dispatch could incentivize industrial companies to exploit their load flexibility options. At the same time, the utilization of a BSS for the reduction of $CO_2$-emissions does not seem practicable. However, there might exist other technologies and measures for industrial companies that offer flexible electricity demand with higher efficiencies and longer lifetime than a BSS.

While the time series of the estimated EFs for the current energy system can be intuitively explained, the results of this study indicate the challenges for future studies. As the AEF presents a more inert behaviour than the MPP, one can still identify a correlation between the value of the EF and the share of RES in the system. However, for a few hours in 2017 the share of RES was so high that nuclear power plants became the marginal generation unit. While this does not influence the AEF, it results in a jump of the MPP from the minimum value in case of a nuclear driven power plant to the maximum value for lignite. In future cases with increasing shares of RES and dispatchable RES, such situations might occur more regularly. Operating hours of formally base-load generation units such as lignite power plants are decreasing. To apply the proposed methodology in such a case, we need to obtain a more detailed knowledge about the must-run conditions and other operational constraints of conventional generators as well as dispatchable RES. This becomes increasingly important, since they may determine the plants dispatch. Furthermore, the coal-phase-out potentially changes the merit order on the energy market and leads to an almost binary EF (zero for RES and positive for the remaining conventional power plants, mainly gas). Increasing prices for $CO_2$-certificates may lead to a fuel switch, which would result in an alignment of production cost and $CO_2$-intensity in the merit order, making a signaling function of EFs redundant.

In addition, the regional aggregation level influences the conceptual approach. Considering smaller regions such as autonomous municipalities or congested electricity grid nodes, introduction of sophisticated regional electricity prices could help to reduce regional emissions. Such prices should orient on dynamic EFs. In these cases, the effect on the non$-CO_2-$emissions, which mostly have a local effect, should be considered. SI E expands the methodology to estimate the EFs for other emissions $SO_2$, $NO_x$ and Dust.

Based on the foregoing discussion, the following recommendations for further work can be given:

- improve method for calculating hourly values based on European Pollutant Release and Transfer Register (E-PRTR) (European Environment Agency, 2019) and EUTL data
- improve modelling of part load and must-run capacities etc.
- extend the validation of the method based on measured/empirical data for power generation and CO2 emissions
- further assess the $CO_2$-reduction potential of BSSs, combining the economic and environmental objectives
- further develop such an approach to a more local/regional context, which may operate in partially off-grid mode with regional markets and prices
- extend the consideration of micro-economic and macro-economic aspects in more integrated framework to overcome the lavine/snowball effects that might be encountered.

## 6. Summary and conclusions

As one possibility to increase flexibility, battery storage systems will play a key role in the transition of the energy system. From an economic point of view, BSSs have been studied and proven in a variety of business cases. How storage system can help to reduce the $CO_2$-emissions of an energy system by flexibly shifting the load is still an open question. In this paper, we introduce a novel data basis for the determination of the energy system's emissions. This is a match between the ENTSO-E and EUTL databases. Furthermore, we postulate four different dynamic EFs to determine the hourly emissions caused through a change in electricity demand. This is the average EF, the marginal power mix, the marginal system response and the marginal power plant. The signaling effect of these EFs are tested for a storage system combined with an

industrial load. We differentiate between a generic storage system, which might be applicable to a variety of technologies offering flexibility, and a specific battery storage system. The linear optimization is divided into two levels. On the first level, the optimization determines the size and economic dispatch of the storage system considering peak-shaving. The second level finds the environmental optimum by minimizing the emissions of the electricity drawn from the grid for the respective EF. The results of the four EFs are statistically evaluated for a set of 50 small and medium sized companies in Germany.

The four different EFs have different signaling effects for an environmental storage dispatch. The AEF and the MPP lead to a similar $CO_2$-reduction and allow for roughly two cycles per day for the generic storage system. The MSR and MPM show a higher volatility, which leads to a higher utilization of the storage system. For the single companies, peak shaving is prioritized over $CO_2$-shifting. Therefore, if a high portion of the storage system is used for peak shaving the $CO_2$-reduction potential is low. Furthermore, a high correlation of the load profile and the profile of the hourly EF supports high $CO_2$-reduction. Similar to an arbitrage trading dispatch, the charging behavior of an environmental dispatch results in high levels of additional degradation of the BSS.

To further assess the $CO_2$-reduction potential of BSSs, future research needs to focus on combining the economic and environmental objectives as well as assessing local/regional energy systems. In addition, future research needs to increase the robustness of the marginal EFs. For this, supplementary information about the behavior of CHP-plants and ramp-up processes of hard-coal and lignite plants should be included in the data basis.

## Declaration of competing interest

The authors declare that they have no known competing financial interests or personal relationships that could have appeared to influence the work reported in this paper.

## CRediT authorship contribution statement

**Fritz Braeuer:** Writing - original draft, Visualization, Methodology, Software, Conceptualization, Data curation, Investigation, Formal analysis. **Rafael Finck:** Writing - original draft, Visualization, Methodology, Software, Conceptualization, Data curation, Investigation, Formal analysis. **Russell McKenna:** Writing - original draft, Conceptualization, Supervision.

## Acknowledgements

The authors thank the Energie Consulting GmbH in Kehl-Goldscheuer, Germany, and its managing director Dr. Jürgen Joseph for the provision of the anonymized data of the 50 SMEs. The third author (RM) acknowledges the financial support of the FlexSUS Project (Project nbr. 91352), which has received funding in the framework of the joint programming initiative ERA-Net Smart Energy Systems' focus initiative Integrated, Regional Energy Systems, with support from the European Union's Horizon 2020 research and innovation programme under grant agreement No 775970, as well as the Smart City Accelerator project. The usual disclaimer applies.

## Appendix A. Supplementary data

Supplementary data to this article can be found online at https://doi.org/10.1016/j.jclepro.2020.121588.

## References

Agora Energiewende, 2019. Agorameter: dokumentation. URL: https://www.agora-energiewende.de/fileadmin2/Projekte/Agorameter/Hintergrunddokumentation_Agorameter_v36_web.pdf.

Alsema, E., 2012. Energy payback time and co2 emissions of pv systems. In: Elsevier Ltd (Ed.), Practical Handbook of Photovoltaics. Elsevier, pp. 1097–1117. https://doi.org/10.1016/B978-0-12-385934-1.00037-4.

Arciniegas, L.M., Hittinger, E., 2018. Tradeoffs between revenue and emissions in energy storage operation. Energy 143, 1–11. https://doi.org/10.1016/j.energy.2017.10.123.

Ardone, A., 2002. Aufgabenstellungen bei der produktionsplanung für energieversorgungsunternehmen. In: Strecker, S., Göbelt, M. (Eds.), Liberalisierte Energiemärkte : Strategie, Prognose, Handel, Fortschritt-Berichte VDI. VDI-Verlag, Düsseldorf, pp. 2–11.

Axsen, J., Kurani, K.S., McCarthy, R., Yang, C., 2011. Plug-in hybrid vehicle ghg impacts in California: integrating consumer-informed recharge profiles with an electricity-dispatch model. Energy Pol. 39, 1617–1629. https://doi.org/10.1016/j.enpol.2010.12.038.

Braeuer, F., Finck, R., McKenna, R., 2019. Data used in "Comparing empirical and model-based approaches for calculating dynamic grid emission factors: an application to co2-minimizing storage dispatch in Germany" (Version 1.2). http://doi.org/10.5281/zenodo.3588418.

Braeuer, F., Rominger, J., McKenna, R., Fichtner, W., 2019. Battery storage systems: an economic model-based analysis of parallel revenue streams and general implications for industry. Appl. Energy 239, 1424–1440. https://doi.org/10.1016/j.apenergy.2019.01.050.

Brouwer, A.S., van den Broek, M., Seebregts, A., Faaij, A., 2015. Operational flexibility and economics of power plants in future low-carbon power systems. Appl. Energy 156, 107–128. https://doi.org/10.1016/j.apenergy.2015.06.065.

Deetjen, T.A., Azevedo, I.L., 2019. Reduced-order dispatch model for simulating marginal emissions factors for the United States power sector. Environ. Sci. Technol. 53, 10506–10513. https://doi.org/10.1021/acs.est.9b02500.

ENTSO-E, 2019. Transparency platform. URL: https://transparency.entsoe.eu.

European Comission, 2019. European Union transaction log (eutl): emission trading data. URL: http://ec.europa.eu/environment/ets/.

European Environment Agency, 2019. The European Pollutant Release and Transfer Register (E-prtr). URL: https://www.eea.europa.eu/data-and-maps/data/member-states-reporting-art-7-under-the-european-pollutant-release-and-transfer-register-e-prtr-regulation-22.

Graf, C., Marcantonini, C., 2017. Renewable energy and its impact on thermal generation. Energy Econ. 66, 421–430. https://doi.org/10.1016/j.eneco.2017.07.009.

Guney, M.S., Tepe, Y., 2017. Classification and assessment of energy storage systems. Renew. Sustain. Energy Rev. 75, 1187–1197. https://doi.org/10.1016/j.rser.2016.11.102.

Hawkes, A.D., 2010. Estimating marginal co2 emissions rates for national electricity systems. Energy Pol. 38, 5977–5987. https://doi.org/10.1016/j.enpol.2010.05.053. URL: https://www.sciencedirect.com/science/article/pii/S0301421510004246/pdfft?md5=a5a989b3443ef0c89ee4be119002a0e5&pid=1-s2.0-S0301421510004246-main.pdf.

Hittinger, E.S., Azevedo, I.M.L., 2015. Bulk energy storage increases United States electricity system emissions. Environ. Sci. Technol. 49, 3203–3210. https://doi.org/10.1021/es505027p.

Holland, S.P., Mansur, E.T., 2008. Is real-time pricing green? the environmental impacts of electricity demand variance. Rev. Econ. Stat. 90, 550–561. https://doi.org/10.1162/rest.90.3.550.

Icha, P., 2019. Entwicklung der spezifischen kohlendioxid-emissionen des deutschen strommix in den jahren 1990 - 2018. URL: https://www.umweltbundesamt.de/publikationen/entwicklung-der-spezifischen-kohlendioxid-5.

Jansen, K.H., Brown, T.M., Samuelsen, G.S., 2010. Emissions impacts of plug-in hybrid electric vehicle deployment on the u.s. western grid. J. Power Sources 195, 5409–5416. https://doi.org/10.1016/j.jpowsour.2010.03.013.

Jochem, P., Babrowski, S., Fichtner, W., 2015. Assessing co2 emissions of electric vehicles in Germany in 2030. Transport. Res. Pol. Pract. 78, 68–83. https://doi.org/10.1016/j.tra.2015.05.007.

Kintner-Meyer, M., Schneider, K., Pratt, R., 2007. Impacts Assessment of Plug-In Hybrid Vehicles on Electric Utilities and Regional Us Power Grids Part 1: Technical Analyses. Pacific Northwest National Laboratory.

Lund, P.D., Lindgren, J., Mikkola, J., Salpakari, J., 2015. Review of energy system flexibility measures to enable high levels of variable renewable electricity. Renew. Sustain. Energy Rev. 45, 785–807. https://doi.org/10.1016/j.rser.2015.01.057.

Pareschi, G., Boulouchos, K., Georges, G., 2017. Assessment of the marginal emission factor associated with electric vehicle charging, 1st E-Mobility Power System Integration Symposium. E-Proceedings. https://doi.org/10.3929/ETHZ-B-000200058.

Rashid, K., Safdarnejad, S.M., Ellingwood, K., Powell, K.M., 2019. Techno-economic evaluation of different hybridization schemes for a solar thermal/gas power plant. Energy 181, 91–106. https://doi.org/10.1016/j.energy.2019.05.130.

Rashid, K., Mohammadi, K., Powell, K., 2020. Dynamic simulation and techno-economic analysis of a concentrated solar power (csp) plant hybridized with both thermal energy storage and natural gas. J. Clean. Prod. 248, 119193. https://doi.org/10.1016/j.jclepro.2019.119193.

Regett, A., Böing, F., Conrad, J., Fattler, S., Kranner, C., 2018. Emission Assessment of Electricity: Mix vs. Marginal Power Plant Method: 15th International Conference on the European Energy Market - Eem 2018. IEEE.

Ruppert, M., Slednev, V., Finck, R., Ardone, A., Fichtner, W., 2020. Utilising distributed flexibilities in the european transmission grid. In: Bertsch, V., Ardone, A., Suriyah, M., Fichtner, W., Leibfried, T., Heuveline, V. (Eds.), Advances in Energy System Optimization. Springer International Publishing, Cham, pp. 81–101.

Ryan, N.A., Johnson, J.X., Keoleian, G.A., Lewis, G.M., 2018. Decision support algorithm for evaluating carbon dioxide emissions from electricity generation in the United States. J. Ind. Ecol. 22, 1318–1330. https://doi.org/10.1111/jiec.12708.

Spork, C.C., Chavez, A., Gabarrell Durany, X., Patel, M.K., Villalba Méndez, G., 2015. Increasing precision in greenhouse gas accounting using real-time emission factors. J. Ind. Ecol. 19, 380–390. https://doi.org/10.1111/jiec.12193.

Stephan, C.H., Sullivan, J., 2008. Environmental and energy implications of plug-in hybrid-electric vehicles. Environ. Sci. Technol. 42, 1185–1190. https://doi.org/10.1021/es062314d.

Tamayao, M.-A.M., Michalek, J.J., Hendrickson, C., Azevedo, I.M.L., 2015. Regional variability and uncertainty of electric vehicle life cycle $co_2$ emissions across the United States. Environ. Sci. Technol. 49, 8844–8855. https://doi.org/10.1021/acs.est.5b00815.

Tomorrow, 2020. Electricitymap: Climate Impact by Area. URL: https://www.electricitymap.org.

Tranberg, B., Corradi, O., Lajoie, B., Gibon, T., Staffell, I., Andresen, G.B., 2019. Real-time carbon accounting method for the european electricity markets. Energy Strategy Review. 26, 100367. https://doi.org/10.1016/j.esr.2019.100367.

Wörner, P., Müller, A., Sauerwein, D., 2019. Dynamische co 2 –emissionsfaktoren für den deutschen strom–mix. Bauphysik 41, 17–29. https://doi.org/10.1002/bapi.201800034.

Yang, C., 2013. A framework for allocating greenhouse gas emissions from electricity generation to plug-in electric vehicle charging. Energy Pol. 60, 722–732. https://doi.org/10.1016/j.enpol.2013.05.013. URL: https://www.sciencedirect.com/science/article/pii/S0301421513003455/pdfft?md5=7bc4430162aa060d70c7edf999722705&pid=1-s2.0-S0301421513003455-main.pdf.

**Supplementary Information**
for

# Comparing empirical and model-based approaches for dynamic grid emission factors: an application to $CO_2$-minimizing storage dispatch in Germany

Fritz Braeuer, *Chair of Energy Economics, Institute for Industrial Production (IIP), Karlsruhe Institute of Technology (KIT), Karlsruhe, Germany*
Rafael Finck, *Chair of Energy Economics, Institute for Industrial Production (IIP), Karlsruhe Institute of Technology (KIT), Karlsruhe, Germany*
Russell McKenna, *DTU Management Engineering, Technical University of Denmark (DTU), Kgs. Lyngby, Denmark*

## SI A. Literature Review

Table A.1: Methods and Models for Calculating $CO_2$-emissions

| Paper | MPM | MPP | AEF | Emp. Data | Mod. | CB | PB | Region |
|---|---|---|---|---|---|---|---|---|
| Arciniegas.2018 | x | | | x | | | | US |
| Finenko.2016 | x | | | | x | | | Asia |
| Hittinger.2015 | x | | | x | | | | US |
| Holland.2008 | x | | | x | | | | US |
| Pareschi.2017 | x | | | x | | x | x | EU |
| Hawkes.2010 | x | | x | x | | x | | UK |
| SilerEvans.2012 | x | | x | x | | | x | US |
| Thind.2017 | x | | x | x | | x | x | US |
| Regett.2018 | x | x | | | x | | x | EU |
| Tamayao.2015 | x | x | x | x | | | x | US |
| Ripp.2018 | | x | x | x | x | x | | - |
| Bettle.2006 | | x | | x | | x | | UK |
| GraffZivin.2014 | | x | | x | | x | | US |
| Jansen.2010 | | x | | | x | x | | US |
| Jochem.2015 | | x | | | x | x | | EU |
| McCarthy.2010 | | x | | | x | x | | US |
| McCarthy.2009 | | x | | | x | | x | US |
| Zheng.2015 | | x | | | | x | | UK |
| Axsen.2011 | | x | x | | x | x | x | US |
| Spork.2015 | | | x | x | | x | | Spain |

Abbreviations
AEF: Average Emission Factor, MPM: Marginal Power Mix, MPP: Marginal Power Plant, Mod. Data: Model based approach, CB: Consumption based, PB: Production based

*MPM.* Hawkes [1] in analogy to Holland and Mansur [2], developed an MPM based on historical data from 2002 to 2009 for the U.K. in various temporal disaggregations. A comparison with an AEF showed that the AEF underestimates the actual emissions by around 30% [1, p. 5986]. Siler-Evans et al. [3] were able to confirm this, when they applied the same approach to different regions in the U.S. using data from 2006 to 2011.

Both studies found substantial deviation for MPM at different time-of-day. Siler-Evans et al. [3] attribute this to demand ramps which are served by gas-fired power plants with lower emissions than coal-fired power plants. This statement is supported by Tamayao et al. [4, p. 8848] and Thind et al. [5]. There have been several more studies applying MPM. Hittinger and Azevedo [6] and Arciniegas and Hittinger [7] use it to analyze the impact of energy storage on the emissions of the U.S electricity system. Thind et al. [5] explore regional differences of the MPM and in contrast to Siler-Evans et al. [3] consider renewable electricity generation for their observations. Pareschi et al. [8] and Tamayao et al. [4] study the differences between a consumption based (allowing for exchanges) and a production based approach (considering only the production inside the system boundaries). Pareschi et al. [8] concludes that inter-regional trade may have an effect on the accuracy of the EF depending on the system size and structure. Tamayao et al. [4] compare the consumption based approach of Graff Zivin et al. [9] and the production based approach of Siler-Evans et al. [3] to an AEF. They conclude that consumption based approaches are more appropriate but lack uncertainties in the data on inter-regional trade.

*MPP.* Jansen et al. [10] similar to Bettle et al. [11] developed a dispatch algorithm to identify the MPP based on a dispatch order derived from capacity factors of the respective fuel type to study the U.S. energy system. McCarthy and Yang [12] developed the EDGE-CA model based on the merit order approach to evaluate the effect of electric vehicles on the MPP. McCarthy and Yang [12] cluster the California power plants into three categories of non-dispatchable, base-load and fossil power plants. In their definition the "marginal generators are the most expensive plants operating in a given hour, and likely, the least efficient" [12, p. 2101]. Axsen et al. [13] built up on the same model to focus on the behavior of owners of plug-in hybrid electric vehicles (PHEV). To consider long term implications of plant retirement and grid expansion they compare the results to the LEDGE-CA model [14].Finenko and Cheah [15] develop a dispatch model for the case of Singapore with a very low share of REs ($< 1\%$) and a high share of natural gas power plants (95%). Jochem et al. [16] use the PERSEUS-NET-TS model to analyse the influence of different EV-charging strategies. They use a nodal pricing approach for the German energy system and consider 440 administrative districts to evaluate the energy system's behavior in case of high share of REs in 2030. Regett et al. [17] develop their own MPP with a merit order approach using the ISAaR model. The model incorporates an electricity market simulation for Europe. Ripp and Steinke [18] published a methodology to properly assess the emissions in a multi-commodity system considering different forms of energy resulting from combined heat and power plants and energy storage systems.Zheng et al. [19] calculate the MPP for the UK. Aligning with Tamayao et al. [4], they emphasize the influence of the accurate constraints of the power plant technologies. It is often stated that is difficult to identify the MPP due to the numerous technical and economic constraints in reality [3, 1, 4].

## SI B. Data inaccuracies

Multiple generation units in ENTSO-E are listed under one single installation name in EUTL. In these cases, we estimate the theoretical share one generation unit has of the total $CO_2$-emissions of the entire power plant listed in EUTL. Table B.2 illustrates

this approach further. The theoretical efficiency per generation unit depends on age and technology. A value for the age-dependent efficiency is linearly interpolated between the values of an old and new installed power generator taken from ENTSO-E [20]. The efficiency factor multiplied with the fuel specific emission factor [21] and the total generation results in the theoretically estimated emissions per generation unit. Looking at the total estimated $CO_2$-emissions all generation units of one power plant emit, one can derive the estimated share of emissions linked to the single generation unit. Finally, adapting the estimated share of emissions to the verified emissions leads to the specific emission factor per generation unit, $EF_j$.

Similarly, the theoretically EF per generation unit is used to compensate missing values for verified emissions as well as unreasonable high EFs per power plant greater than 2 t/MWh.

Table B.2: Example table to illustrate data preparation to derive emission factors per power plant

| **ENTSO Generation Unit** | **EUTL ID** | **Fuel Type** | **Efficiency** | **Fuel EF** | |
|---|---|---|---|---|---|
| Units | | | | $\frac{kg_{CO_2}}{kWh}$ | |
| RDK 4 | 1457 | Gas | 0.4924 | 0.2014 | |
| RDK 7 | 1457 | Coal | 0.3968 | 0.3557 | |
| RDK 8 | 1457 | Coal | 0.4559 | 0.3557 | |
| **ENTSO Generation Unit** | **Total generation per unit** | **Estimated emissions per year** | **Estimated share of emissions** | **Verified emissions** | $EF_j$ |
| Units | GWh | t | | t | $\frac{kg_{CO_2}}{kWh}$ |
| RDK 4 | 10.5 | 4285 | 0.0011 | 3841547 | 0.3970 |
| RDK 7 | 1536.9 | 1377487 | 0.3481 | 3841547 | 0.8701 |
| RDK 8 | 3300.9 | 2575281 | 0.6508 | 3841547 | 0.7574 |

For finalizing the *AEF* and the *MSR*, the outliers in the time series were identified through the median method and replaced through linear interpolation.

## SI C. ESM details

Equation C.1 [22] defines $P_{peak}$ to be at least equal to the amount of electricity ($x_{el,t}$) drawn from the grid during one of the 15-minutes time steps per year. 15-minute time steps are chosen, as the peak price is defined for the peak power demand a 15-minute time step. Equation C.2 [22] shows the electricity flow balance, where $x_{el,t}$ is equals to the electricity demand of the industrial production ($D_{Prod,t}$) minus the electricity flowing from the ESS to the production ($x_{(ESS-Prod),t}$) and the electricity flow from the grid to the ESS ($x_{(grid-ESS)}$).

$$P_{peak} \leq x_{el,t} \cdot \frac{4}{1000}, \quad \forall t \in [1, 2...35040] \tag{C.1}$$

$$x_{el,t} = D_{Prod,t} - x_{(ESS-Prod),t} + x_{(grid-ESS),t},$$
$$x_{(ESS-Prod),t} \geq 0, x_{(grid-ESS),t} \geq 0, \forall t \in [1, 2...35040] \tag{C.2}$$

## SI D. Results GSS

Figure D.1 and Figure D.2 show the results of the environmental dispatch for two companies for two consecutive sample days, February 15th (Wednesday) till 17th (Friday) 2017. The figures are divided into four graphs, one for each EF. The figures show the load profile, the charging and discharging profile as well as the SoC on the left axis. The right axis indicates the respective EF. The horizontal dashed-dot lines indicate the maximum peak load that has to be achieved through peak shaving. While the two sample companies have a similar peak load level (translated into maximum energy per 15-minute interval, company 45 with 327 $kWh$ and company 46 with 370 $kWh$) as well as comparable optimized storage capacities (company 45 with 219 $kWh$ and company 46 with 319 $kWh$), the load profiles are fairly different. Company 45, an iron casting company, shows very high singular peaks of more than 300 $kWh$ followed by periods of low energy demand, not more than 20 $kWh$. It has one of the lowest utilization factors. Similarly, sample company 46, a manufacturer of mixed spices, shows five peaks per day of up to 400 $kWh$. The lowest load during these sample days is around 80 $kWh$. The utilization factor is one of the highest.

Considering Figure D.1, the four graphs illustrate the signaling effect of the different EFs to charge the storage system for different time periods. For all four EFs, charging periods are during hours of low EFs. One can observe roughly four full charging cycles in case the AEF, eight cycles for the MSR, six and a half for MPM and seven for the MPP. Discharging occurs mostly during periods of high loads. The unique load profile of company 45 restricts the storage system to discharge during low load periods as the loads are near zero. Therefore, discharging the storage systems and feeding electricity to the production is not possible. Compared to the AEF, one can observe a high correlation between the load peaks and the peaks of the MSR, MPM and MPP. Thus, shifting the emissions from one period to the other is not restricted by the peak shaving threshold. More to the contrary considering in the fourth graph the second peak in the load on February the 16th, the GSS is utilized for peak shaving during hours of maximum MPP. This results in a synergistic effect of the two objectives leading to the lowest values for $CO_2$-abatement cost among the 50 companies. Simultaneously in the AEF graph during the same time period, the storage dispatch's focus is on peak shaving rather than $CO_2$-reduction.

## SI E. Other emissions

Table E.3 statistically summarizes the EFs applied to the other emissions, $SO_2$, $NO_x$and Dust. Looking at the individual emission factors of the generation units, it is evident that the EF has a weak dependency on the fuel type and generation technology and a rather strong dependency on the air pollution abatement system. This leads to highest volatility among the emission factors for the MPP. In alignment with

Table E.3: Characteristics of the emission factors

| | $CO_2$ *in* $kg_{CO_2}/MWh$ | | | | $SO_2$ *in* $g_{SO_2}/MWh$ | | | |
|---|---|---|---|---|---|---|---|---|
| | AEF | MSR | MPM | MPP | AEF | MSR | MPM | MPP |
| Min | 486.5 | -679.1 | 114.2 | 0.0 | 79.2 | -289.9 | 23.9 | 0.0 |
| Max | 915.6 | 1190.3 | 390.1 | 1189.8 | 272.6 | 456.0 | 131.9 | 13768.8 |
| Mean | 707.5 | 268.1 | 224.1 | 840.2 | 165.6 | 89.5 | 70.3 | 225.6 |
| Std | 76.1 | 304.1 | 90.4 | 267.0 | 31.2 | 125.1 | 33.3 | 691.5 |
| Varcoef | 0.1 | 1.1 | 0.4 | 0.3 | 0.2 | 1.4 | 0.5 | 3.1 |
| | $NO_x$ *in* $g_{NO_x}/MWh$ | | | | *Dust in* $g_{Dust}/MWh$ | | | |
| | AEF | MSR | MPM | MPP | AEF | MSR | MPM | MPP |
| Min | 98.9 | -841.1 | -187.8 | 0.0 | 3.4 | -9.1 | 0.7 | 0.0 |
| Max | 929.0 | 1199.2 | 702.2 | 19436.7 | 8.4 | 14.5 | 4.2 | 546.2 |
| Mean | 436.7 | 229.4 | 170.2 | 695.9 | 5.6 | 2.9 | 2.3 | 7.3 |
| Std | 161.7 | 346.9 | 180.4 | 2062.3 | 0.8 | 4.0 | 1.0 | 26.9 |
| Varcoef | 0.4 | 1.5 | 1.1 | 3.0 | 0.2 | 1.4 | 0.4 | 3.7 |

the $CO_2$-emission factor, the MPP followed by the AEF show the highest mean values for local emissions.

The influence of the environmental dispatch on the other emissions, namely $SO_2$, $NO_x$ and *Dust* is shown in Table E.4.

Table E.4: Statistical overview of results of other emissions

| | | | GSS | | | | BSS | |
|---|---|---|---|---|---|---|---|---|
| | | Unit | AEF | MSR | MPM | MPP | MSR | MPP |
| $\Delta SO_2$ in kg | Min | kg | 0.02 | 0.10 | 0.30 | -0.34 | 0.03 | -0.42 |
| | Max | kg | 4.62 | 25.89 | 78.95 | 2.66 | 6.42 | 0.27 |
| | Mean | kg | 0.38 | 2.25 | 6.45 | 0.36 | 0.55 | -0.02 |
| | Std | kg | 0.70 | 4.04 | 12.23 | 0.66 | 1.02 | 0.11 |
| | Varcoef | % | 188 | 179 | 190 | 184 | 187 | NaN |
| $\Delta NO_x$ in kg | Min | kg | -18.51 | 0.16 | 1.62 | -6.67 | 0.03 | -6.30 |
| | Max | kg | -0.07 | 49.85 | 395.41 | 0.76 | 7.96 | 0.06 |
| | Mean | kg | -1.60 | 4.33 | 32.56 | -0.74 | 0.75 | -0.66 |
| | Std | kg | 2.89 | 7.66 | 62.05 | 1.31 | 1.34 | 1.13 |
| | Varcoef | % | NaN | 177 | 191 | NaN | 180 | NaN |
| $\Delta Dust$ in kg | Min | kg | 0.00 | 0.00 | 0.01 | -0.02 | 0.00 | -0.01 |
| | Max | kg | 0.19 | 0.90 | 2.56 | 0.18 | 0.20 | 0.04 |
| | Mean | kg | 0.02 | 0.07 | 0.21 | 0.02 | 0.02 | 0.00 |
| | Std | kg | 0.03 | 0.13 | 0.40 | 0.03 | 0.03 | 0.01 |
| | Varcoef | % | 188 | 199 | 189 | 212 | 198 | 292 |

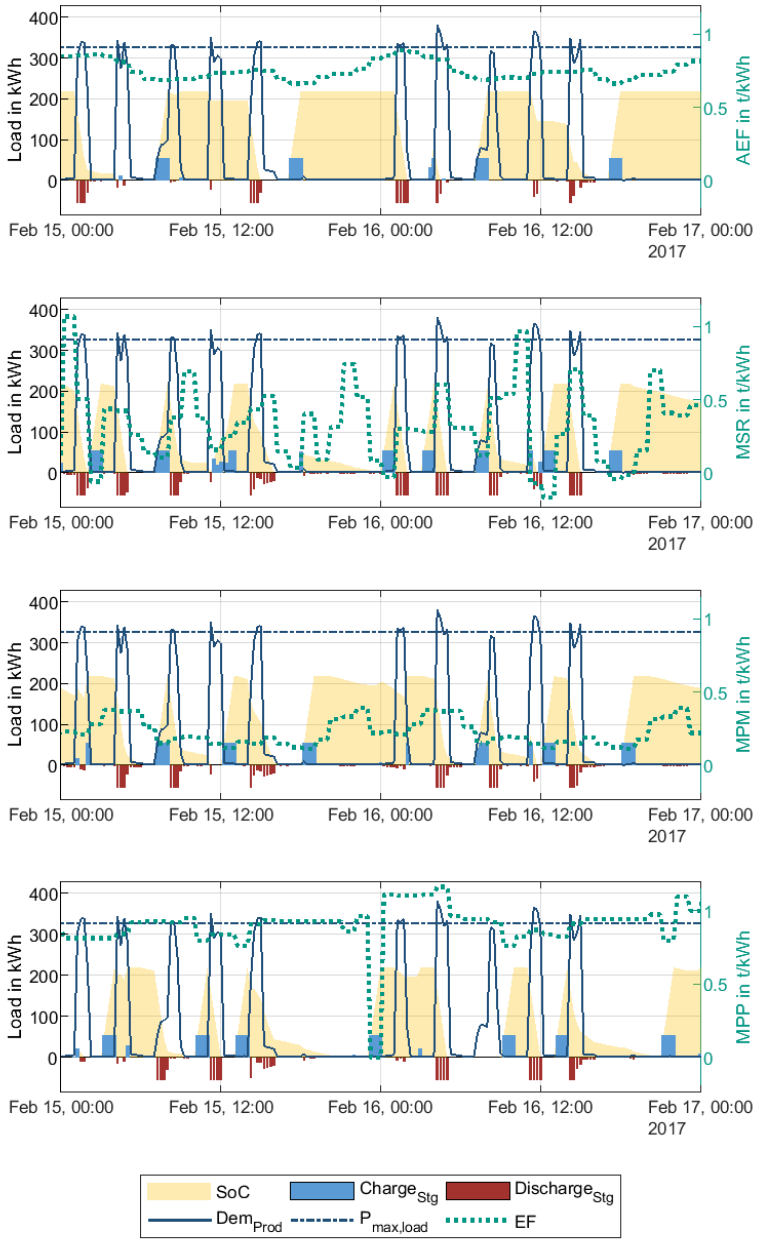


Figure D.1: Load and charging profile of company 45, iron casting, for 2 exemplary days. Optimized GSS capacity is 219 $kWh$

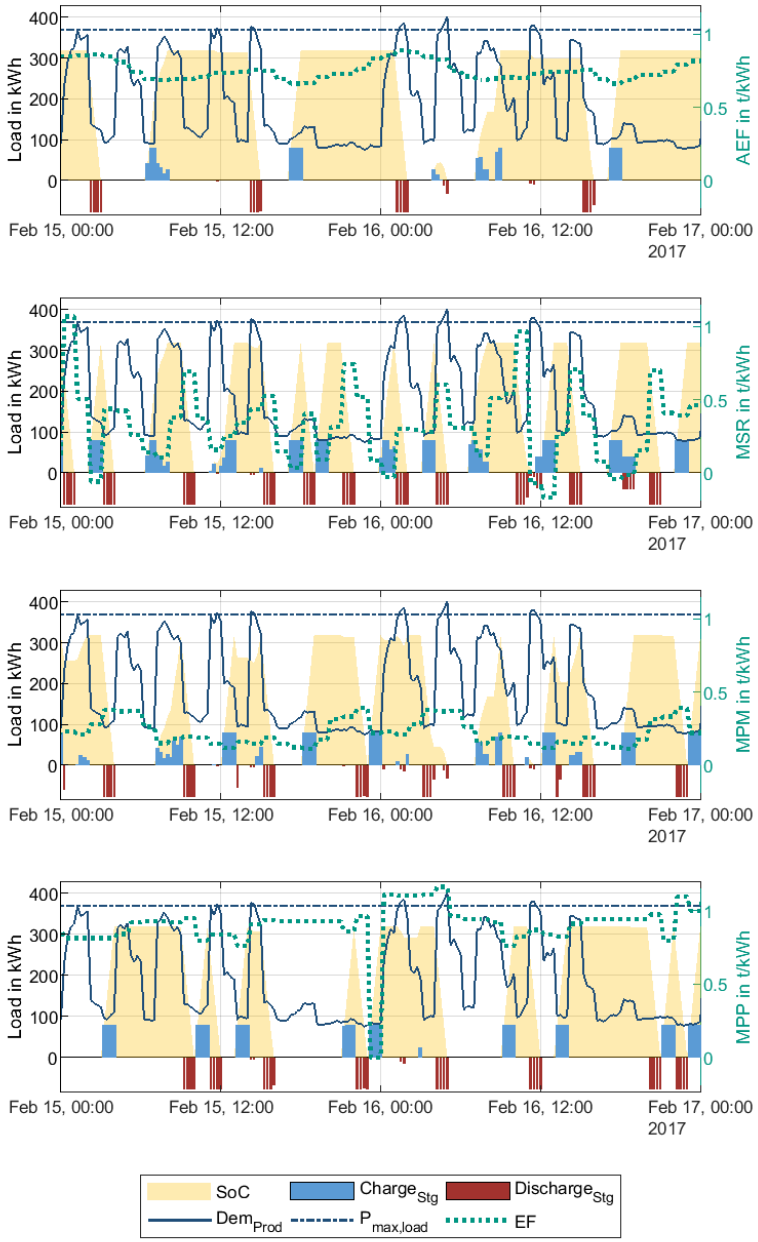


Figure D.2: Load and charging profile of company 46, manufacturer of mixed spices, for 2 exemplary days. Optimized GSS capacity is 319 $kWh$

## SI F. MPM

The *MPM* is derived from the work of Hawkes [1]. He postulates a marginal EF, which is shown in equation F.1 [1] and equation F.2 [1]. Over the course of one year, Hawkes [1] assumes that the energy system reacts similar in every hour of the day. Therefore for every hour of the day $h$, we build a linear regression model consisting of 365 samples, see equation F.1. Equation F.2 defines the slope of the regression line $b_h$ as the *MPM*.

$$\Delta m_{CO_2,(h)} = a_h + b_h \cdot \Delta L_{Res,(h)}, \forall h \in 1, 2, ..., 24 \tag{F.1}$$

$$MPM_h = b_h, \forall h \in 1, 2, ..., 24 \tag{F.2}$$

To derive the MPM, the sample was adjusted for outliers after the median method. The hourly change in $CO_2$-emissions of the power mix ($\Delta m_{CO_2,(h)}$) is the dependent variable and the hourly change in residual load ($\Delta L_{Res,(h)}$) is the the independent variable.

Figure F.3 plots the hourly values of the MPM on the right access. Orientated on the left access, the bar chart indicates the $R^2$-Value of the linear regression model defining the MPM.

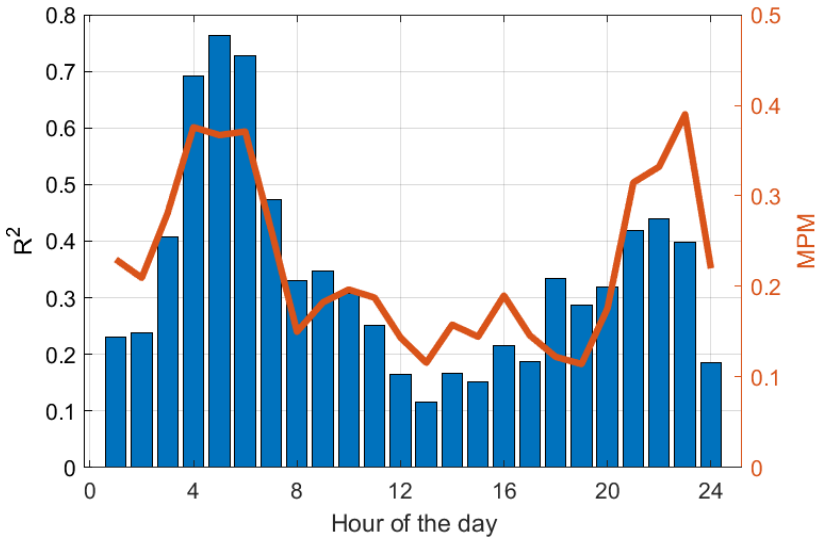


Figure F.3: MPM for all the hour of the day and the values of $R^2$

## References


[1] A. D. Hawkes, Estimating marginal co2 emissions rates for national electricity systems, Energy Policy 38 (2010) 5977–5987. URL: https://www.sciencedirect.com/science/article/pii/S0301421510004246/pdfft?md5=a5a989b3443ef0c89ee4be119002a0e5&pid=1-s2.0-S0301421510004246-main.pdf. doi:10.1016/j.enpol.2010.05.053.

[2] S. P. Holland, E. T. Mansur, Is real-time pricing green? the environmental impacts of electricity demand variance, Review of Economics and Statistics 90 (2008) 550–561. doi:10.1162/rest.90.3.550.

[3] K. Siler-Evans, I. L. Azevedo, M. G. Morgan, Marginal emissions factors for the u.s. electricity system, Environmental science & technology 46 (2012) 4742–4748. doi:10.1021/es300145v.

[4] M.-A. M. Tamayao, J. J. Michalek, C. Hendrickson, I. M. L. Azevedo, Regional variability and uncertainty of electric vehicle life cycle $co_2$ emissions across the united states, Environmental science & technology 49 (2015) 8844–8855. doi:10.1021/acs.est.5b00815.

[5] M. P. S. Thind, E. J. Wilson, I. L. Azevedo, J. D. Marshall, Marginal emissions factors for electricity generation in the midcontinent iso, Environmental science & technology 51 (2017) 14445–14452. doi:10.1021/acs.est.7b03047.

[6] E. S. Hittinger, I. M. L. Azevedo, Bulk energy storage increases united states electricity system emissions, Environmental science & technology 49 (2015) 3203–3210. doi:10.1021/es505027p.

[7] L. M. Arciniegas, E. Hittinger, Tradeoffs between revenue and emissions in energy storage operation, Energy 143 (2018) 1–11. doi:10.1016/j.energy.2017.10.123.

[8] G. Pareschi, K. Boulouchos, G. Georges, Assessment of the marginal emission factor associated with electric vehicle charging, 1st E-Mobility Power System Integration Symposium. E-Proceedings (2017). doi:10.3929/ETHZ-B-000200058.

[9] J. S. Graff Zivin, M. J. Kotchen, E. T. Mansur, Spatial and temporal heterogeneity of marginal emissions: Implications for electric cars and other electricity-shifting policies, Journal of Economic Behavior & Organization 107 (2014) 248–268. doi:10.1016/j.jebo.2014.03.010.

[10] K. H. Jansen, T. M. Brown, G. S. Samuelsen, Emissions impacts of plug-in hybrid electric vehicle deployment on the u.s. western grid, Journal of Power Sources 195 (2010) 5409–5416. doi:10.1016/j.jpowsour.2010.03.013.

[11] R. Bettle, C. H. Pout, E. R. Hitchin, Interactions between electricity-saving measures and carbon emissions from power generation in england and wales, Energy Policy 34 (2006) 3434–3446. doi:10.1016/j.enpol.2005.07.014.

[12] R. McCarthy, C. Yang, Determining marginal electricity for near-term plug-in and fuel cell vehicle dmeands in california: Impacts on vehicle greenhouse gas emissions, Journal of Power Sources (2010) 2099–2109.

[13] J. Axsen, K. S. Kurani, R. McCarthy, C. Yang, Plug-in hybrid vehicle ghg impacts in california: Integrating consumer-informed recharge profiles with an electricity-dispatch model, Energy Policy 39 (2011) 1617–1629. doi:10.1016/j.enpol.2010.12.038.

[14] R. McCarthy, Assessing Vehicle Electricity Demand Impacts on California Electricity Supply, Phd dissertation, University of California, Davis, 2009.

[15] A. Finenko, L. Cheah, Temporal co2 emissions associated with electricity generation: Case study of singapore, Energy Policy 93 (2016) 70–79. doi:10.1016/j.enpol.2016.02.039.

[16] P. Jochem, S. Babrowski, W. Fichtner, Assessing co2 emissions of electric vehicles in germany in 2030, Transportation Research Part A: Policy and Practice 78 (2015) 68–83. doi:10.1016/j.tra.2015.05.007.

[17] A. Regett, F. Böing, J. Conrad, S. Fattler, C. Kranner, Emission assessment of electricity: Mix vs. marginal power plant method: 15th international conference on the european energy market - eem 2018, IEEE (2018).

[18] C. Ripp, F. Steinke, Modeling time-dependent co2 intensities inmulti-modal energy systems with storage: 15th international conference on the european energy market – eem 2018, IEEE (2018).

[19] Z. Zheng, F. Han, F. Li, J. Zhu, Assessment of marginal emissions factor in power systems under ramp-rate constraints, CSEE Power and Energy Syst. (CSEE Journal of Power and Energy Systems) 1 (2015) 37–49. doi:10.17775/CSEEJPES.2015.00049.

[20] ENTSO-E, Tyndp 2018 - maps & data: Joint scenarios data - input data, 2018. URL: https://tyndp.entsoe.eu/maps-data/.

[21] P. Gniffke, Carbon dioxide emissions for the german atmospheric emission reporting: 1990 - 2016, 2018.

[22] F. Braeuer, J. Rominger, R. McKenna, W. Fichtner, Battery storage systems: An economic model-

based analysis of parallel revenue streams and general implications for industry, Applied Energy 239 (2019) 1424–1440. doi:10.1016/j.apenergy.2019.01.050.